EFFECTS OF EPOXY-COATING ON THE BOND OF REINFORCING STEEL TO CONCRETE

by

Hossain Hadje-Ghaffari

David Darwin

Steven L. McCabe

A Report on Research Sponsored by

THE NATIONAL SCIENCE FOUNDATION

Research Grant No. CES-8616228

UNIVERSITY OF KANSAS

LAWRENCE, KANSAS

July 1991

50272-101

REPORT DOCUMENTATION PAGE	1. REPORT NO.	2.	3. Recipient's Accession No.

4. Title and Subtitle
Effects of Epoxy-Coating on the Bond of Reinforcing Steel to Concrete

5. Report Date
July 1991

6.

7. Author(s)
Hossain Hadje-Ghaffari, David Darwin, and Steven L. McCabe

8. Performing Organization Rept. No.
SM Report No. 28

9. Performing Organization Name and Address
Structural Engineering and Materials Laboratory
University of Kansas Center for Research, Inc.
2291 Irving Hill Drive, West Campus
Lawrence, Kansas 66045

10. Project/Task/Work Unit No.

11. Contract(C) or Grant(G) No.
(C)
(G) NFS CES-8616228

12. Sponsoring Organization Name and Address
National Science Foundation
Washington, D.C. 20550

13. Type of Report & Period Covered

14.

15. Supplementary Notes

16. Abstract (Limit: 200 words)

The effects of deformation pattern, bar size, concrete cover, casting position, concrete slump, consolidation, transverse reinforcement, and concrete strength on the reduction in bond strength between reinforcing bars and concrete caused by epoxy coating are described. Tests include beam-end and splice specimens containing No. 5, No. 6, No. 8, and No. 11 bars. A preliminary investigation of the behavior of epoxy-coated hooks is also described. Epoxy coatings reduce bond strength. In general, this reduction increases with bar size and changes with deformation pattern: bars with a relatively large rib-bearing area are affected less by the coating than bars with a smaller bearing area. The bond strength of both uncoated and coated bars increases as concrete cover increases. The bottom to top-cast bar strength ratio, B/T, increases for uncoated bars and decreases for coated bars as concrete slump increases. Transverse steel increases bond strength; coated confined bars had virtually the same bond strength as uncoated unconfined bars. Design recommendations are made.

Analytical studies are conducted on a statical model, consisting of two rigid bodies (steel and concrete) in contact, and a finite element model, representing one-half of a beam-end specimen. Statical model analyses indicate that 0.35 and 0.10 can be adopted as representative coefficients of friction for uncoated and coated bars, respectively. Finite element analyses indicate an increase in bond force will occur with an increase in cover, lead length, or bar size.

17. Document Analysis a. Descriptors
beam-end specimen, beam-splice specimens, bond (concrete to steel), coatings, coefficient of friction, cohesion, deformed reinforcement, epoxy-coated reinforcement, fictitious crack model, fracture mechanics, non-linear finite element analysis, reinforcing steels, splitting crack, structural engineering

b. Identifiers/Open-Ended Terms

c. COSATI Field/Group

18. Availability Statement	19. Security Class (This Report)	21. No. of Pages
Release Unlimited	Unclassified	288
	20. Security Class (This Page) Unclassified	22. Price

(See ANSI-Z39.18) See Instructions on Reverse

OPTIONAL FORM 272 (4-77)
(Formerly NTIS-35)
Department of Commerce

ABSTRACT

The effects of deformation pattern, bar size, concrete cover, casting position, concrete slump, consolidation, transverse reinforcement, and concrete strength on the reduction in bond strength between reinforcing bars and concrete caused by epoxy coating are described. Tests include beam-end specimens containing No. 5, No. 6, No. 8, and No. 11 bars with average coating thicknesses ranging from 3 to 17 mils. Three deformation patterns are evaluated. Specimens with covers of 1, 2, and 3 bar diameters are studied. Concrete slumps range from 2 to 8 in.. Some of the specimens cast with 8 in. slump concrete are vibrated and some are not. Concrete strengths range from 5,000 to 13,000 psi with most concrete at 6,000 psi. Full-scale beam splice specimens are tested to verify the results of the beam-end tests. A preliminary investigation of the behavior of epoxy-coated hooks is carried out.

Epoxy coatings are found to significantly reduce bond strength, but the extent of the reduction is less than used to establish the development length modification factors in the 1989 ACI Building Code and 1989 AASHTO Bridge Specifications. In general, the reduction in bond strength caused by epoxy coating increases with bar size and changes with deformation pattern: bars with a relatively large rib-bearing area are affected less by the coating than bars with a smaller bearing area. The bond strength of both uncoated and coated bars increases as concrete cover increases; for the beam-end specimens tested in this study, the absolute

reduction in bond strength caused by an epoxy coating is nearly independent of cover. The bottom to top-cast bar strength ratio, B/T, increases for uncoated bars and decreases for coated bars as slump increases. The coated bar to uncoated bar bond strength ratio, C/U, is the same for bottom and top-cast bars in low slump concrete; however, C/U for top-cast bars is greater than C/U for bottom-cast bars in high slump concrete. Vibration has a positive effect on uncoated and coated bar bond strengths and on C/U for both bottom and top-cast bars. Confinement provided by transverse steel has a positive effect on bond strength, and in the current tests, coated confined bars had virtually the same bond strength as uncoated unconfined bars.

To better understand the effect of epoxy coating on bond strength and the nature of bond failure, an analytical study is conducted on a statical and a finite element model. The statical model consists of two rigid bodies (steel and concrete) in contact. The finite element model represents one-half of a beam-end specimen. The statical model analysis along with the test results indicates that 0.35 and 0.10 can be adopted as representative coefficients of friction for uncoated and coated bars, respectively. The finite element analyses indicate that an increase in lateral force provided by the concrete, and thus an increase in bond force, will occur with an increase in cover, lead length, or bar size.

ACKNOWLEDGMENTS

This report is based on a thesis submitted by Hossain Hadje-Ghaffari to the Department of Civil Engineering of the University of Kansas in partial fulfillment of the requirements for the Ph.D. degree.

The research was supported by the National Science Foundation under NSF Grant CES-8616228. Reinforcing steel was supplied by Chaparrel Steel Company, North Star Steel Company, Sheffield Steel Corporation, and Structural Metals, Inc. The epoxy coating, 3M Scotchkote 213, was applied by ABC Coating Company, Inc. and Simcote, Inc. Superplasticizer and powdered silica fume were supplied by Master Builders, Inc., and form release agent was provided by Nox-Crete, Inc.

Numerical computations were performed on the Harris 800 computer system operated by the Computer Aided Engineering Laboratory and an Apollo DN3500 workstation operated by the Graphics and Computer Applications Laboratory in the Department of Civil Engineering at the University of Kansas. Finite element models were generated with the PATRAN-II software system and the analysis was carried out using the POLO-FINITE General Purpose Finite Element Program.

TABLE OF CONTENTS

TABLE OF CONTENTS (continued)

TABLE OF CONTENTS (continued)

LIST OF TABLES (continued)

LIST OF TABLES

LIST OF FIGURES (continued)

LIST OF FIGURES (continued)

LIST OF FIGURES (continued)

LIST OF FIGURES (continued)

LIST OF FIGURES (continued)

CHAPTER 1: INTRODUCTION

1.1 General

Corrosion of reinforcing steel is a major design consideration in reinforced concrete structures because corrosion can cause considerable damage, resulting in costly repairs. Corrosion is most likely to occur in structures subjected to harsh environments such as offshore and marine structures, concrete pavements and bridges, and cooling towers where the attack on steel is accelerated because of the presence of excessive amounts of chloride ions found in sea water, deicing chemicals, or chemicals for water treatment. This process damages the structure in two ways. The chloride attack and oxidation process may degrade the bond of the steel to the concrete, and the corroding steel undergoes a volume expansion equal to several times its original volume. This expansion creates tensile stresses in the surrounding concrete which may result in spalling which reduces the bond between the concrete and reinforcing steel and allows access for oxygen and moisture.

Traditionally, the corrosion of reinforcing steel has been controlled by minimizing the extent of cracking and the widths of those cracks in concrete. This is achieved by using a low water-cement ratio, dense concrete, increased concrete cover, and by sealing the concrete surface. These provisions, however, have not always been successful and may not be practical or economical.

A major step toward inhibiting the corrosion of reinforcing steel has been the introduction of epoxy coating to seal the bar surface to eliminate chloride attack. Epoxy was first used as a coating material to inhibit the corrosion of pipelines. Based on experience with pipelines, several coating materials were investigated in one of the earliest studies of coated reinforcing steel (Clifton, Mathey, and Anderson 1979), and fusion-bonded epoxy coatings were found to be practical, economical and effective in controlling corrosion. Epoxy-coated reinforcing steel was introduced to the concrete industry in a Pennsylvania bridge deck in 1973 (ACI Technical Committees 222, 408, and 439, 1988). Ever since, coated steel has found an increasingly wider application in a variety of concrete structures. Currently, 5% of all reinforcing bars being produced in the United States are epoxy coated.

The epoxy coating process used for reinforcing steel produces a smoother surface than the original rough mill scale surface. The geometry of the deformations on the bar also are changed from their original well-defined somewhat sharp corners and edges to more rounded corners and edges. These changes affect the bond between the reinforcing steel and concrete. The ACI Building Code (1983) contained no special design provisions for the use of epoxy-coated bars until the 1989 Building Code was proposed (ACI Committee 318, 1988, 1989).

All of the studies performed to date show that epoxy-coated bars develop less bond strength than uncoated bars. This

observation is important since the bond between concrete and reinforcing steel is critical to safety and integrity of reinforced concrete structures.

Many factors may, in fact, affect the bond of deformed bars to concrete. Since epoxy coatings change the surface properties of a bar and alter the interaction between reinforcing steel and concrete, properties of the bar such as deformation pattern, rib spacing, angle, height, and area may become more important in coated bar performance than in a standard uncoated bar. A study at the University of Kansas by Choi, Darwin, and McCabe (1990) has shown that the type of deformation pattern and the bar size affect the amount of reduction in bond strength caused by epoxy coating.

The KU study has been the most extensive study of the bond strength of epoxy-coated bars, considering deformation pattern, bar size, concrete cover, coating thickness, and bar position. The research program described herein complements the prior KU work by investigating the effects of parameters such as, concrete strength, concrete slump, and stirrup confinement. In addition, the behavior of coated bars in full size beam splice tests as well as the behavior of a limited number of epoxy-coated hooks embedded in beam-end specimens are investigated. The information from this research, combined with that from the current study at the University of Kansas, as well as that from previous studies by other researchers, will be used to obtain a better understanding of the bond behavior of epoxy-coated bars. This improved understanding will be reflected

in improved design provisions for the ACI Building Code that will address the behavior of epoxy-coated bars more accurately than the 1989 design rules (ACI Committee, 1988, 1989). The outcome will be a building code that permits safe, accurate, and economical design.

1.2 Background

Bond is the critical property that joins steel to concrete, thus ensuring strain compatibility. If bond is lost, a bar will move relative to the concrete causing a loss of integrity. The force in the bar is transmitted to the concrete by three mechanisms (Lutz et al. 1966, Lutz 1970) that include chemical adhesion, friction, and mechanical interaction between the concrete and the steel. Chemical adhesion occurs because the cement paste in concrete is closely attached to steel. Contact between the concrete and the bar causes friction upon movement of the bar. The magnitude of adhesion and friction depend on the roughness of the bar surface. Mechanical interaction is mostly influenced by the geometric properties of the deformations or ribs on the bar. As the bond stress increases and the adhesion capacity is exceeded, the adhesion component is lost. After the loss of adhesion, friction and mechanical interaction between the bar and the concrete act together to resist the movement of the bar relative to the concrete.

Since the surface of a epoxy-coated bar is smooth and glossy, the adhesion and friction between an epoxy-coated bar and concrete are much lower than the ones obtained with an uncoated bar, and

mechanical interaction is thought to be the only bond mechanism that is effective.

Several studies have been preformed to investigate the effect of epoxy coating on the bond strength between the concrete and reinforcing steel. The studies performed to date in this area have been done by Mathey and Clifton (1976) on 19 pullout specimens, Johnston and Zia (1982) on 6 slab and 40 beam-end specimens, Treece and Jirsa (1987, 1989) on 21 beam specimens, Cleary and Ramirez (1989) on 8 slab specimens, and Choi, Darwin, and McCabe (1990) on 394 beam-end specimens. These investigations come to somewhat different conclusions about the effects of the epoxy coating, concrete strength, coating thickness, and bar size on bond strength. Except for the study at the University of Kansas (Choi, Darwin, and McCabe 1990), the total number of tests and the number of variables in earlier studies have been low. Therefore, the generality of the conclusions obtained in these studies is quite limited.

Since epoxy coating changes the surface properties of reinforcing bars and mechanical interaction is thought to be the only effective bond mechanism in epoxy-coated bars, the deformations on the bars and their characteristics, such as pattern and height, are parameters that should be considered in any study of the bond strength of epoxy-coated reinforcing steel to concrete. Also, since the concrete surrounding a bar tends to split due to mechanical interaction, the effects of concrete properties, such as compressive

strength and slump, concrete cover, and confinement also should be included in such a study.

Although epoxy-coated reinforcing bars have been used for over fifteen years, only a limited amount of information has been available on the bond strength of epoxy-coated bars (Mathey and Clifton 1976, Johnston and Zia 1982, Treece and Jirsa 1987, 1989). The results from this study, combined with the current study at the University of Kansas, will provide more complete information on of the behavior of epoxy-coated bars. This information will also permit assessment of the new ACI Building Code provisions (ACI Committee 318, 1988, 1989) concerning the development length of epoxy-coated bars and will lead to suggested modifications.

1.3 Previous Work

1.3.1 Bond Strength

Before the introduction of deformed bars to concrete industry, concrete structures were reinforced with hooked smooth bars. Hooks are responsible for locking and developing the strength of smooth bars in concrete so that the bars can resist the pullout force. Deformations were introduced to alleviate the need for hooks. One of the earliest studies on this subject was done by Abrams (1913) in 1913 on the bond strength of both smooth and deformed bars. The test results showed higher bond stresses could be obtained with deformed bars than with smooth bars. The test results also indicated that the higher the bearing area of the deformations per

unit length of the bar (the area of a deformation projected on a plane perpendicular to the bar axis divided by the deformation spacing), the higher was the slip resistance of the bar.

In 1939, Menzel (1939) used pullout tests to investigate many factors affecting bond strength. The factors studied included the type of bar surface, embedment length, type and positions of the deformations, position of the bar, and the thickness of the concrete cover. The test results indicated the superiority of transverse deformations over longitudinal ribs, since the transverse deformations provide some bearing area for mechanical interaction in the direction of the pullout force.

Clark (1946, 1949) carried out beam and pullout tests on 17 different types of deformed bars. The variables included bar position, bar size, bonded length of the bar, and concrete strength. It was concluded that bottom-cast bars develop more bond strength than top-cast bars. The highest bond strengths were obtained by the bars that provided ratios of shearing area (area of the bar-concrete interface between deformations) to bearing area (measured as the projected area of the ribs) of the deformations of less than 10.

Studies by Lutz, Gergely, and Winter (1966), and Lutz (1970) on the bond strength of reinforcing steel to concrete indicate that chemical adhesion, friction, and mechanical interaction contribute to the bond between the bar and concrete. In these studies, bond forces, and the associated slip and cracking were examined for bars with various surface and deformation properties.

According to Lutz et al. (1966), slip of a deformed bar can occur in two ways: 1) the deformations or ribs, can push the concrete away from the bar by a wedging action, and 2) the deformations can crush the concrete in front of them. Lutz also observed that the movement of the bar, the slip, is about the same with all ribs with face angles greater than about 40°. This means that for rib face angles greater than about 40° to 45° (Fig. 1.1), the friction between the rib face and concrete is sufficient to prevent relative movement at the rib interface. In this case, slip occurs only once the concrete in front of the ribs is crushed by the high bearing pressure exerted by the ribs. For bars with face angles less than about 30°, slip is primarily due to the relative movement between the concrete and bar along the face of the rib.

A study done by Skorobogatov and Edwards (1979) on bars with face angles of 48.5° and 57.8° supports the earlier work (Lutz et al 1966). Skorobogatov and Edwards concluded that the rib face angle does not affect the maximum bond strength since the large rib face angle is flattened by a crushed concrete wedge in front of the ribs which effectively reduces the rib face angle to a smaller value (Fig. 1.1).

Tepfers (1979) suggested that the concrete around a bar acts as a thick ring with mechanical interaction of bond action acting as an internal pressure. The behavior of the ring at the point of failure may be perfectly elastic, perfectly plastic, or partly cracked elastic, depending on the thickness of the concrete cover.

He concluded that the partly cracked elastic analysis gives cracking loads on the safe side of the experimental results. Tepfers compared the predicted results from the partly cracked elastic analysis to the experimental results of lap splices in 193 beams, and the values agreed for lap splices and concrete covers normally used in practice (Tepfers 1982).

Donahey and Darwin (1985) and Brettmann, Darwin, and Donahey (1986) investigated the effects of concrete properties and construction procedures on bond strength. Concrete slump, consolidation practice, bar position, and concrete cover were the factors considered in these studies. They observed that for concrete with the same compressive strength, bond strength decreases with increased concrete slump. They also observed that high density internal vibration improves the bond strength compared to low density internal vibration. Superplasticizer was used to obtain high slump concrete with temperatures ranging form 53° to 84°. They (Brettmann et al. 1986) observed that the use of superplasticizer to increase the slump has relatively little effect on the bond strength, if the concrete is vibrated and the concrete temperature is high (about 84°). However, if the concrete is not vibrated or if the concrete temperature is low (about 53°), the addition of a superplasticizer to increase the slump will decrease the bond strength.

Pinc, Watkins, and Jirsa (1977) investigated the influence of lead embedment, the straight segment of the bar before the bend of

the hook, on the strength of hooked bar anchorages in beam-column joints. They tested sixteen specimens with different lead embedment lengths. Two different bar sizes, No. 9 and No. 11, of grade 60 steel were used. Concrete strengths ranged from 3600 to 5400 psi. Both 90° and 180° hooks were tested. They concluded that the major factors affecting anchorage capacity are the length of embedment and the degree of lateral confinement of the joint. Most of the slip in hooks occurs in the straight lead embedment and the curved portion of the hooked bar, with very little slip occurring at the tail extensions of the hooks. In general, longer lead embedment lengths result in higher stresses at failure. They found little difference in the strength of 90° and 180° hooks with the failure of the hooks being governed primarily by a loss of cover rather than by pullout.

1.3.2 Design Relationships

Experimental results from studies on bond strength have been used to derive relationships for use in determining bond capacity. For instance, the ultimate bond stress in the 1963 ACI Building Code (1963) was based on studies done by Ferguson and Thompson at the University of Texas (1962) and Mathey and Watstein at the National Bureau of Standards (1961). From these studies, the ultimate average bond force per unit length of the bar (in pounds per inch) was expressed as

$$u = 35\sqrt{f'_c} \qquad (1.1)$$

in which f'_c is the compressive strength of the concrete in psi.

Another design relationship was developed by Jimenez, White and Gergely (1978) using regression analysis applied to 314 development and splice tests from different studies (Chamberlin 1956, 1958; Chin et al. 1955; Ferguson and Breen 1965; Ferguson and Krishnaswamy 1971; Mathey and Watstein 1961; Tephers 1973). They suggested that the axial stress in the bar (in ksi) at which the bond failure occurs is

$$f_s = \frac{L}{d_b}\left[\frac{c\sqrt{f'_c}}{(27.8\ d_b + 0.45\ L)} + 0.573\ \frac{A_v}{bs}\ f_{yt}\right] \qquad (1.2)$$

in which f_s is the stress in the steel bar in ksi; c is the lesser concrete top or side cover; d_b is the bar diameter; L is the bonded length; b is the beam width; s is the spacing of the transverse reinforcement, all in in.; A_v is the area of transverse reinforcement in in^2; and f_{yt} is the yield stress of transverse reinforcement in ksi.

Orangun, Jirsa, and Breen (1977) used nonlinear regression analysis on about 500 test results to arrive at an empirical equation for calculating the strength of splices of deformed bars. From the analysis, the following equation was obtained as the best fit line through the data points.

$$f_s = \frac{41_s}{d_b}\left(1.22 + \frac{3.23c}{d_b} + \frac{53d_b}{1_s} + \frac{A_{tr}f_{yt}}{500sd_b}\right)\sqrt{f'_c} \qquad [1.3(a)]$$

Orangun, Jirsa, and Breen (1977) recommended Eq. 1.3(b) as the design equation.

$$f_s = \frac{41_s}{d_b}\left(1.2 + \frac{3c}{d_b} + \frac{50d_b}{l_s} + \frac{A_{tr}f_{yt}}{500sd_b}\right)\sqrt{f'_c} \qquad [1.3(b)]$$

in which l_s is the splice length, in in.; A_{tr} is the area of the transverse reinforcement in in^2; f_{yt} is the yield strength of transverse reinforcement in psi; and s is the spacing of the transverse reinforcement in in.

Zsutty (1985) developed an empirical equation for predicting the strength of lapped splices with or without transverse reinforcement. The resulting equation is

$$f_s = 560(f'_c)^{1/3}\left(\frac{l_d}{d_b}\right)^{1/2}\left(\frac{c}{d_b} + 2r\right)^{1/2} \qquad (1.4)$$

in which f_s is the bar stress of tension lapped splice in psi and r is the transverse steel ratio (area of transverse steel divided by the product of the spacing of transverse steel and the beam width).

1.3.3 Epoxy-Coated Reinforcement

Mathey et al. (1947, 1973, 1975, 1983) were the first to investigate the bond of epoxy-coated bars to concrete in a study at the National Bureau of Standards (NBS). The study included 5 uncoated, 23 epoxy-coated and 6 polyvinyl chloride coated bars. No.

6 bars with two deformation patterns, diamond and barrel (similar to Bethleham pattern), were used. They used pullout specimens consisting of No. 6 bars with a 12 inch bonded length embedded at the middle of a 10x10x12 inch concrete prism. Concrete strength was in the range of 5730 to 6620 psi.

Mathey and Clifton concluded that the polyvinyl chloride coated bars and epoxy-coated bars with thick coatings (about 25 mils) had unsatisfactory bond strength, but that the bars with epoxy coatings between 1 and 11 mils performed satisfactorily. While bond failure occurred for the bars with the polyvinyl chloride coatings and in the single epoxy-coated bar having a coating thickness of 25 mils, all of the uncoated bars and the coated bars with an epoxy thickness between 1 and 11 mils yielded during the tests. The average bond strength of the 19 pullout specimens with bars having an epoxy coating between 1 and 11 mils was just 6% less than that for specimens with uncoated bars. This result indicated a relatively small loss of bond.

The applicability of these test results to the bond of reinforcing steel in an actual structure is limited because the pullout specimens employed in the tests place the concrete in compression while the bar is in tension. This provides additional confinement for the concrete, making it effectively stronger and thus increasing the bond. In actual structures, if the reinforcement is in tension, the concrete around it is also in tension. The test results are further undermined by the fact that the bars

yielded in all of the specimens exhibiting adequate bond. Yielding of bars in bond tests is not desirable since the cross section of the bar changes upon yielding.

To obtain a more realistic measure and a better understanding of the effect of epoxy coating on bond strength than was obtained by the NBS study, Johnston and Zia (1982), at North Carolina State University (NCSU), investigated the bond of epoxy-coated bars by testing 6 slab specimens and 40 beam-end specimens with No. 6 and No. 11 bars. The advantage that modified cantilever beam-end specimens have over pullout specimens is that in beam-end specimens, both the steel bar and the concrete surrounding it are simultaneously placed in tension. The slab specimens were used to evaluate the effect of epoxy coating on crack width and crack spacing. The beam-end specimens were used to compare the slip and bond strength of coated and uncoated bars. The beam-end tests consisted of 26 static loaded specimens (12 uncoated, 12 epoxy-coated, and 2 blast-cleaned bars), and 14 fatigue specimens (6 uncoated, 6 epoxy-coated, and 2 blast-cleaned bars). One deformation pattern (diamond) was used and the concrete strength ranged from 5720 to 7040 psi. The coating thickness of epoxy-coated bars varied between 6.7 and 11.1 mils, with the majority of the test bars having a coating thickness between 8 and 9 mils. All of the specimens were confined using No. 3 bar stirrups with spacings of 6 and 3 inches for No. 6 and 11 bars, respectively, to satisfy the minimum requirements of ACI 318 (1983). Three different bonded

lengths were used for No. 6 (8, 13, and 18 inches) and No. 11 (16, 24, and 30 inches) bars. The bonded length of the bars started 10 inches away from the loaded end of the specimen to avoid local failure of the concrete at the loaded end of the specimen (a conical shape piece of concrete is pulled out by the bar). The concrete cover was approximately 3.0 d_b for the No. 6 bars and 1.5 d_b for the No. 11 bars.

Johnston and Zia observed that the slab specimens with epoxy-coated bars had slightly higher deflection and wider cracks and exhibited about 4% less strength than those with uncoated bars. However, the beam-end specimens with epoxy-coated bars developed about 85% of the bond strength of specimens with uncoated bars. Some of the tests were terminated after yielding of the bars and some were continued past the yield point until the bar was pulled out by splitting of the concrete. The high bond strengths which resulted in yielding of most of the specimens may have been caused by confinement provided by the stirrups, by embedding the bar so far from the loaded end, and by the long bonded length of the bars. Based on the few tests which resulted in bond failure (9 specimens, out of which only two failed prior to yielding), Johnston and Zia recommended that development length should be increased by 15 percent for epoxy-coated bars. This recommendation is also suscept because of the low number of specimens that failed without yielding the reinforcement.

Kobayashi and Takewaka (1984) studied the bond of epoxy-coated bars to concrete as a part of their experimental studies on epoxy-coated reinforcing steel for corrosion protection. They used two types of specimens. One type of specimens consisted of a reinforcing bar centrally located in a 15 cm concrete cube that was reinforced by spirals. The bonded length of the bars was 10 cm starting 3 cm from the loaded end of the specimen. The second type of specimen was a simply supported beam specimen, 15x20x180 cm, with an effective span of 160 cm. The beams had continuous bars as reinforcement and were loaded with two concentrated loads, 25 cm on either side of the midspan. Two types of epoxy coating with two different thicknesses, 100 and 200 μm (approximately 4 and 8 mils), were used on 10 and 16 mm nominal diameter bars, with perpendicular-lug (bamboo) deformations. They concluded that the bond strength tends to decrease as the coating thickness increases, and it is about 80% of the value obtained with uncoated bars. However, they surmized that the influence of epoxy coating on bond strength would decrease with increasing bar size. They stated that since the rib height is increased as the diameter of the bar becomes larger, the effect of epoxy coating on bond strength may be expected to become smaller. Beams with epoxy-coated bars showed about 10% more deflection and about 10% more crack widths than beams with uncoated bars. They also concluded that a minimum of about 200 μm (8 mils) of epoxy-coating thickness is necessary for "complete" corrosion protection of steel.

Treece and Jirsa (1987, 1989), at the University of Texas at Austin, investigated the bond strength of epoxy-coated bars by testing splices in beams. Twenty-one specimens were tested using No. 6 and No. 11 bars with a diamond-shaped deformation pattern. All of the beams were simply supported with concentrated loads at the third points of the span and had three splices at midspan. The tests consisted of 10 specimens with No. 6 bars (4 with uncoated and 6 with coated bars) and 11 specimens with No. 11 bars (5 with uncoated and 6 with coated bars). Four of the specimens had bottom-cast bars and seventeen had top-cast bars. Concrete strengths ranged from 3860 to 12600 psi, and epoxy-coating thicknesses ranged from 4.5 to 14 mils. The concrete cover was less than 1.5 d_b for 16 specimens and greater than 2.5 d_b for 3 specimens. It is important to note that four out of the ten No. 6 bar specimens had covers less than or equal to the maximum size of the aggregate, which can be expected to reduce bond strength (Donahey and Darwin 1985). None of the test specimens were replicated.

From the test results, Treece and Jirsa concluded that epoxy-coating significantly reduces the bond strength of reinforcing bars in tension. They concluded that this reduction in the splice strength is independent of bar size, concrete strength, and coating thickness for coatings between 5 and 14 mils. However, the trend of the data provided in their report seems to indicate that coating thickness has a direct effect on No. 6 bars (thicker coating results in lower strength), but not on No. 11 bars. The test results also

show that in terms of strength, there is a size factor, that is, No. 6 bars appear to be affected less than No. 11 bars by epoxy coating. The specimens with coated bars showed a significant increase in crack width and crack spacing in comparison to specimens with uncoated bars; No. 6 epoxy-coated bar specimens showed an average crack width of twice the crack width in uncoated bar specimens. However, both types of specimens had about the same stiffness.

The main conclusion of the study by Treece and Jirsa was that the amount of bond strength reduction due to epoxy coating depends on the mode of failure, pullout or splitting. In their analysis, Treece and Jirsa assumed that the tests done by Mathey and Clifton (NBS) and Johnston and Zia (NCSU) failed in a pullout mode because the steel was confined by large concrete cover and transverse steel, preventing a splitting failure [In fact, all of the NBS and NCSU specimens failed in a splitting mode]. Treece and Jirse concluded that if a pullout failure occurs, the bond strength of epoxy-coated bars is about 85% of the bond strength of uncoated bars, but if a splitting failure occurs, as did in their tests, the bond strength of epoxy-coated bars is about 65% of the bond strength of coated bars. Based on these conclusions, Treece and Jirsa recommended that the basic development length of the uncoated bars be multiplied by a factor of 1.5 for epoxy-coated bars with a cover of less than 3 d_b or a clear spacing between bars of less than 6 d_b. For all other cases, this factor should be 1.15. The 1.15 factor corresponds to the recommendations by Johnston and Zia. Cover and bar spacing are

important in these recommendations since the larger the cover and the spacing of the bars, the thicker is the concrete cylinder around a bar and presumably the more force it takes to split that concrete cylinder and fail the bars in bond. The tests by Johnston and Zia, however, was accompanied by a longitudinal crack above the test bar through the concrete cover, which indicates a splitting failure, as verified by Zia (1989). In the NCSU tests, although the cover for No. 6 bars was greater than 3.0 d_b and the bars were confined by stirrups, all specimens failed in the splitting mode. Thus, the conclusion that bars with 3.0 d_b or greater cover or with transverse reinforcement fail in the pullout mode is not based on observations. The relatively greater strength of the coated bars tested by Johnston and Zia may have been due to the effect of the confining reinforcement which is not included in the Treece-Jirsa recommendations.

Cleary and Ramirez (1989) tested 8 slab specimens (4 with uncoated and 4 with epoxy-coated bars). Each specimen was constructed with three No. 6 bars spliced at midspan. All of the bars had a spiral type deformation pattern and a mean coating thickness of 9.0 mils. The concrete strength ranged from 3990 to 8200 psi. Cleary and Ramirez stated that two sets of the specimens (2 coated and 2 uncoated bars) were valid since they failed in bond rather than by yielding. Based on their tests and the tests by Johnston and Zia (1982) and Treece and Jirsa (1987, 1989), Cleary and Ramirez concluded that there was no loss of stiffness due to use

of epoxy-coated bars and there was no significant difference in deflection between specimens with coated and uncoated bars. This contradicts the observations by Johnston and Zia that the specimens with epoxy-coated bars showed 6% to 20% more deflection than those with uncoated bars (6% at a load of 45 kips and 20% at a load of 54 kips on the slabs). They also concluded that specimens with epoxy-coated bars had fewer but wider cracks. One major conclusion made in this study was that the amount of the reduction in the bond strength caused by epoxy coating increases with increasing compressive strength of the concrete and increasing splice length. However, the validity of this conclusion is in question because of two reasons. First, the data cited from the NCSU study in this report represents the splitting load rather than the ultimate load of the specimens. The coated to uncoated bond strength ratios of the NCSU specimens are 0.78, 0.64, and 0.63 for splitting loads and 0.85, 0.95, and 1.0 for ultimate loads for specimens with No. 11 bars and bonded lengths of 16, 24, and 30 inches, respectively. As it can be seen, not only is there a considerable difference in the bond ratios of splitting and ultimate loads, but also the ultimate bond ratio increases as the bonded length of the bar increases. Second, the report by the University of Texas shows no relation between the concrete strength and the bond ratio and thus contradicts the conclusion by Cleary and Ramirez that the amount of reduction in the bond strength of coated bars is dependent on concrete strength. Cleary and Ramirez, however, state that Treece

and Jirsa used the Orangun, Jirsa and Breen proposed expression (Eq. 1.3) (Orangun et al. 1977) to normalize their results and that is why Treece and Jirsa did not notice any effect of concrete strength on bond reduction of epoxy-coated bars. They state that the proposed equation was derived based on tests on uncoated bars and can not be applied to epoxy-coated bars. Thus, it can be seen that there has been some misunderstanding of the results of the NCSU and the Univrsity of Texas studies.

Based primarily on recommendations by Treece and Jirsa, design provisions for the use of epoxy-coated steel were included in the proposed Building Code Requirements for Reinforced Concrete (ACI 318-89) (ACI Committee 318, 1988, 1989). These new provisions require that the basic development length of uncoated bars be multiplied by 1.5 for bottom cast epoxy-coated bars with cover of less than 3 d_b or clear spacing between the bars of less than 6 d_b and by 1.2 for all other conditions. These factors should be multiplied by 1.3 for top cast epoxy-coated bars but the product should not exceed 1.7.

It is clear that, in spite of the available research, there is only a limited amount of information available on the bond of epoxy-coated bars. Factors such as concrete cover, bar size, concrete strength and coating thickness, have been only partially investigated using a small number of specimens. Moreover, the majority of the early tests used only the diamond deformation pattern.

Due to ever increasing use of epoxy-coated bars in a variety of concrete structures, there is a clear need to develop a better understanding of the behavior and bond strength of epoxy-coated bars. Information is needed on the effects of parameters such as deformation pattern, bar position, concrete cover, concrete slump, concrete strength, confinement, and enough specimens should be tested to minimize the effects of scatter in the data. Some of these parameters such as deformation pattern, bar size, concrete cover, coating thickness, and bar position have been investigated by Choi, Darwin, and McCabe (1990) at the University of Kansas as the first part of this study. Other parameters such as concrete strength, confinement, and concrete slump, along with splices in full scale beam specimens and epoxy-coated hooks will be investigated in this part of the study.

1.4 Object and Scope

The object of this study is to extend the research by Choi, Darwin, and McCabe (1990). The goal is to obtain a better understanding of the effect of epoxy coating on the bond strength between reinforcing steel and concrete and to develop recommendations for changes in the development length provisions of the Building Code Requirements for Reinforced Concrete (ACI 318-89) (ACI Committee 318, 1989).

The bond strength between reinforcing steel and concrete is evaluated based on flexural bond strength; bond performance is

evaluated based on slip, load, deflection and crack width. The key parameters in this study include deformation pattern (three are evaluated), bar size (No. 5, 6, 8, and 11), and concrete cover (1, 2, and 3 bar diameters). In addition, the effects of bar position, confinement of the test bars with stirrups, concrete strength (6000 and 12000 psi), and concrete slump (3 and 9 inches) are investigated. A preliminary evaluation of the behavior of epoxy-coated hooks, using No. 5 and No. 8 hooks with 90° and 180° bends, is also included.

The testing program uses two different test specimens. Bond strength is measured using modified cantilever beam-end specimens which are similar to those used by Brettmann, Darwin, and Donahey (1986), Choi, Darwin, and McCabe (1990), and Johnston and Zia (1982). Full scale beam splices, similar to those used by Treece and Jirsa (1987, 1989) are also employed. Test measurements on the modified cantilever beam specimens include load, loaded end slip, and free end slip of the bar. Test measurements on beam splices include load, deflection and transverse crack width. The beam-end specimens are used to investigate the effects of bar position, slump, concrete strength, confinement of the bars with stirrups, and concrete cover. These specimens are also used to investigate the performance of epoxy-coated hooks. Full scale beam specimens are used to investigate epoxy-coated splices and to complement the results of Choi, Darwin, and McCabe. The results of the splice

specimens are also compared to those obtained by Treece and Jirsa (1987, 1989).

To better understand the effect of epoxy coating on bond strength, an analytical study is conducted to evaluate the effects of the major variables on bond strength. The analytical study consists of two parts. The first part is a statical model of two rigid bodies in contact to simulate a reinforcing bar in contact with concrete. This model is used to study the values of coefficient of friction between uncoated or coated bars and concrete and the rib face angle of reinforcing bars. The second part is a finite element study using a model developed by Choi, Darwin, and McCabe (1990). The finite element model is used to study the effect of concrete cover, lead length, and bar size on the bond strength of reinforcing steel to concrete. The results from the analytical study are compared to the experimental results and the results from the finite element study by Choi, Darwin, and McCabe (1990).

The test results of this study along with the results of the analytical model and the results from previous studies are used to develop rational design recommendations for the use of both uncoated and epoxy-coated reinforcing steel in practice.

CHAPTER 2: EXPERIMENTAL PROGRAM

2.1 General

The study of effect of epoxy coating on the bond strength between reinforcing steel and concrete involved a wide range of variables, including bar surface, deformation pattern, bar size, concrete cover, casting position, concrete slump, consolidation, confinement of reinforcing steel with stirrups, and concrete strength. In addition, a preliminary investigation of the behavior of epoxy-coated hooks was carried out.

In this chapter, the variables of the test program and the configurations of beam-end and beam splice specimens are described. The material properties, specimen fabrication, test procedures, the appearance of specimens after failure, the mode of failure for each type of specimen, and the specimen strengths are also presented in this chapter.

Two types of test specimens were used to evaluate the effect of epoxy coating on bond strength. 630 beam-end specimens and 15 beam-splice specimens were tested. 394 of the beam-end specimens were tested by Choi et al. (1990). Beam-end specimens were used for the majority of the tests because they provide a realistic model, as will be discussed in Section 3.2, for measuring bond between reinforcing steel and concrete and are small enough to allow for the economical replication of tests to minimize the scatter in the data. Full scale beam-splice specimens also were used to verify the

results from the beam-end specimens and to compare with the results obtained by Treece and Jirsa (1987, 1989), the basis for the design provisions for epoxy-coated bars in ACI 318-89.

2.2 Variables of Test Program

Specimens were cast in groups to study the effects of specific variables. In each group two and, in most groups, three replications were cast for every variable. Two groups of specimens, groups 22 and 30, provided six and four replications, respectively. The variables are described in more detail as follows:

Bar surface: The effect of the bar surface on bond performance is the main variable in this study. Two different bar surfaces were considered: mill scale (uncoated) and fusion-bonded epoxy-coated.

Deformation pattern: Reinforcing bars with three commercial deformation patterns (S, C, and N pattern, described in Section 2.4) were tested.

Bar size: Four bar sizes, No. 5, No. 6, No. 8, and No. 11 were tested.

Concrete cover: One, two, and three bar diameter covers were used in the beam-end specimens, while about 1.5 bar diameter cover was used for the splices.

Casting position: Both top and bottom-cast bars were investigated to ascertain the top-bar effect for coated bars.

Concrete slump and consolidation: Low slump (3-4 in.) and high slump (8 in.) concretes were investigated. For the high slump concrete specimens, half of the specimens were vibrated and the other half were placed without vibration to investigate the effect of consolidation on bond strength.

Confinement: Uncoated and coated No. 3 C-pattern stirrups were used for confining uncoated and coated test bars, respectively, in three groups of beam-end specimens.

Concrete strength: One group of specimens was cast with 13,000 psi concrete for comparison to other groups which had 5000 and 6000 psi concrete.

Hooks: Uncoated and coated C-pattern No. 5 and 8 hooks with 90° and 180° bends were investigated as a preliminary study on the effects of epoxy coating on hooks.

2.3 Test Specimens

Standard beam-end specimen were used for 28 test groups while deep beam-end specimens were used for 2 groups. Fig. 2.1(a) shows the dimensions of both standard and deep beam-end specimens for No. 8 bars. The standard beam-end specimens were 9 in. wide, 24 in. long and about 18 in. high. The amount of concrete above bottom-cast bars and below top-cast bars was 15 in. for all the specimens. The height of the specimens varied slightly to accommodate different bar sizes and concrete cover. Thus, the height of the specimen was 15 in. plus the diameter of the bar and the amount of the cover.

The width of the specimen was increased to 10 in. for No. 11 bars to avoid splice failure between the test and auxiliary bars. Auxiliary bars [Fig. 2.1(b)] were provided to prevent the specimens from failing in flexure. Deep specimens had the same width and length as standard specimens but were 39 in. high to provide 36 in. of concrete below top cast bars or above bottom cast bars for No. 8 bars [Fig. 2.1(a)]. The specimen dimensions were based on a previous study (Brettmann, Donahey, and Darwin, 1984, 1986).

Test bars extended 22 in. out from the face of the specimen. Two auxiliary bars, parallel to the test bar, were provided to prevent the specimen from failing in flexure [Fig. 2.1(b)]. The size of the auxiliary bars varied depending on the test bar size and the expected ultimate bond force. No. 4 auxiliary bars for No. 5 and No. 6 test bars and No. 5 auxiliary bars for No. 8 test bars with top and side covers of $1\frac{3}{4}$ and $1\frac{1}{4}$ in., respectively, were used. For specimens with No. 8 confined bars and No. 11 bars, No. 6 auxiliary bars with 90° hooks at both ends were used to avoid bond failure of the auxiliary bars. A single transverse bar was used to support the test bar. Two lifting bars were provided at the mid height of the specimen to help move the specimens, as shown in Fig. 2.1(a).

Bonded lengths (length of test bars in contact with the concrete) of $3\frac{1}{2}$, $4\frac{1}{2}$, 8, and 9 in. were used for No. 5, 6, 8, and 11 bars, respectively. The bonded lengths of straight bars were selected to ensure that the bars did not yield before bond failure (Brettmann, Donahey, and Darwin, 1984, 1986).

As shown in Fig. 2.1(b), polyvinyl chloride (PVC) pipes were used as bond breakers to control the bonded length of the bar and to avoid localized cone-type failure of the concrete at the loaded end of the specimen. The length of the PVC pipes at the loaded-end of the bar (lead lengths) were $2\frac{3}{8}$, $2\frac{3}{4}$, $3\frac{3}{4}$, and $1\frac{1}{2}$ in. for No. 5, 6, 8, and 11 bars, respectively. The inside diameter of PVC pipe matched the diameter of the bar. The PVC pipes were carefully sealed against mortar seepage using silicone caulking between the PVC pipe and the test bar. A steel pipe was extended to the end of the specimen to allow access for measuring unloaded end slip through an LVDT touching the end of the test bar. 3.0 and $4\frac{1}{2}$ in. PVC pipes were used at the loaded end only for No. 5 and No. 8 hooks, respectively. Unloaded end slips were not measured for the hooks. Forms were constructed using $\frac{3}{4}$ in. B-B plyform and 2x4 studs. Test bars were cleaned with acetone before placing concrete.

No. 3 stirrups, at $5\frac{1}{2}$ in. spacing starting $2\frac{1}{2}$ in. from the loaded face of the specimen, were used to investigate the effect of confinement on the bond of epoxy-coated bars to concrete.

The beam-splice specimens consisted of simply supported beams, similar to those tested by Treece and Jirsa (1987, 1989) (Fig. 2.2). Splice lengths ranged from 12 in. for No. 5 and No. 6 bars to 16 in. for No. 8 bars and 24 in. for No. 11 bars. Two or three adjacent splices were located within the constant moment region. Three splices were used for No. 5 bars. An additional test beam with two splices of uncoated No. 5 bars was used to evaluate the usefulness

of double splice specimens for later tests. The strength of the double and triple splice specimens were nearly proportional to the number of splices. Based on this limited evidence, double splice beams were used for No. 6, No. 8, and No. 11 bars. A cover of 1 in. was used for No. 5 and No. 6 bars, $1\frac{1}{2}$ in. for No. 8, and 2 in. for No. 11 bars. The clear spacing between splices was equal to 4 in., and the side cover was equal to 2 in. for all beams. Additional dimensions and information for beam-splice specimens are included in Fig. 2.2. The spliced bars were all bottom-cast, in contrast to the Treece/Jirsa specimens, which primarily used top-cast bars and thus potentially introduced a top-bar effect into the tests.

2.4 Materials

Reinforcing Steel: ASTM A 615 (1987), Grade 60, No. 3, 5, 6, 8, and 11 bars were used. Bars with three deformation patterns, designated S, C, and N, were tested (Fig. 2.3). Deformation pattern S consisted of ribs perpendicular to the axis of the bar. Deformation pattern C consisted of diagonal ribs inclined at an angle of 60° with respect to the axis of the bar. Deformation pattern N consisted of diagonal ribs inclined at an angle of 70° with respect to the axis of the bar. C-pattern No. 3 bars were used as stirrups. Bars of each size and deformation pattern were from the same heat of steel. Yield strengths and deformation properties are shown in Table 2.1. The method of measuring the bearing area and face angle of deformations is presented in Appendix A.

Epoxy coating was commercially applied 3M Scotch Kote 213 powder in accordance with ASTM A 775 (1988) and ranged in thickness from 3 to 17 mils as measured by a pull-off type thickness gauge (Mikro-test III Thickness Gage). Readings were taken at 6 points around the circumference of the bar between each set of deformations within the bonded length. Average readings within the bonded lengths are reported. A wide range in coating thickness, outside of the ASTM A 775 limits (5 to 12 mils), was used to help evaluate the effects of coating thickness on bond strength.

Concrete: Non-air entrained concrete was supplied by a local ready mix plant. Type I portland cement, $\frac{3}{4}$ in. nominal maximum size crushed limestone and Kansas River sand, were used. Water-cement ratios from 0.55 to 0.25 were used to obtain concrete with nominal strengths of 5,000, 6,000, and 13,000 psi. 5,000 and 6,000 psi concrete were used for 29 groups of the specimens as ordinary strength concrete. Master Builders Rheobuild 1000 superplasticizer was used to obtain high slump concrete. Master Builders MBSF powdered silica fume and superplasticizer along with a low w/c ratio were used to obtain high strength concrete. Mixture proportions are shown in Table 2.2. Concrete properties for individual specimen groups are given in Table 2.3.

2.5 Placement Procedures

Concrete was placed in two lifts in the standard beam-end specimens and beam-splice specimens. The first lift was placed in

all specimens in a group before any specimen received a second lift. Each lift in the beam-end specimens was vibrated at 6 evenly spaced points. Each lift in the beam-splice specimens was vibrated on each side of the beams at staggered one foot intervals. Concrete was placed in three lifts for deep specimens.

Standard 6 x 12 in. test cylinders were cast in steel molds and cured in the same manner as the test specimens. Concrete cylinders in group 27 were cut in half due to honeycombing, caused by low slump and high concrete temperature, and the strengths of the 6 in. cylinders were corrected to that of standard cylinders, ASTM C39 (1986). Forms were stripped after the concrete had reached a strength in excess of 3,000 psi.

2.6 Test Procedures

Beam-end specimens: Tests were made at nominal concrete strengths of 5,000, 6,000, and 13,000 psi. The beam-end specimens were tested using an apparatus developed by Donahey and Darwin (1983, 1985) and modified by Brettmann et al. (1984, 1986) [Fig. 2.1(c)]. Specimens from a group were tested within a 12 hour period (except for groups 18-20, for which tests were completed over a 48 hour period) at ages ranging from 3 to 11 days. Specimens with 13,000 psi concrete were tested at 132 days. Specimens with No. 5 and No. 6 bars were loaded at approximately 3.0 kips per minute. Specimens with No. 8 and No. 11 bars were tested at about 6.0 kips per minute (Brettmann et al. 1984, 1986, Choi et al. 1990).

The specimen and the testing apparatus were tied down to the structural floor by two wide flange sections and four tie-down rods. Load was applied to the test bar by two 60-ton hollow-core hydraulic jacks, powered by an Amsler hydraulic testing machine through two 1-in. diameter load rods instrumented as load cells using two longitudinal and two transverse strain gages. As shown in Fig. 2.1(c), the hydraulic jacks exerted a pulling force on the yokes while the test bar was loaded in tension by the yokes through a grip assembly. The tensile force on the bar was counteracted by a compressive force that the frame of the testing assembly imposed on the concrete specimen through a bearing pad. The center of this pad was located 7 in. below the center of No. 5 and 6 test bars and 5 in. below the center of No. 8 and 11 test bars. Loaded-end slip was measured using two spring-loaded LVDTs attached to an aluminum block mounted on the test bar. Unloaded-end slip was measured using a single spring-loaded LVDT mounted at the end of the steel conduit [Fig. 2.1(b)].

Beam-splices: Splice specimens were inverted and tested as illustrated in Fig. 2.2(b). The beams were supported at two points by a pin and roller support. Loads were applied by four hydraulic jacks through four $1\frac{1}{2}$ in. load roads instrumented as load cells. The deflections at each end and middle of the beam were measured by one LVDT at each location. Loads were applied at the ends of the cantilever regions, resulting in a constant moment region between the two supports.

Specimens were loaded monotonically. Crack locations and widths were recorded at 2 kip intervals during the progress of the tests, at loads of $\frac{1}{3}$ and $\frac{2}{3}$ of ultimate load. Crack measurements ceased at a load of about $\frac{2}{3}$ of the expected failure load to insure that the balance of the test would not be interrupted so as to provide a consistent measure of member strength by minimizing creep. Two specimens, C-pattern No. 6 coated and S-pattern No. 8 uncoated, however, failed immediately after the crack measurements were terminated. Splice tests lasted 20 to 25 minutes. The beams were loaded so that the steel stress would increase by 400 psi per second.

General: The load rods and the LVDTs were connected to a Hewlett-Packard data acquisition system to record the load and the bar slip or beam deflection throughout the tests. Data was acquired every second throughout the test.

2.7 Test Results

Beam-end specimens: The load, loaded and unloaded end slips were recorded throughout each test. The ultimate bond force, epoxy coating thickness, concrete cover, and concrete strength for each test, are listed in Table 2.4. The specimens in groups 1 through 19 were tested by Choi et al. (1990) during the first part of this study.

Typical load versus unloaded end slip curves for different bar sizes are presented in Figs. 2.4 through 2.7. The unloaded end slip

is used since it depends on the bond over the entire bonded length of the bar and generally is a smoother function of the load than the loaded end slip. Loaded end slip is highly dependent upon local effects since the loaded end is closer to the loaded face of the member than the unloaded end. Figs. 2.4 through 2.7 clearly show the effects of epoxy coating on bond strength. At small loads, loads corresponding to bar stresses of about 5 ksi for all the bar sizes, the slope of the curves for all the bars is very close. However, as the load increases, the slope quickly drops for coated bars. Overall, uncoated bars obtained a higher bond strength than coated bars. At any given load, coated bars slip more than uncoated bars, and in most cases, coated bars fail at greater values of slip than uncoated bars.

Beam-splices: The load and the deflections at the middle and the ends of the beams were recorded throughout each test. The ultimate moment, along with bar size, deformation pattern, splice length, coating thickness, crack comparison, and C/U ratio for each test, are listed in Table 2.5. The ultimate stress in the splices, listed in Table 2.5, is calculated by allowable stress method using the ultimate moment. Ultimate strength method was used in calculating the stress in the splices by Choi et al. (1990).

The total deflection at the middle of the beam is used to compare the stiffness of the beams with coated and uncoated bars. The total deflection is the average of deflection at both ends plus the deflection at the middle of the beam. The load-deflection

curves for all of the beam-splice specimens are presented in Figs. 2.8 through 2.14. These figures indicate little difference in the stiffness and the amount of deflection for members with coated and uncoated bars. However, beams with coated bars consistently failed at a lower load than beams with uncoated bars of the same bar size.

2.8 Specimen Behavior

Beam-end specimens: A splitting type bond failure was observed in all tests. On the front surface of the beam-end specimens, one crack ran up through the cover from the test bar to the top surface. The top surface crack continued parallel to and above the test bar, over the bonded section of the bar, and fanned out over the rear PVC bond breaker, as shown in Fig. 2.15. On the front surface, one or two cracks ran down below the test bar. Although two different crack patterns were observed, the concrete around the bar always split into three parts: wedges on either side of the bar, and the remaining specimen below the bar.

In the specimens with only one crack below the bar at the front face of the specimen, the vertical crack ran down from the bottom of the test bar to the top of the bearing pad, where it intersected a horizontal crack across the specimen's loaded face. This horizontal crack extended to the sides of the specimen where it continued at an angle towards the top of the specimen up to the rear PVC bond breaker.

A similar cracking pattern was evident for specimens with two cracks at the bottom of the test bar. The two cracks formed at the loaded face of the specimen, approximately 120, from the vertical crack at the top of the bar, as shown in Fig. 2.15.

In specimens with stirrups, there were small transverse cracks above every stirrup perpendicular to the splitting crack, as shown in Fig. 2.16. The transverse crack closest to the loaded end was the widest. These transverse cracks ran only as deep as the center of the test bar.

All of the unconfined specimens failed in a brittle manner, meaning that, they failed immediately after the formation of the longitudinal splitting crack above the bar. However, the specimens with the 90, hooks and most of the specimens with confining stirrups, failed in a ductile manner. In these specimens, the top crack appeared as a hairline crack at a load of about 90% of ultimate and became a wide splitting crack at failure.

Beam-splices: At failure, beam-splice specimens exhibited extensive longitudinal and transverse cracking in the region of the splices, Fig. 2.17. Concrete above the splices was easily removed, exposing a nearly horizontal crack running the full width of the beam in the plane of the splices. The transverse cracks on the tension face of the beam ran all the way to the compression zone. Except for the beam with No. 5 epoxy-coated bars [third beam in group SP1 (Table 2.5)], which failed gradually in a ductile manner, all the specimens failed suddenly.

Crack widths were measured within a region spanning 12 in. on either side of the splice. The comparison of the crack widths and number of cracks in the beams were based on the cracks through the concrete cover over the splice length in each beam. The number of cracks and maximum crack widths are summarized in Table 2.5. For three out of seven pairs of the beams, the widest crack in the beams with coated reinforcement was about 2 mils wider than the widest crack in the beams with uncoated bars. For two pairs, the maximum crack widths were identical, and for two pairs the widest crack in the beams with uncoated bars was about 2 mils wider than the widest crack in the beams with coated bars. For four pairs, the beams with the uncoated bars had 2 more cracks than the beams with coated bars, while in one case the two beams had an identical number of cracks and in two cases the beams with the coated bars had 2 more cracks than the beams with uncoated bars.

2.9 Appearance of Test Bars After Failure

In both types of specimens, the test bars were examined following the tests by removing the concrete cover. Uncoated bars showed evidence of good adhesion to the concrete. Particles of concrete were left on the shafts of the bars and on the sides of the deformations. Wedges of compacted concrete powder were lodged in front of the ribs, adhering to the ribs on the pull side only [Fig. 2.18(a)]. Coated bars showed virtually no adhesion to the concrete. No concrete particles were left on the deformations or the shafts of

the coated bars [Fig. 2.18(b)]. The concrete in contact with the epoxy-coated bars had a smooth, glossy surface (Fig. 2.19). In a few cases, there were signs of the epoxy coating being crushed against the concrete, but, in general, the epoxy was undamaged. These observations agree with the ones made by Johnston and Zia (1982) and Treece and Jirsa (1987, 1989) in earlier tests of coated bars.

High strength specimens provided an exception to these observations. In these specimens, the epoxy on top of the deformations was damaged throughout the bonded length of the test bars, with the deformation closest to the unloaded end being damaged the most. This may have been caused by the high strength of the concrete since, unlike the bars in the low strength concrete specimens, there were clear signs of abrasion on the top of the deformations of uncoated bars.

Based on the ultimate loads and load-slip curves from the tests, the effects of different test variables on the bond of epoxy-coated will be discussed in the next chapter. For example, as seen in Fig. 2.4, coated bars slip more than uncoated bars at any given load, and, eventually, coated bars fail at greater slip values and lower loads than uncoated bars. This greater slip indicates a reduction in both the adhesion and friction components of the bond mechanism for the epoxy-coated bars.

CHAPTER 3: EVALUATION OF EXPERIMENTAL RESULTS

3.1 General

In this chapter, the results of the tests described in Chapter 2 are analyzed to determine the effects of the test variables on the bond strength of epoxy-coated reinforcing bars to concrete. The method of correcting the values of bond strength obtained from the test specimens to account for the variation in concrete cover and coating thickness from nominal values and a discussion on the validity of beam-end specimens for bond tests are also presented. The test results are compared to the bond strengths predicted by the ACI Building Code (1989), and the Orangun, Jirsa, Breen (1977) equation, and design recommendations are made.

In this part of the study, the results from 236 beam-end specimens and 15 beam splice specimens are combined with the test results of Choi, Darwin, and McCabe (1990). The effect of epoxy-coating on bond strength is evaluated by calculating the ratio of the bond strength of coated bars to the bond strength of uncoated bars, C/U.

An analysis of test groups 2 through 22 for the effects of deformation pattern, bar size, and coating thickness on the bond of epoxy-coated bars to concrete, along with some analysis of beam-splices, was included in a report by Choi, Hadje-Ghaffari, Darwin, and McCabe (1990). Choi et al. observed that unlike No. 6 and larger bars, No. 5 bars are sensitive to coating thickness. They

also observed that epoxy coating reduces the bond strength of coated bars but that the amount of this reduction depends on the type of the deformation pattern and the reduction in bond strength caused by epoxy coating increases with bar size for No. 5 and larger bars.

3.2 Data Correction

To compare the results on a similar basis, the ultimate bond strengths of individual specimens are corrected for variations in actual concrete cover and coating thickness. The individual test results are then normalized with respect to a nominal concrete strength of 6,000 psi, using the assumption that, within the concrete strength range used, bond strength is proportional to the square root of the compressive strength. Thus, corrected bond strengths are multiplied by $(6000/f'_c)^{1/2}$ to obtain the final modified values. Both the original and the corrected values of bond strengths are summarized in Table 2.4.

The bond strengths of individual specimens are corrected for variations in actual concrete cover from nominal values of 1, 2, and 3 d_b. This correction is obtained by plotting the bond strength versus the actual cover for all beam-end specimens with bars of one size. In Fig. 3.1, the ultimate bond force of No. 8 bars is plotted versus the concrete cover. It is observed that the best fit lines for different groups of specimens are nearly parallel for bars of the same size, regardless of deformation pattern or bar surface condition.

Using the technique of dummy variables (Draper and Smith 1981), parallel best fit lines are constructed based on the assumption that changes in concrete cover cause the same incremental change in bond strength for bars of the same size, regardless of deformation pattern, test group, or bar surface condition. The technique of dummy variables is applied only to those groups of specimens in which at least two different covers were used. For No. 6 bars which were tested with only 2 d_b covers, the cover correction slope is obtained by interpolating the correction slopes of No. 5 and No. 8 bars. A typical plot using dummy variables, in this case for No. 11 bars, is shown in Fig. 3.2, where the ultimate bond force of No. 11 bars is plotted versus the cover.

The best fit slopes for the ultimate bond force versus cover are 3936, 5964, 13,614, and 7948 lb per inch of cover for standard specimens with No. 5, No. 6, No. 8, and No. 11 bars, respectively. Individual specimen strengths are corrected to covers of 1, 2, and 3 d_b by shifting the measured bond strength parallel to the best fit lines. The impact of this correction is small, and an analysis using No. 5 and No. 6 bar data that was uncorrected for cover altered no conclusions obtained with the cover-corrected data (Choi, Darwin, and McCabe 1990). This is fortunate because a cover correction is not possible for test groups 1 through 6 since the actual cover for the specimens in those groups was not measured.

A similar correction should be made for variations in the epoxy coating thickness (9 mils is taken as the standard). However,

work by Choi, Darwin, and McCabe (1990) and Choi et al. (1990), showed that of the bars tested, only No. 5 bars are sensitive to coating thickness, while No. 6 and larger bars are not sensitive to coating thickness.

The effect of coating thickness on bond strength is shown in Figs. 3.3 - 3.5 for No. 5, No. 6, and No. 8 bars, respectively. In these figures, C/U is plotted as a function of the epoxy-coating thickness for each deformation pattern. The data presented in these figures are from groups 2 - 6, 8 - 15, and 17 - 22. Each data point represents the ratio of the bond strength of an individual epoxy-coated bar to the average bond strength of uncoated bars with the same deformation pattern and bar size in the same group of specimens. The data points are based on the specimens that had 2 d_b nominal cover, since 2 d_b is the standard cover in ACI 318-89. Using the technique of dummy variables (Draper and Smith 1981), the best fit lines for each deformation pattern are obtained using the assumption that there may be differences in the effect of the coating due to deformation pattern, but that the effect of coating thickness is the same for all deformation patterns. The best fit lines in Figs. 3.4 and 3.5, for No. 6 and No. 8 bars, have very slight negative slopes, which result in decreases in the C/U ratio of only 0.002 and 0.012, respectively, as the coating thickness increases from 5 to 12 mils. Thus, No. 6 and larger bars appear to be largely insensitive to coating thickness, an observation which agrees with the observations made by Johnston and Zia (1982) and

Treece and Jirsa (1987, 1989). However, Fig. 3.3 shows that No. 5 bars are indeed sensitive to coating thickness, with C/U dropping by 0.09 as the coating thickness increases from 5 to 12 mils. This observation does not conflict with the earlier studies (Johnston and Zia 1982; Treece and Jirsa 1987, 1989) since those studies included only No. 6 and larger bars, and it agrees with the observations made by Kobayashi and Takewaka (1984) for 16 and 10 mm diameter bars, which are very close to No. 5 and No. 3 bars, respectively. The "coating correction slope" for No. 5 bars is 164 lb/mil of coating thickness for standard specimens.

3.3 Specimen Evaluation

Due to the large number of variables in the overall study, it was considered desirable to use a single bonded length in the beam-end specimens for each bar size. At the outset, however, it was not clear what effect the specimen geometry and either the bonded length (the contact length between the concrete and the steel) or the lead length (the distance from the loaded face of the specimen to the start of the bonded length) had on the reduction in bond strength caused by the epoxy coating. To answer these questions, Choi, Darwin, and McCabe (1990) and Choi et al. (1990) conducted tests with different bonded lengths and lead lengths (groups 7, 8, 11, 12, and 16). They established that the reduction in bond strength caused by epoxy-coated bars is independent of bonded length and lead length.

Some beam-splices were tested to verify the results of the beam-end specimens with a more realistic model and to compare the results with the splice tests of Treece and Jirsa (1987, 1989), which serve as the basis for the development length provisions for epoxy-coated bars in ACI 318-89. Splice tests may provide a more realistic model of bond behavior in an actual structure and, therefore, it is important to compare the C/U ratio from the beam-end specimens to the C/U ratio from the splice specimens. As will be demonstrated later in this chapter, the results of beam splices generally lie within the range of the results obtained from beam-end specimens. It appears evident that the beam-end specimens are valid specimens to study the bond behavior of coated bars.

3.4 Deformation Pattern and Bar Size

Figs. 3.3 - 3.5 provide convincing evidence that the effect of epoxy coating varies considerably with deformation pattern. For the three bar sizes illustrated, the S pattern is affected the most. For example, based on the values of the best fit lines at 9 mils coating thickness, the C/U ratios for S, C, and N-pattern bars are 0.83, 0.91, and 0.91 for No. 5, 0.81, 0.91, and 0.93 for No. 6, and 0.74, 0.90, and 0.84 for No. 8 bars, respectively. Also, it can be observed that the smaller bars, on the average, are affected less than the larger bars. For example, for a 9 mil coating, the C/U ratios for No. 5, No. 6, and No. 8 S-pattern bars are 0.83, 0.81, and 0.74, respectively. However, some smaller bars exhibit lower

values of C/U than do larger bars of different deformation patterns. For example, the C/U ratio for S-pattern No. 5 bars, 0.83, is lower than the C/U ratio for C-pattern No. 8 bars, 0.90 (Table 3.1).

Table 3.1 provides the normalized ultimate bond force and the C/U ratios for the beam-end specimens for different bar sizes and deformation patterns. Figs. 3.6 - 3.8 show the relative bond strength, U/U and C/U, as a function of related rib area of the bars, R_r, bearing area ratio of the bars, R_b, and bar size, respectively. U/U and C/U are the ratios of the bond strength of uncoated and coated bars, respectively, to that of uncoated bars. Related rib area, R_r, and bearing area ratio, R_b, are defined in Table 2.1. Both R_r and R_b are measures of the bearing area of the deformations relative to the bar size.

Table 3.1 and Figs. 3.6 - 3.8 show that the C/U ratio changes with-deformation pattern and bar size. The U/U and C/U values presented in this table and these figures are obtained from groups 2 - 6, 8 - 15, and 17 - 22 for bottom-cast bars with 2 d_b cover. The bond strengths for the No. 5 coated bars are normalized to 9 mils coating thickness. Table 3.1 shows that the mean values of C/U, based on group, for the S, C, and N deformation patterns are, respectively, 0.83, 0.91 and 0.91 for No. 5 bars; 0.81, 0.91 and 0.93 for No. 6 bars; 0.74, 0.90 and 0.84 for No. 8 bars; and 0.92, 0.83 and 0.74 for No. 11 bars. These results were also presented by Choi et al. (1990).

It should be noted that the C/U ratios based on the results from individual groups do not give a fair comparison of the deformation patterns because these values of C/U are evaluated individually by deformation pattern. Thus, a coated bar may have a low C/U based on uncoated bars of the same deformation pattern, but, in fact, have a higher bond strength than another coated bar that has a high value of C/U because its uncoated bars have a low bond strength. Thus, it is fairer to base the values of C/U on the mean strength of all uncoated bars of the same size. Therefore, the values of U in the denominator of "C/U all" and "U/U all" in Table 3.1 and Figs. 3.6 - 3.8 are based on the mean strengths of all uncoated bars of the same size for all deformation patterns; each deformation pattern weighted equally. For a 9 mil coating and 2 d_b cover, the mean values of C/U calculated on this basis for the S, C, and N patterns are 0.85, 0.93, and 0.87 for No. 5 bars; 0.80, 0.89, and 0.97 for No. 6 bars; 0.73, 0.83, and 0.90 for No. 8 bars; and 0.90, 0.80, and 0.78 for No. 11 bars, respectively. The mean values of U/U for the S, C and N patterns are, respectively, 1.03, 1.02 and 0.95 for No. 5 bars; 0.99, 0.97 and 1.04 for No. 6 bars; 0.98, 0.96 and 1.06 for No. 8 bars; and 0.98, 0.97 and 1.05 for No. 11 bars. It is worth noting that the range in the mean values of C/U significantly exceeds the range in the mean values of U/U, except for No. 5 bars where the range of relative strengths is identical. The wider spread in the bond strengths of coated bars emphasizes the strong dependence of bond strength reduction on deformation pattern.

The effect of epoxy coating on bond strength as a function of bar size is illustrated in Fig. 3.8, which compares the relative bond strengths of coated and uncoated bars, U/U and C/U, by deformation pattern. As with Figs. 3.6 and 3.7, the relative strengths are expressed in terms of the mean strength of all uncoated bars of the same size. For the coated bars, the overall trend is a reduction in C/U with increasing bar size. For all bars of a given size, the mean values of C/U are 0.88, 0.89, 0.83, and 0.83 for No. 5, No. 6, No. 8, and No. 11 bars, respectively. Based on deformation pattern, the lowest mean values of C/U for each bar size are 0.85, 0.80 and 0.73 for S-pattern No. 5, No. 6 and No. 8 bars, respectively, and 0.78 for N-pattern No. 11 bars.

3.5 Concrete Slump, Degree of Consolidation, Concrete Cover, and Bar Position

The effects of concrete slump, degree of consolidation (vibration) of plastic concrete, and bar position are shown in Fig. 3.9. Fig. 3.9 provides a summary of normalized ultimate bond strengths obtained from standard beam-end specimens with slumps below 6 in. and for deep beam-end specimens with slumps both below and above 6 in. Results for both bottom and top-cast bars are shown. Some of the specimens made with high slump concrete (obtained with a superplasticizer) were vibrated and some were not vibrated. For the tests illustrated, top-cast bars exhibit a lower bond strength than the corresponding bottom-cast bars, and bars cast in high slump

concrete exhibit a reduced bond strength if the concrete is not vibrated. The top-cast bars in high slump concrete, whether vibrated or not, have a lower bond strength than the top-cast bars in the lower slump concrete. The bond strength of bottom-cast bars appears to be little affected by concrete slump.

3.5.1 Concrete Slump and Degree of Consolidation

The effects of slump and degree of consolidation were investigated using deep beam-end specimens in groups 23 and 24. It is important to note that the high slump concrete had about 14 percent higher compressive strength than its base low slump concrete. For the current discussion, the ultimate bond strength of the bars in both low and high slump concrete is normalized to 6000 psi concrete, as described in Section 3.2.

The normalized ultimate bond strengths of uncoated and coated bars are plotted versus the concrete slump in Figs. 3.10 and 3.11 for vibrated bottom and top-cast N-pattern No. 8 bars, respectively. Fig. 3.12 shows the top-bar effect for N-pattern No. 8 bars in deep specimens for high and low slump concrete. In Fig. 3.12, the ratios of the best fit lines for the bond strengths of bottom and top-cast bars in Figs. 3.10 and 3.11 are plotted versus concrete slump. The normalized ultimate bond strengths, the C/U ratios, and the ratios of bottom to top-cast bar strength for the groups containing specimens with both top and bottom-cast bars (groups 9 - 11, 15, 17, 18, 23, and 24) are summarized in Table 3.2. As shown in Table 3.2,

bottom-cast bars are, with one exception (coated bars in group 23), stronger in bond than top-cast bars in the same slump concrete, regardless of the amount of slump.

In Table 3.3, the B/T and C/U ratios from Table 3.2 are averaged based on bar size and concrete slump. No. 8 bars with 8 in. slump and No. 6 bars with $5\frac{3}{4}$ in. slump are considered to be the bars cast in high slump concrete. The average B/T ratios for uncoated and coated bars and the average C/U ratios for bottom and top-cast bars and the average bottom-cast uncoated to top-cast coated (U/C) ratios for all bar sizes and concrete slumps are statistically analyzed, using hypothesis testing, to see if these ratios or the difference between these ratios is statistically significant or not significant [i.e., in case of No. 6 bars, does the average B/T ratio for uncoated bars, 1.340, represent a significant difference in bond strengths (due to the top-bar effect) or is the value of B/T due to the scatter in the data, and is the difference between B/T ratios for uncoated bars, 1.340, and coated bars, 1.114, significant (due to coating effect) or is it not significant (due to scatter in the data)?]. The hypothesis testing procedure is presented in Appendix B.

The results of hypothesis testing are also presented in Table 3.3. The hypothesis testing indicates that, with at least a 97.5 percent level of confidence, the differences obtained in the bond tests, as represented by B/T and C/U, are significant (not due to scatter) with the exception of the B/T ratio of No. 8 coated bars in

vibrated 8 in. slump concrete, 1.051, and the C/U ratios of No. 6 top-cast bars, 0.998, and No. 8 top-cast bars in vibrated 8 in. slump concrete, 0.938.

Table 3.3 shows that for low slump concrete, B/T is virtually the same for uncoated and coated bars for both standard and deep specimens. The average B/T for No. 5 and No. 8 bars in low slump concrete is 1.13 and 1.14 for uncoated and coated bars, respectively. Also for low slump concrete, C/U is virtually the same, at 0.89, for bottom and top-cast bars in both standard and deep specimens. For high slump concrete, however, B/T is significantly different for uncoated and coated bars. The average B/T for No. 6 and No. 8 bars in high slump concrete is 1.28 for uncoated bars compared to 1.08 for coated bars. It is interesting to note that, as slump increases, B/T for coated bars decreases from 1.14 to 1.08 while B/T for uncoated bars increases from 1.13 to 1.28. Also, for high slump concrete, C/U is significantly different for bottom and top-cast bars. The average C/U for bars in high slump concrete is 0.82 for bottom-cast bars, but 0.97 for top-cast bars. It is also important to note that C/U decreases, from 0.89 to 0.82, for bottom-cast bars but increases, from 0.89 to 0.97, for top-cast bars as slump increases.

In general, the top-bar effect is expected to increase as slump increases due to increased settlement and bleeding. Table 3.3 and Fig. 3.12 bear out this expectation for uncoated bars. The coated bars, however, exhibit a reduced top-bar effect as slump

increases. This reduction in the top-bar effect can be attributed to the fact that the effect of epoxy coating and the effect of weakened concrete at the interface caused by bleeding and settlement have similar effects on the bond strength of coated bars. As seen in Table 3.2, for No. 8 bars in group 24, uncoated bottom-cast bars show a small increase in bond strength with an increase in slump, unlike uncoated top-cast bars and coated bottom and top-cast bars which show a decrease in bond strength with an increase in slump. Coated bottom-cast bars show the greatest decrease in bond strength, 14 percent, with increasing slump, which also explains the trend observed in Fig. 3.12. Brettman, Darwin, and Donahey (1986) observed a decrease in the bond strength of both bottom and top-cast bars with increasing slump. The number of the bars tested in high slump concrete in the current study, however, is very limited.

The observation that the bars in low slump concrete are stronger in bond than the bars in high slump concrete is based on the results from beam end-specimens whose bond forces for both low and high slump concrete are normalized to a concrete strength of 6,000 psi. It is worthwhile to look at bond strengths that are not normalized with respect to concrete strength. Table 3.4 summarizes the bond forces of bottom and top-cast bars in both low and high slump concrete in group 24 without normalizing the bond forces to the same concrete strength. As seen in Table 3.4, the adverse effect of high slump on bond strength is somewhat compensated by the higher strength of the superplasticized concrete (5880 psi) in

comparison to its low slump base concrete (5150 psi). With the exception of the coated bottom-cast bars, where the bond strength of the bars in high slump vibrated concrete is about 7 percent less than the bond strength in low slump concrete, bars cast in high slump vibrated concrete have a higher bond strength than bars cast in low slump concrete due to the higher strength of the high slump concrete. For example, the ultimate bond forces for uncoated bottom-cast bars are 39297 and 43417 lbs. and for uncoated top-cast bars are 34646 and 35658 lbs. for the bars in 2-1/2 and 8 in. slump vibrated concrete, respectively. These observations agree with the observations made by Brettmann, et al. (1986). As pointed out by Brettman et al. (1986), however, the extra bond strength obtained here is not available in practice, because the compressive strength of the high slump concrete would be adjusted down to that required in the field.

Vibration has a positive effect on bond strength, regardless of casting position for both coated and uncoated bars, as seen in Tables 3.2 and 3.4 and Fig. 3.9 for specimens in group 24. For example, the normalized ultimate bond force values (Table 3.2) for uncoated bottom-cast bars are 43,848 and 42,656 lbs. and for uncoated top-cast bars are 36,008 and 35,080 lbs. for vibrated and unvibrated specimens, respectively. The differences are even greater for coated bars. The relative strengths agree with the observations made by Brettmann, Darwin and Donahey (1986). For concrete with an 8 in. slump, a lack of vibration causes a reduction

as high as 15 percent (coated top-cast bars) (Table 3.2). As seen in Table 3.2, the ratio of bottom-cast bar strength to top-cast bar strength, B/T, remains at 1.22 for uncoated bars but rises from 1.05 to 1.12 for coated bars when the concrete is not vibrated. Also, C/U drops from 0.81 to 0.77 for bottom-cast bars and from 0.94 to 0.84 for top-cast bars when the concrete is not vibrated. Thus, vibration improves C/U for both bottom and top-cast bars, and, as for the vibrated high slump concrete, C/U for bars in non-vibrated high slump concrete is higher for the top-cast bars, 0.84, than for bottom-cast bars, 0.77.

3.5.2 Concrete Cover and Bar Position

a) Concrete Cover: Cover affects the confinement around bars. Its effect on the normalized ultimate bond forces for No. 5, No. 8, and No. 11 bars in groups 1 - 2, 8, 13, and 18 - 20 is shown in Figs. 3.13, 3.14, and 3.15, respectively. These figures show that, regardless of bar position, bar size, or deformation pattern, there is a nearly linear relationship between bond force and concrete cover. This means that as the cover increases, the ultimate bond force increases. The best fit lines for coated and uncoated bars are nearly parallel, but the absolute magnitude of the increase in bond strength with cover is slightly greater for uncoated bars than for coated bars.

The nearly parallel best fit lines for coated and uncoated bars in Figs. 3.13 - 3.15 result in higher values of C/U for bars

with greater covers. This is also shown in Table 3.5 for C/U ratios based both on the best fit lines for specimens in groups 1, 4, 6, 8, 11-13, 17-20, 23, and 24 (groups with specimens with more than one cover) and on the average of bond strengths for a group of specimens. For example, for bottom-cast N-pattern No. 8 bars, the C/U ratio (based on the best fit lines) increases from 0.85 to 0.91 as the concrete cover increases from 1 to 3 d_b. For top-cast N-pattern No. 8 bars, C/U ratio increases from 0.83 to 0.91.

Table 3.6 summarizes the U/C ratios (inverse of C/U ratios in Table 3.5) for bottom-cast bars with different covers in beam-end specimens as a function of bar size along with the ACI modification factors for epoxy-coated bars (1.5 for bars with a cover less than 3 d_b or spacing between the bars less than 6 d_b and 1.2 for bars with a cover of at least 3 d_b or spacing between the bars of at least 6 d_b). Table 3.6 shows that the largest U/C value for bars with a cover of 3 d_b or greater, 1.22 for No. 11 bars, is in agreement with the ACI modification factor of 1.20 for bars with 3 d_b or more cover. For No. 8 and smaller bars, however, this comparison indicates that the factor could be safely dropped to 1.10. Also, based on the largest U/C value for bars with cover of less than 3 d_b, 1.38 for No. 11 N-pattern bars with 2 d_b cover in group 20 (Table 3.6), the ACI modification factor of 1.5 could be reduced to 1.35 or 1.40 for No. 11 bars and even further, down to 1.20, for No. 8 and smaller bars. The current tests provide no direct information on factors for No. 14 and No. 18 bars.

As will be discussed shortly, no modification factor may be necessary for bars with covers of 3 d_b or more because the design codes (AASHTO 1989, ACI 1989) do not take into account the higher bond strength of uncoated bars with a cover greater than 2 d_b. The argument could be made that, since uncoated bars with 2 d_b cover represent the standard, coated bars with equal bond strength because of added cover should not require a greater development length, even if the bond is weaker than uncoated bars with the same added cover.

In Figs. 3.16 - 3.18, the bond forces represented by the best fit lines in Figs. 3.13 - 3.15 are normalized with respect to the values at 2 d_b cover and plotted versus concrete cover in bar diameters. As shown in these figures, the bond strength of coated bars is slightly more sensitive to concrete cover than is the bond strength of uncoated bars, regardless of bar size, deformation pattern, or the casting position. For example, in Fig. 3.16, the bond force (normalized to the bond force at 2 d_b cover) for N-pattern No. 5 bars changes from 0.74 to 1.26 for uncoated bars, but from 0.73 to 1.27 for coated bars, as the cover increases from 1 to 3 d_b. Similar trends are observed for No. 8 and No. 11 bars.

The Orangun, Jirsa, and Breen (1977) best fit equation [Eq. 1.3(a)] is used in conjunction with the results shown in Figs. 3.13 - 3.15 to investigate the possibility of increasing the cover, rather than development length, to account for the reduced bond strength of coated bars. The goal is to calculate an additional cover, ΔC, for coated bars that will allow coated bars to be developed in the same

length as uncoated bars when the bars are just yielding ($f_s = f_y$). Eq. 1.3(a), without including the factor of transverse steel, can be written in terms of pullout force as:

$$\text{Pullout force} = \text{POF} = A_b f_s = [3.23\ \pi \ell_s\ C + 1.22\ \pi \ell_s\ d_b + 212\ A_b]\sqrt{f'_c} \qquad (3.1)$$

If Eq. 3.1 is generalized by substituting K_{1U}, K_{2U}, K_{3U}, and C_U for the factors 3.23, 1.22, 212, and C, respectively, for uncoated bars, and if it is assumed that there is a similar set of factors, K_{1C}, K_{2C}, K_{3C}, and C_C for coated bars, Eq. 3.1 can be rewritten as

$$\text{POF}_{\text{uncoated}} = [K_{1U}\ \pi \ell_s\ C_U + K_{2U}\ \pi \ell_s\ d_b + K_{3U}\ A_b]\sqrt{f'_c} \qquad (3.2)$$

$$\text{POF}_{\text{coated}} = [K_{1C}\ \pi \ell_s\ C_C + K_{2C}\ \pi \ell_s\ d_b + K_{3C}\ A_b]\sqrt{f'_c} \qquad (3.3)$$

Using f'_c = 6000 psi, and values of 5.875, 11.75, and 10.5 in. (lead length plus bonded length in test specimens) for ℓ_s in No. 5, No. 8, and No. 11 bars, respectively, Eqs. 3.2 and 3.3 can be set equal to the equations of the best fit lines for uncoated and coated bottom-cast bars of No. 5, No. 8, and No. 11 bars in Figs. 3.13 - 3.15. These equations are:

for No. 5 bars:

$$\text{POF}_{\text{uncoated}} = (5545\ C_U + 6515)\sqrt{6000}$$

$$POF_{coated} = (5441\ C_U + 5763)\sqrt{6000}$$

for No. 8 bars:

$$POF_{uncoated} = (13692\ C_U + 17239)\sqrt{6000} \qquad (3.4)$$

$$POF_{coated} = (13540\ C_U + 12618)\sqrt{6000}$$

and for No. 11 bars:

$$POF_{uncoated} = (8331\ C_U + 22014)\sqrt{6000}$$

$$POF_{coated} = (6949\ C_U + 15662)\sqrt{6000}$$

The coefficients of C_U and C_C in Eqs. 3.2 and 3.3, K_{1U} and K_{1C}, respectively, are simply the slopes of the lines in Eqs. 3.4. The values of K_{2U}, K_{3U}, K_{2C}, and K_{3C}, however, cannot be solved for directly. The terms containing K_2 and K_3 in Eqs. 3.2 and 3.3 are the intercepts of the lines in Figs. 3.13 - 3.15. Thus, to simplify the solution of Eqs. 3.2 and 3.3 to obtain the K_2 and K_3 values, two approaches are taken. The first approach is to set $K_{2U} = K_{2C} = 1.22$ (the value in Eq. 3.1) and solve for K_{3U} and K_{3C}. Then by setting $(PoF)_{uncoated} = (PoF)_{coated}$ and $C_C = C_U + \Delta C$ and solving for ΔC:

$$\Delta C = \frac{\frac{A_b}{\pi \ell_s}(K_{3U} - K_{3C}) - (K_{1C} - K_{1U})\ C_U}{K_{1C}} \qquad (3.5)$$

in which $\ell_s = [(A_b f_y/\sqrt{f'_c}) - K_{3U}\ A_b]/[\pi(1.22\ d_b + K_{IU} C_U)]$, the value of ℓ_s for which $(PoF)_{uncoated} = A_b f_y$, $f_y = 60{,}000$ psi, and $f'_c = 6000$ psi.

The second approach is to set $K_{3U} = K_{3C} = 212$ (the value in Eq. 3.1) and solve for K_{2U} and K_{2C}. This gives:

$$\Delta C = \frac{d_b (K_{2U} - K_{2C}) - (K_{IC} - K_{IU}) C_U}{K_{1C}} \qquad (3.6)$$

The K_{1U}, K_{1C}, K_{2U}, K_{2C}, K_{3U}, K_{3C}, and ΔC values for C_U values of 1, 2, and 3 d_b for No. 5, No. 8, and No. 11 bars are presented in Table 3.7 for both approaches.

As seen in Table 3.7, the ΔC values from the first approach are, with the exception of No. 8 bars with 3 d_b cover, less than the ΔC values from the second approach. Since a cover of 2 d_b is the standard in ACI 318-89 (1989), the largest ΔC values (second approach) at 2 d_b cover will be used for each bar size. Therefore, assuming that Eq. 1.3(a) (Orangun, Jirsa, and Breen) is applicable for the test results of this study, the ΔC values for 2 d_b cover in Table 3.7 suggest that, instead of increasing the development length of coated bars, increasing the cover of coated No. 5, No. 8, and No. 11 bars by 0.2, 0.4, and 1.5 in., respectively, will compensate for the reduction in bond strength of those bars caused by coating. For example, from the best fit lines for N-pattern No. 11 bars shown in Fig. 3.15, the uncoated bars with 2.82 in. (2.0 d_b) cover provide an ultimate bond force of 45,508 lbs., while the coated bars with 4.32 in. (2.0 d_b + 1.5 in.) cover provide an ultimate bond force of 45,680 lbs. A coated bar with 4.32 in. cover has a slightly greater bond strength than an uncoated bar with 2.82 in. cover. Thus, an

increase in concrete cover appears to be a viable alternative to modifying the development length of coated bars. A particularly clear comparison is made in Table 3.5 using the term C'/U, the ratio of the bond strength of coated bars to the bond strength of uncoated bars with 1 d_b less cover. With the exception of C'/U based on average test values for No. 11 N-pattern coated bars with 2 d_b cover, the C'/U ratios in Table 3.5 are greater than 1.0, meaning that, in all other cases, the development length of coated bars need not be increased if an additional bar diameter of cover is provided. This is true in all cases for coated bars with 3 d_b cover, since in every case, these bars exhibited greater bond strength than the uncoated bars with 2 d_b cover.

The comparisons can be used to develop design provisions to take advantage of the extra bond strength obtained with added cover. The values of ΔC calculated above translate into 0.32, 0.4, and 1.07 d_b for No. 5, No. 8, and No. 11 bars, respectively. For the sake of simplicity, it seems prudent to recommend a cover increase of 0.5 d_b for coated No. 8 bars and smaller and 1.0 d_b for No. 9, No. 10, and No. 11 bars to compensate for the reduction in bond strength caused by the epoxy coating. In any case, the experimental data shows specifically that no increase in development length is needed for coated bars with 3 d_b cover. The beneficial effect of covers greater than 2 d_b is not considered for uncoated bars in the ACI 318-89. The beneficial effect of increased spacing, however, is considered for both uncoated and coated bars in ACI 318-89. The

current observations about the effects of increased cover suggest that for bars with cover less than 3 d_b or clear spacing between bars less than 6 d_b, the factor for epoxy-coated bars can be lowered to 1.35 (recommended value of the current study, Section 3.11) and for all other conditions, the factor for epoxy-coated bars can be lowered to 1.0 as long as ACI 318 Section 12.2.3.4 (0.8 factor for bars with clear spacing greater than 5 d_b) is not applied to coated bars. The later exclusion is necessary since the 0.8 factor for added spacing is already accounted for by the 1.0 epoxy factor. An alternative would be to retain the current 0.8 factor for wide spacing and the 1.2 factor for epoxy-coated bars with at least 3 d_b cover and 6 d_b clear spacing (0.8 x 1.2 = 0.96). Tests on No. 14 and No. 18 bars are needed to extend the recommendations to the larger size bars.

b) Bar Position: The effect of bar position on bond strength is shown in Fig. 3.9 for No. 5, No. 6 and No. 8 bars in standard and deep specimens and for high and low slump concrete. As Fig. 3.9 shows, bottom-cast bars have a higher bond strength than top-cast bars, regardless of bar size, bar surface condition, or concrete slump.

Table 3.3 shows that, for low slump concrete, the average B/T ratio is virtually the same for uncoated and coated bars (1.132 versus 1.137) and the C/U ratio is virtually the same for bottom and top-cast bars (0.893 versus 0.889). For high slump concrete, however, the average value of B/T is significantly greater for

uncoated bars, at 1.28, than for coated bars, at 1.08. Also, for high slump concrete, the average value of C/U is significantly lower for bottom-cast bars, at 0.82, than for top-cast bars, at 0.97.

Table 3.3 and Fig. 3.12 show that the values of B/T are similar for uncoated and coated bars for slumps between 2 and 4 in. For increasing slump, however, B/T increases for uncoated bars, as expected, but decreases for coated bars. As shown in Table 3.3, the highest average value of B/T for uncoated bars, 1.28, occurs for bars cast in high slump concrete, while the highest average value of B/T for coated bars, 1.14, occurs for bars cast in low slump concrete. These trends in the B/T ratio are important because the value of top-bar modification factor, used in the ACI Building Code (1989), 1.3, is based on a worst case assumption, i.e., bars cast in high slump concrete. The B/T ratio of 1.28 for uncoated bars agrees well with ACI top-bar factor of 1.30. Since coated bars do not appear to be affected as greatly as uncoated bars at higher slumps, it can be argued that a top-bar factor below 1.3, such as 1.15, should be used for epoxy-coated bars. A value of 1.15 compares favorably with the defacto top-bar factor for epoxy-coated bars in ACI 318-89, 1.13, which is obtained by dividing the upper limit on the combined effects of bar position and epoxy coating, 1.7, by the epoxy bar factor, 1.5.

The values of U/C ratio of uncoated bottom-cast bar strength to coated top-cast bar strength, in Tables 3.2 and 3.3 show the combined effects of coating and bar position on the bond strength of

"top coated bars". Average U/C ratios of 1.29, 1.32 and 1.45 (Table 3.3) for low slump, high slump vibrated, and high slump non-vibrated concrete, respectively, demonstrate that the effects of coating and bar position on the bond strength are not additive and that the ACI upper limit on the combined factors, 1.70, can be dropped to 1.50 for top coated bars. The 1.50 factor agrees closely with 1.55, which is the product of 1.35, the higher of two recommended epoxy factors (Section 3.11), and 1.15, the top-bar factor for coated bars developed in this section.

Overall, it appears that either a top-bar factor of 1.15 for coated bars, applied to the development length of bottom-cast coated bars, or an upper limit of 1.50 on the combined factors, applied to the development length of bottom-cast uncoated bars, will provide satisfactory development lengths.

c) Concrete Cover and Bar Position: The combined effects of concrete cover and bar position (top and bottom-cast bars) is illustrated in Fig. 3.14, where the normalized ultimate bond forces for S and N-pattern No. 8 bars with covers of 1, 2, and 3 d_b are plotted versus the concrete cover. As this figure shows, the bottom-cast bars exhibit a higher bond strength than the corresponding top-cast bars. The Commissie Voor Uitvoering Van Research Ingesteld door de Betonrereniging in the Netherlands, CUR, (1963) and Ferguson and Thompson (1965) observed a reduction in B/T with increased cover. Similar observations are made in this study, but not to the same degree as in the two earlier studies. Table 3.8 presents the B/T

ratios for both uncoated and coated N-pattern No. 8 bars in group 18. The bars had covers of 1, 2, and 3 d_b. B/T drops from 1.15 to 1.14 for uncoated bars and from 1.24 to 1.18 for coated bars, based on the average of individual tests, as cover increases from 1 d_b to 3 d_b.

Fig. 3.14 shows that, for N-pattern No. 8 bars, at a concrete cover of about 2 d_b, the normalized bond strength of the uncoated top-cast bars and coated bottom-cast bars are approximately the same. For 1 d_b cover, the uncoated top-cast bars are about 4 percent stronger than the coated bottom-cast bars; for 3 d_b cover, the uncoated top-cast bars are about 4 percent weaker than the coated bottom-cast bars. This would suggest that, based on the current ACI top-bar factor of 1.3, the increase in the development length of epoxy-coated bottom bars need not be more than about 35 percent (from the product of 1.3, the current top-bar factor, and 1.04, the strength ratio of uncoated top-cast bars with 1 d_b cover to coated bottom-cast bars with 1 d_b cover = 1.30 x 1.04 = 1.35). Fig. 3.14, of course, only presents the data for a single bar size. A 35 percent increase in development length of coated bars, however, matches the recommended maximum epoxy factor of this study of 35 percent (Section 3.11).

3.6 Confinement With Transverse Reinforcement

A limited number of specimens, in groups 27, 28, and 30, contained transverse reinforcement in the form of No. 3 C-pattern stir-

rups spaced at 5.5 in. Uncoated and coated No. 3 stirrups were used for confining uncoated and coated bars, respectively. The normalized ultimate bond forces obtained from these confined specimens are compared to those of unconfined specimens in Table 3.9. The comparison shows that confined bars have higher bond strengths than unconfined bars, regardless of bar size, deformation pattern, or surface properties. This can be seen in Table 3.9 where the CU/UU (confined uncoated to unconfined uncoated bars) and CC/UC (confined coated to unconfined coated bars) values are all greater than 1.0. Based on average bond forces for uncoated and coated bars in each group, the C/U ratios for confined bars (CC/CU) range from 0.81, for S-pattern No. 8 bars, to 0.98, for S-pattern No. 11 bars. The average value of C/U for all of the confined bars, 0.88, is similar and slightly higher than the average obtained for all unconfined bars, 0.85 (Table 3.1). The average ratios of bond strengths of confined coated bars to unconfined uncoated bars, CC/UU, [UU = the current standard for development length design (ACI 318-89)] are 0.94, 0.92, and 1.14 for No. 5, No. 8, and No. 11 bars, respectively. The average CC/UU for all bar sizes, 0.999, is high, primarily due to high value of CC/UU for S-pattern No. 11 bars, 1.21. Based on the lowest average value of CC/UU for all bar sizes, 0.92 for No. 8 bars, using a development length modification factor of 1.10 appears to be appropriate for confined coated bars if the added bond strength due to confinement is not accounted for otherwise. The observations on the combined effects of confinement and coating are summarized in Fig.

3.19, where the average normalized bond forces of unconfined and confined bars are presented graphically. It can be seen from Fig. 3.19 that, when considering all of the bar sizes and deformation patterns tested, coated confined bars have virtually the same bond strength as the uncoated unconfined bars.

The average values of C/U for unconfined bars (Table 3.1) and for confined bars (Table 3.9) are 0.88 and 0.87 for No. 5 bars, 0.82 and 0.85 for No. 8 Bars, and 0.83 and 0.93 for No. 11 bars, respectively. Thus, for beam-end specimens, C/U for confined bars increases with bar size, unlike C/U for unconfined bars which decreases with bar size. Also, based on the average values for individual bar sizes, CC/UC and CU/UU increase with bar size. In the current study, it appears that transverse reinforcement enhances the bond strength of coated bars more than it does the bond strength of uncoated bars. The degree of enhancement appears to increase with bar size, which helps to compensate for the greater reduction obtained for unconfined coated bars as bar size increases. This observation can be seen graphically in Fig. 3.20, where the percent increase in bond force of confined bars relative to unconfined bars is compared to bar diameter for both coated and uncoated bars. The trend observed in Fig. 3.20 may be related to deformation height, which increases with bar diameter. Deformation height is important in specimens with confined bars since the specimen can sustain significant additional load after cracks appear, in contrast to specimens with unconfined bars that fail just as the splitting crack

appears. When a specimen cracks, the stirrups limit crack width. As a result, for bars with higher deformations, bond failure occurs at a wider crack width and a higher load than it does for a bar with small deformations.

Fig. 3.21 compares the bond strength ratios for coated confined bars to uncoated unconfined bars (CC/UU) versus K_{tr} for No. 5, No. 8, and No. 11 bars. K_{tr}, which is part of Eq. 1.3, is

$$K_{tr} = \frac{A_{tr} f_{yt}}{500 S d_b} \tag{3.7}$$

in which $A_{tr} = 0.11$ in^2 is the area of one leg of the stirrup (since only one leg of the stirrups cross the crack); $f_{yt} = 68,900$ psi is the yield strength of the stirrups; $S = 5.5$ in. is the spacing of the stirrups; and d_b is the diameter of the confined test bar. The values of K_{tr} for the current study are listed in Table 3.9. Orangun, Jirsa, and Breen (1977) observed that for the values of K_{tr} greater than 3.0, the additional transverse reinforcement is not particularly effective. As Fig. 3.21 indicates, the average CC/UU values for No. 5 and No. 8 bars are about the same, at 0.92, while the average CC/UU value for No. 11 bars are at 1.14. As a general trend, however, CC/UU ratio increases with bar size, not K_{tr}, mainly because of the effect of higher deformations on larger bars, as discussed earlier.

3.7 Concrete Strength

A limited number of tests, group 29, were carried out to evaluate the effect of concrete strength on the reduction in bond strength caused by epoxy coating. Bond strengths are compared for S-pattern No. 6 bars using beam-end specimens prepared with 13,000 psi and 6,000 psi concrete. Table 3.10 summarizes the ultimate normalized and non-normalized bond forces of uncoated and coated No. 6 bars cast in 6,000 and 13,000 psi concrete. Fig. 3.22 compares the non-normalized ultimate bond forces to concrete strength.

Table 3.10 and Fig. 3.22 show that, in this limited comparison, as the concrete strength increases, the bond strength increases for top-cast bars and remains almost unchanged for bottom-cast bars. As concrete strength increases from 6,000 to 13,000 psi, bond strength increases 21 percent and 14 percent for top-cast uncoated and coated bars, respectively. However, the bond strength of bottom-cast bars remains virtually unchanged (decreases 1 percent for uncoated bars and increases 2 percent for coated bars). If the bond strengths are normalized (Section 3.2) to 6,000 psi, the projected bond strengths of bars cast in 13,000 psi concrete are lower by 51 and 44 percent for bottom-cast uncoated and coated bars and lower by 24 and 31 percent for top-cast uncoated and coated bars in comparison to bars cast in 6,000 psi concrete. The increase in bond strength due to the increase in concrete strength is clearly not proportional to $\sqrt{f'_c}$; there is only a maximum of a 21 percent increase in bond strength, in case of uncoated top-cast bars, for a

120 percent increase in concrete strength, which should have provided a 48 percent increase in bond strength based on $\sqrt{f'_c}$. This behavior may be due to the following factors:

1) Bond failure of a reinforcing bar results from the fracture of concrete around that bar. Therefore, the fracture energy of concrete, not the tensile or compressive strength of the concrete, is the governing factor in a splitting bond failure. Gettu, Bazant and Karr (1990) found that, for an increase in compressive strength of 160 percent, the fracture energy increases by only 12 percent.
2) A smaller gradation of 3/4 in. coarse aggregate was used in 13,000 psi concrete than in 6,000 psi concrete. In addition, there were 184 lbs less coarse aggregate and 250 lbs more cement in every cubic yard of concrete in the 13,000 psi concrete. This reduces aggregate interlock across the splitting crack, further reducing the fracture energy in the high strength concrete.
3) According to Gettu et. al (1990), more microcracks occur in normal strength concrete than in high strength concrete. Microcracks help reduce the stress concentration at the tip of major cracks. Also, there is a weak interface between the paste and aggregate in normal strength concrete, which results in tortuous crack paths following the aggregate boundaries, instead of rupturing the aggregates as occurs in high strength concrete. Such charac-

teristics increase the brittleness of concrete as concrete strength increases.

4) The 6,000 psi concrete specimens were cured for 3 days and air dried for about 4 days prior to testing. The 13,000 psi concrete specimens were cured for 77 days and air dried for 55 days. The extra air drying for the high strength concrete may have caused more drying shrinkage cracks than were obtained in the 6,000 psi specimens.

As seen in Table 3.10, the high-strength specimens have C/U values of 0.84 and 0.94 for bottom and top-cast specimens, respectively, compared to 0.82 and 1.00 for corresponding lower strength specimens. These differences in C/U are not considered to be significant.

Since only 12 specimens were tested with 13,000 psi concrete, these results are not conclusive, and more research is clearly needed on the bond strength of reinforcing steel to high strength concrete.

3.8 Hooks

A preliminary evaluation of epoxy-coated hooks is made based on tests of 26 C-pattern No. 5 and No. 8 hooks with 180° and 90° bends. These hooks were tested in beam-end specimens in groups 25 and 26. In each group, three uncoated, three coated, and three "repaired" coated hooks were tested. All the coated hooks had coating damage due to the fabrication of the hooks. Liquid epoxy

was used to repair the coating. Table 3.11 summarizes the normalized ultimate bond forces and C/U ratios for the hooks and corresponding values for straight bars (0° bend from groups 2, 5, 6, 10, and 21). The repaired epoxy-coated hooks were expected to be weaker than unrepaired hooks, since the liquid epoxy does not stick to steel bar as well as the powdered epoxy (the visual examination of the hooks after testing showed that all the repaired patches were pealed off the bar). The test results, however, show that there is no significant difference between the bond strengths of unrepaired and repaired coated hooks (Table 3.11).

The values of C/U for the hooks are 0.94 and 0.95 for No. 5 and No. 8 bars, respectively, compared to 0.91 and 0.90 for corresponding straight bars (Table 3.1). The increase in C/U obtained by hooks may be explained by the fact that there are two parts to the failure mechanism of hooks: 1) movement of the bar relative to the concrete and 2) mechanical interlock between the hook and the concrete due to the geometry of hook. Epoxy coating appears to affect the first mechanism much more than the second mechanism. Therefore hooks should have a higher C/U ratio than straight bars, since only the first mechanism exists for straight bars.

For bars with 90° hooks, movement of the straight portion of the bars was accompanied by crushing of the concrete on the inside of the bend. For bars with 180° hooks, movement of both straight and bent portions of the bars was observed. These observations agree with those made by Minor and Jirsa (1975). Minor and Jirsa

(1975) also observed that, for a given bond stress, bars with a 180° hook slip more than bars with a 90° hook.

In the current study, the 90° hooks were stronger than 180° hooks. For example, as seen in Table 3.11, the values of bond force for 90° and 180° No. 5 hooks, respectively, are 20278 lbs. and 17165 lbs. for uncoated bars and 18505 lbs. and 17994 lbs. for coated bars. This may be due to the fact that 90° hooks provide better anchorage and exhibit a different failure mode in the beam-end specimens than do the 180° hooks. A splitting type bond failure, similar to the straight bar specimens, was observed in all the hook specimens. Specimens with 90° hooks failed in a ductile manner; the hook was not completely pulled out of the specimen. In comparison, specimens with 180° hooks failed in a brittle manner, and in some specimens, the hook was pulled clear out of the specimen.

Since only a limited number of hooks were tested, these observations are not conclusive. More research is needed to investigate the effects of additional parameters, such as bar size, coating thickness, deformation pattern, and confining reinforcement, on epoxy-coated hooks.

3.9 Splices

Splice test specimens are larger and more costly than beam-end specimens. Therefore, it is desirable to run fewer splice tests than beam-end tests in a study. The question arises: Why run splice tests at all? The reasons are two-fold. Splice tests may

provide a more realistic model of what happens in an actual structure, and the development length provisions for epoxy-coated bars in ACI 318-89 are based on the splice tests run by Treece and Jirsa (1987, 1989). With this in mind, it is important to know 1) if beam-end specimens give the same results as splice specimens, and 2) if the test results in the current study, both beam-end and splice tests, match the earlier splice tests (Treese and Jirsa 1987, 1989).

Before these questions are answered, the variability that is inherent in bond tests should be considered. Bond tests exhibit a great deal of scatter, as shown in Figs. 3.3 - 3.5. However, the scatter shown in these figures is only one-half of the picture, since the values of C/U are based on mean bond strengths of uncoated bars.

Imagine if the bond strength of each coated bar is divided by the bond strength of each uncoated bar in the same test group. Clearly, the scatter in C/U will increase. The extent of the scatter is illustrated in Fig. 3.23 (Choi, Hadje-Ghaffari, Darwin, and McCabe 1990), where these individual values of C/U are compared as a function of the bearing-area ratio, R_b. Since the splice tests in this study, as well as those performed by Treece and Jirsa (1987, 1989), were executed with individual coated and uncoated bar specimens, i.e., no replications, the expected scatter in C/U for splices should be like that shown for the beam-end specimens in Fig. 3.23.

The C/U values for the splice tests in this study and those from Treece and Jirsa (1987, 1989) also appear in Fig. 3.23. As

illustrated, the splice tests generally lie within the scatter band obtained from the beam-end tests.

For the current study, some splice results are on the high side of the scatter band (S-pattern No. 6, 0.94, S-pattern No. 8, 0.90, and N-pattern No. 8, 0.86) and some are on the low side (N-pattern No. 5, 0.75, C-pattern No. 6, 0.76, and S-pattern No. 11, 0.72). Overall, the key aspects of bond strength reduction caused by epoxy-coating appear to be the same for both beam-end and splice specimens.

Table 2.5 summarizes the strengths obtained for the splice specimens in terms of bending moment and bar stress. Bar stress is calculated by allowable stress method using the ultimate moment. Splice specimens with epoxy-coated bars were uniformly weaker than specimens with uncoated bars, with the relative strengths ranging between 0.94 (S-pattern No. 6 bars) and 0.72 (S-pattern No. 11 bars). The mean value of C/U for the current splice tests, 0.82 (Table 2.5) is slightly lower than the mean for all beam-end tests, 0.85 (Table 3.1). However, the mean value of C/U from Treece and Jirsa (1987, 1989), 0.66 if weighted by test group or 0.69 if weighted by individual specimen, is considerably below the mean for the beam-end tests. The lower relative strength of the splices compared to the beam-end specimens in this study can be traced to the fact that most of the splices had a cover that was less than the 2 d_b used for the beam-end specimens. As discussed in section 3.5.2, the C/U ratio increases as cover increases. Also, a lower

strength is statistically expected for unconfined multiple splice specimens than for single splice or single bar specimens.

3.10 Comparison of Experimental Results to the Predicted Values by ACI (1989) and Orangun, Jirsa, Breen (1977)

Results of the beam-end splice tests from this study and the study by Choi, Darwin, and McCabe (1990) are compared to the bond strengths predicted by the Orangun, Jirsa, and Breen (1977) equation, Eq. 1.3(a), and the ACI Building Code (1989). For this comparison, the epoxy-bar development length modification factors are not used.

The Orangun et al. equation, Eq. 1.3(a), represents a best fit of bond stress data for uncoated bars of different sizes.

The expression for the basic development in ACI 318-89, ℓ_d in inches, is given by

$$\ell_d = \frac{0.04\ A_b\ f_y}{\sqrt{f'_c}} \tag{3.8}$$

in which A_b is the area of an individual bar in square in., f_y is the yield strength of the bar in psi, and f'_c is the compressive strength of concrete in psi. Substituting the bar stress, f_s, for f_y, and the bonded length or bonded length plus lead length in beam-end specimens and the splice length in splice specimens, ℓ_s, for ℓ_d,

and solving for $A_b f_s$ provides an expression for the predicted bar stress at failure.

$$A_b f_s = \frac{\ell_s \sqrt{f'_c}}{0.04} \tag{3.9}$$

For the beam-end specimens, the predicted values are calculated once using the bonded length (BL) of the bar and once using bonded length plus the lead length (BL + LL) for ℓ_s in Eqs. 1.3(a) and 3.8.

Table 3.12 compares the normalized bond strength of beam-end specimens to the values predicted by the two equations for each bar size and deformation pattern. Tables 3.13 and 3.14 present similar comparisons for confined beam-end and splice specimens, respectively. The following factors are used, where applicable, in calculating the bond force by the provisions of ACI 318-89: 0.8 (Section 12.2.3.4 for bars with edge cover of more than 2.5 d_b), 2.0 (Section 12.2.3.2 for bars with a cover of d_b or less), 1.3 (Section 12.2.4.1 for top-cast bars), and 1.4 [Section 12.2.3.3 for bars with a cover between 1 d_b and 2 d_b (splices)]. The Orangun, Jirsa, and Breen equation includes no provision for top reinforcement. In Tables 3.12 and 3.13, the bond strengths of the tests are normalized to a concrete strength of 6,000 psi and a coating thickness (for No. 5 bars only) of 9 mils and are corrected to the appropriate nominal cover (using the procedures outlined in section 3.2). No correction

is made based on concrete strength or coating thickness for the splice tests in Table 3.14.

Comparison -- Test/prediction ratios are presented in Tables 3.12 - 3.14 based on bar size, deformation pattern, casting position (bottom and top-cast), and bar surface condition (uncoated and coated). Average bond strengths are used for comparison in each category. Average test/prediction ratios and coefficients of variation (COV) for the ratios are obtained for each bar size and deformation pattern based on casting position and bar surface condition. The comparison presented below are based primarily on the bonded length plus lead length, since the concrete in the lead length region participates in the bond strength of the bars. Overall, the test/prediction ratios obtained from the Orangun et al. equation are more consistent, closer to 1.0, and exhibit signifi-cantly less scatter, as demonstrated by lower coefficients of variation than do the test/prediction ratios obtained from the ACI provisions.

Comparisons in Table 3.12 show that, for bottom-cast bars, the Orangun et al. equation is conservative for No. 5, No. 6, and No. 8 bars and unconservative for No. 11 bars, with respective test/prediction ratios of 1.15, 1.12, 1.24, and 0.81. The ACI provisions are conservative in all cases, and significantly more conservative than the Orangun et al. equation for No. 8 and No. 11 bars. For the No. 5, No. 6, No. 8, and No. 11 bars the respective ACI test/prediction ratios are 1.09, 1.10, 1.64, and 1.87.

For coated bottom-cast bars, the Orangun et al. equation produces test/prediction ratios close to 1.0, except for No. 11 bars where the ratio is only 0.66. For uncoated top-cast and coated top-cast bars, the Orangun et al. equation produces test/prediction ratios that are, on the average, slightly unconservative, ranging from a high of 1.11 for uncoated top-cast No. 8 bars to a low of 0.80 for coated top-cast No. 6 bars. The average is 0.97 for all uncoated top-cast bars and 0.90 for all coated top-cast bars. The unconservative nature of these comparisons is, of course, due to the lack of consideration of bar position or surface condition. The ACI provisions provide a conservative representation for coated bottom-cast bars, and uncoated and coated top-cast bars. The only exceptions are coated bottom-cast No. 5 and No. 6 bars, where the test/prediction ratios are 0.96 and 0.97, respectively.

The comparisons in Table 3.13 for the beam-end specimens with transverse reinforcement produce generally less conservative comparisons than obtained for the beam-end specimens without transverse reinforcement. For comparisons using the bonded length plus lead length, as done with Table 3.12, the Orangun et al. equation produces unconservative prediction in all cases. When the comparisons are based on bonded length only, the Orangun et al. equation gives a considerably better match with the data. It is, however, still unconservative for the comparison for No. 11 bars. In contrast, the ACI provisions, using bonded length plus lead length, provide a conservative prediction in all cases except for coated No. 5 bars,

where the test/prediction ratio is 0.91. The level of conservativeness increases as the bar size increases, reflecting the greater effectiveness of the transverse reinforcement with an increase in bar size, as observed in Section 3.6.

As with the comparisons for the beam-end specimens, the comparisons for the splice specimens presented in Table 3.14 show that the Orangun et al. equation provides, in general, more accurate and less conservative predictions for splice strength than do the ACI provisions. The Orangun equation becomes progressively less conservative as the bar size increases, while the opposite is true for the ACI provisions. For all splice specimens with uncoated bars, the mean test/prediction ratio and COV for the Orangun et al. equation are 1.03 and 0.15, respectively. The respective values for the ACI provisions are 1.77 and 0.26. For specimens with coated bars, the test/prediction ratio for the Orangun et al. equation drops to 0.82 with a COV of 0.15, while the mean test/prediction ratio for the ACI provisions is 1.50 with a COV of 0.24. Once again, these comparisons are made without the use of an epoxy bar development length modification factor.

3.11 Design Recommendations

The current study points the way to a number of modifications in the provisions for epoxy-coated bars in the ACI Building Code (1989) and the AASHTO Bridge Specifications (1989). Those provisions consist of a 1.5 development length modification factor for

epoxy-coated bars with less than 3 bar diameters of cover or a clear spacing between bars less than 6 bar diameters, a 1.2 (ACI) or 1.15 (AASHTO) modification factor for epoxy-coated bars with a 3 bar diameter cover or more and a clear spacing between bars of 6 bar diameters or more, and an upper limit of 1.7 on the product of the epoxy-coating factor and the top-bar factor.

As Table 3.1 shows, the lowest average value of C/U obtained for any size or deformation pattern of unconfined bottom-cast bars with 2 d_b cover in the current study is 0.73, for S-pattern No. 8 bars. This translates into a modification factor of 1.37. No. 5, No. 6, and No. 11 bars were affected even less, with modification factors of 1.18, 1.25, and 1.28, respectively, based on the deformation pattern with the lowest value of C/U. These modification factors represent bars with covers of 2, not 3, bar diameters. Also, as discussed in section 3.10, by comparing the bond strength values of the tests to those of ACI (Tables 3.12 - 3.14), ACI overestimates the required development length of epoxy-coated bars in virtually all cases, even without including the current ACI factor for epoxy coating. Thus, it appears that development length modification factors can safely be reduced to 1.25 for No. 6 bars and smaller and 1.35 for No. 7 bars and larger (care should be taken in selecting values for No. 3, No. 4, No. 14, and No. 18 bars, since no tests have been performed on these bar sizes). A modification factor of 1.25 for No. 5 bars is more than adequate, based on a 9 mil coating, but will help to take into account the lower bond strengths obtained

by small bars with thicker coatings. Recent work by Cleary and Ramirez (1989) provides additional evidence suggesting that the current design provisions for epoxy-coated bars (1987, 1989) are overconservative. Before finalizing these numbers, it would be prudent to evaluate at least a portion of the patterns that have not yet been tested.

The test results also suggest that development length modification factors can be reduced further by 1) altering deformation patterns to improve the bond strength of epoxy-coated bars or 2) standardizing on "strong" deformation patterns on an industry wide basis. The deformation pattern tested by Treece and Jirsa (1987, 1989), which produced lower values of C/U than obtained in this study, is no longer used for epoxy-coated bars because of difficulties in coating.

The insensitivity to coating thickness for bars larger than No. 5 indicates that coatings thicker than 12 mils could be used on larger bars to improve corrosion protection. This improved protection could be obtained with little reduction in bond strength beyond that currently observed. Additional study is necessary, however, before new limits on coating thickness can be established.

The relative insensitivity of coated bars to the top-bar effect with slump increase, strongly suggests that either a lower top-bar factor or a limit below 1.7 be applied for top-cast epoxy-coated bars. As seen in Table 3.3 and as discussed in section 3.5.2(b), it is reasonable to use a top-bar factor of 1.3 for uncoated bars.

However, the top-bar factor can be reduced to 1.15 or the product of top-bar and epoxy factors can be limited to 1.50 for epoxy-coated bars.

The beneficial effect of confinement of bars by transverse reinforcement should be considered when using epoxy-coated bars. As Table 3.9 shows, the lowest C/U ratio obtained for any size or deformation pattern, 0.81 for S-pattern No. 8 bars, translates into a modification factor of 1.24. Also the lowest ratio of average bond strengths of coated confined to uncoated unconfined bars obtained for any size or deformation pattern bar, 0.86 for S-pattern No. 5 bars, translates into a modification factor of 1.17. Thus, it appears that, based on the current limited data, a development length modification factor of 1.25 would be appropriate for confined coated bars when used in place of confined uncoated bars while a factor of 1.20 would be appropriate for confined coated bars when used in place of unconfined uncoated bars.

The beneficial effect of increased cover on C/U can be translated into the use of increased cover rather than increased development length to account for the reduced bond strength caused by epoxy coating. The results of this study indicate that an increased concrete cover of 0.5 d_b for No. 8 and smaller coated bars and 1.0 d_b for No. 9 and larger coated bars may be an alternate to applying development length modification factors for epoxy-coated bars. More simply, since bars with 2 d_b cover represent the standard for design (ACI 318-89), any bar with 3 d_b or greater cover

and 6 d_b or greater clear spacing should have an epoxy modification factor of 1.0. If this provision is applied, the current 0.8 modification factor for bars with a 5 d_b clear spacing (ACI 318-89 Section 12.2.3.4) should not be applied to epoxy-coated bars.

CHAPTER 4: ANALYTICAL STUDY OF BOND

4.1 Introduction

In this chapter, the effects of the interfacial properties of reinforcing steel and specimen geometry on the bond strength of both coated and uncoated bars are studied analytically using a simple statical model of two rigid bodies in contact and a finite element model incorporating a nonlinear fracture mechanics approach to represent cracking.

Beam-end specimens were used for the major part of the experimental study. These specimens fail with the major crack running through the concrete along the length of the test bar. The crack is caused by the wedging action of the bar as it slips. The studies explore the effects of concrete cover, lead length, face angle of the deformations, and the coefficient of friction between concrete and reinforcing steel on bond strength.

The statical model, Fig. 4.1, consists of two rigid bodies in contact along an inclined plane. One rigid body represents the concrete and the other rigid body represents the reinforcing steel. The angle of the plane represents the face angle of the bar deformations. The rigid bodies are constrained so that relative motion can occur only parallel to the interface. The confining force provided by the concrete and the force in the steel are shown in the figure.

The finite element model (Fig. 4.2) is based on the model developed by Choi, Darwin, and McCabe (1990) to represent a beam-end specimen. This model represents a beam-end specimen using three substructures. These consist of an exterior concrete substructure [Fig. 4.2(a)], a refined interior concrete substructure [Fig. 4.2(b)], and a reinforcing bar substructure [Fig. 4.2(c)]. Special two-node nonlinear rod link elements (Fig. 4.3) are used along with the first substructure to represent fracture of the concrete (the splitting crack), and to attach the substructure to the plane of symmetry. The crack is modeled using a nonlinear fracture mechanics scheme, Hillerborg's fictitious crack model (Hillerborg et al. 1976). The second substructure is associated with the third substructure through special three-node nonlinear interface link elements (Fig. 4.4) to simulate slippage of the bar-concrete interface.

Choi, Darwin, and McCabe (1990) carry out the modeling in two stages. The first stage represents cracking of the concrete along the crack surface, while the second stage represents the slippage of the bar. In the first stage, using the substructuring technique, the exterior concrete substructure [Fig. 4.2(a)] is attached to the crack plane by the two-node link elements. At this stage, the model is loaded by imposing displacements, perpendicular to crack surface, only at the nodes where the reinforcing bar substructure is located. This generates a lateral load-lateral displacement curve for the model. The load-displacement curve is then used to define a nonlinear spring for use in the second stage to represent the confinement

provided by the concrete. This reduces the balance of the analysis to a two-dimension problem, greatly simplifying the solution.

In the second stage, the interior concrete model and the reinforcing steel model are connected to each other through the three-node interface link elements. The nodes on the straight edge of the interior concrete model, top edge of Fig. 4.2(b), are constrained to have the same lateral displacement and are attached to a single spring whose properties are determined in the first stage. In this stage, bar slip is represented by applying displacement to the reinforcing bar substructure. Fig. 4.5 illustrates the overall finite element model.

Using the cracking load from the first stage, Choi, Darwin, and McCabe (1990) compare the bond force obtained from the second stage of finite element analysis to that obtained from the statical model at the same confining force, P (Fig. 4.1), and find, as expected, that the bond forces from the two approaches are identical. Furthermore, the relative bond strength of coated and uncoated reinforcement, C/U, from both analyses depend only on coefficients of friction and face angle of the deformation, not on the confining force. Thus, in this study, the first stage of finite element analysis (cracking) is used to study the effects of specimen geometry, while the statical model is used to study the interfacial material properties.

No definitive experimental tests have been performed to evaluate the actual interfacial properties of either coated or uncoated

reinforcing steel. The statical model is used with the current experimental study to develop representative values for the coefficients of friction between concrete and uncoated and coated bars. The effects of lead length and concrete cover on the bond force of uncoated and coated bars are studied using the finite element model. By comparison with the analytical results of Choi, Darwin, and McCabe (1990), the effect of bar size on the fracture behavior of beam-end specimens also is studied. Specific aspects of the statical model and the finite element model are discussed next.

4.2 Statical Model

The statical model consists of two rigid bodies in contact (Fig. 4.1). The upper rigid body represents the concrete cover. It is constrained in the horizontal direction and has a vertical compressive force, P, representing the confining force provided by the concrete. The lower rigid body represents the reinforcing steel. It is constrained in the vertical direction and has a horizontal sliding force, H, representing the bond force between the bar and the concrete. The angle of the interface, γ, represents the face angle of the deformations on the bar.

The system is assumed to be in equilibrium. To maintain equilibrium, the normal force, $A\sigma_n$, and the tangential force, $A\sigma_s = A(C + \mu\sigma_n)$, along the interface must each be in equilibrium with the sum of the appropriate components of the external forces P and H. σ_n is the normal stress, σ_s is the tangential stress, A is the contact

area, μ is the coefficient of friction, and C is the cohesion stress between the two rigid bodies. The equilibrium equations in the normal and tangential directions are, respectively:

$$A\sigma_n = P \cos \gamma + H \sin \gamma \tag{4.1}$$

$$A(C + \mu\sigma_n) = H \cos \gamma - P \sin \gamma \tag{4.2}$$

Substituting $A\sigma_n$ from Eq. 4.1 into Eq. 4.2 and solving for the sliding force, H, gives:

$$H = P \frac{(\tan \gamma + \mu)}{(1 - \mu \tan \gamma)} + \frac{AC}{\cos \gamma(1 - \mu \tan \gamma)} \tag{4.3}$$

The value of C drops to zero once any relative movement occurs between the two bodies. Since the slip of the bar occurs at very early stages of loading, as seen in Figs. 2.4 - 2.7, only the first term on the right side of the Eq. 4.3 is of interest in terms of strength. Choi, Darwin and McCabe (1990) also demonstrate that, for expected values of C, cohesion plays only a minor role, even in load-slip behavior. Therefore, the statical model will be studied using a zero value for the cohesion stress, C.

4.3 Numerical Results of the Statical Model

Eq. 4.3 is used to study the effects of the face angle of the deformations and the coefficient of friction on the relative bond

strengths of reinforcing bars. Rehm (1961) and Lutz and Gergely (1967), in tests of uncoated bars, observed that bars with rib face angles, γ, between 40° and 105° produce about the same movement of the bar relative to the surrounding concrete because the concrete in front of the ribs crushes, producing ribs with effective face angles between 30° and 40°. They did not observe crushing for bars with γ less than 40°. As discussed in section 2.9, in the current study, crushed concrete was rarely observed in front of the ribs of coated bars but was observed in all cases with uncoated bars. Therefore, for this analysis, in studying the coefficients of friction of uncoated and coated bars, the face angle, γ, is limited first to 40° and then to 30° for uncoated bars. γ is not limited for coated bars.

Three different methods are used to describe the face angle of the test bars. In all three methods, a "local" face angle is calculated on both sides of the deformation based on the slope of the face at twenty points around the circumference of the bar. For the first and second methods, the slope is measured from the base to the top of the face of the deformation. For the first method, the face angles on both faces of the deformation at the twenty points around the circumference are averaged to obtain a single value. The second method uses the maximum individual value from the measurements. The third method is similar to the second method, but the slopes are measured only from the base to the midheight of the deformations. These methods are discussed in detail in Appendix A.

Of the face angles obtained from the three methods, the largest (the third method) is used in this analysis, since it can be argued that it is the largest face angle that controls the slip of a deformation, and in effect the slip of a bar, relative to concrete. The face angles obtained using the three different methods for each bar size are presented in Table 4.1. The bars in this study have face angles ranging from 28° to 38°, from 40° to 57°, and from 43° to 57° for the first, second, and third methods, respectively (Table 4.1).

The bond force, H, for uncoated and coated bars is calculated using Eq. 4.3 for different values of face angle as a function of the coefficients of friction. For each combination of coefficients of friction for the coated and uncoated bars, the ratio of H for coated bars to H for uncoated bars, C/U, is plotted versus the face angle. Figs. 4.6 - 4.8 correspond to uncoated bar coefficients of friction of 0.2, 0.3, and 0.4, respectively. In each figure, coated bar coefficients of friction range from 0.0 to 0.20. The C/U ratios obtained from the test specimens for different bar sizes and deformation patterns ("C/U group" in Table 3.1) are also plotted. In these figures, the maximum face angle around the circumference of the bar at the mid-height of the deformations (method 3) is used to represent the test results. The abrupt change in the shape of the C/U versus face angle curves at $\gamma = 40°$ is the result of the limitation on γ (to 40°) for the uncoated bars.

In Fig. 4.6, the majority of the data points fall outside of the C/U curves. Since the coefficient of friction for coated bars cannot be less than zero, the coefficient of friction for uncoated bars must be greater than 0.2. Comparison of the C/U curves with the test data in Figs. 4.7 and 4.8 indicates that the coefficient of friction of uncoated bars should be between 0.3 and 0.4, if the assumption of an effective value for γ of 40° for uncoated bars is correct.

Fig. 4.9 compares C/U with face angle for an uncoated bar coefficient of friction of 0.35. The experimental C/U values are clustered between curves representing coated bar coefficient of friction of 0.0 and 0.20. Thus, 0.35 and 0.10 appear to be representative values for the coefficients of friction of uncoated and coated bars, respectively. It should be noted that, in all cases where γ is greater than 40°, the coefficient of friction for uncoated bars represents the coefficient for a crushed concrete-concrete interface.

It is worthwhile to investigate C/U when the γ for uncoated bars is not limited to 40°. Fig. 4.10 shows three C/U versus face angle curves where no limits are placed on γ for uncoated bars. The three curves represent coefficients of friction for coated bars of 0.0, 0.20, and 0.33. As Fig. 4.10 shows, all of the experimental results lie between the curves for coated bar coefficients of friction of 0.20 and 0.33, suggesting that the coated bars have coefficients of friction nearly as high as the uncoated bars. This cannot

be true since test results (Fig. 2.18) indicate that the friction between the coated bars and concrete is considerably less than that between the uncoated bars and concrete. Comparison of Figs. 4.9 and 4.10 further strengthens the validity of limiting γ to a maximum of 40° for uncoated bars in the current investigation, as well as the validity of the observations made by Rehm (1961) and Lutz and Gergely (1967).

If γ is limited to 30°, instead of 40°, for uncoated bars, a similar analysis indicates that 0.56 and 0.10 are representative values for the coefficients of friction of uncoated and coated bars, respectively. This is seen in Fig. 4.11 where the C/U curves are plotted versus face angle for an uncoated bar coefficient of friction of 0.56. Fig. 4.12 compares the C/U versus face angle curves for uncoated and coated bar coefficients of friction of 0.35 and 0.0, respectively, with 30° and 40° serving as the limiting face angle for the uncoated bars. Since the test results fall between the two curves and the coated bar coefficient of friction cannot be less than zero, 0.35 appears to be a reasonable lower bound of the uncoated bar coefficient of friction.

The maximum confining force provided by the concrete around a bar, P in Eq. 4.3, is the same for both uncoated and coated bars. Since the cohesion, C, drops to zero at early stages of loading, the sliding force of the bar, H, can be determined based on the face angle, γ, and coefficient of friction, μ. The values of H are H_U and H_C for uncoated and coated bars, respectively. Since C/U is the

ratio of H_C to H_U, this suggests that C/U is independent of lead length and cover. The test results of Choi, Darwin, and McCabe (1990) indicate that C/U is insensitive to lead length, but the test results discussed in Section 3.5.2 indicate some increase in C/U as cover increases.

Choi, Darwin, and McCabe (1990) used $\gamma = 36.9°$ and values of 0.3 and 0.03 as the coefficients of friction for uncoated and coated bars in Eq. 4.3. They obtained a value of C/U of 0.59, which is lower than the lowest average experimental results for any bar size or deformation pattern, 0.72 (S-pattern No. 8 bars). The analyses illustrated in Figs. 4.6 - 4.12 and the face angle values in Table 4.1 suggest that both the assumed face angle and coefficients of friction of uncoated and coated bars used in the earlier study are not representative of the actual bars.

It is important to note that C and N-pattern bars in this study have ribs that are inclined with respect to the longitudinal axes of the bars. The statical analysis in this study is based on the assumption that ribs are perpendicular to the axes of the bar (S-pattern). A three-dimensional statical model is required to study the effect of the inclination of the ribs.

4.4 Finite Element Analysis

The specific aspects of the finite element model, including the crack representations and concrete are discussed in the following sections.

4.4.1 Crack Representation

Following the tests, beam-end specimens consistently reveal a splitting crack, with a dominant fracture surface or running crack. Since the dominant crack splits the specimen vertically as the reinforcing steel wedges against the concrete, the fracture surfaces can be characterized as being in an opening mode, with symmetrical displacements perpendicular to the fracture surfaces (Barsom and Rolfe 1987). This basic behavior can be represented using a simple nonlinear fracture mechanics approach.

Hillerborg et al. (1976) proposed the fictitious crack model for predicting crack propagation in concrete. In concrete, it is presumed that although the tensile strength of the material has been attained, the concrete can still resist a tensile load since the zone around the cracks can transfer tensile stress until the crack propagates through that zone. This stress transfer capability is represented using a stress-displacement relationship, such as illustrated in Fig. 4.13 (Petersson, 1980), in which the tensile-stress carrying capability of the material decreases with increasing crack width. Once the crack width reaches a value of w_o, all of the energy that can be dissipated by the crack is accounted for, and the tensile stress becomes zero. In Fig. 4.13, the area under the stress-displacement curve represents the energy absorbed per unit area of crack surface as the crack is fully opened. This fracture energy, G_c, can be calculated as:

$$G_c = \int_0^{w_o} \sigma \, dw \qquad (4.4)$$

in which w is the crack width and σ is the tensile stress across the crack. This expression for G_c has been shown to be accurate in representing the overall fracture behavior of concrete, and its applicability has been firmly established on a theoretical basis (Petersson 1981).

For the current study, the fictitious crack model is used in the finite element analysis to represent the splitting crack that forms at the center line of the specimen. The crack is modeled using special nonlinear link elements (Fig. 4.3) which are perpendicular to the defined fracture surface. The link elements are two-node rod elements; each node has only one degree of freedom, parallel to the elements. The elements have a unit length and a total area equal to the total contact area across the crack plane. Since the specimen splits symmetrically, only one-half of the specimen needs to be modeled; the tip of the crack is always at the specimen center line.

Prior to attaining the tensile strength of the concrete, f'_t, the link elements are intentionally modeled as being very stiff, using a modulus of elasticity of 400,000 ksi. Upon reaching f'_t, the elements are then forced to follow a linear stress-displacement relationship, as illustrated in Fig. 4.14. For this study, the tensile strength of rod elements is 0.4 ksi and G_c, the area under

the stress-displacement relationship in Fig. 4.14, is 0.57 lb/in., which correspond to concrete with compressive strength of 6 ksi (Petersson 1981, Leibengood, Darwin and Dodds 1984). The corresponding value of w_o is 0.0029 in.

The stress-strain function for the link elements to represent this nonlinear material behavior is illustrated in Fig. 4.15. Prior to cracking, the material is assumed to be isotropic and linear elastic. After cracking, when the stress in the link element is on the descending branch of the stress-strain function, the secant modulus is used as the stiffness of the material in the finite element formulation.

4.4.2 Concrete Material Model

With the exception of the material at the crack plane, concrete is treated as a linear elastic material using 8-node three-dimensional isoparametric brick elements, with a modulus of elasticity of 4000 ksi and a Poisson's ratio of 0.20. The three-dimensional elements are used to construct the exterior concrete model [Fig. 4.2(a)].

The linear 8-node brick elements, having no midside node, are used to produce a linear shape function, which produces stresses that are compatible with the stresses that are produced by the linear shape function of the rod link elements at the crack surface (Herrmann 1978).

4.4.3 Beam-end Specimen Model

The finite element model represents the concrete in a beam-end specimen in contact with a single deformation of a 5/8 square in. reinforcing bar. Due to symmetry, only one half of the specimen is modeled. The plane of symmetry represents the splitting crack. The notch in the model represents the position of the reinforcing bar.

The exterior concrete substructure represents the test specimen. Three covers, 1, 2, and 3 bar diameters, and three lead lengths, 1, 2, and 3 in., are evaluated. The specimen depth consists of 5 in. of concrete below the bar, 5/8 in. for the bar dimension, and the concrete cover. The length of the block consists of 9 in. behind the deformation plus 0.40 in. for the deformation length [equal to the spacing of the deformations on No. 5 bars (Table 2.1)], and the lead length. The model is 4.5 in. wide.

The finite element models are generated with the PATRAN-II software system (1990). Nodal renumbering also is performed by PATRAN-II to minimize the band width, using the minimum wave front criteria. The models are analyzed using the POLO-FINITE finite element analysis software system (1991). The number of nodes and elements for the cases described in the following section is summarized in Table 4.2.

4.5 Solution Procedure

Loads are applied by imposing displacements, in the positive Y direction, on the nodes where the bar deformation is located (hashed

area in Fig. 4.16). Small increments of displacement (typically, 0.00005 in. for the first 5 steps, 0.00015 for steps up to peak load, and 0.00002 to pinpoint the peak load) are used to obtain a stable solution with a minimum number of iterations. An incremental iterative Newton-Raphson procedure is used to obtain convergence. Cracking is the only nonlinear process modeled. Unbalanced forces that result from cracking are reapplied in successive iterations until convergence is obtained. The iterations continue until the Euclidean norm of the residual nodal loads is less than 0.1 percent of the corresponding norm of the total nodal loads. Convergence is typically rapid, generally requiring only three iterations per load step. To limit the computational effort, the initial material properties of the elements are used to form the global stiffness matrix for the initial load application. The global stiffness matrix for the further load applications is updated for every iteration until convergence of each load step.

4.6 Numerical Results of Finite Element Study

In this section, the results of the finite element analysis of the beam-end specimens are presented and the effects of the key parameters are evaluated. The results for models using different covers and lead lengths are presented and discussed based on the observed behavior of the test specimens. The finite element results in this study is compared to those of Choi, Darwin, and McCabe (1990), the experimental results, and empirical equations.

4.6.1 Splitting of Concrete

This section presents the results of finite element analysis and the effects of cover, lead length, and bar size are examined.

Fig. 4.17 shows the lateral force-lateral displacement curves for the models with 2 in. lead length and 1, 2, and 3 bar diameter covers. Fig. 4.18 shows the lateral force-lateral displacement curves for the models with 2 bar diameter cover and 1, 2, and 3 in. lead lengths. It can be seen in both of these figures that, as the cover thickness or the lead length increase, the lateral force required for splitting increases and the ascending and descending branches of the load-displacement curves become steeper.

Crack propagation from the splitting of the concrete is shown in Fig. 4.16 for a model with a 3 bar diameter cover and a 2 in. lead length. In this figure, each contour line represents the load and the displacement at which the enclosed link elements just reach the descending branch of the stress-strain curve (Fig. 4.15). As expected, the crack surface starts propagating adjacent to the loaded area (location of bar deformation) and spreads in all directions away from the reinforcing bar. The crack surface rapidly reaches the top and front of the specimen. At the peak load, the crack surface has propagated through the lead length, cover, and depth of the concrete block, while parts of the concrete below and at the back of the loaded area remain elastic (Fig. 4.16). This cracking pattern generally matches the pattern observed in the test specimens (Section 2.8). Similar crack patterns are observed for the other

configurations of the covers and lead lengths. The following sections describe the effect of concrete cover and lead length on the splitting load.

4.6.2 Effect of Concrete Cover

The load-displacement curves in Fig. 4.17 show that as the cover increases, the lateral force to split the concrete increases. This is also shown in Fig. 4.19 where the values of lateral force are plotted versus the cover for the models with 2 in. lead length and 1, 2, and 3 d_b covers for both this study and the study by Choi, Darwin, and McCabe (1990). The maximum lateral forces for the 1, 2, and 3 bar diameter cover models are 9,375, 10,130, and 11,081 lbs., respectively. Choi, Darwin, and McCabe (1990) observed that once the peak lateral force, P, is obtained, Eq. 4.3 gives an accurate value for the sliding or the bond force, H. Therefore, it is evident that as the cover increases, the bond force increases.

The increase in the bond or sliding force, H, with an increase in cover agrees with the observations made on the test results. Further comparison with the test results is presented in Section 4.6.5.

4.6.3 Effect of Lead Length

The load-displacement curves in Fig. 4.18 show that as the lead length increases, the lateral force to split the concrete increases. This is also shown in Fig. 4.20 where the values of

lateral force are plotted versus the lead length for the models with 2 d_b cover and 1, 2, and 3 in. lead lengths for both this study and the study by Choi, Darwin, and McCabe (1990). The maximum lateral forces for models with the 1, 2, and 3 in. lead lengths are 8,883, 10,130, and 12,444 lbs., respectively. It is evident that as the lead length increases, the bond force increases.

The increase in the bond or sliding force, H, with an increase in lead length, agrees with the test results of Choi, Darwin, and McCabe (1990). Further comparisons with the test results are presented in Section 4.6.5.

4.6.4 Comparison to the Results by Choi, Darwin, and McCabe (1990)

Choi, Darwin, and McCabe (1990) performed the finite element analysis using a No. 8 bar as the bar model. The peak load and the corresponding displacement for all of the models with different covers and lead lengths from this study and the study by Choi, Darwin, and McCabe (1990) are presented in Table 4.3. Choi et al. observed an increase in bond strength with an increase of cover and lead length, which agrees with observations made in this study. Fig. 4.19 shows the values of the lateral force versus cover for both studies. This comparison seems to indicate that the bond strength of No. 5 bars is less sensitive to cover than the bond strength of No. 8 bars. This trend agrees with experimental results as seen in Fig. 4.21. In Fig. 4.21, the ultimate bond strengths (ultimate bond forces divided by the bonded length plus lead length

in beam-end specimens) are plotted versus cover for No. 5 and No. 8 uncoated bottom-cast bars and a best fit line is drawn for each bar size. The lower sensitivity of the bond strength of No. 5 bars to cover is apparent from the flatter slope of the best fit line for the No. 5 bars in comparison to the slope of the best fit line for the No. 8 bars in Fig. 4.21. Fig. 4.20 shows the values of the lateral force versus the lead length for both studies. The two bar sizes behave similarly as the lead length increases, and the two bar sizes show similar sensitivity to lead length.

A major difference, however, other than bar size, exists between the models used in the two studies. The model used by Choi et al. was constrained at the lower front edge against vertical displacement. This allowed the model to rotate about the x and z axes while the load was applied, and as a result, it allowed the model to have a lower peak load than obtained in the current study. The boundary condition used in this study, which simulates the constraints on the actual specimen more realistically, constrains the bottom surface of the model (x-y place) against vertical displacement and the center line of the bottom surface against horizontal displacement in the x direction. Thus, the base of the model does not rotate about any axis while the load is applied, resulting in a higher peak load than obtained by Choi et al.

The effects of the boundary conditions and the loaded area are shown in Fig. 4.22. In this figure, the lateral force-lateral displacement curves for three finite element models are presented. All

three models have a 2 in. cover and a 2 in. lead length. Case 1 is the model used by Choi, Darwin, and McCabe (1990) (loaded area simulating a No. 8 bar with a single deformation) but with the new boundary conditions. Case 2 is the same as Case 1 with the exception that the loaded area simulates a No. 5 bar deformation. Case 3 is the model used by Choi, Darwin, and McCabe (1990). Comparing cases 1 and 3 shows that, with the new boundary conditions, the model is stiffer, and has a greater strength and corresponding displacement than the model used by Choi, Darwin, and McCabe (1990). Comparing cases 1 and 2 shows that the model with the larger loaded area (model with No. 8 bar) is stiffer, and has a slightly greater strength than the model with the smaller loaded area (model with No. 5 bar). The comparison of cases 1 and 2 indicates that the absolute value of cover is the prime controller of bond strength, not cover as a multiple of bar diameter. It also indicates that larger bars should exhibit slightly higher bond forces than smaller bars for a given development length.

4.6.5 Comparison to the Test Results and Empirical Equations

In this section, the results obtained from the finite element models are compared to test results for No. 5 N-pattern bars (groups 7 - 13 and 21) and the bond strengths predicted by Eq. 1.3 (Orangun, Jirsa, and Breen 1977), Eq. 1.2 (Jimenez, White, and Gergely 1978), and Eq. 1.4 (Zsutty 1985) in Figs. 4.23 and 4.24. In Fig. 4.23, the results are normalized with respect to the respective cases with 2

d_b cover. In Fig. 4.24, the results are normalized with respect to the respective cases with a 1.0 in. lead length. For the predictive equations, lead length is used in place of development length.

As seen in Fig. 4.23, the test results, the finite element results, and the predicted results from the Orangun, Jirsa, and Breen (1977) equation and the Zsutty (1985) equation are in general agreement with each other and show a similar sensitivity to cover, within the range of the covers used for the test specimens. The finite element model exhibits less sensitivity to cover than do the test results or the three predictive equations (Orangun et al., Jimenez et al., and Zsutty). The Jimenez, White, and Gergely (1978) equation shows a much greater sensitivity to the cover than is exhibited by the test results.

As shown in Fig. 4.24, the test results, the finite element results, and the predicted results from the Orangun, Jirsa, and Breen (1977) equation and the Zsutty (1985) equation are in general agreement with each other and show a similar sensitivity to lead length, within the range of the lead lengths tested, while the Jimenez, White, and Gergely (1978) equation again shows a much greater sensitivity to the lead length than actually exists.

4.7 Summary

The statical model analysis along with the test results indicate that 0.35 and 0.10 can be adopted as representative coefficients of friction values for uncoated and coated bars,

respectively, when the face angle of uncoated bars is limited to an effective value of 40°. The corresponding values are 0.56 and 0.10, when the face angle of uncoated bars is limited to an effective value of 30°.

The finite element analyses indicate that an increase in lateral force provided by the concrete, and thus an increase in bond force, will occur with an increase in cover, lead length, or bar size. These observations agree with experimental results. The finite element results and the general predictions of the Orangun, Jirsa, and Breen (1977) and Zsutty (1985) equations agree with test results for N-pattern No. 5 bars when the results and predictions are normalized with respect to values at 2 d_b cover and 1.0 in. lead length.

CHAPTER 5: SUMMARY, CONCLUSIONS, AND DESIGN RECOMMENDATIONS

5.1 Summary

The purpose of this study is to obtain a better understanding of the effect of epoxy coating on the bond strength between reinforcing steel and concrete. The study involved 630 beam-end specimens and 15 beam-splice specimens. 394 of the beam-end specimens were tested by Choi et al. (1990). The key parameters in this study are bar surface condition (coated and uncoated), deformation pattern, bar size, concrete cover, casting position, concrete slump, degree of consolidation, confinement of reinforcing steel with transverse reinforcement, and concrete strength. In addition, a preliminary investigation of the behavior of epoxy-coated hooks is carried out.

To better understand the effect of epoxy coating on bond strength and the nature of bond failure, analytical studies are conducted using a statical model and a finite element model. The statical model consists of two rigid bodies in contact while the finite element model represents the concrete portion of a beam-end specimen. The statical model is used to study the roles of coefficient of friction between coated or uncoated steel and concrete and rib face angle of reinforcing bars on the reduction in bond strength caused by epoxy coating. The finite element model is used to study the effects of concrete cover and lead length on bond strength. The

effect of bar size on bond strength is investigated by comparing the finite element analysis results to those obtained by Choi, Darwin, and McCabe (1990).

5.2 Observations and Conclusions

The following observations and conclusions are based on the test results and analyses presented in this report.

5.2.1 Experimental Study

5.2.1.1 Beam-end Specimens

1. Epoxy coating reduces the bond strength of reinforcing bars to concrete. The extent of this reduction, however, is less than that used to establish the development length modification factors in the 1989 ACI Building Code and 1989 AASHTO Bridge Specifications.
2. Splitting failure was observed for all specimens.
3. The load-slip stiffness of coated bars is lower than that of uncoated bars. Coated bars slip more than uncoated bars at any load.
4. For coatings between 3 and 17 mils in thickness, the coating thickness does not affect the bond strength reduction caused by epoxy coating for No. 6 and larger bars. Thicker coatings cause a greater reduction in bond strength than thinner coatings for No. 5 bars.

5. The reduction in bond strength caused by epoxy coating increases with bar size. The mean values of the relative bond strength, C/U, are 0.88, 0.89, 0.82, and 0.83 for No. 5, No. 6, No. 8, and No. 11 bars, respectively.
6. The extent of the reduction in bond strength caused by epoxy coatings depends on deformation pattern. The height of the ribs and their spacing and inclination can have a profound effect on the performance of epoxy-coated bars. Bars with a larger rib bearing area per unit length are affected less by the epoxy coating than bars with a smaller rib bearing area per unit length.
7. The bond strength of both coated and uncoated bars increases as cover increases, regardless of bar position, bar size, or deformation pattern. For beam-end tests, epoxy coating causes a nearly fixed drop in bond strength, independent of cover or bar position. This results in an increase in C/U as cover increases.
8. As the depth of concrete below a bar increases, the bond strength decreases, regardless of bar size, deformation pattern, or bar surface condition.
9. Bars cast in low slump concrete are stronger in bond than bars cast in high slump concrete of the same compressive strength.

10. The bottom to top-cast bar strength ratio, B/T, increases for uncoated bars and decreases for coated bars as slump increases.
11. In low slump concrete, B/T is the same for uncoated and coated bars, and C/U is the same for bottom and top-cast bars.
12. In high slump vibrated concrete, B/T for uncoated bars is greater than B/T for coated bars, and C/U for top-cast bars is greater than C/U for bottom-cast bars.
13. Vibration has a positive effect on bond strength for both coated and uncoated, bottom and top-cast bars. Vibration also has a positive effect on C/U for bottom and top-cast bars.
14. Confinement of reinforcing bars with transverse steel has a positive effect on bond strength for both coated and uncoated bars. C/U for confined bars, 0.88, is approximately the same as C/U for unconfined bars, 0.85.
15. The limited study of the effect of transverse steel indicates that coated confined bars have virtually the same bond strength as uncoated unconfined bars. The bond strength of coated bars was enhanced more by confinement than the bond strength of uncoated bars. The degree of this enhancement increased with bar size.
16. The limited study of the effect of concrete strength showed little or no increase in bond strength as concrete

strength increases from 6,000 to 13,000 psi. C/U does not appear to change as concrete strength increases.

17. The average value of C/U for hooks in beam-end specimens, 0.95, was 5 percent higher than the average value of C/U for straight bars, 0.90, with the same deformation pattern and bar size.

5.2.1.2 Splice Specimens

1. The key aspects of bond strength reduction caused by epoxy coating appear to be the same for both beam-end and splice specimens.
2. Splice specimens with epoxy-coated bars were uniformly weaker than specimens with uncoated bars.
3. The mean value of C/U for the current splice tests, 0.82, is slightly lower than the mean for all beam-end tests, 0.85. However, the mean value of C/U from Treece and Jirsa (1987, 1989), 0.66 if weighted by test group or 0.69 if weighted by individual specimen, is considerably below the mean for the beam-end tests.

5.2.2 Comparison of Experimental Results to the Predicted Values by ACI (1989) and Orangun, Jirsa, Breen (1977)

1. The test/prediction ratios obtained from the Orangun, Jirsa, and Breen equation are more consistent, closer to 1.0, and exhibit significantly less scatter than do the test/prediction ratios obtained from the ACI provisions.

2. For the beam-end specimens, the Orangun, et al. equation overestimates the effect of transverse reinforcement on the bond strength of uncoated and coated bars.
3. Overall, ACI is conservative in estimating the bond strength of uncoated and coated bars, even without considering the development length modification factors in ACI 318-89 for epoxy coating.

5.2.3 Analytical Study of Bond

5.2.3.1 Statical Model

1. The statical model analysis, along with the test results, indicates that 0.35 and 0.10 can be adopted as representative coefficients of friction for uncoated and coated bars, respectively, when the maximum effective face angle of uncoated bars is limited to a value of 40°. The corresponding values are 0.56 and 0.10, when the maximum effective face angle of uncoated bars is limited to a value of 30°.

5.2.3.2 Finite Element Analysis

1. The finite element analyses indicate that an increase in lateral force provided by the concrete, and thus an increase in bond force, will occur with an increase in cover, lead length, or bar size.
2. The finite element results and the general predictions of the Orangun, Jirsa, and Breen (1977) and Zsutty (1985)

equations agree with test results for N-pattern No. 5 bars when the results and predictions are normalized with respect to values at 2 d_b cover and 1.0 in. lead length.

5.3 Design Recommendations

The current study points the way to a number of modifications in the provisions for epoxy-coated bars in the ACI Building Code (1989) and the AASHTO Bridge Specifications (1989). Those provisions consist of a 1.5 development length modification factor for epoxy-coated bars with less than 3 bar diameters of cover or a clear spacing between bars less than 6 bar diameters, a 1.2 (ACI) or 1.15 (AASHTO) modification factor for epoxy-coated bars with a 3 bar diameter cover or more and a clear spacing between bars of 6 bar diameters or more, and an upper limit of 1.7 on the product of the epoxy-coating factor and the top-bar factor.

As discussed in section 3.10, ACI 318-89 overestimates the required development length of epoxy-coated bars in virtually all cases, even without including the current ACI factor for epoxy coating. The results obtained in this study indicate that the current development length modification factor of 1.50 can realistically be reduced to 1.25 for No. 6 bars and smaller and 1.35 for No. 7 bars and larger. Care should be taken in selecting values for No. 3, No. 4, No. 14, and No. 18 bars, since no tests have been performed on these bar sizes. Before finalizing these numbers, it

would be prudent to evaluate at least a portion of the patterns that have not yet been tested.

The test results also suggest that development length modification factors can be reduced further by 1) altering deformation patterns to improve the bond strength of epoxy-coated bars or 2) standardizing on "strong" deformation patterns on an industry wide basis. The deformation pattern tested by Treece and Jirsa (1987, 1989), which produced lower values of C/U than obtained in this study, is no longer used for epoxy-coated bars because of difficulties in coating.

The insensitivity to coating thickness for bars larger than No. 5 indicates that coatings thicker than 12 mils could be used on larger bars to improve corrosion protection. This improved protection could be obtained with little reduction in bond strength beyond that currently observed. Additional study is necessary, however, before new limits on coating thickness can be established.

The relative insensitivity of coated bars to the top-bar effect with slump increase, strongly suggests that either a lower top-bar factor or a limit below 1.7 be applied for top-cast epoxy-coated bars. The results of this study indicate that it is reasonable to use a top-bar factor of 1.3 for uncoated bars. However, the top-bar factor can be reduced to 1.15 and/or the product of top-bar and epoxy factors can be limited to 1.50 for epoxy-coated bars.

The beneficial effect of confinement of bars by transverse reinforcement should be considered when using epoxy-coated bars.

The results of this study indictate that based on the current limited data, a development length modification factor of 1.25 would be appropriate for confined coated bars when used in place of confined uncoated bars while a factor of 1.20 would be appropriate for con-fined coated bars when used in place of unconfined uncoated bars.

The beneficial effect of increased cover on C/U can be translated into the use of increased cover rather than increased development length to account for the reduced bond strength caused by epoxy coating. The results of this study indicate that, since bars with 2 d_b cover represent the standard for design (ACI 318-89), any bar with 3 d_b or greater cover and 6 d_b or greater clear spacing can have an epoxy modification factor of 1.0 in place of current 1.20 factor. If this provision is applied, the current 0.8 modification factor for bars with a 5 d_b clear spacing (ACI 318-89, Section 12.2.3.4) should not be applied to epoxy-coated bars.

5.4 Recommendations for Future Study

Research on the effect of epoxy coating on the bond strength of reinforcing steel is continuing at the University of Kansas. This report complements the initial study by Choi, Darwin, and McCabe (1990). The following is a partial list of questions related to the bond of epoxy-coated reinforcement needed to be studied in subsequent research efforts.

1. What deformation pattern has the best bond performance when bars are epoxy coated?
2. What are the limits of coating thickness to improve corrosion protection with acceptable reductions in bond strength?
3. How effective is transverse reinforcement for improving the development of epoxy-coated splices? (A study of the effect of the transverse reinforcement on the bond performance of splices by Hester, Salamizavaregh, Darwin, and McCabe (1991) will help answer this question).
4. More information is needed about the bond performance of epoxy-coated bars in high strength concrete.
5. More information is needed about the bond performance of epoxy-coated hooks.
6. Is there an effective way to increase friction and cohesion for epoxy-coated bars?
7. What is the bond performance of repaired epoxy-coated bars?
8. Actual development length of coated bars should be determined by testing different embedment lengths for all bar sizes and deformation patterns.
9. What are the actual values for cohesion and coefficient of friction of coated and uncoated bars?
10. How would a finite element model containing a circular deformed bar, with multiple lugs and different deformation

configurations, predict the bond performance of both coated and uncoated bars?

BIBLIOGRAPHY

AASHTO Highway Sub-Committee on Bridges and Structures. (1989). Standard Specification for Highway Bridges, 14th Edition, American Association of State Highway and Transportation Officials, Washington, DC.

Abrams, D. A. (1913). "Tests of Bond between Concrete and Steel," Bulletin No. 71, Engineering Experiment Station, University of Illinois, Urbana, IL, 105 pp.

ACI Committee 318. (1963). "Building Code Requirements for Reinforced Concrete (ACI 318-63)", American Concrete Institute, Detroit, MI, June, 144 pp.

ACI Committee 318. (1983). "Building Code Requirements for Reinforced Concrete (ACI 318-83)," American Concrete Institute, Detroit, MI, 111 pp.

ACI Committee 318. (1989). "Building Code Requirements for Reinforced Concrete (ACI 318-89) and Commentary-ACI 318R-89," American Concrete Institute, Detroit, MI, 353 pp.

ACI Technical Committees 222, 408, and 439. (1988). "ACI Workshop on Epoxy-Coated Reinforcement," Concrete International, Vol 10., No. 12, December, pp. 80-84.

ACI Committee 318. (1988). "Proposed Revisions to: Building Code Requirements for Reinforced Concrete (ACI 318-83) (Revised 1986)," ACI Structural Journal, Vol. 85, No. 6, November, pp. 645-674.

ACI Committee 318. (1989). "Proposed Revisions to: Building Code Requirements for Reinforced Concrete (ACI 318-83) (Revised 1986)," Discussion and Closure, ACI Structural Journal, Vol. 86, No. 3, May-June, pp. 323-352.

ASTM. (1989). "Standard Specification for Deformed and Plain Billet-Steel Bars for Concrete Reinforcement," (ASTM A 615-87a) 1989 Annual Book of ASTM Standards, Vol. 1.04, American Society for Testing and Materials, Philadelphia, PA, pp. 381-384.

ASTM. (1989). "Standard Specification for Epoxy-Coated Reinforcing Steel Bars," (ASTM A 775/A 775M-88a) 1989 Annual Book of ASTM Standards, Vol. 1.04, American Society for Testing and Materials, Philadelphia, PA, pp. 548-552.

Barsom, John and Rolfe, Stanley. (1987). Fracture and Fatigue Control in Structures, 2nd Edition, Prentice-Hall, pp. 30-38.

Brettmann, Barie B., Darwin, David, and Donahey, Rex C. (1986). "Bond of Reinforcement to Superplasticized Concrete," Journal of the American Concrete Institute, Proceedings Vol. 83, No. 1, January-February, pp. 98-107.

Chamberlin, S. J. (1956). "Spacing of Reinforcement in Beams," Journal of American Concrete Institute, Proceedings Vol. 53, July, pp. 113-134.

Chamberlin, S. J. (1958). "Spacing of Spliced Bars in Beams," Journal of American Concrete Institute, Proceedings Vol. 54, February, pp. 689-697.

Chinn, J., Ferguson, P. M., and Thompson, J. M. (1955). "Lapped Splices in Reinforced Concrete Beams," Journal of American Concrete Institute, Proceedings Vol. 52, October, pp. 201-213.

Choi, Oan C., Darwin, David, and McCabe, Steven L. (1990). "Bond Strength of Epoxy-Coated Reinforcement to Concrete," SM Report No. 25, University of Kansas Center for Research, Lawrence, Kansas, July, 217 pp.

Choi, Oan C., Hadje-Ghaffari, H., Darwin, David, and McCabe, Steven L. (1990). "Bond Epoxy-Coated Reinforcement to Concrete: Bar Parameters," SL Report 90-1, University of Kansas Center for Research, Lawrence, Kansas, January, 43 pp.

Clark, A. P. (1946). "Comparative Bond Efficiency of Deformed Concrete Reinforcing Bars," Journal of American Concrete Institute, Proceedings Vol. 43, No. 4, December, pp. 381-400.

Clark, A. P. (1949). "Bond of Concrete Reinforcing Bars," Journal of American Concrete Institute, Proceedings Vol. 46, No. 3, November, pp. 161-184.

Cleary, D. B. and Ramirez, J. A. (1989). "Bond of Epoxy Coated Reinforcing Steel in Concrete Bridge Decks," Joint Highway Research Project Informational Report, JHRP 89-7, Purdue University, 127 pp.

Clifton, James R., Beeghly, Hugh F., and Mathey, Robert G. (1975). "Nonmetallic Coatings for Concrete Reinforcing Bars," Building Science Series, No. 65, National Bureau of Standards, Washington, DC, 34 pp.

Clifton, James R., Mathey, Robert G., and Anderson, Erik D. (1979). "Creep of Coated Reinforcing Bars in Concrete," Journal of the Structural Division, ASCE, Vol. 105, ST10, October, pp. 1935-1947.

Clifton, James R. and Mathey, Robert G. (1983). "Bond and Creep Characteristics of Coated Reinforcement Bars in Concrete," Journal of the American Concrete Institute, Proceedings Vol. 80, No. 4, July-August, pp. 288-293.

Dodds, Robert H. and Lopez, Leonard A. (1980). "Generalized Software System for Non-Linear Analysis," Advances in Engineering Software, Vol. 2, No. 4, October, pp. 161-168.

Donahey, Rex C. and Darwin, David. (1985). "Bond of Top-Cast Bars in Bridge Decks," Journal of the American Concrete Institute, Proceedings Vol. 82, No. 1, January-February, pp. 57-66.

Ferguson, P. M. and Breen, J. E. (1965). "Lapped Splices for High Strength Reinforcing Bars," Journal of the American Concrete Institute, Proceedings Vol. 62, No. 9, September, pp. 1063-1078.

Ferguson, P. M. and Krishnaswamy, C. N. (1971). "Tensile Lap Splices -- Part 2: Design Recommendations for Retaining Wall Splices and Large Bar Splices," Research Report No. 113-3, Center for Highway Research, University of Texas at Austin, April, 60 pp.

Ferguson, Phil M. and Thompson, J. Neils. (1962). "Development Length of High Strength Reinforcing Bars in Bond," Journal of

the American Concrete Institute, Proceedings Vol. 59, No. 7, July, pp. 887-927.

Ferguson, Phil M. and Thompson, J. Neils. (1965). "Development Length for Large High Strength Reinforcing Bars," Journal of the American Concrete Institute, Proceedings Vol. 62, No. 1, January, pp. 71-91.

Herrmann, L. R. (1978). "Finite Element Analysis of Contact Problems," Journal of the Engineering Mechanics Division, ASCE, Vol. 104, No. EM5, October, pp. 1043-1057.

Hestor, Cynthia J., Salamizavaregh, Shahin, Darwin, David, and McCabe, Steven L. (1991). "Bond of Epoxy-Coated Reinforcement to Concrete: Splices," SL Report 91-1, University of Kansas Center for Research, Lawrence, Kansas, May.

Hillerborg, A., Modeer, M., and Petersson, P. E. (1976). "Analysis of Crack Formation and Crack Growth in Concrete by Means of Fracture Mechanics and Finite Elements," Cement and Concrete Research, Vol. 6, No. 6, November, pp. 773-782.

Jimenez, Rafael, Gergely, Peter, and White, Richard N. (1978). "Shear Transfer Across Cracks in Reinforced Concrete," Department of Structural Engineering, Cornell University, Ithaca, NY, August, 35 pp.

Johnston, David W. and Zia, Paul. (1982). "Bond Characteristics of Epoxy Coated Reinforcing Bars," Report No. FHWA-NC-82-002, Federal Highway Administration, Washington, DC, 163 pp.

Kobayashi, K. and Takewaka, K. (1984). "Experimental Studies on Epoxy Coated Reinforcing Steel for Corrosion Protection," The International Journal of Cement and Lightweight Concrete, Volume 6, Number 2, May, pp. 99-116.

Leibengood, L., Darwin, D., and Dodds, R. H. (1984). "Finite Element Analysis of Concrete Fracture Specimens," SM Report No. 11, University of Kansas Center for Research, Lawrence, Kansas, May, 120 pp.

Lopez, L. A., Dodds, R. H., Jr., Rehak, D. R., and Schmidt, R. S. (1991). Polo-finite: A Structural Mechanics System for Linear and Nonlinear Analysis. A technical report by the University of Illinois at Urbana-Champaign.

Lutz, L. A., Gergely, P., and Winter, G. (1966). "The Mechanics of Bond and Slip of Deformed Reinforcing Bars in Concrete," Report No. 324, Department of Structural Engineering, Cornell University, August, 306 pp.

Lutz, L. and Gergely, P.. (1967). "Mechanics of Bond and Slip of Deformed Bars in Concrete," Journal of the American Concrete Institute, Proceedings Vol. 64, No. 11, November, pp. 711-721.

Lutz, L. A. (1970). "Analysis of Stresses in Concrete near a Reinforcing Bar due to Bond and Transverse Cracking," Journal of the American Concrete Institute, Proceedings Vol. 67, No. 10, October, pp. 778-787.

Mathey, Robert G. and Watstein, David. (1961). "An Investigation of Bond in Beam and Pull-out Specimens with High-strength Deformed

Bars," Journal of the American Concrete Institute, Proceedings Vol. 57, No. 3, March, pp. 1071-1098.

Mathey, Robert G. and Clifton, James R. (1976). "Bond of Coated Reinforcing Bars in Concrete," Journal of the Structural Division, ASCE, Vol. 102, ST1, January, pp. 215-229.

Menzel, Carl A. (1939). "Some Factors Influencing Results of Pull-Out Bond Tests," Journal of the American Concrete Institute, Proceedings Vol. 35, No. 10, June, pp. 517-542.

Minor, J. and Jirsa, J. O. (1975). "Behavior of Bent Bar Anchorages," Journal of the American Concrete Institute, Proceedings Vol. 72, No. 4, April, pp. 141-149.

Orangun, C. O., Jirsa, J. O., and Breen, J. E. (1977). "A Reevaluation of Test Data on Development Length and Splices," Journal of the American Concrete Institute, Proceedings Vol. 74, No. 3, March, pp. 114-122.

PATRAN-II Modeling Software. (1990). PDA Engineering, 1560 Brookhollow Dr., Santa Ana, Calif. 92705.

Petersson, P-E. (1980). "Fracture Energy of Concrete: Method of Determination," Cement and Concrete Research, Vol. 10, No. 1, January, pp. 79-89.

Petersson, P-E. (1981). "Crack Growth and Development of Fracture Zones in Plain Concrete and Similar Materials," Report TVBM-1006, Div. of Bldg Materials, University of Lund, Sweden, 174 pp.

Pike, Robert G., Hay, Richard E., Clifton, James R., Beeghly, Hugh F., and Mathey, Robert F. (1973). "Nonmetallic Coatings for Concrete Reinforcing Bars," Public Roads, Vol. 37, No. 5, June, pp. 185-197.

Pinc, Robert L., Watkins, Michael D., and Jirsa, James O. (1977). "Strength of Hooked Bar Anchorages in Beam Column Joints," The Reinforced Concrete Research Council, Project 33, The University of Texas at Austin, November, 67 pp.

Rehm, G. (1961). "Ueber die Grundlagen des Verbundeszwischen Stahlund Beton. (The Fundamentals of Bond Between Steel Reinforcement and Concrete)," Berlin, Wilhelm Ernst and Sohn, Deutscher Ausschuss fur Stahlbeton, Heft 138, p. 59.

Skorobogatov, S. M. and Edwards, A. D. (1979). "The Influence of the Geometry of Deformed Steel Bars on Their Bond Strength in Concrete," The Institute of Civil Engineers, Proc., Vol. 67, Part 2, June, pp. 327-339.

Tepfers, R. (1973). "A Theory of Bond Applied to Overlapped Tensile Reinforcement Splices for Deformed Bars," Publication 73:2, Division of Concrete Structures, Chalmers University of Technology, Grotegorg, Sweden.

Tepfers, R. (1979). "Cracking of Concrete Cover Along Anchored Deformed Reinforcing Bars," Magazine of Concrete Research, Vol. 31, No. 106, March, pp. 3-12.

Tepfers, R. (1982). "Lapped Tensile Reinforcement Splices," Journal of the Structural Division, ASCE, Vol. 108, No. ST1, January, pp. 283-301.

Treece, R. A. and Jirsa, J. O. (1987). "Bond Strength of Epoxy-Coated Reinforcing Bars," PMFSEL Report No. 87-1, Phil M. Ferguson Structural Engineering Laboratory, The University of Texas at Austin, January, 85 pp.

Treece, R. A. and Jirsa, J. O. (1989). "Bond Strength of Epoxy-Coated Reinforcing Bars," ACI Materials Journal, Vol. 86, No. 2, March-April, pp. 167-174.

Zia, Paul. (1989). Personal Communication, North Carolina State University.

Zsutty, T. (1985). "Empirical Study of Bar Development Behavior," Journal of Structural Engineering, ASCE, Vol. 111, No. 1, January, pp. 205-219.

Table 2.1 : Average Test Bar Data

Bar size	Def. patt.	Yield stre. (ksi)	Def. height (in.)	Def. spac (in.)	Def. gap (in.)	Def. angle (deg.)	Def. face angle (deg.)	Bearing area per inch * (in.)	Related rib area +	Bearing area ratio $ (in.-1)
3	C	68.9	0.018	0.249	0.116	60	45	0.058	0.049	0.527
5	S	70.6	0.031	0.423	0.159	90	47	0.112	0.057	0.361
5	C	72.3	0.040	0.413	0.140	60	45	0.146	0.074	0.471
5	N	68.4	0.041	0.379	0.158	70	51	0.169	0.086	0.545
6	S	63.8	0.040	0.502	0.154	90	45	0.141	0.060	0.320
6	C	70.9	0.047	0.467	0.122	60	57	0.185	0.079	0.420
6	N	64.2	0.051	0.462	0.151	70	49	0.197	0.084	0.448
8	S	67.0	0.053	0.674	0.176	90	50	0.202	0.064	0.256
8	C	**	0.062	0.656	0.195	60	56	0.241	0.077	0.305
8	N	63.8	0.057	0.602	0.160	70	55	0.250	0.080	0.316
11	S	64.6	0.076	0.945	0.217	90	55	0.315	0.071	0.202
11	C	63.1	0.074	0.840	0.196	60	45	0.306	0.069	0.196
11	N	64.3	0.077	0.914	0.195	70	43	0.289	0.065	0.185

* bearing area of the deformations devided by the spacing of the deformations. Bearing area based on closely spaced measurements of ribs.

+ The ratio of the bearing area of the deformations to the shearing area between the deformations (bearing area devided by the nominal perimeter of the bar)

$ The ratio of the bearing area of the deformations to the area of the bar (bearing area devided by the nominal area of the bar)

** Yield strength is greater than 70.0 ksi.

Table 2.2 : Concrete Mixture Proportions (Cubic Yard Batch Weights)

Group	Nominal Strength (psi)	W/C ratio	Cement (lb)	Water (lb)	Aggregate Fine+ (lb)	Aggregate Coarse* (lb)
1	5000	0.55	509	280	1537	1575
2	6000	0.41	756	310	1245	1575
3-7	6000	0.45	622	280	1437	1575
8-17,21,22 27,28 SP2-SP4	6000	0.45	733	330	1213	1575
18-20,23**, 24++,25,26, 30,SP1	5000	0.55	600	330	1324	1575
29$	12000	0.25	935***	234	1524	1391+++

+ Kansas River Sand - Lawrence Sand Co., Lawrence, KS, bulk specific gravity = 2.62, absorption = 0.5%, fineness modulus = 3.0.

* Crushed limestone - Hamm's Quarry, Perry, KS, bulk specific gravity = 2.52, absorption = 3.5%, maximum size = 3/4 in., unit weigth = 97.2 lb/cubic ft.

$ 5500 cc 'Rheobuild 1000' superplasticizer by Master Builders was added

** 13000 cc 'Rheobuild 1000' was added

++ 10000 cc 'Rheobuild 1000' was added

*** 85 pounds of the total 935 pounds of cement weight is powder silica fume by master Builders. Bulk specific gravity = 2.20

+++ Crushed limestone - Hamm's Quarry, perry, KS -- Bulk specific gravity = 2.64, Absorption = 3.5%, maximum size = 1/2 inch, Unit weight=97.2 lb/ft3

Table 2.3 : Concrete Properties

Group	Slump (in.)	Concrete Temperature (F)	Age at Test (days)	Average Compressive Strength (psi)
1	1	57	3 - 4	4060 - 4910
2	2 1/2	60	3	5700
3	1 1/4	65	5	6090
4	1 1/4	73	4	6130
5	1 1/2	60	4	5920
6	1 1/2	70	5	5870
7	1	68	6	6000
8	3	80	4	5800
9	4	89	6	5650
10	4 1/2	85	7	5990
11	3 1/4	89	6	5970
12	3 1/4	92	7	5940
13	3 1/4	93	9	5840
14	4	88	7	5800
15	4 1/4	74	8	6000
16	3 1/2	72	4	6240
17	5 3/4	78	9	5850
18	4 1/4	57	3	4790
			4	5010
			5	5430
19	3 3/4	68	4	5070
			5	5270
20	2 3/4	89	9	5290
			10	5260

*, + refer to last page of table

Table 2.3 (cont.) : Concrete Properties

Group	Slump (in.)	Concrete Temperature (F)	Age at Test (days)	Average Compressive Strength (psi)
21	4	92	5	5990
22	4 1/2	64	7	6300
23	2-1/4	75	3	5120
	2-1/4	75	4	5580
	8	76	3	5580
	8	76	4	5790
24	2-1/2	70	5	4980
	2-1/2	70	6	5240
	8	71	5	5680
	8	71	6	5980
25	2-1/2	84	4	5030
26	2-1/2	71	5	4940
27+	1	99	8	6710
28	4	89	7	5810
			8	5960
29	8-1/2	70	132	12920
30	5-1/2	66	11	5110
SP1	4 3/4	70	11	5360
SP2	2 3/4	78	6	6010
SP3	5 1/2	74	6	5980
SP4	3 1/2	87	7	5850

* SP = Splice groups

+ Standard cylinders were cut in half due to honeycombing at the top half of the cylinders and the strengths were corrected to that of the standard cylinders in accordance to ASTM C 39.

Table 2.4 : Beam-end specimen results

Group No.	Specimen label ***	Average coating thickness (mils)	Cover ** (in.)	Concrete strength (psi)	Ultimate bond force (lbs)	Modified bond ++ force (lbs)	Lead length (in.)
1	8TS-E 5- 8.0	4.9	1.000	4480	23090	26721	3.75
1	8TS-E 9- 8.0	8.5	1.000	4820	21910	24445	3.75
1	8TS-E12- 8.0	13.8	1.000	4820	23640	26375	3.75
1	8TS-B 0- 8.0	0.0	1.000	4420	24180	28172	3.75
1	8TS-M 0- 8.0	0.0	1.000	4410	27090	31598	3.75
1	8TS-E 5- 8.0	4.1	2.000	4750	33680	37853	3.75
1	8TS-E 9- 8.0	7.9	2.000	4720	33360	37612	3.75
1	8TS-E12- 8.0	12.5	2.000	4710	36000	40631	3.75
1	8TS-B 0- 8.0	0.0	2.000	4770	39000	43740	3.75
1	8TS-M 0- 8.0	0.0	2.000	4780	38410	43033	3.75
1	8TS-E 5- 8.0	3.5	3.000	4110	43730	52836	3.75
1	8TS-E 9- 8.0	7.7	3.000	4080	40000	48507	3.75
1	8TS-E12- 8.0	11.0	3.000	4060	41450	50389	3.75
1	8TS-B 0- 8.0	0.0	3.000	4910	53420	59052	3.75
1	8TS-M 0- 8.0	0.0	3.000	4910	52170	57670	3.75
2	8BC-E12- 8.0	11.0	1.000	5700	24840	25485	3.75
2	8BC-E 9- 8.0	9.1	1.000	5700	25660	26326	3.75
2	8BC-E 5- 8.0	5.4	1.000	5700	25000	25649	3.75
2	8BC-B 0- 8.0	0.0	1.000	5700	33020	33877	3.75
2	8BC-M 0- 8.0	0.0	1.000	5700	31040	31846	3.75
2	8BC-E12- 8.0	13.3	2.000	5700	38300	39294	3.75
2	8BC-E 9- 8.0	10.0	2.000	5700	36760	37714	3.75
2	8BC-E 5- 8.0	5.3	2.000	5700	35990	36924	3.75
2	8BC-B 0- 8.0	0.0	2.000	5700	40000	41039	3.75
2	8BC-M 0- 8.0	0.0	2.000	5700	45990	47184	3.75
3	8BS-E12- 8.0	12.8	2.000	6090	27030	26829	3.75
3	8BS-E12- 8.0A	13.0	2.000	6090	32040	31802	3.75
3	8BS-E12- 8.0B	12.3	2.000	6090	29110	28894	3.75
3	8BS-E 9- 8.0	9.7	2.000	6090	29940	29717	3.75
3	8BS-E 9- 8.0A	10.2	2.000	6090	28140	27931	3.75
3	8BS-E 9- 8.0B	10.2	2.000	6090	31100	30869	3.75
3	8BS-E 5- 8.0	5.4	2.000	6090	28990	28774	3.75
3	8BS-E 5- 8.0A	6.4	2.000	6090	28580	28368	3.75

Note : Refer to the last page of the table for footnotes

Table 2.4 (cont.) : Beam-end specimen results

Group No.	Specimen label ***	Average coating thickness (mils)	Cover ** (in.)	Concrete strength (psi)	Ultimate bond force (lbs)	Modified bond ++ force (lbs)	Lead length (in.)
3	8BS-E 5- 8.0B	6.5	2.000	6090	32280	32040	3.75
3	8BS-B 0- 8.0	0.0	2.000	6090	44290	43961	3.75
3	8BS-B 0- 8.0A	0.0	2.000	6090	45640	45301	3.75
3	8BS-B 0- 8.0B	0.0	2.000	6090	43920	43594	3.75
3	8BS-M 0- 8.0	0.0	2.000	6090	43480	43157	3.75
3	8BS-M 0- 8.0A	0.0	2.000	6090	40960	40656	3.75
3	8BS-M 0- 8.0B	0.0	2.000	6090	40640	40338	3.75
4	8BN-E 9- 8.0	8.6	2.000	6130	35820	35438	3.75
4	8BN-E 9- 8.0A	8.5	2.000	6130	42030	41581	3.75
4	8BN-E 9- 8.0B	8.8	2.000	6130	34970	34597	3.75
4	8BN-B 0- 8.0	0.0	2.000	6130	46630	46132	3.75
4	8BN-B 0- 8.0A	0.0	2.000	6130	41620	41176	3.75
4	8BN-B 0- 8.0B	0.0	2.000	6130	41920	41473	3.75
4	8BN-M 0- 8.0	0.0	2.000	6130	45220	44737	3.75
4	8BN-M 0- 8.0A	0.0	2.000	6130	50000	49466	3.75
4	8BN-M 0- 8.0B	0.0	2.000	6130	44580	44104	3.75
5	8BC-E12- 8.0	13.8	2.000	5920	37370	37621	3.75
5	8BC-E12- 8.0A	13.2	2.000	5920	30590	30795	3.75
5	8BC-E12- 8.0B	12.7	2.000	5920	34560	34792	3.75
5	8BC-E 9- 8.0	9.5	2.000	5920	36070	36312	3.75
5	8BC-E 9- 8.0A	10.0	2.000	5920	33560	33785	3.75
5	8BC-E 9- 8.0B	9.4	2.000	5920	34290	34520	3.75
5	8BC-E 5- 8.0	5.5	2.000	5920	33440	33665	3.75
5	8BC-E 5- 8.0A	4.6	2.000	5920	35550	35789	3.75
5	8BC-E 5- 8.0B	3.7	2.000	5920	35560	35799	3.75
5	8BC-B 0- 8.0	0.0	2.000	5920	37520	37772	3.75
5	8BC-B 0- 8.0A	0.0	2.000	5920	46920	47235	3.75
5	8BC-B 0- 8.0B	0.0	2.000	5920	41150	41427	3.75
5	8BC-M 0- 8.0	0.0	2.000	5920	34550	34782	3.75
5	8BC-M 0- 8.0A	0.0	2.000	5920	34740	34973	3.75
5	8BC-M 0- 8.0B	0.0	2.000	5920	39490	39755	3.75

Note : Refer to the last page of the table for footnotes

Table 2.4 (cont.) : Beam-end specimen results

Group No.	Specimen label ***	Average coating thickness (mils)	Cover ** (in.)	Concrete strength (psi)	Ultimate bond force (lbs)	Modified bond ++ force (lbs)	Lead length (in.)
6	8BS-E 9- 8.0	7.9	2.000	5870	35430	35820	3.75
6	8BS-E 9- 8.0A	10.8	2.000	5870	32840	33201	3.75
6	8BS-B 0- 8.0	0.0	2.000	5870	47530	48053	3.75
6	8BS-B 0- 8.0A	0.0	2.000	5870	35930	36325	3.75
6	8BS-M 0- 8.0	0.0	2.000	5870	46500	47012	3.75
6	8BS-M 0- 8.0A	0.0	2.000	5870	42710	43180	3.75
6	8BC-E 9- 8.0	10.7	2.000	5870	33790	34162	3.75
6	8BC-E 9- 8.0A	9.1	2.000	5870	36630	37033	3.75
6	8BC-B 0- 8.0	0.0	2.000	5870	51430	51996	3.75
6	8BC-B 0- 8.0A	0.0	2.000	5870	42510	42978	3.75
6	8BC-M 0- 8.0	0.0	2.000	5870	43930	44413	3.75
6	8BC-M 0- 8.0A	0.0	2.000	5870	46820	47335	3.75
6	8BN-E 9- 8.0	9.2	2.000	5870	36620	37023	3.75
6	8BN-E 9- 8.0A	10.4	2.000	5870	45070	45566	3.75
6	8BN-B 0- 8.0	0.0	2.000	5870	50810	51369	3.75
6	8BN-B 0- 8.0A	0.0	2.000	5870	39150	39581	3.75
6	8BN-M 0- 8.0	0.0	2.000	5870	38000	38418	3.75
6	8BN-M 0- 8.0A	0.0	2.000	5870	47670	48194	3.75
7	5BN-E 9- 3.5	9.5	1.250	6000	16000	16000	3.75
7	5BN-E 9- 3.5A	10.1	1.250	6000	16080	16080	3.75
7	5BN-E 9- 3.5B	8.9	1.625	6000	16200	16200	3.75
7	5BN-B 0- 3.5	0.0	1.313	6000	15730	15730	3.75
7	5BN-B 0- 3.5A	0.0	1.281	6000	16050	16050	3.75
7	5BN-B 0- 3.5B	0.0	1.250	6000	16680	16680	3.75
7	5BN-M 0- 3.5	0.0	1.281	6000	16890	16890	3.75
7	5BN-M 0- 3.5A	0.0	1.250	6000	15930	15930	3.75
7	5BN-M 0- 3.5B	0.0	1.563	6000	17100	17100	3.75
7	5TN-E 9- 3.5	10.3	1.313	6000	14480	14480	3.75
7	5TN-E 9- 3.5A	10.0	1.313	6000	15200	15200	3.75
7	5TN-E 9- 3.5B	9.0	1.313	6000	15360	15360	3.75
7	5TN-B 0- 3.5	0.0	1.344	6000	15620	15620	3.75
7	5TN-B 0- 3.5B	0.0	1.344	6000	15440	15440	3.75
7	5TN-M 0- 3.5	0.0	1.313	6000	16330	16330	3.75
7	5TN-M 0- 3.5B	0.0	1.375	6000	16480	16480	3.75
7	5TN-M 0- 3.5	0.0	0.750	6000	14580	14580	3.75
7	5BN-M 0- 3.5	0.0	0.687	6000	12970	12970	3.75

Note : Refer to the last page of the table for footnotes

Table 2.4 (cont.) : Beam-end specimen results

Group No.	Specimen label ***	Average coating thickness (mils)	Cover ** (in.)	Concrete strength (psi)	Ultimate bond force (lbs)	Modified bond ++ force (lbs)	Lead length (in.)
8	5BN-M 0- 3.5	0.0	0.656	5800	13860	14096	3.75
8	5BN-E 9- 3.5	6.1	0.656	5800	13440	13669	3.75
8	5BN-M 0- 3.5	0.0	0.656	5800	10180	10228	2.38
8	5TN-M 0- 3.5	0.0	0.719	5800	10610	10346	2.38
8	5BN-E 9- 3.5	5.7	0.687	5800	11780	11185	2.38
8	5TN-E 9- 3.5	6.5	0.687	5800	9160	8767	2.38
8	5BN-M 0- 3.5	0.0	0.625	5800	10270	10445	1.50
8	5TN-M 0- 3.5	0.0	0.687	5800	8340	8482	1.50
8	5BN-E 9- 3.5	6.5	0.656	5800	7850	7984	1.50
8	5TN-E 9- 3.5	8.3	0.687	5800	8420	8563	1.50
8	5BN-M 0- 3.5	0.0	0.687	5800	8500	8645	0.75
8	5BN-M 0- 3.5	0.0	1.250	5800	18110	18419	3.75
8	5BN-E 9- 3.5	5.6	1.281	5800	15860	16131	3.75
8	5BN-M 0- 3.5	0.0	1.313	5800	14580	14577	2.38
8	5TN-M 0- 3.5	0.0	1.250	5800	12700	12917	2.38
8	5BN-E 9- 3.5	7.0	1.344	5800	14100	13633	2.38
8	5TN-E 9- 3.5	5.9	1.281	5800	12700	12455	2.38
8	5BN-M 0- 3.5	0.0	1.250	5800	10850	11035	1.50
8	5TN-M 0- 3.5	0.0	1.313	5800	10990	11177	1.50
8	5BN-E 9- 3.5	5.1	1.250	5800	11180	11371	1.50
8	5TN-E 9- 3.5	6.0	1.250	5800	10330	10506	1.50
9	5BS-E 5- 3.5	6.9	1.313	5650	11160	10902	2.38
9	5BS-E 5- 3.5A	5.5	1.313	5650	11910	11444	2.38
9	5BS-E 5- 3.5B	4.4	1.313	5650	13590	12994	2.38
9	5BS-E12- 3.5	14.5	1.313	5650	10520	11494	2.38
9	5BS-E12- 3.5A	17.1	1.375	5650	11340	12516	2.38
9	5BS-E12- 3.5B	11.8	1.313	5650	10630	11163	2.38
9	5BS-B 0- 3.5	0.0	1.313	5650	12440	12567	2.38
9	5BS-B 0- 3.5A	0.0	1.344	5650	13690	13729	2.38
9	5BS-B 0- 3.5B	0.0	1.313	5650	13890	14061	2.38
9	5BS-M 0- 3.5	0.0	1.313	5650	14770	14968	2.38
9	5BS-M 0- 3.5A	0.0	1.313	6310	14870	14248	2.38
9	5BS-M 0- 3.5B	0.0	1.344	5650	13220	13245	2.38
9	5TS-E 5- 3.5	5.8	1.438	5650	12080	11235	2.38

Note : Refer to the last page of the table for footnotes

Table 2.4 (cont.) : Beam-end specimen results

Group No.	Specimen label ***	Average coating thickness (mils)	Cover ** (in.)	Concrete strength (psi)	Ultimate bond force (lbs)	Modified bond ++ force (lbs)	Lead length (in.)
9	5TS-E 5- 3.5A	6.9	1.375	5650	11300	10839	2.38
9	5TS-E 5- 3.5B	5.9	1.344	5650	10410	9969	2.38
9	5TS-E12- 3.5	14.3	1.281	5650	10470	11175	2.38
9	5TS-E12- 3.5A	15.6	1.375	5650	10800	11202	2.38
9	5TS-E12- 3.5B	12.2	1.375	5650	9820	9849	2.38
9	5TS-B 0- 3.5	0.0	1.375	5650	11220	10969	2.38
9	5TS-B 0- 3.5A	0.0	1.438	5650	12520	12012	2.38
9	5TS-B 0- 3.5B	0.0	1.438	5650	12590	12084	2.38
9	5TS-M 0- 3.5	0.0	1.281	5650	10770	10950	2.38
9	5TS-M 0- 3.5A	0.0	1.406	5650	11860	11480	2.38
9	5TS-M 0- 3.5B	0.0	1.313	5650	12060	12131	2.38
10	5BC-E 9- 3.5	9.3	1.188	5990	12660	12971	2.38
10	5BC-E 9- 3.5A	10.1	1.250	5990	12950	13141	2.38
10	5BC-E 9- 3.5B	8.7	1.250	5990	12880	12841	2.38
10	5BC-E 5- 3.5	3.0	1.313	5990	14700	13472	2.38
10	5BC-E 5- 3.5A	4.5	1.250	5990	13370	12640	2.38
10	5BC-E 5- 3.5B	3.7	1.313	5990	14110	12996	2.38
10	5BC-B 0- 3.5	0.0	1.281	5990	13370	13255	2.38
10	5BC-B 0- 3.5A	0.0	1.250	5990	14560	14572	2.38
10	5BC-B 0- 3.5B	0.0	1.250	5990	13850	13861	2.38
10	5BC-M 0- 3.5	0.0	1.281	5990	13660	13545	2.38
10	5BC-M 0- 3.5A	0.0	1.250	5990	13340	13351	2.38
10	5BC-M 0- 3.5B	0.0	1.375	5990	14340	13847	2.38
10	5TC-E 9- 3.5	9.7	1.313	5990	11460	11243	2.38
10	5TC-E 9- 3.5A	7.7	1.406	5990	12070	11207	2.38
10	5TC-E 9- 3.5B	8.9	1.375	5990	11980	11386	2.38
10	5TC-E 5- 3.5	3.4	1.313	5990	12620	11768	2.38
10	5TC-E 5- 3.5A	4.0	1.313	5990	12390	11599	2.38
10	5TC-E 5- 3.5B	3.9	1.344	5990	11990	11040	2.38
10	5TC-B 0- 3.5	0.0	1.281	5990	12020	11881	2.38
10	5TC-B 0- 3.5A	0.0	1.250	5990	12060	12070	2.38
10	5TC-B 0- 3.5B	0.0	1.313	5990	12090	11803	2.38
10	5TC-M 0- 3.5	0.0	1.344	5990	12080	11645	2.38
10	5TC-M 0- 3.5A	0.0	1.313	5990	12210	11923	2.38
10	5TC-M 0- 3.5B	0.0	1.313	5990	12510	12223	2.38
10	5BC-M 0- 3.5	0.0	1.875	5990	17330	17344	2.38

Note : Refer to the last page of the table for footnotes

Table 2.4 (cont.) : Beam-end specimen results

Group No.	Specimen label ***	Average coating thickness (mils)	Cover ** (in.)	Concrete strength (psi)	Ultimate bond force (lbs)	Modified bond ++ force (lbs)	Lead length (in.)
10	5TC-M 0- 3.5	0.0	1.875	5990	14430	14442	2.38
11	5BN-E 9- 3.5	9.6	1.219	5970	12180	12435	2.38
11	5BN-E 9- 3.5A	10.0	1.250	5970	11630	11823	2.38
11	5BN-E 9- 3.5B	9.9	1.344	5970	11930	11730	2.38
11	5BN-B 0- 3.5	0.0	1.344	5970	12700	12353	2.38
11	5BN-B 0- 3.5A	0.0	1.344	5970	12870	12524	2.38
11	5BN-B 0- 3.5B	0.0	1.250	5970	14220	14255	2.38
11	5BN-M 0- 3.5	0.0	1.281	5970	12180	12084	2.38
11	5BN-M 0- 3.5A	0.0	1.250	5970	12800	12832	2.38
11	5BN-M 0- 3.5B	0.0	1.250	5970	13940	13974	2.38
11	5TN-E 9- 3.5	9.0	1.375	5970	11980	11416	2.38
11	5TN-E 9- 3.5A	9.5	1.313	5970	9010	8786	2.38
11	5TN-E 9- 3.5B	10.6	1.313	5970	8980	8867	2.38
11	5TN-B 0- 3.5	0.0	1.313	5970	11910	11643	2.38
11	5TN-B 0- 3.5A	0.0	1.313	5970	11710	11442	2.38
11	5TN-B 0- 3.5B	0.0	1.219	5970	11060	11236	2.38
11	5TN-M 0- 3.5	0.0	1.281	5970	11790	11671	2.38
11	5TN-M 0- 3.5A	0.0	1.250	5970	12080	12110	2.38
11	5TN-M 0- 3.5B	0.0	1.313	5970	11680	11412	2.38
11	5BN-M 0- 3.5	0.0	1.281	6090	7050	6997	0.00
11	5BN-M 0- 3.5A	0.0	1.188	6090	7000	6948	0.00
11	5TN-M 0- 3.5	0.0	1.313	6090	6770	6719	0.00
11	5TN-M 0- 3.5A	0.0	1.313	6090	6720	6670	0.00
12	5BN-M 0- 3.5	0.0	1.250	5940	15320	15397	2.38
12	5BN-M 0- 3.5A	0.0	1.250	5940	13830	13899	2.38
12	5BN-M 0- 3.5B	0.0	1.250	5940	12650	12713	2.38
12	5BN-E 9- 3.5	9.8	1.188	5940	12080	12524	2.38
12	5BN-E 9- 3.5A	10.5	1.188	5940	12570	13132	2.38
12	5BN-E 9- 3.5B	9.3	1.344	5940	11890	11621	2.38
12	5BN-M 0- 3.5	0.0	1.250	5940	10460	10512	1.50
12	5BN-M 0- 3.5A	0.0	1.250	5940	11250	11306	1.50
12	5BN-E 9- 3.5	8.3	1.250	5940	10690	10743	1.50
12	5BN-E 9- 3.5A	9.8	1.125	5940	11350	11407	1.50

Note : Refer to the last page of the table for footnotes

Table 2.4 (cont.) : Beam-end specimen results

Group No.	Specimen label ***	Average coating thickness (mils)	Cover ** (in.)	Concrete strength (psi)	Ultimate bond force (lbs)	Modified bond ++ force (lbs)	Lead length (in.)
12	5BN-M 0- 3.5	0.0	1.250	5940	9550	9598	1.00
12	5BN-M 0- 3.5A	0.0	1.313	5940	10730	10784	1.00
12	5BN-E 9- 3.5	9.0	1.281	5940	9260	9306	1.00
12	5BN-E 9- 3.5A	9.4	1.219	5940	10520	10572	1.00
12	5BN-M 0- 3.5	0.0	1.281	5940	9930	9980	0.50
12	5BN-M 0- 3.5A	0.0	1.063	5940	8720	8763	0.50
12	5BN-M 0- 3.5B	0.0	1.188	5940	9290	9336	0.50
12	5BN-E 9- 3.5	9.2	1.219	5940	8310	8351	0.50
12	5BN-E 9- 3.5A	9.6	1.313	5940	8360	8402	0.50
12	5BN-E 9- 3.5B	8.8	1.438	5940	8150	8191	0.50
12	5BN-M 0- 3.5	0.0	1.281	5940	7980	8020	0.00
12	5BN-M 0- 3.5A	0.0	1.188	5940	7980	8020	0.00
12	5BN-E 9- 3.5	9.8	1.313	5940	6870	6904	0.00
12	5BN-E 9- 3.5A	8.1	1.219	5940	7950	7990	0.00
13	5BN-M 0- 3.5	0.0	0.625	5844	10420	10558	2.38
13	5BN-M 0- 3.5A	0.0	0.625	5844	10130	10264	2.38
13	5BN-M 0- 3.5B	0.0	0.656	5844	11160	11181	2.38
13	5BN-E 5- 3.5	6.2	0.625	5844	9960	9630	2.38
13	5BN-E 5- 3.5A	5.7	0.625	5844	9970	9558	2.38
13	5BN-E 5- 3.5B	6.8	0.656	5844	10520	10171	2.38
13	5BN-M 0- 3.5	0.0	1.281	5844	12170	12205	2.38
13	5BN-M 0- 3.5A	0.0	1.250	5844	13660	13841	2.38
13	5BN-M 0- 3.5B	0.0	1.188	5844	12850	13272	2.38
13	5BN-E 5- 3.5	7.1	1.281	5844	13110	12844	2.38
13	5BN-E 5- 3.5A	6.2	1.250	5844	12000	11697	2.38
13	5BN-E 5- 3.5B	6.2	1.250	5844	11700	11393	2.38
13	5BN-M 0- 3.5	0.0	1.875	5844	14580	14773	2.38
13	5BN-M 0- 3.5A	0.0	1.938	5844	14650	14592	2.38
13	5BN-M 0- 3.5B	0.0	1.875	5844	16090	16303	2.38
13	5BN-E 5- 3.5	5.8	1.844	5844	14600	14392	2.38
13	5BN-E 5- 3.5A	6.4	1.875	5844	16080	15864	2.38
13	5BN-E 5- 3.5B	6.2	1.906	5844	14810	14419	2.38
14	6BS-M 0- 4.5	0.0	1.469	5800	20130	20660	2.75

Note : Refer to the last page of the table for footnotes

Table 2.4 (cont.) : Beam-end specimen results

Group No.	Specimen label ***	Average coating thickness (mils)	Cover ** (in.)	Concrete strength (psi)	Ultimate bond force (lbs)	Modified bond ++ force (lbs)	Lead length (in.)
14	6BS-M 0- 4.5A	0.0	1.469	5800	20210	20741	2.75
14	6BS-M 0- 4.5B	0.0	1.500	5800	16410	16690	2.75
14	6BS-E 5- 4.5	4.1	1.563	5800	15630	15524	2.75
14	6BS-E 5- 4.5A	4.8	1.500	5800	16140	16415	2.75
14	6BS-E 5- 4.5B	4.2	1.500	5800	14560	14808	2.75
14	6BS-E12- 4.5	11.8	1.500	5800	15430	15693	2.75
14	6BS-E12- 4.5A	10.9	1.563	5800	15250	15137	2.75
14	6BS-E12- 4.5B	11.6	1.531	5800	15330	15405	2.75
14	6BN-M 0- 4.5	0.0	1.500	5800	18000	18307	2.75
14	6BN-M 0- 4.5A	0.0	1.438	5800	18340	19026	2.75
14	6BN-M 0- 4.5B	0.0	1.500	5800	20240	20586	2.75
14	6BN-E 9- 4.5	7.2	1.563	5800	20680	20660	2.75
14	6BN-E 9- 4.5A	8.8	1.719	5800	19880	18915	2.75
14	6BN-E 9- 4.5B	8.0	1.563	5800	17760	17690	2.75
14	6BC-M 0- 4.5	0.0	1.500	5800	18850	19172	2.75
14	6BC-M 0- 4.5A	0.0	1.594	5800	17960	17707	2.75
14	6BC-M 0- 4.5B	0.0	1.500	5800	19000	19324	2.75
14	6BC-E 5- 4.5	4.7	1.563	5800	17290	17212	2.75
14	6BC-E 5- 4.5A	4.2	1.594	5800	18460	18216	2.75
14	6BC-E 5- 4.5B	4.1	1.563	5800	16970	16887	2.75
14	6BC-E12- 4.5	9.5	1.500	5800	18750	19070	2.75
14	6BC-E12- 4.5A	10.2	1.500	5800	18930	19253	2.75
14	6BC-E12- 4.5B	11.4	1.531	5800	17900	18019	2.75
15	8BS-M 0- 8.0	0.0	1.938	6000	41800	42650	3.75
15	8BS-M 0- 8.0A	0.0	2.000	6000	42700	42700	3.75
15	8BS-E 5- 8.0	4.1	2.000	6000	29050	29050	3.75
15	8BS-E 5- 8.0A	4.7	2.000	6000	33340	33340	3.75
15	8BS-E 5- 8.0B	6.8	1.938	6000	34730	35580	3.75
15	8BS-E12- 8.0	16.5	2.000	6000	30500	30500	3.75
15	8BS-E12- 8.0A	11.7	2.063	6000	29100	28249	3.75
15	8BS-E12- 8.0B	14.1	1.938	6000	32000	32850	3.75
15	8TS-E12- 8.0	7.0	2.063	6000	27400	26634	3.75
15	8TS-E12- 8.0A	12.1	2.000	6000	30200	30200	3.75
15	8BN-M 0- 8.0	0.0	2.000	5830	40600	41187	3.75
15	8BN-M 0- 8.0A	0.0	2.000	5830	42800	43419	3.75
15	8BN-M 0- 8.0B	0.0	2.000	5830	45140	45793	3.75

Note : Refer to the last page of the table for footnotes

Table 2.4 (cont.) : Beam-end specimen results

Group No.	Specimen label ***	Average coating thickness (mils)	Cover ** (in.)	Concrete strength (psi)	Ultimate bond force (lbs)	Modified bond ++ force (lbs)	Lead length (in.)
15	8TN-M 0- 8.0	0.0	2.063	5830	38900	38697	3.75
15	8TN-M 0- 8.0A	0.0	2.063	5830	43020	42876	3.75
15	8TN-M 0- 8.0B	0.0	2.125	5830	38900	37931	3.75
15	8TN-E 5- 8.0B	4.2	2.125	5830	33000	31945	3.75
16	6BN-M 0-10.5	0.0	1.563	6240	25200	24710	0.50
16	6BN-M 0-10.5A	0.0	1.469	6240	26500	25985	0.50
16	6BN-M 0-10.5B	0.0	1.563	6240	22900	22455	0.50
16	6BN-E 9-10.5	7.2	1.500	6240	26300	25789	0.50
16	6BN-E 9-10.5A	8.9	1.500	6240	23600	23141	0.50
16	6BN-E 9-10.5B	9.5	1.531	6240	25300	24808	0.50
16	8BN-M 0-14.0	0.0	2.031	6240	36800	36085	0.50
16	8BN-M 0-14.0A	0.0	2.000	6240	38800	38046	0.50
16	8BN-M 0-14.0B	0.0	2.031	6240	37800	37065	0.50
16	8BN-E 9-14.0	10.3	2.000	6240	31900	31280	0.50
16	8BN-E 9-14.0A	7.7	2.000	6240	36100	35398	0.50
16	8BN-E 9-14.0B	10.0	2.000	6240	31900	31280	0.50
16	5BN-M 0- 8.5	0.0	1.250	6240	18400	18042	0.50
16	5BN-M 0- 8.5A	0.0	1.281	6240	15800	15493	0.50
16	5BN-M 0- 8.5B	0.0	1.281	6240	19400	19023	0.50
16	5BN-E 9- 8.5	7.0	1.156	6240	17600	17258	0.50
16	5BN-E 9- 8.5A	5.6	1.219	6240	16600	16277	0.50
16	5BN-E 9- 8.5B	6.5	1.344	6240	18500	18140	0.50
16	5BS-M 0- 8.5	0.0	1.344	6240	18200	17846	0.50
16	5BS-M 0- 8.5A	0.0	1.313	6240	17400	17062	0.50
16	5BS-M 0- 8.5B	0.0	1.313	6240	17700	17356	0.50
16	5BS-E 9- 8.5	9.6	1.281	6240	11200	10982	0.50
16	5BS-E 9- 8.5A	9.0	1.250	6240	17000	16669	0.50
16	5BS-E 9- 8.5B	10.3	1.250	6240	12100	11865	0.50
17	6BC-M 0- 4.5	0.0	1.500	5850	17900	18128	2.75
17	6BC-M 0- 4.5A	0.0	1.563	5850	19800	19679	2.75
17	6BC-M 0- 4.5B	0.0	1.438	5850	17870	18470	2.75
17	6BC-E 5- 4.5	7.1	1.563	5850	16020	15851	2.75
17	6BC-E 5- 4.5A	5.9	1.500	5850	16740	16953	2.75

Note : Refer to the last page of the table for footnotes

Table 2.4 (cont.) : Beam-end specimen results

Group No.	Specimen label ***	Average coating thickness (mils)	Cover ** (in.)	Concrete strength (psi)	Ultimate bond force (lbs)	Modified bond ++ force (lbs)	Lead length (in.)
17	6BC-E 5- 4.5B	6.5	1.500	5850	16100	16305	2.75
17	6BC-E12- 4.5	9.3	1.500	5850	15890	16092	2.75
17	6BC-E12- 4.5A	10.5	1.500	5850	14570	14755	2.75
17	6BC-E12- 4.5B	10.9	1.500	5850	16160	16365	2.75
17	6BS-M 0- 4.5	0.0	1.469	5850	17400	17808	2.75
17	6BS-M 0- 4.5A	0.0	1.438	5850	18300	18905	2.75
17	6BS-M 0- 4.5B	0.0	1.500	5850	19200	19444	2.75
17	6BS-E 5- 4.5	5.7	1.500	5850	15130	15322	2.75
17	6BS-E 5- 4.5A	3.8	1.531	5850	15800	15814	2.75
17	6BS-E 5- 4.5B	3.6	1.531	5850	14900	14903	2.75
17	6BS-E12- 4.5	12.9	1.469	5850	15900	16288	2.75
17	6BS-E12- 4.5A	11.5	1.531	5850	16900	16928	2.75
17	6BS-E12- 4.5B	11.1	1.531	5850	13900	13890	2.75
17	6TS-M 0- 4.5	0.0	1.594	5850	13600	13189	2.75
17	6TS-M 0- 4.5A	0.0	1.656	5850	14200	13407	2.75
17	6TS-M 0- 4.5B	0.0	1.625	5850	15900	15323	2.75
17	6TS-E12- 4.5	13.2	1.438	5850	14400	14972	2.75
17	6TS-E12- 4.5A	10.4	1.656	5850	13700	12901	2.75
18	8BN-M 0- 8.0	0.0	0.937	5060	29200	32647	3.75
18	8BN-M 0- 8.0A	0.0	1.063	5060	29500	31272	3.75
18	8BN-M 0- 8.0B	0.0	1.063	5060	28660	30357	3.75
18	8BN-E12- 8.0	13.4	0.937	5060	23600	26549	3.75
18	8BN-E12- 8.0A	11.7	1.063	5060	27190	28757	3.75
18	8BN-E12- 8.0B	13.5	0.969	5060	27400	30262	3.75
18	8TN-M 0- 8.0	0.0	1.063	5060	25200	26675	3.75
18	8TN-M 0- 8.0A	0.0	1.156	5060	27200	27704	3.75
18	8TN-M 0- 8.0B	0.0	1.156	5060	27180	27682	3.75
18	8TN-E12- 8.0	11.1	1.063	5060	22800	24061	3.75
18	8TN-E12- 8.0A	12.6	1.094	5060	21840	22633	3.75
18	8TN-E12- 8.0B	14.2	1.063	5060	21300	22428	3.75
18	8BN-M 0- 8.0	0.0	1.875	5060	45600	51357	3.75
18	8BN-M 0- 8.0A	0.0	1.938	5060	42400	47021	3.75
18	8BN-M 0- 8.0B	0.0	1.875	5060	41040	46391	3.75
18	8BN-E12- 8.0	12.2	1.969	5060	33700	37122	3.75
18	8BN-E12- 8.0A	9.3	1.969	5060	35700	39300	3.75
18	8BN-E12- 8.0B	8.6	1.938	5060	35950	39997	3.75

Note : Refer to the last page of the table for footnotes

Table 2.4 (cont.) : Beam-end specimen results

Group No.	Specimen label ***	Average coating thickness (mils)	Cover ** (in.)	Concrete strength (psi)	Ultimate bond force (lbs)	Modified bond ++ force (lbs)	Lead length (in.)
18	8TN-M 0- 8.0	0.0	2.063	5060	32900	35059	3.75
18	8TN-M 0- 8.0A	0.0	1.938	5060	38600	41264	3.75
18	8TN-M 0- 8.0B	0.0	2.000	5060	35800	38983	3.75
18	8TN-E12- 8.0	11.8	2.000	5060	32630	35531	3.75
18	8TN-E12- 8.0A	13.7	2.063	5060	29800	31684	3.75
18	8TN-E12- 8.0B	12.7	2.063	5060	31530	33568	3.75
18	8BN-M 0- 8.0A	0.0	3.188	4790	58400	62808	3.75
18	8BN-M 0- 8.0B	0.0	3.000	4790	49600	55512	3.75
18	8BN-E12- 8.0	9.7	3.031	4790	47100	52288	3.75
18	8BN-E12- 8.0A	10.3	2.938	4790	51600	58601	3.75
18	8BN-E12- 8.0B	12.0	3.031	4790	50600	56206	3.75
18	8TN-M 0- 8.0A	0.0	3.063	4790	47110	51959	3.75
18	8TN-E12- 8.0	12.6	3.063	4790	42400	46688	3.75
18	8TN-E12- 8.0A	9.8	3.063	4790	43300	47695	3.75
18	8TN-E12- 8.0B	12.4	3.094	4790	43200	47200	3.75
18	8BS-M 0- 8.0	0.0	1.969	5440	36920	39199	3.75
18	8BS-M 0- 8.0A	0.0	2.031	5440	43540	45300	3.75
18	8BS-M 0- 8.0B	0.0	2.031	5440	37940	39419	3.75
18	8BS-E12- 8.0	8.1	2.063	5440	32660	33448	3.75
18	8BS-E12- 8.0A	9.7	1.906	5440	29510	32268	3.75
18	8BS-E12- 8.0B	11.6	1.906	5440	33510	36468	3.75
18	8TS-M 0- 8.0	0.0	2.094	5440	32120	32583	3.75
18	8TS-M 0- 8.0A	0.0	2.156	5440	34270	34075	3.75
18	8TS-M 0- 8.0B	0.0	2.063	5440	36490	37556	3.75
18	8TS-E12- 8.0	12.7	2.094	5440	29010	29317	3.75
18	8TS-E12- 8.0A	13.5	2.125	5440	29000	28924	3.75
18	8TS-E12- 8.0B	12.9	2.063	5440	29650	30372	3.75
19	11BN-M 0- 9.0	0.0	2.883	5070	36000	38666	1.50
19	11BN-M 0- 9.0A	0.0	2.945	5270	46100	48195	1.50
19	11BN-M 0- 9.0B	0.0	2.633	5270	36100	40009	1.50
19	11BN-E 9- 9.0	10.3	2.820	5270	32000	34144	1.50
19	11BN-E 9- 9.0A	8.5	2.820	5070	29600	32200	1.50
19	11BN-E 9- 9.0B	8.1	2.820	5270	28200	30089	1.50
19	11BN-M 0- 9.0	0.0	4.230	5070	48300	52543	1.50
19	11BN-M 0- 9.0A	0.0	4.230	5270	47500	50683	1.50
19	11BN-M 0- 9.0B	0.0	4.355	5270	42900	44781	1.50

Note : Refer to the last page of the table for footnotes

Table 2.4 (cont.) : Beam-end specimen results

Group No.	Specimen label ***	Average coating thickness (mils)	Cover ** (in.)	Concrete strength (psi)	Ultimate bond force (lbs)	Modified bond ++ force (lbs)	Lead length (in.)
19	11BN-E 9- 9.0	9.6	4.355	5070	37000	39257	1.50
19	11BN-E 9- 9.0A	9.4	4.293	5270	44200	46665	1.50
19	11BN-E 9- 9.0B	12.2	4.293	5270	40900	43144	1.50
19	11BS-M 0- 9.0	0.0	2.758	5270	38600	41683	1.50
19	11BS-M 0- 9.0A	0.0	2.851	5270	36300	38484	1.50
19	11BS-M 0- 9.0B	0.0	2.883	5070	34400	36925	1.50
19	11BS-E 9- 9.0	11.0	2.820	5270	27600	29449	1.50
19	11BS-E 9- 9.0A	10.9	2.695	5070	27700	31127	1.50
19	11BS-E 9- 9.0B	12.6	2.820	5270	36400	38839	1.50
19	11BC-M 0- 9.0	0.0	2.570	5070	37500	42781	1.50
19	11BC-M 0- 9.0A	0.0	2.789	5270	37800	40581	1.50
19	11BC-M 0- 9.0B	0.0	2.758	5270	35100	37948	1.50
19	11BC-E 9- 9.0	12.1	2.820	5070	29000	31547	1.50
19	11BC-E 9- 9.0A	13.1	2.820	5270	27700	29556	1.50
19	11BC-E 9- 9.0B	12.4	2.883	5270	29100	30553	1.50
20	11BN-M 0- 9.0	0.0	1.410	5290	34120	36337	1.50
20	11BN-M 0- 9.0A	0.0	1.160	5260	31260	35373	1.50
20	11BN-M 0- 9.0B	0.0	1.410	5260	32480	34689	1.50
20	11BN-E 9- 9.0	10.5	1.285	5290	23570	26095	1.50
20	11BN-E 9- 9.0A	7.9	1.410	5260	27900	29797	1.50
20	11BN-E 9- 9.0B	6.9	1.348	5260	25690	27934	1.50
20	11BN-M 0- 9.0	0.0	2.883	5290	47380	49962	1.50
20	11BN-M 0- 9.0A	0.0	3.070	5260	39500	40200	1.50
20	11BN-M 0- 9.0B	0.0	2.758	5260	41330	44638	1.50
20	11BN-E 9- 9.0	10.4	2.945	5290	29300	30210	1.50
20	11BN-E 9- 9.0A	8.7	3.008	5260	33700	33012	1.50
20	11BN-E 9- 9.0B	9.2	2.883	5260	32910	34652	1.50
20	11BN-M 0- 9.0	0.0	4.136	5260	52550	63278	1.50
20	11BN-M 0- 9.0A	0.0	4.230	5260	48300	51585	1.50
20	11BN-M 0- 9.0B	0.0	4.168	5260	58610	63093	1.50
20	11BN-E 9- 9.0	9.0	4.230	5260	48660	51970	1.50
20	11BN-E 9- 9.0A	9.1	4.043	5260	44680	49209	1.50
20	11BN-E 9- 9.0B	8.9	4.230	5260	46280	49428	1.50
20	11BS-M 0- 9.0	0.0	2.883	5290	36480	38354	1.50
20	11BS-M 0- 9.0A	0.0	2.883	5260	43990	46485	1.50
20	11BS-M 0- 9.0B	0.0	2.758	5260	38060	41145	1.50

Note : Refer to the last page of the table for footnotes

Table 2.4 (cont.) : Beam-end specimen results

Group No.	Specimen label ***	Average coating thickness (mils)	Cover ** (in.)	Concrete strength (psi)	Ultimate bond force (lbs)	Modified bond ++ force (lbs)	Lead length (in.)
20	11BS-E 9- 9.0	10.9	2.883	5290	41780	43998	1.50
20	11BS-E 9- 9.0A	9.4	2.820	5260	36030	38481	1.50
20	11BS-E 9- 9.0B	9.7	2.820	5260	39560	42251	1.50
20	11BC-M 0- 9.0	0.0	2.945	5290	41580	43289	1.50
20	11BC-M 0- 9.0A	0.0	2.883	5260	34500	36350	1.50
20	11BC-M 0- 9.0B	0.0	2.883	5260	39440	41626	1.50
20	11BC-E 9- 9.0	9.4	2.820	5290	28320	30160	1.50
20	11BC-E 9- 9.0A	8.2	2.758	5260	38600	41722	1.50
20	11BC-E 9- 9.0B	8.4	2.758	5260	33800	36596	1.50
21	5BC-M 0- 3.5	0.0	0.969	5990	14180	15325	2.38
21	5BC-M 0- 3.5A	0.0	1.188	5990	14530	14794	2.38
21	5BC-M 0- 3.5B	0.0	1.188	5990	14850	15114	2.38
21	5BC-E 5- 3.5	4.3	1.219	5990	12880	12242	2.38
21	5BC-E 5- 3.5A	5.0	1.219	5990	13030	12508	2.38
21	5BC-E 5- 3.5B	4.7	1.000	5990	12990	13300	2.38
21	5BC-E12- 3.5	11.2	1.375	5990	12840	12709	2.38
21	5BC-E12- 3.5A	11.3	1.250	5990	12670	13059	2.38
21	5BC-E12- 3.5B	10.8	1.250	5990	13900	14208	2.38
21	5BS-M 0- 3.5	0.0	0.875	5990	12790	14312	2.38
21	5BS-M 0- 3.5A	0.0	1.250	5990	14750	14762	2.38
21	5BS-M 0- 3.5B	0.0	1.188	5990	14460	14724	2.38
21	5BS-E 5- 3.5	4.7	1.250	5990	12460	11762	2.38
21	5BS-E 5- 3.5A	5.3	1.125	5990	12850	12755	2.38
21	5BS-E 5- 3.5B	5.6	1.250	5990	12880	12330	2.38
21	5BS-E12- 3.5	13.8	1.250	5990	10220	11019	2.38
21	5BS-E12- 3.5A	10.0	1.031	5990	11340	12396	2.38
21	5BS-E12- 3.5B	11.7	1.375	5990	11820	11770	2.38
22	6BN-M 0- 4.5	0.0	1.375	6300	19290	19570	2.75
22	6BN-M 0- 4.5A	0.0	1.500	6300	19970	19488	2.75
22	6BN-M 0- 4.5B	0.0	1.500	6300	19440	18971	2.75
22	6BN-M 0- 4.5C	0.0	1.625	6300	24530	23193	2.75
22	6BN-M 0- 4.5D	0.0	1.313	6300	19880	20519	2.75
22	6BN-M 0- 4.5E	0.0	1.500	6300	21080	20571	2.75

Note : Refer to the last page of the table for footnotes

Table 2.4 (cont.) : Beam-end specimen results

Group No.	Specimen label ***	Average coating thickness (mils)	Cover ** (in.)	Concrete strength (psi)	Ultimate bond force (lbs)	Modified bond ++ force (lbs)	Lead length (in.)
22	6BN-E 9- 4.5	9.8	1.406	6300	18390	18505	2.75
22	6BN-E 9- 4.5A	8.0	1.438	6300	19330	19236	2.75
22	6BN-E 9- 4.5B	9.7	1.313	6300	16140	16869	2.75
22	6BN-E 9- 4.5C	8.6	1.375	6300	19560	19834	2.75
22	6BN-E 9- 4.5D	8.9	1.469	6300	17870	17625	2.75
22	6BN-E 9- 4.5E	8.0	1.281	6300	17960	18831	2.75
23+	8BN-M 0- 8.0	0.0	1.938	5580	42200	44610	3.75
23	8BN-M 0- 8.0A	0.0	1.938	5580	37850	40099	3.75
23	8BN-M 0- 8.0B	0.0	2.063	5120	41000	43532	3.75
23	8BN-E12- 8.0	12.5	2.000	5120	30870	33417	3.75
23	8BN-E12- 8.0A	10.2	1.875	5580	35270	38275	3.75
23	8BN-E12- 8.0B	11.3	2.000	5580	36210	37548	3.75
23	8TN-M 0- 8.0	0.0	2.031	5580	42800	43998	3.75
23	8TN-M 0- 8.0A	0.0	1.969	5580	39280	41114	3.75
23	8TN-M 0- 8.0B	0.0	2.000	5120	38100	41244	3.75
23	8TN-E12- 8.0	12.4	2.000	5120	33580	36351	3.75
23	8TN-E12- 8.0A	11.7	2.063	5580	37400	38016	3.75
23	8TN-E12- 8.0B	11.9	2.063	5580	34690	35205	3.75
23	8BN-M 0- 8.0	0.0	1.938	5790	37210	38729	3.75
23	8BN-M 0- 8.0A	0.0	1.969	5790	38980	40106	3.75
23	8BN-M 0- 8.0B	0.0	2.000	5580	43200	44796	3.75
23	8BN-E12- 8.0	10.1	1.875	5580	31300	34158	3.75
23	8BN-E12- 8.0A	11.0	1.906	5790	34020	35907	3.75
23	8BN-E12- 8.0B	10.0	1.875	5790	31710	33981	3.75
23	8TN-M 0- 8.0	0.0	2.063	5790	37280	37184	3.75
23	8TN-M 0- 8.0A	0.0	2.063	5790	40680	40645	3.75
23	8TN-M 0- 8.0B	0.0	2.063	5580	34100	34594	3.75
23	8TN-E12- 8.0	12.2	2.000	5580	34040	35297	3.75
23	8TN-E12- 8.0A	10.3	2.000	5790	36190	36840	3.75
23	8TN-E12- 8.0B	9.8	2.000	5790	33260	33857	3.75
23	8BN-M 0- 8.0	0.0	2.125	5580	34600	34176	3.75
23	8BN-M 0- 8.0A	0.0	2.000	5790	36650	37308	3.75
23	8BN-M 0- 8.0B	0.0	2.000	5790	29300	29826	3.75
23	8BN-E12- 8.0	12.6	1.938	5790	29930	31318	3.75
23	8BN-E12- 8.0A	13.0	1.875	5790	28500	30713	3.75
23	8BN-E12- 8.0B	12.1	1.938	5580	28190	30082	3.75

Note : Refer to the last page of the table for footnotes

Table 2.4 (cont.) : Beam-end specimen results

Group No.	Specimen label ***	Average coating thickness (mils)	Cover ** (in.)	Concrete strength (psi)	Ultimate bond force (lbs)	Modified bond ++ force (lbs)	Lead length (in.)
23	8TN-M 0- 8.0	0.0	2.063	5580	32360	32789	3.75
23	8TN-M 0- 8.0A	0.0	2.125	5790	27990	26961	3.75
23	8TN-M 0- 8.0B	0.0	2.000	5790	36100	36748	3.75
23	8TN-E12- 8.0	10.7	2.031	5790	25160	25229	3.75
23	8TN-E12- 8.0A	10.1	2.000	5790	23500	23922	3.75
23	8TN-E12- 8.0B	10.2	2.000	5580	19940	20676	3.75
24+	8BN-M 0- 8.0	0.0	2.125	4980	37520	42886	3.75
24	8BN-M 0- 8.0A	0.0	2.031	5240	37830	40055	3.75
24	8BN-M 0- 8.0B	0.0	1.969	5240	40840	44126	3.75
24	8BN-E12- 8.0	11.1	1.938	4980	36400	40805	3.75
24	8BN-E12- 8.0A	10.4	1.938	5240	35430	38763	3.75
24	8BN-E12- 8.0B	12.4	1.875	5240	37560	41893	3.75
24	8TN-M 0- 8.0	0.0	2.063	4980	35810	38540	3.75
24	8TN-M 0- 8.0A	0.0	2.156	5240	34790	35312	3.75
24	8TN-M 0- 8.0B	0.0	2.000	5240	36020	38543	3.75
24	8TN-E12- 8.0	11.6	2.094	4980	34680	36917	3.75
24	8TN-E12- 8.0A	8.7	2.125	5250	34190	35018	3.75
24	8TN-E12- 8.0B	8.8	2.063	5240	30430	31796	3.75
24	8BN-M 0- 8.0	0.0	1.906	5680	41650	44083	3.75
24	8BN-M 0- 8.0A	0.0	1.813	5980	43610	46235	3.75
24	8BN-M 0- 8.0B	0.0	1.938	5980	40310	41228	3.75
24	8BN-E12- 8.0	11.8	1.875	5680	35830	38527	3.75
24	8BN-E12- 8.0A	12.3	1.906	5980	31640	32969	3.75
24	8BN-E12- 8.0B	10.8	1.938	5980	34090	34997	3.75
24	8TN-M 0- 8.0	0.0	2.000	5680	33760	34697	3.75
24	8TN-M 0- 8.0A	0.0	2.094	5980	38350	37265	3.75
24	8TN-M 0- 8.0B	0.0	2.063	5980	36780	36075	3.75
24	8TN-E12- 8.0	11.5	2.031	5680	32650	33174	3.75
24	8TN-E12- 8.0A	12.0	1.906	5980	36930	38140	3.75
24	8TN-E12- 8.0B	8.3	2.031	5980	30340	30007	3.75
24	8BN-M 0- 8.0	0.0	1.813	5680	38290	41906	3.75
24	8BN-M 0- 8.0A	0.0	1.813	5980	41570	44192	3.75
24	8BN-M 0- 8.0B	0.0	1.875	5980	40100	41868	3.75
24	8BN-E12- 8.0	12.2	1.938	5680	32940	34706	3.75
24	8BN-E12- 8.0A	8.2	1.938	5980	34260	35168	3.75
24	8BN-E12- 8.0B	12.4	1.844	5980	26200	28370	3.75

Note : Refer to the last page of the table for footnotes

Table 2.4 (cont.) : Beam-end specimen results

Group No.	Specimen label ***	Average coating thickness (mils)	Cover ** (in.)	Concrete strength (psi)	Ultimate bond force (lbs)	Modified bond ++ force (lbs)	Lead length (in.)
24	8TN-M 0- 8.0	0.0	2.031	5680	34820	35404	3.75
24	8TN-M 0- 8.0A	0.0	2.094	5980	36330	35241	3.75
24	8TN-M 0- 8.0B	0.0	2.063	5980	35300	34593	3.75
24	8TN-E12- 8.0	10.3	1.938	5680	27260	28783	3.75
24	8TN-E12- 8.0A	11.6	2.031	5980	31340	31009	3.75
24	8TN-E12- 8.0B	8.9	2.063	5980	28960	28242	3.75
25*	5BC-M 0- 90	0.0	1.313	5030	18220	19899	3.00
25	5BC-M 0- 90A	0.0	1.313	5030	18760	20489	3.00
25	5BC-M 0- 90B	0.0	1.188	5030	18720	20445	3.00
25	5BC-E12- 90	9.7	1.313	5030	17520	19134	3.00
25	5BC-E12- 90A	9.1	1.281	5030	16530	18053	3.00
25	5BC-E12- 90B	9.5	1.469	5030	16780	18326	3.00
25	5BC-E12- 90	9.1	1.219	5030	16270	17769	3.00
25	5BC-E12- 90A	8.2	1.188	5030	17360	18960	3.00
25	5BC-E12- 90B	9.6	1.188	5030	15120	16513	3.00
25	5BC-M 0- 180	0.0	1.250	5030	16000	17474	3.00
25	5BC-M 0- 180A	0.0	1.313	5030	14510	15847	3.00
25	5BC-M 0- 180B	0.0	1.250	5030	16640	18173	3.00
25	5BC-E12- 180	8.3	1.344	5030	0	0	3.00
25	5BC-E12- 180A	10.0	1.344	5030	16960	18523	3.00
25	5BC-E12- 180B	10.9	1.219	5030	15990	17463	3.00
25	5BC-E12- 180	8.3	1.219	5030	15770	17223	3.00
25	5BC-E12- 180A	9.2	1.375	5030	12990	14187	3.00
25	5BC-E12- 180B	8.2	1.250	5030	16250	17747	3.00
26*	8BC-M 0- 90	0.0	2.063	4940	47970	52866	4.50
26	8BC-M 0- 90A	0.0	1.875	4940	50760	55941	4.50
26	8BC-M 0- 90B	0.0	1.813	4940	49490	54541	4.50
26	8BC-E12- 90	9.8	1.750	4940	48670	53638	4.50
26	8BC-E12- 90A	9.3	1.938	4940	41140	45339	4.50
26	8BC-E12- 90B	11.9	2.063	4940	45500	50144	4.50
26	8BC-E12- 90	11.3	1.813	4940	51420	56668	4.50
26	8BC-E12- 90A	10.1	2.031	4940	46570	51323	4.50
26	8BC-E12- 90B	10.1	2.063	4940	48060	52965	4.50

Note : Refer to the last page of the table for footnotes

Table 2.4 (cont.) : Beam-end specimen results

Group No.	Specimen label ***	Average coating thickness (mils)	Cover ** (in.)	Concrete strength (psi)	Ultimate bond force (lbs)	Modified bond ++ force (lbs)	Lead length (in.)
27$	8BN-M 0- 8.0	0.0	1.875	6710	29110	27526	1.00
27	8BN-M 0- 8.0A	0.0	1.813	6710	39640	37484	1.00
27	8BN-M 0- 8.0B	0.0	2.000	6710	39600	37446	1.00
27	8BN-E 9- 8.0	8.7	1.938	6710	30710	29039	1.00
27	8BN-E 9- 8.0A	8.8	2.000	6710	31800	30070	1.00
27	8BN-E 9- 8.0B	7.4	2.063	6710	32300	30543	1.00
27	8BS-M 0- 8.0	0.0	1.875	6710	35200	33285	1.00
27	8BS-M 0- 8.0A	0.0	1.875	6710	33490	31668	1.00
27	8BS-M 0- 8.0B	0.0	1.813	6710	35280	33361	1.00
27	8BS-E 9- 8.0	7.3	1.875	6710	27890	26373	1.00
27	8BS-E 9- 8.0A	7.5	1.938	6710	32540	30770	1.00
27	8BS-E 9- 8.0B	7.4	1.875	6710	28300	26760	1.00
27	5BN-M 0- 3.5	0.0	1.250	6710	9930	9389	0.62
27	5BN-M 0- 3.5A	0.0	1.375	6710	9480	8964	0.62
27	5BN-M 0- 3.5B	0.0	1.250	6710	10380	9815	0.62
27	5BN-E 9- 3.5	6.8	1.188	6710	8430	7971	0.62
27	5BN-E 9- 3.5A	6.8	1.250	6710	7820	7394	0.62
27	5BN-E 9- 3.5B	8.7	1.250	6710	9140	8642	0.62
27	5BS-M 0- 3.5	0.0	1.063	6710	8730	8255	0.62
27	5BS-M 0- 3.5A	0.0	1.125	6710	9050	8557	0.62
27	5BS-M 0- 3.5B	0.0	1.156	6710	10220	9664	0.62
27	5BS-E 9- 3.5	8.5	1.250	6710	9920	9380	0.62
27	5BS-E 9- 3.5A	9.4	1.156	6710	5670	5361	0.62
27	5BS-E 9- 3.5B	10.9	1.250	6710	8240	7791	0.62
28$	8BN-M 0- 8.0	0.0	1.813	5810	43850	47113	3.75
28	8BN-M 0- 8.0A	0.0	1.938	5810	47360	48979	3.75
28	8BN-M 0- 8.0B	0.0	2.188	5810	45260	43441	3.75
28	8BN-E 9- 8.0	7.6	1.625	5810	37830	43548	3.75
28	8BN-E 9- 8.0A	8.5	1.938	5810	40150	41652	3.75
28	8BN-E 9- 8.0B	8.3	1.906	5810	37490	39374	3.75
28	8BS-M 0- 8.0	0.0	1.813	5810	44520	47794	3.75
28	8BS-M 0- 8.0A	0.0	1.750	5810	41990	46074	3.75
28	8BS-M 0- 8.0B	0.0	1.750	5810	47440	51612	3.75

Note : Refer to the last page of the table for footnotes

Table 2.4 (cont.) : Beam-end specimen results

Group No.	Specimen label ***	Average coating thickness (mils)	Cover ** (in.)	Concrete strength (psi)	Ultimate bond force (lbs)	Modified bond ++ force (lbs)	Lead length (in.)
28	8BS-E 9- 8.0	6.6	1.875	5810	36700	38997	3.75
28	8BS-E 9- 8.0A	9.3	1.875	5810	40430	42787	3.75
28	8BS-E 9- 8.0B	9.6	1.750	5810	31730	35648	3.75
28	5BN-M 0- 3.5	0.0	1.250	5960	15690	15742	2.38
28	5BN-M 0- 3.5A	0.0	1.188	5960	14250	14549	2.38
28	5BN-M 0- 3.5B	0.0	1.125	5960	14580	15132	2.38
28	5BN-E 9- 3.5	9.4	1.125	5960	12950	13563	2.38
28	5BN-E 9- 3.5A	10.8	1.188	5960	12870	13461	2.38
28	5BN-E 9- 3.5B	9.6	1.188	5960	13200	13595	2.38
28	5BS-M 0- 3.5	0.0	1.375	5960	15450	14997	2.38
28	5BS-M 0- 3.5A	0.0	1.188	5960	14550	14850	2.38
28	5BS-M 0- 3.5B	0.0	1.250	5960	14020	14066	2.38
28	5BS-E 9- 3.5	10.5	1.125	5960	12120	12911	2.38
28	5BS-E 9- 3.5A	10.6	1.375	5960	12250	12050	2.38
28	5BS-E 9- 3.5B	9.3	1.188	5960	11600	11940	2.38
29	6BS-M 0- 4.5	0.0	1.469	12920	17720	17263	2.75
29	6BS-M 0- 4.5A	0.0	1.563	12920	19410	18333	2.75
29	6BS-M 0- 4.5B	0.0	1.500	12920	18800	18118	2.75
29	6BS-E12- 4.5	9.3	1.375	12920	15540	15722	2.75
29	6BS-E12- 4.5A	13.5	1.438	12920	15580	15387	2.75
29	6BS-E12- 4.5B	14.5	1.500	12920	14680	14147	2.75
29	6TS-M 0- 4.5	0.0	1.563	12920	18920	17844	2.75
29	6TS-M 0- 4.5A	0.0	1.625	12920	16890	15498	2.75
29	6TS-M 0- 4.5B	0.0	1.531	12920	15580	14820	2.75
29	6TS-E12- 4.5	16.4	1.625	12920	17860	16433	2.75
29	6TS-E12- 4.5A	14.8	1.563	12920	16680	15685	2.75
29	6TS-E12- 4.5B	11.2	1.375	12920	12830	13143	2.75
30$	11BN-M 0- 9.0	0.0	2.633	5110	52420	58292	1.50
30	11BN-M 0- 9.0A	0.0	2.820	5110	48960	53052	1.50
30	11BN-M 0- 9.0B	0.0	2.820	5110	45870	49704	1.50
30	11BN-M 0- 9.0C	0.0	2.758	5110	49250	53863	1.50
30	11BN-M 0- 9.0D	0.0	2.820	5110	50500	54721	1.50
30	11BN-E 9- 9.0	8.3	2.789	5110	43810	47720	1.50

Note : Refer to the last page of the table for footnotes

Table 2.4 (cont.) : Beam-end specimen results

Group No.	Specimen label ***	Average coating thickness (mils)	Cover ** (in.)	Concrete strength (psi)	Ultimate bond force (lbs)	Modified bond ++ force (lbs)	Lead length (in.)
30	11BN-E 9- 9.0A	7.0	2.820	5110	41660	45142	1.50
30	11BN-E 9- 9.0B	8.8	2.758	5110	44300	48499	1.50
30	11BN-E 9- 9.0C	9.1	2.851	5110	42380	45674	1.50
30	11BS-M 0- 9.0	0.0	2.820	5110	45010	48772	1.50
30	11BS-M 0- 9.0A	0.0	2.758	5110	45610	49919	1.50
30	11BS-M 0- 9.0B	0.0	2.820	5110	49160	53269	1.50
30	11BS-M 0- 9.0C	0.0	2.883	5110	44850	48102	1.50
30	11BS-E 9- 9.0	8.9	2.633	5110	47470	52928	1.50
30	11BS-E 9- 9.0A	10.1	2.633	5110	45640	50945	1.50
30	11BS-E 9- 9.0B	9.0	2.758	5110	41460	45422	1.50
30	11BS-E 9- 9.0C	8.1	2.883	5110	44100	47289	1.50

* These specimens had either a 90.0 or 180.0 degrees hoohs.

\+ Deep specimens.

$ The test bar in these specimens were confined with No. 3 stirrups.

** The actual measured cover before testing. The cover was not measured for the specimens in groups 1-6, and, therefore, the cover was assumed to be equal to the nominal cover.

++ Modified bond force is the corrected ultimate bond force for the variations in the concrete cover of 1, 2, or 3 db, coating thickness of 5, 9, or 12 mils, and concrete strength of 6000 or 12000 psi.

*** Specimen label

#PD-SC-LR

: Bar size : 5, 6, 8, 11

P : Bar position : B = bottom, t = top

D : Deformation pattern : S, C, N

S : Bar surface condition : M = uncoated, C = coated

C : Nominal coating thickness : 0, 5, 9, 12 mils

L : Bonded length of the test bar

Note : In groups 25 and 26 : 90 = 90 degrees bend

180 = 180 degrees bend

R : Replication I.D. : blank, A, B, C, D, E

Table 2.5 : Summary of the Beam Splice Tests

Group	Bar No.	Def. patt.	Splice length (in.)	Average Coating Thickness (mils)	Concrete Strength (psi)	No. of cracks	Widest crack (mils)	Bar stress for crack comparison (ksi)	Ult. moment (k-in)	Ult. stress (ksi)	+ C/U
SP1	5	N	12	0.0	5360	7	9	40.9	521	62.5	
	5*	N	12	0.0		8	7	42.1	813	65.3	
	5*	N	12	9.5		6	7	42.1	609	49.0	0.75
SP2	6	S	12	0.0	6010	6	7	36.7	543	45.8	
	6	S	12	8.3		3	9	36.7	511	43.1	0.94
	6	C	12	0.0		5	5	36.7	610	51.4	
	6	C	12	8.8		6	5	36.7	466	39.3	0.76
SP3	8	S	16	0.0	5980	6	7	25.9	854	43.1	
	8	S	16	9.4		4	5	25.9	768	38.7	0.90
	8	N	16	0.0		5	9	25.9	858	43.3	
	8	N	16	9.5		7	7	25.9	737	37.2	0.86

*, + refer to last page of table

Table 2.5 (cont.) : Summary of the Beam Splice Tests

Group	Bar No.	Def. patt.	Splice length (in.)	Average Coating Thickness (mils)	Concrete Strength (psi)	No. of cracks	Widest crack (mils)	Bar stress for crack comparison (ksi)	Ult. moment (k-in)	Ult. stress (ksi)	+ C/U
SP4	11	S	24	0.0	5850	5	7	24.0	1459	40.2	
:	11	S	24	9.3		5	9	24.0	1053	29.0	0.72
	11	C	24	0.0		7	7	24.0	1372	37.8	
	11	C	24	10.3		6	10	24.0	1128	31.1	0.82
	Mean =										0.82

* These beams contained 3 splices

\+ C/U = Ratio of bond strengths of coated to uncoated bars

Table 3.1 Summary of beam-end tests for specimens with standard configuration (bond strength normalized to 2db cover and, for No. 5 bars, a 9 mil coating thickness)

Bar size	Def. pattern	Group No.	Concrete strength (psi)	No. of uncoated bars***	Uncoated bars Normalized bond force (lbs.)	No. of coated bars***	Coated bars Normalized bond force (lbs.)	C/U+ group	U/U++ all	C/U++ all
5	S	9	5650	3	14154	6	11753	0.83	1.01	0.84
5	S	21	5990	3	14598	6	12005	0.82	1.04	0.86
Average =					14376		11879	0.83	1.03	0.85
5	C	10	5990	3	13580	6	13009	0.96	0.97	0.93
5	C	21	5990	3	15078	6	13020	0.86	1.08	0.93
Average =					14329		13014	0.91	1.02	0.93
5	N	11	5970	3	12964	3	11998	0.93	0.92	0.86
5	N	12	5940	3	14003	3	12425	0.89	1.00	0.89
5	N	13	5840	3	13107	3	11977	0.91	0.93	0.85
Average =					13358		12133	0.91	0.95	0.87
Average of all No. 5 bars * =					14021		12342	0.88	1.00	0.88
6	S	14	5800	3	19363	6	15498	0.80	1.00	0.80
6	S	17	5850	3	18720	6	15525	0.83	0.97	0.81
Average =					19041		15511	0.81	0.99	0.80

+, ++, *, **, *** refer to last page of table

Table 3.1 (cont.) : Summary of beam-end tests for specimens with standard configuration (bond strength normalized to 2db cover and, for No. 5 bars, a 9 mil coating thickness)

Bar size	Def. pattern	Group No.	Concrete strength (psi)	No. of uncoated bars***	Uncoated bars Normalized bond force (lbs.)	No. of coated bars***	Coated bars Normalized bond force (lbs.)	C/U+ group	U/U++ all	C/U++ all
6	C	14	5800	3	18733	6	18112	0.97	0.97	0.94
6	C	17	5850	3	18760	6	16056	0.86	0.97	0.83
Average =					18746		17084	0.91	0.97	0.89
6	N	14	5800	3	19309	3	19089	0.99	1.00	0.99
6	N	22	6300	6	20385	6	18486	0.91	1.06	0.96
Average =					20026		18687	0.93	1.04	0.97
Average of all No. 6 bars * =					19271		17094	0.89	1.00	0.89
8	S	3	6090	3	41384	9	29472	0.71	0.96	0.68
8	S	6	5870	2	45104	2	34512	0.77	1.05	0.80
8	S	15	6000	2	42680	6	31600	0.74	0.99	0.73
8	S	18	4790 - 5430	3	41312	3	34064	0.82	0.96	0.79
Average =					42365		31303	0.74	0.98	0.73

+, ++, *, **, *** refer to last page of table

Table 3.1 (cont.) : Summary of beam-end tests for specimens with standard configuration (bond strength normalized to 2db cover and, for No. 5 bars, a 9 mil coating thickness)

Bar size	Def. pattern	Group No.	Concrete strength (psi)	No. of uncoated bars***	Uncoated bars Normalized bond force (lbs.)	No. of coated bars***	Coated bars Normalized bond force (lbs.)	C/U+ group	U/U++ all	C/U++ all
8	C	2	5700	1	47184	3	37976	0.80	1.10	0.88
8	C	5	5920	3	36504	9	34784	0.95	0.85	0.81
8	C	6	5870	2	45880	2	35600	0.78	1.07	0.83
Average =					41409		35584	0.90	0.96	0.83
8	N	4	6130	3	46104	3	37208	0.81	1.07	0.86
8	N	6	5870	2	43304	2	41296	0.95	1.01	0.96
8	N	15	6000	3	43464	0	0	0.00	1.01	0.00
8	N	18	4790 - 5430	3	48256	3	38800	0.80	1.12	0.90
Average =					45461		38827	0.84	1.06	0.90
Average of all No. 8 bars * =					43078		35238	0.83	1.00	0.82
11	S	19	5070 - 5270	3	39033	3	33138	0.85	0.94	0.80
11	S	20	5260 - 5290	3	41994	3	41580	0.99	1.01	1.00
Average =					40513		37359	0.92	0.98	0.90

+, ++, *, **, *** refer to last page of table

Table 3.1 (cont.) : Summary of beam-end tests for specimens with standard configuration (bond strength normalized to 2db cover and, for No. 5 bars, a 9 mil coating thickness)

Bar size	Def. pattern	Group No.	Concrete strength (psi)	No. of uncoated bars***	Uncoated bars Normalized bond force (lbs.)	No. of coated bars***	Coated bars Normalized bond force (lbs.)	C/U+ group	U/U++ all	C/U++ all
11	C	19	5070 - 5270	3	40437	3	30555	0.76	0.97	0.74
11	C	20	5260 - 5290	3	40419	3	36162	0.89	0.97	0.87
Average =					40428		33358	0.83	0.97	0.80
11	N	19	5070 - 5270	3	42291	3	32148	0.76	1.02	0.77
11	N	20	5260 - 5290	3	44937	3	32625	0.73	1.08	0.79
Average =					43614		32386	0.74	1.05	0.78
Average of all No. 11 bars * =					41518		34367	0.83	1.00	0.83
Average of all bars ** =								0.86	1.00	0.85

\+ Numerator and denominator based on group average

++ Numerator based on group average. Denominator based on average for all deformation patterns of all groups for each bar size; each deformation pattern weighted equally

* Each deformation pattern weighted equally

** Each bar size weighted equally

*** Bars are bottom-cast with nominal 2db cover, the bond forces are corrected to 2db cover and for No. 5 coated bars, corrected to 9 mil coating

Table 3.2 Summary of beam-end tests with bottom and top-cast bars in standard and deep specimens with different slump concretes and degrees of consolidation

Bar size	Group No.	Def pattern	Slump (in.)	Cover (db)	No. Of uncoated bars	Uncoated bars normalized bond force (lbs.)	No. Of coated bars	Coated bars normalized bond force (lbs.)	CP*	B/T* U/U*	B/T* C/C*	B/T* U/C*	C/U* group
5	9	S	4	2	3	14154	6	11753	B	1.228	1.097	1.321	0.830
					3	11522	6	10714	T				0.930
5	10	C	4 1/2	2	3	13580	6	13010	B	1.138	1.144	1.194	0.958
					3	11932	6	11375	T				0.953
5	11	N	3 1/4	2	3	12964	3	11998	B	1.105	1.238	1.338	0.925
					3	11732	3	9688	T				0.826
Average of No. 5 bars =										1.157	1.160	1.284	
6	17	S	5 3/4	2	3	18720	6	15525	B	1.340	1.114	1.343	0.829
					3	13973	2	13941	T				0.998
Average of No. 6 bars =										1.340	1.114	1.343	

* Refer to the last page of the table

Table 3.2 (cont.) Summary of beam-end tests with bottom and top-cast bars in standard and deep specimens with different slump concretes and degrees of consolidation

Bar size	Group No.	Def pattern	Slump (in.)	Cover (db)	No. Of uncoated bars	Uncoated bars normalized bond force (lbs.)	No. Of coated bars	Coated bars normalized bond force (lbs.)	CP*	B/T*			C/U* group
										U/U*	C/C*	U/C*	
8	15	N	4 1/4	2	3	43464	-	-	B	1.091	-	-	-
					3	39832	-	-	T				-
8	15	S	4 1/4	2	2	42680	6	31600	B	-	1.112	1.502	0.740
					-	-	2	28416	T				-
8	18	N	4 1/4	1	3	31424	3	28520	B	1.149	1.238	1.364	0.908
					3	27352	3	23040	T				0.842
8	18	N	4 1/4	2	3	48256	3	38800	B	1.256	1.155	1.437	0.804
					3	38432	3	33592	T				0.874
8	18	N	4 1/4	3	2	59160	3	55696	B	1.139	1.180	1.254	0.941
					1	51960	3	47192	T				0.908

* Refer to the last page of the table

Table 3.2 (cont.) Summary of beam-end tests with bottom and top-cast bars in standard and deep specimens with different slump concretes and degrees of consolidation

Bar size	Group No.	Def pattern	Slump (in.)	Cover (db)	No. Of uncoated bars	Uncoated bars normalized bond force (lbs.)	No. Of coated bars	Coated bars normalized bond force (lbs.)	CP*	B/T* U/U*	B/T* C/C*	B/T* U/C*	C/U* group
					3	41312	3	34064	B				0.825
8	18	S	4 1/4	2						1.189	1.153	1.399	
					3	34736	3	29536	T				0.850
Average of No. 8 bars in standard specimens =										1.165	1.168	1.391	
					3	42744	3	36416	B				0.852
8+	23	N	2 1/4	2						1.015	0.997	1.170	
					3	42120	3	36520	T				0.867
					3	42360	3	40488	B				0.956
8+	24	N	2 1/2	2						1.131	1.170	1.225	
					3	37464	3	34592	T				0.923
Average of No. 8 bars in deep specimens (low slump vibrated) =										1.073	1.084	1.198	
					3	43848	3	35504	B				0.810
8+	24	N	8	2						1.218	1.051	1.298	
					3	36008	3	33776	T				0.938
Average of No. 8 bars in deep specimens (high slump vibrated)										1.121	1.073	1.231	

* Refer to the last page of the table

Table 3.2 (cont.) Summary of beam-end tests with bottom and top-cast bars in standard and deep specimens with different slump concretes and degrees of consolidation

Bar size	Group No.	Def pattern	Slump (in.)	Cover (db)	No. Of uncoated bars	Uncoated bars normalized bond force (lbs.)	No. Of coated bars	Coated bars normalized bond force (lbs.)	CP*	B/T* U/U*	B/T* C/C*	B/T* U/C*	C/U* group
					3	42656	3	32752	B				0.768
8+$	24	N	8	2						1.216	1.116	1.454	
					3	35080	3	29344	T				0.836
Average of No. 8 bars in deep specimens =										1.145	1.084	1.287	
Average of all No. 8 bars =										1.156	1.130	1.345	
AVERAGE OF ALL BARS =										1.170	1.136	1.331	

\+ Deep specimens

$ Non-vibrated specimens

* CP : Casting position

B : Bottom

T : Top

B/T : Ratio, bottom-cast bars to top-cast bars

U/U : Ratio, uncoated bottom-cast bars to uncoated top-cast bars

C/C : Ratio, coated bottom-cast bars to coated top-cast bars

U/C : Ratio, uncoated bottom-cast bars to coated top-cast bars

C/U : Ratio, coated bars to uncoated bars

Table 3.3 Summary of the hypothesis testing on the average values from Table 3.2

Bar size	Slump (in.)	V NV *	Spec type **	Bottom / Top (B/T)					Coated / Uncoated (C/U)					U/C	
				Uncoated		Coated		U&C $ H test	Bottom		Top		B&T + H test	ratio	H test*
				ratio	H test*	ratio	H test*		ratio	H test*	ratio	H test*			
5	3 1/4 - 4 1/2	V	ST	1.157	S	1.160	S	NS	0.904	S	0.903	S	NS	1.284	S
8	4 1/2	V	ST	1.165	S	1.168	S	NS	0.870	S	0.869	S	NS	1.391	S
8	2 1/4 - 2 1/2	V	D	1.073	S	1.084	S	NS	0.904	S	0.895	S	NS	1.200	S
Average - low slump				1.132	-	1.137	-	-	0.893	-	0.889	-	-	1.292	-
6	5 3/4	V	ST	1.340	S	1.114	S	S	0.829	S	0.998	NS	S	1.343	S
8	8	V	D	1.218	S	1.051	NS	S	0.810	S	0.938	NS	S	1.298	S
Average - high slump				1.279	-	1.083	-	-	0.820	-	0.968	-	-	1.321	-
8	8	NV	D	1.216	S	1.116	S	S	0.768	S	0.836	S	S	1.454	S

* H test : The results of hypothesis testing
S = difference in bond strengths indicated by the ratio is significant with a confidence of 97.5 percent
NS = difference in bond strengths indicated by the ratio is not significant with a confidence of 97.5 percent
V : Vibrated
NV : Not Vibrated

** Specimen type
ST : standard
D : deep

$ Hypothesis test for the difference in the B/T ratio for the uncoated and coated bars.

+ Hypothesis test for the difference in the C/U ratio for the bottom and top bars.

Table 3.4 Summary of ultimate bond forces for vibrated and non-vibrated specimens with different slump concretes.

CP*	Slump (in.)	Cosolidation *	Concrete strength (psi)	Ultimate bond force (lbs.) U*	Ultimate bond force (lbs.) C*
B	2 1/2	V	5150	39297	37598
	8	V	5880	43417	35130
	8	NV	5880	42256	32410
T	2 1/2	V	5150	34646	31951
	8	V	5880	35658	33434
	8	NV	5880	34717	29059

* CP : Casting position
B : Bottom cast
T : Top cast
V : Vibrated
NV : Non-vibrated
U : Ultimate bond force of uncoated bars (not normalized based on concrete strength)
C : Ultimate bond force of coated bars (not normalized based on concrete strength)

Table 3.5 Summary of beam-end tests for bars with different covers

Bar No.	Def pat*	P*	C*	U* Cover (db*)	Normalized ultimate test bond force (lbs.) BF*	AV*	NB *	C/U group BF*	AV*	C'/U + BF*	AV*
(Group No.)											
	(8,13)			1	9980	10558	4	-	-	-	-
	(8,11,12,13)		U	2	13446	13480	10	-	-	-	-
	(13)			3	16912	15223	3	-	-	-	-
	(13)			4.8	23150	25856	1	-	-	-	-
5	N	B									
	(8,13)			1	9163	10136	4	0.918	0.960	-	-
	(8,11,12,13)		C	2	12564	12284	10	0.934	0.911	1.259	1.163
	(13)			3	15965	14891	3	0.944	0.978	1.187	1.105
	(13)			4.8	22086	24571	1	0.954	0.950	-	-
	(17)		U	2	-	18720	3	-	-	-	-
		B									
	(17)		C	2	-	15525	6	-	0.829	-	-
6	S										
	(17)		U	2	-	13973	3	-	-	-	-
		T									
	(17)		C	2	-	13941	2	-	0.998	-	-
	(1)			1	27180	31598	1	-	-	-	-
	(1,18)		U	2	39420	36812	4	-	-	-	-
	(1)			3	51661	57671	1	-	-	-	-
8	S	T									
	(1)			1	23052	25847	3	0.848	0.818	-	-
	(1,15,18)		C	2	35065	32693	8	0.890	0.888	1.290	1.035
	(1)			3	47077	50578	3	0.911	0.877	1.194	1.374
	(18)			1	30931	31426	3	-	-	-	-
	(4,6,15,18,23,24)		U	2	44623	44436	17	-	-	-	-
	(18)			3	58316	59160	2	-	-	-	-
		B									
	(18)			1	26158	28523	3	0.846	0.908	-	-
	(4,6,18,23,24)		C	2	39698	38666	14	0.890	0.870	1.283	1.230
	(18)			3	53238	55699	3	0.913	0.941	1.193	1.253
8	N										
	(18)			1	27187	27354	3	-	-	-	-
	(15,18)		U	2	39320	39136	6	-	-	-	-
	(18)			3	51454	51960	1	-	-	-	-
		T									
	(18)			1	22551	23041	3	0.829	0.842	-	-
	(18)		C	2	34622	33595	3	0.881	0.858	1.273	1.228
	(18)			3	46692	47194	3	0.907	0.908	1.187	1.206

* Refer to the last page of the table

Table 3.5 (cont.) Summary of beam-end tests for bars with different covers

Bar No.	Def pat*	C P*	U C*	Cover (db*)	Normalized ultimate test bond force (lbs.)			C/U group		C'/U +	
(Group No.)					BF*	AV*	NB *	BF*	AV*	BF*	AV*
	(20)			1	34918	35467	3	-	-	-	-
	(20)		U	2	46579	44934	3	-	-	-	-
	(20)			3	58240	59319	3	-	-	-	-
11	N	B									
	(20)			1	26128	27943	3	0.748	0.788	-	-
	(20)			2	36930	32625	3	0.793	0.726	1.058	0.920
	(20)			3	47731	50203	3	0.820	0.846	1.025	1.117
			C								
	(19)			2	32197	32145	3	-	-	-	-
	(19)			3	42994	43022	3	-	-	-	-

* Def Pat : Deformation pattern
C P : Casting position
B : bottom
T : top
U C : Uncoated or coated
U : Uncoated
C : Coated
db : bar diameter
BF : best fit value
AV : average value
BL : bonded length
BL+LL : bonded length plus lead length
NB : number of test bars

\+ This C/U ratio is the ratio of the bond force for a coated bar to the bond force of an uncoated bar with 1db less cover

Table 3.6 U/C values for bottom-cast bars in beam-end specimens with different covers and comparison to the ACI epoxy bar factors

Bar size	Deformation pattern (group)	Cover (db)	U/C bottom bars $ BF *	U/C bottom bars $ AV *	ACI factors **
5	N (8,11,12,13)	1	1.089	1.042	1.5
		2	1.071	1.098	1.5
		3	1.059	1.022	1.2
		4.8	1.048	1.053	1.2
6	S (17)	2	-	1.206	1.5
8	N (4,6,15,18,23,24)	1	1.182	1.101	1.5
		2	1.124	1.149	1.5
		3	1.095	1.063	1.2
11	N (20)	1	1.337	1.269	1.5
		2	1.261	1.377	1.5
		3	1.220	1.182	1.2

$ Strength ratio of uncoated to coated bottom bars

* BF = best fit values
AV = average values

** ACI 318-89, section 12.2.4.3 (Epoxy factors)
1.5 = bars with cover less than 3 db
1.2 = bars with cover of 3 db and greater

Table 3.7 Application of Orangun, Jirsa, Breen equation to the results of the beam-end specimens with different covers

Bar size	Best fit line Eq. Y = AX + B		K1 values *		Cu** (in.)	Approach 1			Approach 2		
	A	B	K1u	K1c		K2 & K3 values *		ΔC ** (in.)	K2 & K3 values *		ΔC ** (in.)
5	uncoated		3.879	3.806	0.625	K2u =	1.220	0.060	K2u =	1.594	0.150
	5545.30	6514.59			-------	K3u =	225.9	-------	K3u =	212.0	-------
	----------				1.250	K2c =	1.220	0.108	K2c =	0.752	0.162
	coated				-------	K3c =	194.6	-------	K3c =	212.0	-------
	5440.98	5762.69			1.875			0.156			0.174
8	uncoated		4.789	4.735	1.000	K2u =	1.220	0.186	K2u =	1.492	0.353
	13692.11	17239.19			-------	K3u =	224.7	-------	K3u =	212.0	-------
	----------				2.000	K2c =	1.220	0.336	K2c =	-0.124	0.364
	coated				-------	K3c =	149.2	-------	K3c =	212.0	-------
	13539.78	12618.25			3.000			0.486			0.376
11	uncoated		3.261	2.719	1.410	K2u =	1.220	0.475	K2u =	-1.000	1.195
	8331.13	22013.85			-------	K3u =	145.8	-------	K3u =	212.0	-------
	----------				2.820	K2c =	1.220	0.898	K2c =	-2.763	1.476
	coated				-------	K3c =	93.2	-------	K3c =	212.0	-------
	6948.54	15662.35			4.230			1.320			1.757

Orangun, Jirsa, Breen equation ===> Pullout force = POF = $A_b f_s = [K1\ \pi \ell_s\ C + K2\ \pi \ell_s\ d_b + K3\ A_b]\sqrt{f'_c}$

* K1u = K1 for uncoated bars; K2c = K2 for coated bars
K1c = K1 for coated bars; K3u = K3 for uncoated bars
K2u = K2 for uncoated bars; K3c = K3 for coated bars

** = Cc - Cu; Cc = cover of coated bars; Cu = cover of uncoated bars

Table 3.8 Top-bar factors

Bar No.	Def. Pattern	Cover (db)	B/T* best fit value U/U*	B/T* best fit value C/C*	B/T* best fit value U/C*	B/T* average values U/U*	B/T* average values C/C*	B/T* average values U/C*
8	N	1	1.138	1.160	1.372	1.149	1.238	1.364
		2	1.135	1.147	1.289	1.135	1.151	1.323
		3	1.133	1.140	1.249	1.139	1.180	1.254

* B/T : Ratio of the bottom bars to top bars
U/U : Ratio of uncoated bottom bars to uncoated top bars
C/C : Ratio of coated bottom bars to coated top bars
U/C : Ratio of uncoated bottom bars to coated top bars
C/U : Ratio of coated bars to uncoated bars

Table 3.9 Summary of the beam-end tests for specimens with transverse reinforcement and comparison with the specimens without transverse reinforcement

B S	D P	Standard lead length: Normalized ultimate Bond force (lbs.) N UU* B*	N UC* B*	N CU* B*	N CC* B*	Ratios: CC/CU	CC/UC	CC/UU	CU/UU	Non-standard lead +: Normalized ultimate bond force (lbs.) N CU* B*	N CC* B*	Ratio CC/CU	Ktr
S		3 14154	6 11753										
		3 14598	6 12005	3 14639	3 12301	0.840	1.036	0.856	1.018	3 9372	3 7737	0.826	
		avg 14376	11879										
5													4.41
		3 12964	3 11998										
N		3 14003	3 12425	3 15142	3 13540	0.894	1.116	1.014	1.134	3 9222	3 7829	0.849	
		3 13107	3 11977										
		avg 13358	12133										
Average of No. 5 bars						0.867	1.076	0.935	1.076			0.838	
		3 41384	9 29472										
S		2 45104	2 34512										
		2 42680	6 31600	3 48494	3 39145	0.807	1.251	0.924	1.145	3 34758	3 29386	0.845	
		3 41312	3 34064										
8													2.76
		avg 42365	31303										

\+ No. 5 lead length = 0.625 standard lead length = 2.375
No. 8 lead length = 1.000 standard lead length = 3.750

* B S : Bar size UU : Unconfined uncoated bars UC : Unconfined coated bars
D P : Deformation pattern CU : Confined uncoated bars CC : Confined coated bars
N B : Number of the bars in each group

Table 3.9 (cont.) Summary of the beam-end tests for specimens with transverse reinforcement and comparison with the specimens without transverse reinforcement

B S	D P	Standard lead length: Normalized ultimate Bond force (lbs.) N UU* B*	N UC* B*	N CU* B*	N CC* B*	Ratios: CC/CU	CC/UC	CC/UU	CU/UU	Non-standard lead +: Normalized ultimate bond force (lbs.) N CU* B*	N CC* B*	Ratio CC/CU	Ktr
		3 46104	3 37208										
	N	2 43304	2 41296										
		3 43464	- -	3 46511	3 41525	0.893	1.069	0.913	1.023	3 35571	3 29885	0.840	
		3 48256	3 38800										
8													2.76
	avg	45461	38827										
	Average of No. 8 bars					0.850	1.160	0.919	1.084			0.843	
	S	3 39033	3 33138										
		3 41994	3 41580	4 50016	4 49146	0.983	1.316	1.213	1.235	- -	- -	-	
		---	---										
	avg	40513	37359										
11													1.95
	N	3 42291	3 32148										
		3 44937	3 32625	5 53927	4 46759	0.867	1.444	1.072	1.236	- -	- -	-	
		---	---										
	avg	43614	32386										
	Average of No. 11 bars					0.925	1.380	1.143	1.236			-	
	Average of all bars					0.881	1.205	0.999	1.132			0.840	

+, * refer to the first page of table

Table 3.10 Summary of beam-end tests for specimens with high strength and normal strength concrete containing No. 6 bars (Bonded length = 4.5 in.)

C P *	Def pat	Group No.	Concrete strength (psi)	NU*	NC*	Ultimate bond force (lbs.)				
						Normalized bond force (lbs.) +		C/U	Non-normalized bond force (lbs.)	
						U*	C*		U*	C*
B	N	14	5800	3	3	19310	19089	0.989	18986	18756
	C	14	5800	3	6	18734	18113	0.967	18414	17802
	C	17	5850	3	6	18761	16056	0.856	18522	15854
	N	22	6300	6		20385	18486	0.907	20885	18923
	Average of all N & C pattern					19515	17771	0.921	19538	17702
	S	14	5800	3	6	19364	15498	0.800	19040	15237
	S	17	5850	3	6	18720	15525	0.829	18486	15332
	Average of all S pattern					19042	15512	0.815	18763	15285
	Average of all the patterns					19380	16950	0.882	19317	16823
	S	29	12920	3	3	12642	10776	0.843	18581	15638
T	S	17	5850	3	2	13973	13941	0.998	13788	13761
	S	29	12920	3	3	11238	10637	0.940	16677	15660

* C P : Casting position
NU : Number of uncoated bars in each group
NC : Number of coated bars in each group
U : Uncoated bars
C : Coated bars

\+ The bond forces are normalized to 6000 psi concrete strength

Table 3.11 Summary of beam-end tests for specimens with hooks

Bar size	Degree of bend	No. of bars U*	No. of bars UC*	No. of bars RC*	Group No.	Normalized ultimate bond force (lbs.) U*	Normalized ultimate bond force (lbs.) UC*	Normalized ultimate bond force (lbs.) RC*	C/U All*	C/U UC*	C/U RC*
5	0 +	3	6	-	10	13791	12841	-	0.931	-	-
		3	6	-	21	14532	13181	-	0.907	-	-
	90	3	3	3	25	20278	18505	17748	0.894	0.913	0.875
	180	3	2	3	25	17165	17994	16386	0.992	1.048	0.955
	Average of No. 5 hooks =								0.939	0.981	0.915
8		1	3	-	2	47184	37976	-	0.805	-	-
	0 +	3	9	-	5	36504	34784	-	0.953	-	-
		2	2	-	6	45874	35598	-	0.776	-	-
	90	3	3	3	26	54450	49707	53653	0.949	0.913	0.985
	Average of all hooks ++ =								0.945	0.958	0.938

* U : Uncoated bar
UC : Unrepaired coated hook or straight coated bars
RC : Repaired coated hook
All : The value of C in the C/U ratio is the average of all of the repaired and unrepaired coated hooks

\+ : Straight bars
++ : Average of all C - pattern hooks in groups 25 and 26
(Average of 0.894 , 0.992 , 0.949)

Table 3.12 Comparison of the unconfined beam-end tests with the Orangun, Jirsa, and Breen (1977) equation and ACI (1989) design provisions

B S *	D P *	C P *	U C *	C C *	N B *	Ultimate bond force (lbs.) Test (normalized)	Predicted OJB* BL*	Predicted OJB* BL+LL*	predicted ACI BL*	predicted ACI BL+LL*	Comparison test / OJB BL*	Comparison test / OJB BL+LL*	Comparison test / ACI BL*	Comparison test / ACI BL+LL*	ACI factors +
			U	2	6	14376					1.559	1.196	1.697	1.011	
		B					9222	12025	8472	14221					0.8
			C	2	12	11879					1.288	0.988	1.402	0.835	
	S														
			U	2	3	11522					1.249	0.958	1.768	1.053	
		T					9222	12025	6517	10939					0.8,1.3
			C	2	6	10714					1.162	0.891	1.644	0.979	
			U	2	6	14329					1.554	1.192	1.691	1.008	
		B					9222	12025	8472	14221					0.8
			C	2	12	13014					1.411	1.082	1.536	0.915	
	C														
			U	2	3	11932					1.294	0.992	1.831	1.091	
		T					9222	12025	6517	10939					0.8,1.3
			C	2	6	11375					1.233	0.946	1.745	1.040	
5															
				1	4	10558	7484	9108	4236	7111	1.411	1.159	2.492	1.485	0.8,2.0
	B	U	2	9		13358	9222	12025	8472	14221	1.448	1.111	1.577	0.939	
			3	3		15223	10959	14941	8472	14221	1.389	1.019	1.797	1.070	0.8
			4.8	1		25856	14086	20190	8472	14221	1.836	1.281	3.052	1.818	

* , + Refer to last page of table

Table 3.12 (cont.) Comparison of the unconfined beam-end tests with the Orangun, Jirsa, and Breen (1977) equation and ACI (1989) design provisions

B S *	D P *	C P *	U C *	C C *	N B *	Ultimate bond force (lbs.) Test (normalized)	Predicted OJB* BL*	Predicted OJB* BL+LL*	predicted ACI BL*	predicted ACI BL+LL*	Comparison test / OJB BL*	Comparison test / OJB BL+LL*	Comparison test / ACI BL*	Comparison test / ACI BL+LL*	ACI factors +
				1	4	10136	7484	9108	4236	7111	1.354	1.113	2.393	1.425	0.8,2.0
			C	2	9	12133	9222	12025	8472	14221	1.316	1.009	1.432	0.853	
				3	3	14891	10959	14941	8472	14221	1.359	0.997	1.758	1.047	0.8
				4.8	1	24571	14086	20190	8472	14221	1.744	1.217	2.900	1.728	
N															
				1	1	10165	7484	9108	3259	5470	1.358	1.116	3.119	1.858	0.8,2.0,1.3
			U	2	4	12028	9222	12025	6517	10939	1.304	1.000	1.846	1.100	0.8,1.3
T															
				1	1	8768	7484	9108	3259	5470	1.172	0.963	2.690	1.603	0.8,2.0,1.3
			C	2	3	9688	9222	12025	6517	10939	1.051	0.806	1.487	0.886	0.8,1.3
Average of all No. 5 bars						uncoated bottom					1.495	1.148	1.825	1.087	
						coefficient of variation					0.061	0.053	0.205	0.205	
						coated bottom					1.353	1.039	1.607	0.957	
						coefficient of variation					0.058	0.052	0.218	0.219	
						uncoated top					1.291	0.997	1.936	1.154	
						coefficient of variation					0.024	0.042	0.194	0.194	
						coated top					1.168	0.900	1.718	1.023	
						coefficient of variation					0.055	0.058	0.156	0.156	

* , + Refer to last page of table

Table 3.12 (cont.) Comparison of the unconfined beam-end tests with the Orangun, Jirsa, and Breen (1977) equation and ACI (1989) design provisions

BS*	DP*	CP*	UCC*	NB*	Ultimate bond force (lbs.) Test (normalized)	Predicted OJB* BL*	Predicted OJB* BL+LL*	predicted ACI BL*	predicted ACI BL+LL*	Comparison test / OJB BL*	Comparison test / OJB BL+LL*	Comparison test / ACI BL*	Comparison test / ACI BL+LL*	ACI factors +
	U	2	6		19041					1.410	1.098	1.748	1.085	
B						13507	17347	10893	17549					0.8
	C	2	12		15511					1.148	0.894	1.424	0.884	
S														
	U	2	3		13973					1.035	0.805	1.668	1.035	
T						13507	17347	8379	13500					0.8,1.3
	C	2	2		13941					1.032	0.804	1.664	1.033	
6														
	U	2	6		18746					1.388	1.081	1.721	1.068	
C	B					13507	17347	10893	17549					
	C	2	12		17084					1.265	0.985	1.568	0.974	
														0.8
	U	2	9		20026					1.483	1.154	1.838	1.141	
N	B					13507	17347	10893	17549					
	C	2	9		18687					1.384	1.077	1.716	1.065	
Average of all No. 6 bars					uncoated bottom					1.435	1.117	1.779	1.104	
					coefficient of variation					0.030	0.029	0.029	0.030	
					coated bottom					1.255	0.977	1.556	0.966	
					coefficient of variation					0.075	0.074	0.074	0.074	

* , + Refer to last page of table

Table 3.12 (cont.) Comparison of the unconfined beam-end tests with the Orangun, Jirsa, and Breen (1977) equation and ACI (1989) design provisions

B S *	D P *	C P *	U C *	C C *	N B *	Ultimate bond force (lbs.) Test (normalized)	Predicted OJB* BL*	Predicted OJB* BL+LL*	predicted ACI BL*	predicted ACI BL+LL*	Comparison test / OJB BL*	Comparison test / OJB BL+LL*	Comparison test / ACI BL*	Comparison test / ACI BL+LL*	ACI factors +
						uncoated top					1.035	0.805	1.668	1.035	
						coefficient of variation					-	-	-	-	
						coated top					1.032	0.804	1.664	1.033	
						coefficient of variation					-	-	-	-	
			U	2	10	42365	28012	35061	19365	28442	1.512	1.208	2.188	1.490	
	B														0.8
			C	2	20	31303	28012	35061	19365	28442	1.117	0.893	1.616	1.101	
S															
				1	1	31598	21687	25771	7448	10939	1.457	1.226	4.242	2.889	0.8,2.0,1.3
			U	2	4	36812	28012	35061	14896	21879	1.314	1.050	2.471	1.683	
				3	1	57671	34337	44351	14896	21879	1.680	1.300	3.872	2.636	0.8,1.3
	T														
				1	3	25847	21687	25771	7448	10939	1.192	1.003	3.470	2.363	0.8,2.0,1.3
			C	2	8	32693	28012	35061	14896	21879	1.167	0.932	2.195	1.494	
				3	3	50578	34337	44351	14896	21879	1.473	1.140	3.395	2.312	0.8,1.3
8															
				1	1	31846	21687	25771	9682	14221	1.468	1.236	3.289	2.239	0.8,2.0
			U	2	6	41409	28012	35061	19365	28442	1.478	1.181	2.138	1.456	0.8
C	B														
				1	3	25820	21687	25771	9682	14221	1.191	1.002	2.667	1.816	0.8,2.0
			C	2	14	35584	28012	35061	19365	28442	1.270	1.015	1.838	1.251	0.8

* , + Refer to last page of table

Table 3.12 (cont.) Comparison of the unconfined beam-end tests with the Orangun, Jirsa, and Breen (1977) equation and ACI (1989) design provisions

B S *	D P *	C P *	U C *	C C *	N B *	Ultimate bond force (lbs.) Test (normalized)	Predicted OJB* BL*	Predicted OJB* BL+LL*	predicted ACI BL*	predicted ACI BL+LL*	Comparison test / OJB BL*	Comparison test / OJB BL+LL*	Comparison test / ACI BL*	Comparison test / ACI BL+LL*	ACI factors +
				1	3	31426	21687	25771	9682	14221	1.449	1.219	3.246	2.210	0.8,2.0
			U	2	11	45461	28012	35061	19365	28442	1.623	1.297	2.348	1.598	
				3	2	59160	34337	44351	19365	28442	1.723	1.334	3.055	2.080	0.8
	B														
				1	3	28523	21687	25771	9682	14221	1.315	1.107	2.946	2.006	0.8,2.0
			C	2	8	38827	28012	35061	19365	28442	1.386	1.107	2.005	1.365	
				3	3	55699	34337	44351	19365	28442	1.622	1.256	2.876	1.958	0.8
	8	N													
				1	3	27354	21687	25771	7448	10939	1.261	1.061	3.673	2.501	0.8,2.0,1.3
			U	2	6	39136	28012	35061	14896	21879	1.397	1.116	2.627	1.789	
				3	1	51960	34337	44351	14896	21879	1.513	1.172	3.488	2.375	0.8,1.3
	T														
				1	3	23041	21687	25771	7448	10939	1.062	0.894	3.094	2.106	0.8,2.0,1.3
			C	2	3	33595	28012	35061	14896	21879	1.199	0.958	2.255	1.535	
				3	3	47194	34337	44351	14896	21879	1.374	1.064	3.168	2.157	0.8,1.3
Average of all No. 8 bars						uncoated bottom					1.549	1.242	2.414	1.644	
						coefficient of variation					0.050	0.041	0.156	0.156	
						coated bottom					1.247	1.000	1.952	1.329	
						coefficient of variation					0.109	0.104	0.221	0.221	

* , + Refer to last page of table

Table 3.12 (cont.) Comparison of the unconfined beam-end tests with the Orangun, Jirsa, and Breen (1977) equation and ACI (1989) design provisions

B S *	D P *	C P *	U C *	C C *	N B *	Ultimate bond force (lbs.) Test (normalized)	Predicted OJB* BL*	Predicted OJB* BL+LL*	predicted ACI BL*	predicted ACI BL+LL*	Comparison test / OJB BL*	Comparison test / OJB BL+LL*	Comparison test / ACI BL*	Comparison test / ACI BL+LL*	ACI factors +
						uncoated top					1.379	1.111	3.017	2.054	
						coefficient of variation					0.076	0.062	0.200	0.200	
						coated top					1.228	0.984	2.770	1.886	
						coefficient of variation					0.102	0.080	0.197	0.198	
			U	2	6	40513					0.822	0.761	1.860	1.594	
S	B						49312	53261	21786	25416					
			C	2	6	37359					0.758	0.701	1.715	1.470	
															0.8
			U	2	6	40428					0.820	0.759	1.856	1.591	
C	B						49312	53261	21786	25416					
			C	2	6	33358					0.676	0.626	1.531	1.312	
11															
				1	3	35467	39347	41635	10893	12708	0.901	0.852	3.256	2.791	0.8,2.0
			U	2	6	43614	49312	53261	21786	25416	0.884	0.819	2.002	1.716	
				3	3	59319	59277	64887	21786	25416	1.001	0.914	2.723	2.334	0.8
N	B														
				1	3	27943	39347	41635	10893	12708	0.710	0.671	2.565	2.199	0.8,2.0
			C	2	6	32386	49312	53261	21786	25416	0.657	0.608	1.487	1.274	
				3	6	46613	59277	64887	21786	25416	0.786	0.718	2.140	1.834	0.8

* , + Refer to last page of table

Table 3.12 (cont.) Comparison of the unconfined beam-end tests with the Orangun, Jirsa, and Breen (1977) equation and ACI (1989) design provisions

B S *	D P *	C P *	U C *	C C *	N B *		Ultimate bond force (lbs.) Test (normalized)		Predicted OJB*		predicted ACI		Comparison test / OJB		test / ACI		ACI factors +
									BL*	BL+LL*	BL*	BL+LL*	BL*	BL+LL*	BL*	BL+LL*	
Average of all No. 11 bars						uncoated bottom							0.869	0.806	2.177	1.866	
						coefficient of variation							0.068	0.066	0.226	0.226	
						coated bottom							0.718	0.664	1.812	1.553	
						coefficient of variation							0.071	0.067	0.199	0.199	
Average of all bars						uncoated bottom							1.337	1.078	2.049	1.425	
						coefficient of variation							0.052	0.047	0.154	0.154	
						coated bottom							1.143	0.920	1.732	1.201	
						coefficient of variation							0.078	0.074	0.178	0.178	
						uncoated top							1.235	0.971	2.207	1.414	
						coefficient of variation							0.050	0.052	0.197	0.197	
						coated top							1.143	0.896	2.051	1.314	
						coefficient of variation							0.079	0.069	0.177	0.177	

\+ ACI 318-89 factors for development length
0.8 : ACI 12.2.3.4 (for bars with edge cover of more than 2.5db)
2.0 : ACI 12.2.3.2 (for bars with cover of 1 db or less)
1.3 : ACI 12.2.4.1 (for top-bar factor)

* BS : Bar Size CC : Concrete cover in terms of bar diameter
DP : Deformation pattern OJB : Orangun, Jirsa, Breen (1977)
BL : Bonded length BL+LL : Bonded length plus lead length
NB : Number of bars in each group
UC : Uncoated or coated (U : Uncoated C : Coated)
CP : Casting position (B : Bottom T : Top)

Table 3.13 Comparison of the confined beam-end tests with the Orangun, Jirsa, and Breen (1977) equation and ACI (1989) design provisions

B S *	D P *	C P *	U C *	C C *	N B *	Ultimate bond force (lbs.) Test (normalized)	Predicted OJB* BL*	Predicted OJB* BL+LL*	predicted ACI BL*	predicted ACI BL+LL*	Comparison test / OJB BL*	Comparison test / OJB BL+LL*	Comparison test / ACI BL*	Comparison test / ACI BL+LL*
			U	2	3	14639					1.043	0.728	1.728	1.029
	S	B												
			C	2	3	12301					0.876	0.612	1.452	0.865
5							14041	20114	8472	14221				
			U	2	3	15142					1.078	0.753	1.787	1.065
	N	B												
			C	2	3	13540					0.964	0.673	1.598	0.952
Average of all No. 5 uncoated bars											1.061	0.741	1.758	1.047
Average of all No. 5 coated bars											0.920	0.643	1.525	0.909
			U	2	3	48494					1.244	0.948	2.504	1.705
	S	B												
			C	2	3	39145					1.004	0.765	2.021	1.376
8							38978	51167	19365	28442				
			U	2	3	46511					1.193	0.909	2.402	1.635
	N	B												
			C	2	3	41525					1.065	0.812	2.144	1.460
Average of all No. 8 uncoated bars											1.219	0.929	2.453	1.670
Average of all No. 8 coated bars											1.035	0.789	2.083	1.418

* refer to the last page of table

Table 3.13 (cont.) Comparison of the confined beam-end tests with the Orangun, Jirsa, and Breen (1977) equation and ACI (1989) design provisions

BS*	DP*	CP*	UC*	CC*	NB*	Ultimate bond force (lbs.) Test (normalized)	Predicted OJB* BL*	Predicted OJB* BL+LL*	predicted ACI BL*	predicted ACI BL+LL*	Comparison test / OJB BL*	Comparison test / OJB BL+LL*	Comparison test / ACI BL*	Comparison test / ACI BL+LL*
			U	2	4	50016					0.812	0.740	2.296	1.968
	S	B												
			C	2	4	49146					0.798	0.727	2.256	1.934
11							61565	67556	21786	25416				
			U	2	5	53927					0.876	0.798	2.475	2.122
	N	B												
			C	2	4	46759					0.760	0.692	2.146	1.840
Average of all No. 11 uncoated bars											0.844	0.769	2.386	2.045
Average of all No. 11 coated bars											0.779	0.710	2.201	1.887
Average of all uncoated bars											1.041	0.813	2.199	1.587
Coefficient of variation											0.148	0.102	0.162	0.259
Average of all coated bars											0.911	0.714	1.936	1.405
Coefficient of variation											0.115	0.084	0.152	0.284

* BS : Bar Size
DP : Deformation pattern
CP : Casting position
B : Bottom
T : Top
UC : Uncoated or coated
U : Uncoated C : Coated
CC : Concrete cover in terms of bar diameter
NB : Number of bars in each group
BL : Bonded length
BL+LL : Bonded length plus lead length
OJB : Orangun, Jirsa, Breen (1977) equation

Table 3.14 Comparison of the splice tests with the Orangun, Jirsa, and Breen (1977) equation and ACI (1989) design provisions

BS *	Concrete strength (psi)	DP *	UC *	Cover (db*)	Bar Force (lbs.) Test	OJB*	ACI	test/OJB	test/ACI	ACI factors **
			U	1.60	19375			1.215	1.284	0.8,1.4,1.3
			U+	1.60	20243			1.269	1.342	
5	5360	N	C+	1.60	15190	15946	15085	0.953	1.007	0.8,1.4,1.3
	Average of uncoated No. 5 splices							1.242	1.313	
	Average of coated No. 5 splices							0.953	1.007	
			U	1.33	20152			1.044	1.262	
		S	C	1.33	18964			0.983	1.187	0.8,1.4,1.3
6	6010		U	1.33	22616	19298	15973	1.172	1.416	
		C	C	1.33	17292			0.896	1.083	0.8,1.4,1.3
	Average of uncoated No. 6 splices							1.108	1.339	
	Average of coated No. 6 splices							0.940	1.135	
			U	1.50	34049			0.929	2.003	
		S	C	1.50	30573			0.834	1.799	1.4,1.3
8	5980		U	1.50	34207	36664	16996	0.933	2.013	
		N	C	1.50	29388			0.802	1.729	1.4,1.3
	Average of uncoated No. 8 splices							0.931	2.008	
	Average of coated No. 8 splices							0.818	1.764	

*, **, + Refer to last page of table

Table 3.14 (cont.) Comparison of the splice tests with the Orangun, Jirsa, and Breen (1977) equation and ACI (1989) design provisions

BS*	Concrete strength (psi)	DP*	UC*	Cover (db*)	Bar Force (lbs.) Test	OJB*	ACI	test/OJB	test/ACI	ACI factors **
			U	1.42	62712			0.866	2.487	
		S								1.4,1.3
			C	1.42	45240			0.625	1.794	
11	5850					72431	25215			
			U	1.42	58968			0.814	2.339	
		C								1.4,1.3
			C	1.42	48516			0.670	1.924	
	Average of uncoated No. 11 splices							0.840	2.413	
	Average of coated No. 11 splices							0.648	1.859	
	Average of all uncoated splices							1.030	1.768	
	Coefficient of variation							0.151	0.263	
	Average of all coated splices							0.824	1.503	
	Coefficient of variation							0.149	0.239	

\+ These beams contained three splices

* BS : Bar size
DP : Deformation pattern
UC : Uncoated or Coated
U : Uncoated
C : Coated
db : Bar diameter
OJB : Orangun, Jirsa, Breen (1977) equation

** ACI factors : ACI factors for development length, ACI 318-89, Sections 12.2.3.1 - 12.2.3.4 and 12.2.4.1
0.8 : ACI 12.2.3.4 (for bars with edge cover of more than 2.5db)
1.4 : ACI 12.2.3.3 (for bars with a cover between 1 and 2db)
1.3 : ACI 12.2.4.1 (for top-bar factor)

Table 4.1 Face angle of the test bars

Bar size	Deformation pattern	Face angle (degrees) 1*	2*	3*	Average face angle for all deformation patterns (degrees) 1*	2*	3*
5	S	28.22	43.77	47.18	31.43	46.98	47.83
	C	29.35	45.93	45.29			
	N	36.71	51.25	51.03			
6	S	27.35	39.53	45.16	33.44	48.67	50.22
	C	37.87	56.73	56.57			
	N	35.09	49.74	48.94			
8	S	31.23	46.66	49.75	31.61	51.54	53.52
	C	28.49	52.15	55.61			
	N	35.10	55.80	55.20			
11	S	36.20	54.04	55.21	31.41	47.74	47.98
	C	28.63	46.09	45.42			
	N	29.41	43.10	43.32			
Average of all bars					31.97	48.73	49.89

* 1 : Average face angle around the circumference of the bar (Appendix A)
2 : Maximum face angle around the circumference of the bar (Appendix A)
3 : Maximum face angle around the circumference of the bar at the mid-height of the deformations (Appendix A)

Table 4.2 Number of nodes and elements in the finite element model (exterior concrete substructure and link elements) for each case

Case	Structure *	Nodes	Elements
1 in. lead length	block	1717	1200
2 db cover	links	-	374
2 in. lead length	block	1653	1152
1 db cover	links	-	342
2 in. lead length	block	1919	1350
2 db cover	links	-	418
2 in. lead length	block	2166	1548
3 db cover	links	-	494
3 in. lead length	block	2121	1500
2 db cover	links	-	462

* block : eigth node brick elements for the exterior concrete model
links : two node rod elements conecting the exterior concrete model to the crack plane

Table 4.3 Ultimate lateral force and corresponding displacement of the finite element models

Case	This study		Choi, Darwin, McCabe (1990)	
	Peak load (lb.)	Displacement (in.)	Peak load (lb.)	Displacement (in.)
1 in. lead length 2 db cover	8883	0.00380	7984	0.00237
2 in. lead length 1 db cover	9375	0.00371	7270	0.00223
2 in. lead length 2 db cover	10130	0.00358	9550	0.00197
2 in. lead length 3 db cover	11081	0.00351	12221	0.00241
3 in. lead length 2 db cover	12444	0.00414	11649	0.00205

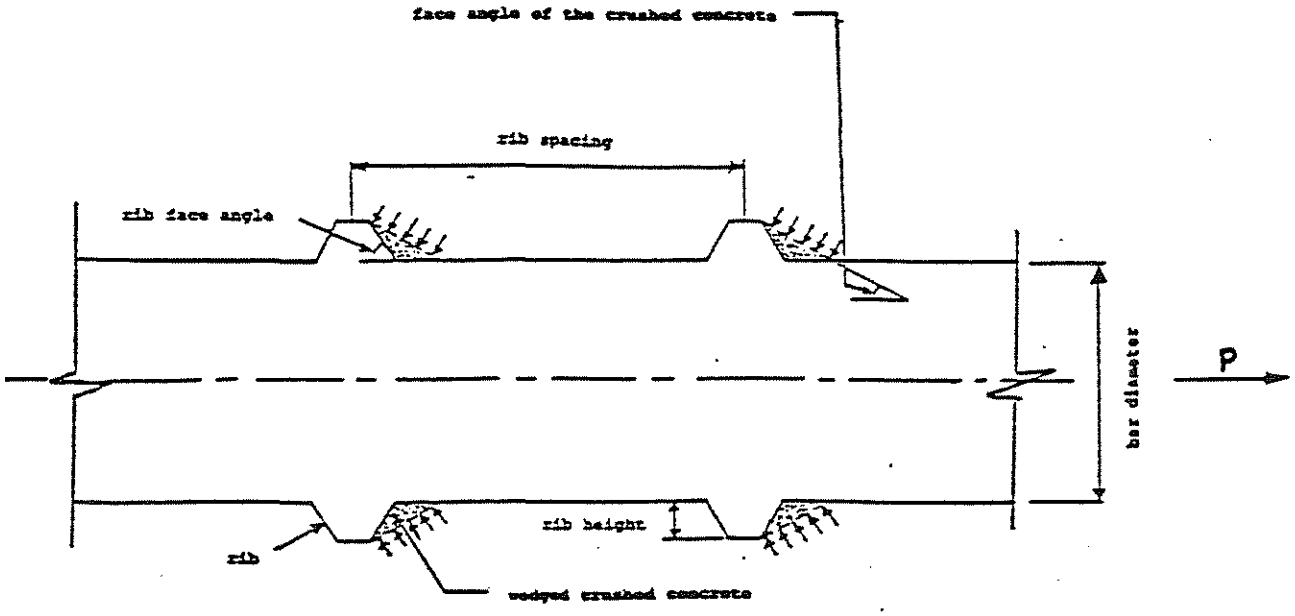

Fig. 1.1 The Geometry of a Deformed Reinforcing Bar and the Mechanical Interaction Between the Bar and the Concrete (Tepfers 1979)

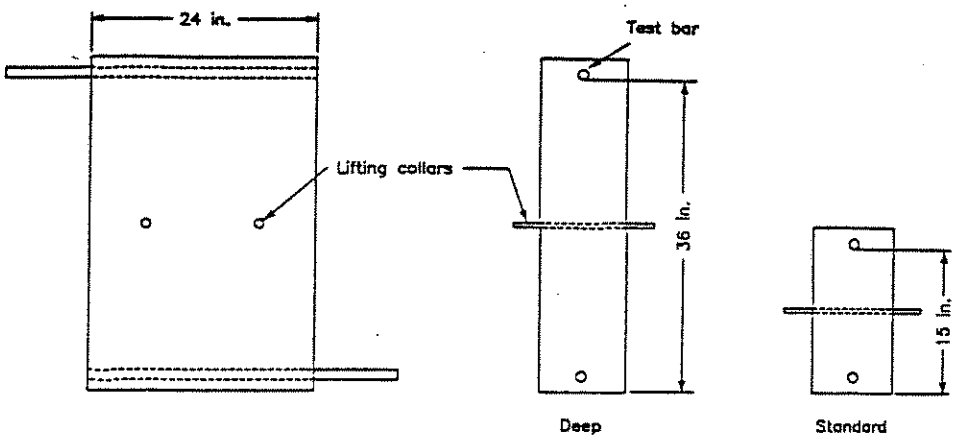

(a)

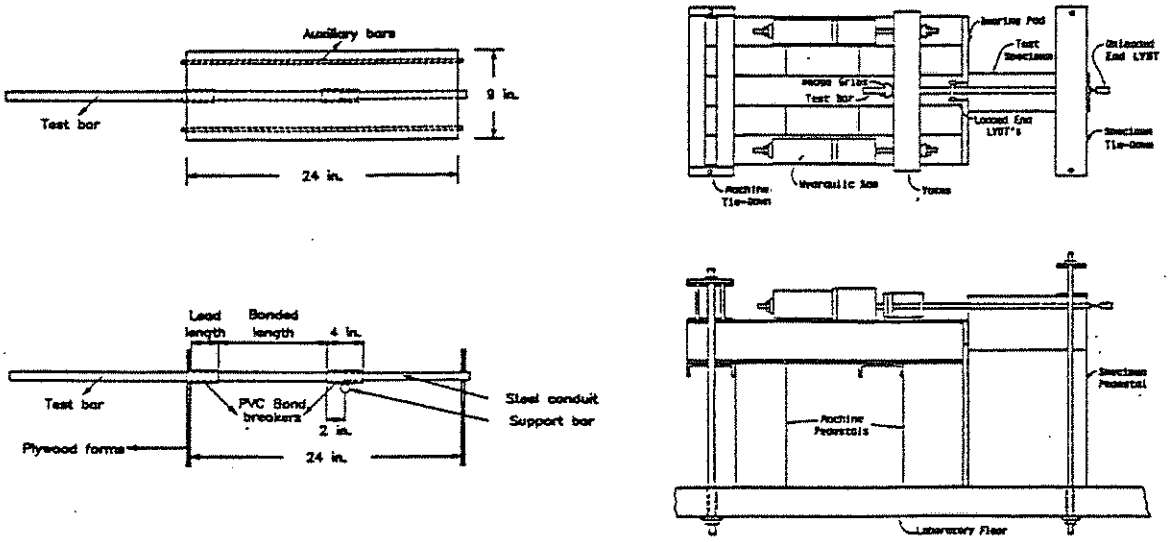

(b) (c)

Fig. 2.1 Beam End Specimen and Test Set-up

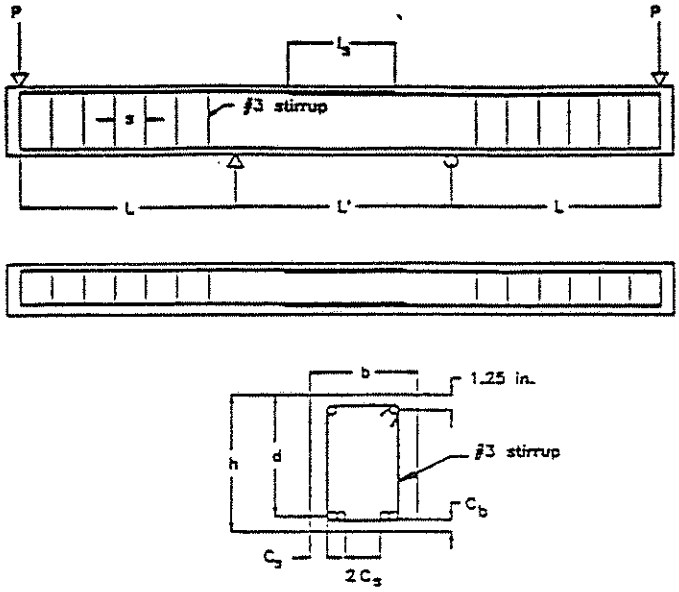

Bar Size	L (ft.)	L' (ft.)	l_s (in.)	No. of splices	s (in.)	b (in.)	d (in.)	h (in.)	Cs (in.)	Cb (in.)
#5	4	4	12	3	6	15.75	14.69	16	2	1
#5	4	4	12	2	6	10.5	14.69	16	2	1
#6	4	4	12	2	7	11	14.63	16	2	1
#8	4	4	16	2	7	12	14	16	2	1.5
#11	4.5	6	24	2	6	13.65	13.30	16	2	2

(a)

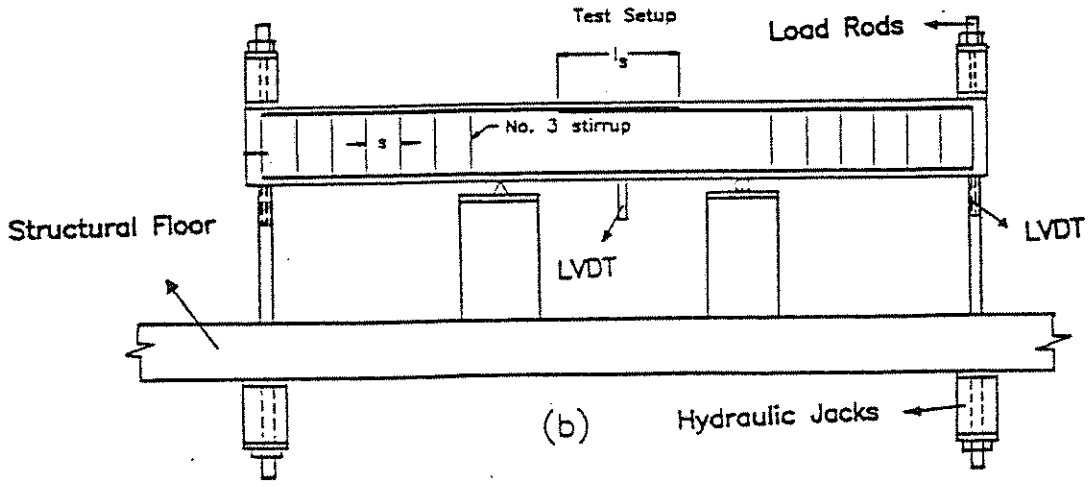

Fig. 2.2 Beam Splice Specimen and Test Set-up

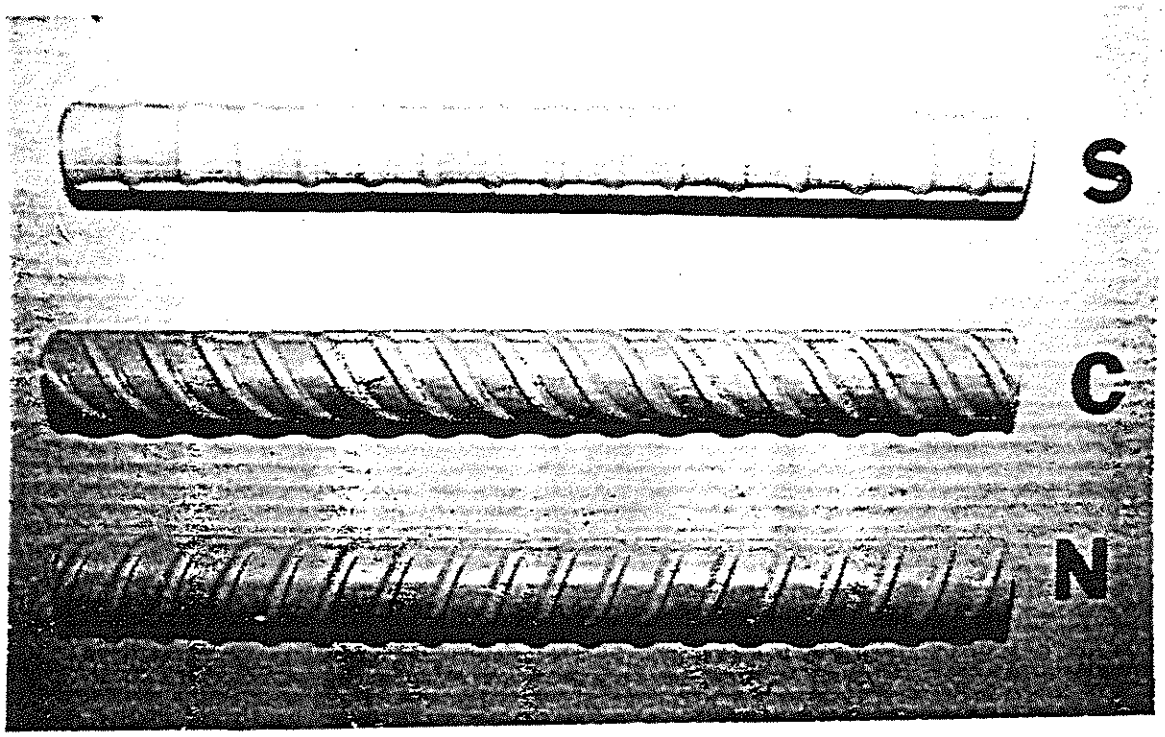

Fig. 2.3 Reinforcing Bar Deformation Patterns

Fig. 2.3 Reinforcing Bar Deformation Patterns

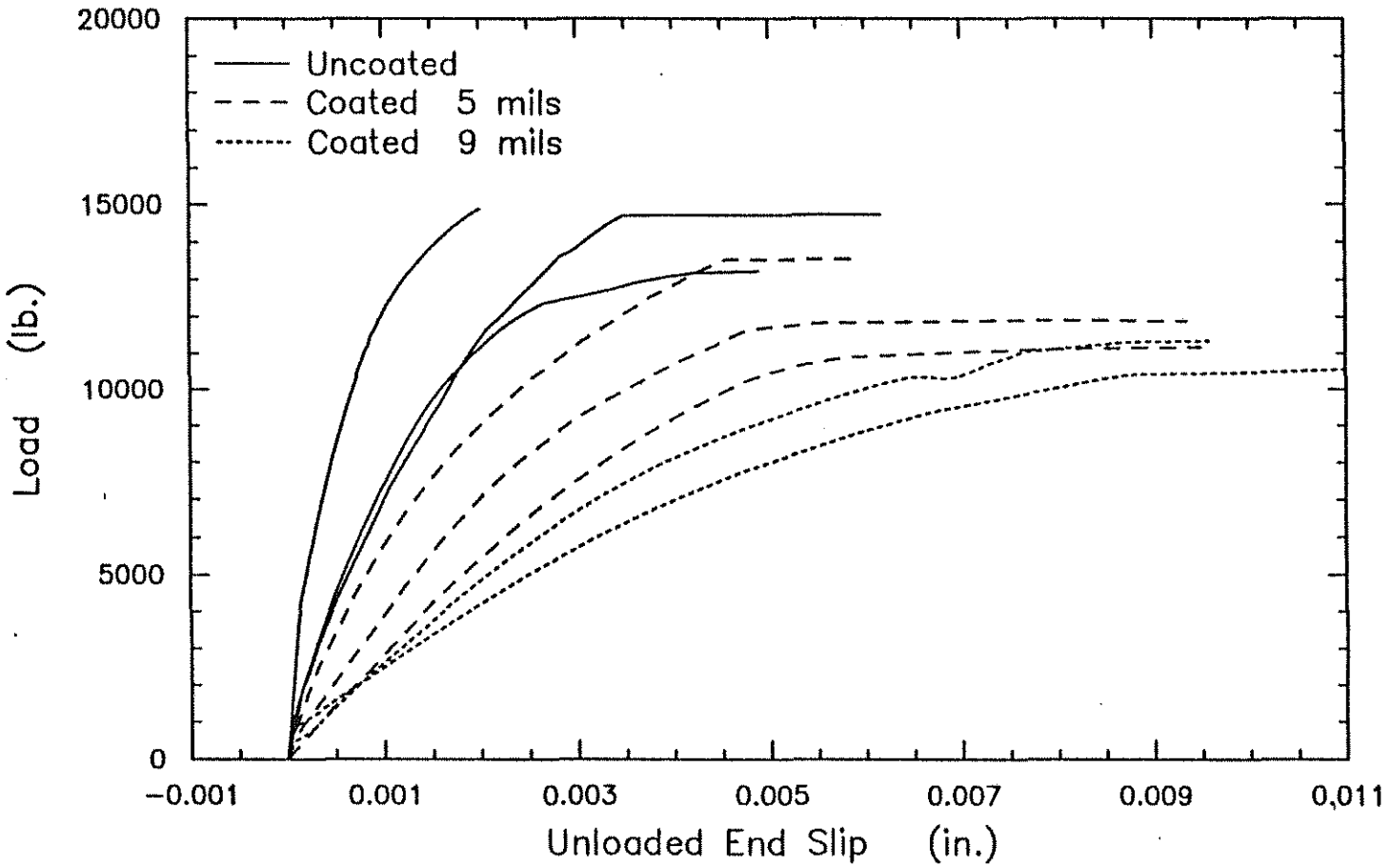

Fig. 2.4 Load – Slip Curves of Beam–end Specimens with S – pattern No. 5 Bars

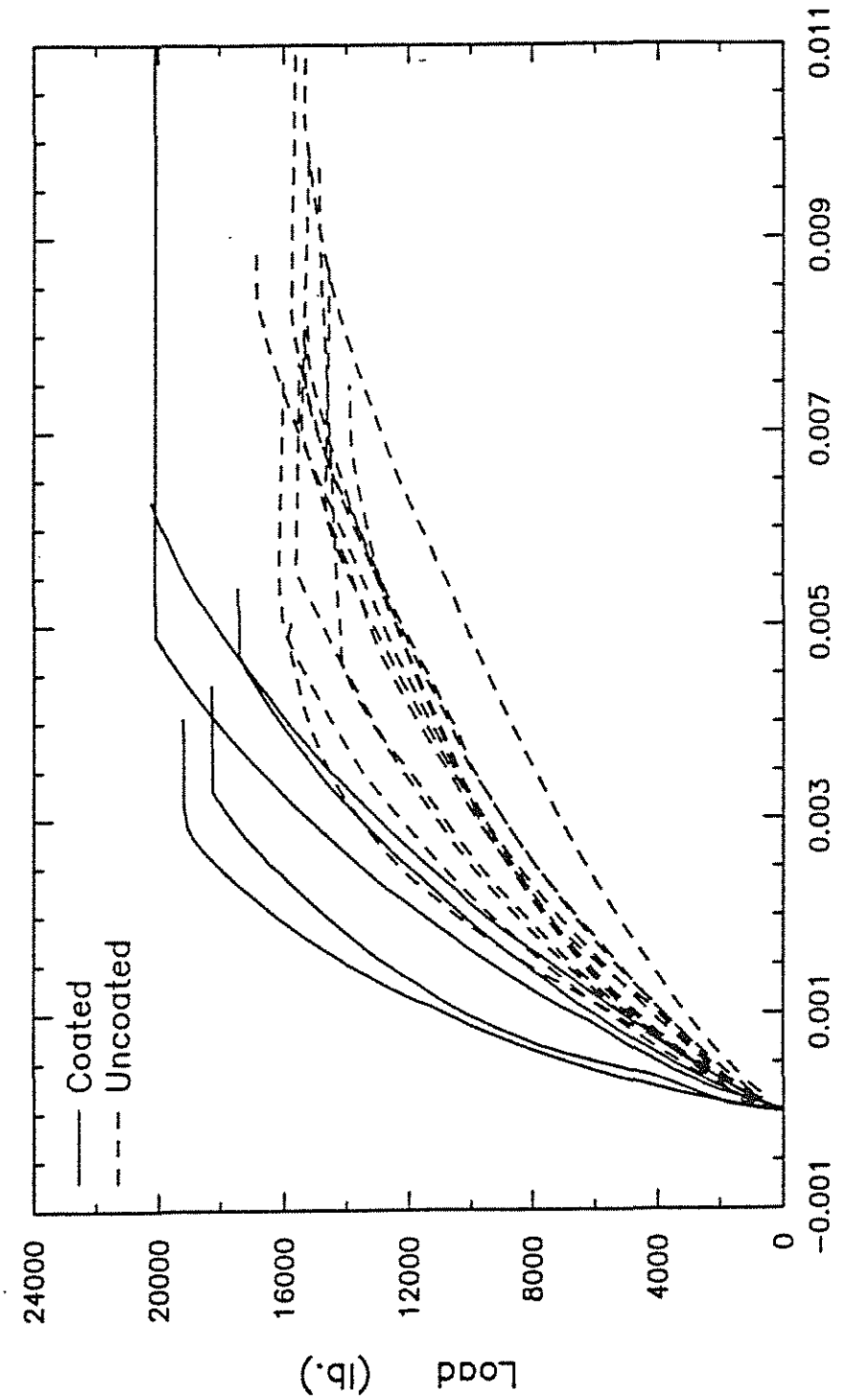

Fig. 2.5 Load – Slip Curves of Beam–end Specimens with S – pattern No. 6 Bars

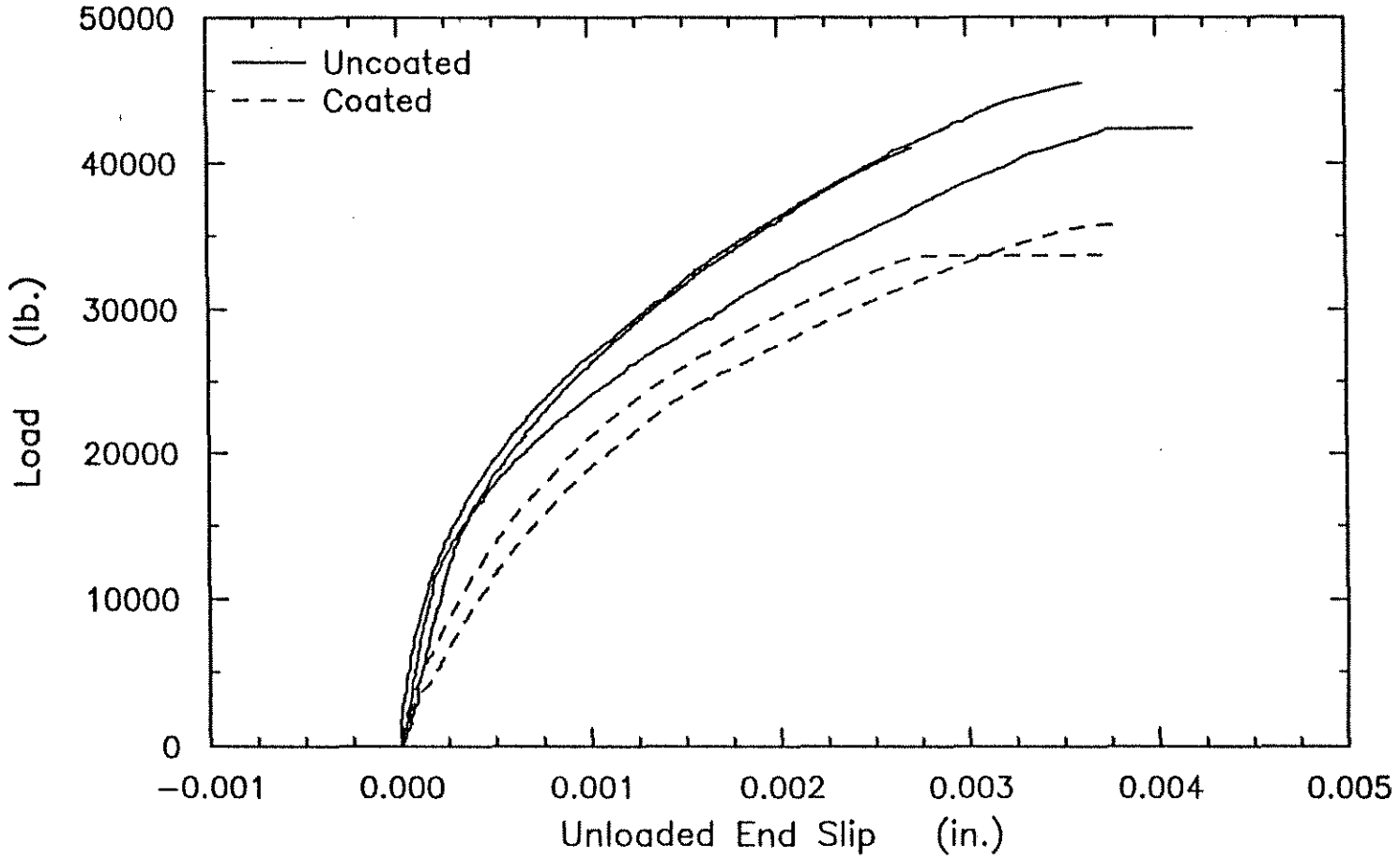

Fig. 2.6 Load – Slip Curves of Beam–end Specimens with N – pattern No. 8 Bars

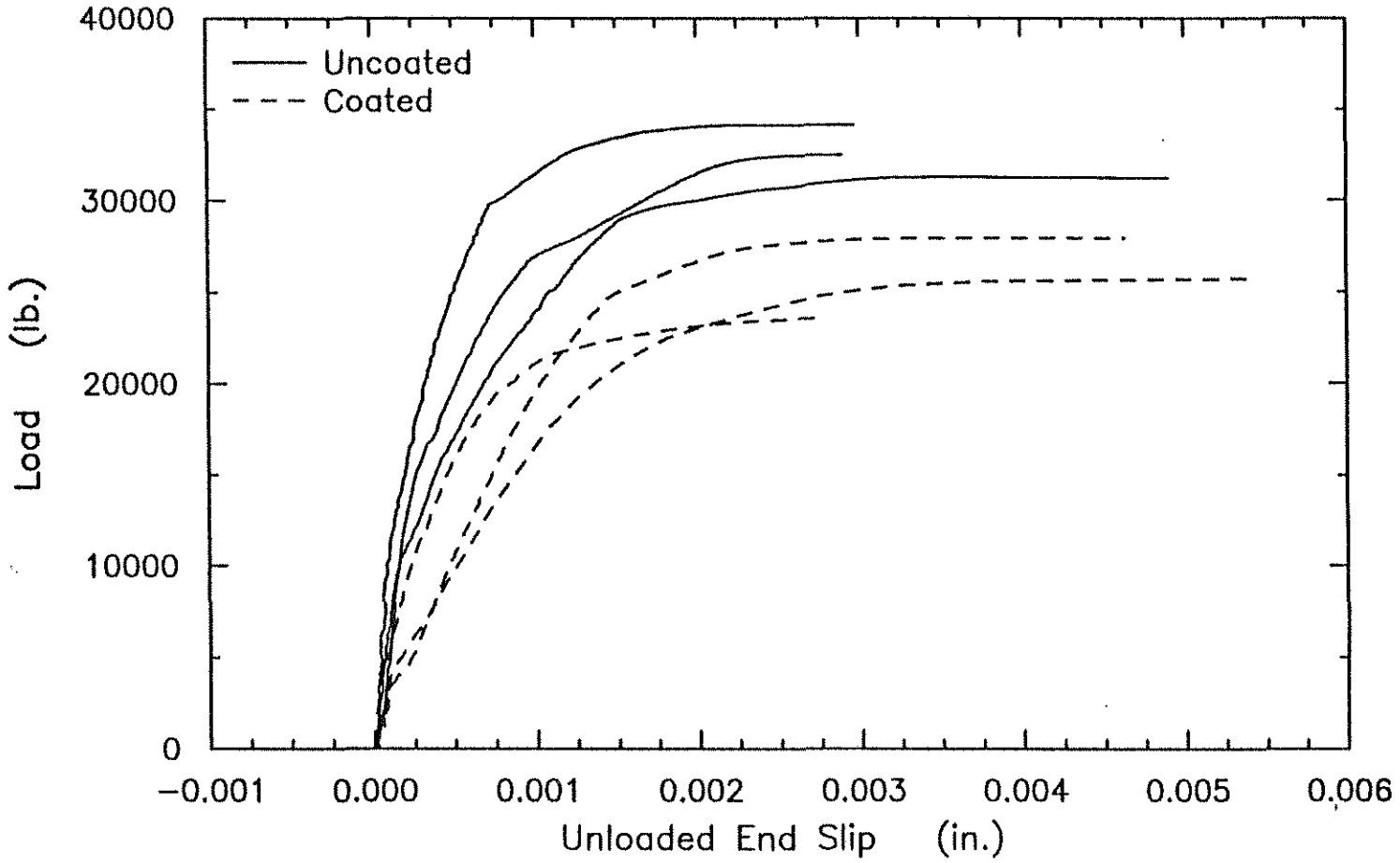

Fig. 2.7 Load – Slip Curves of Beam–end Specimens with N – pattern No. 11 Bars

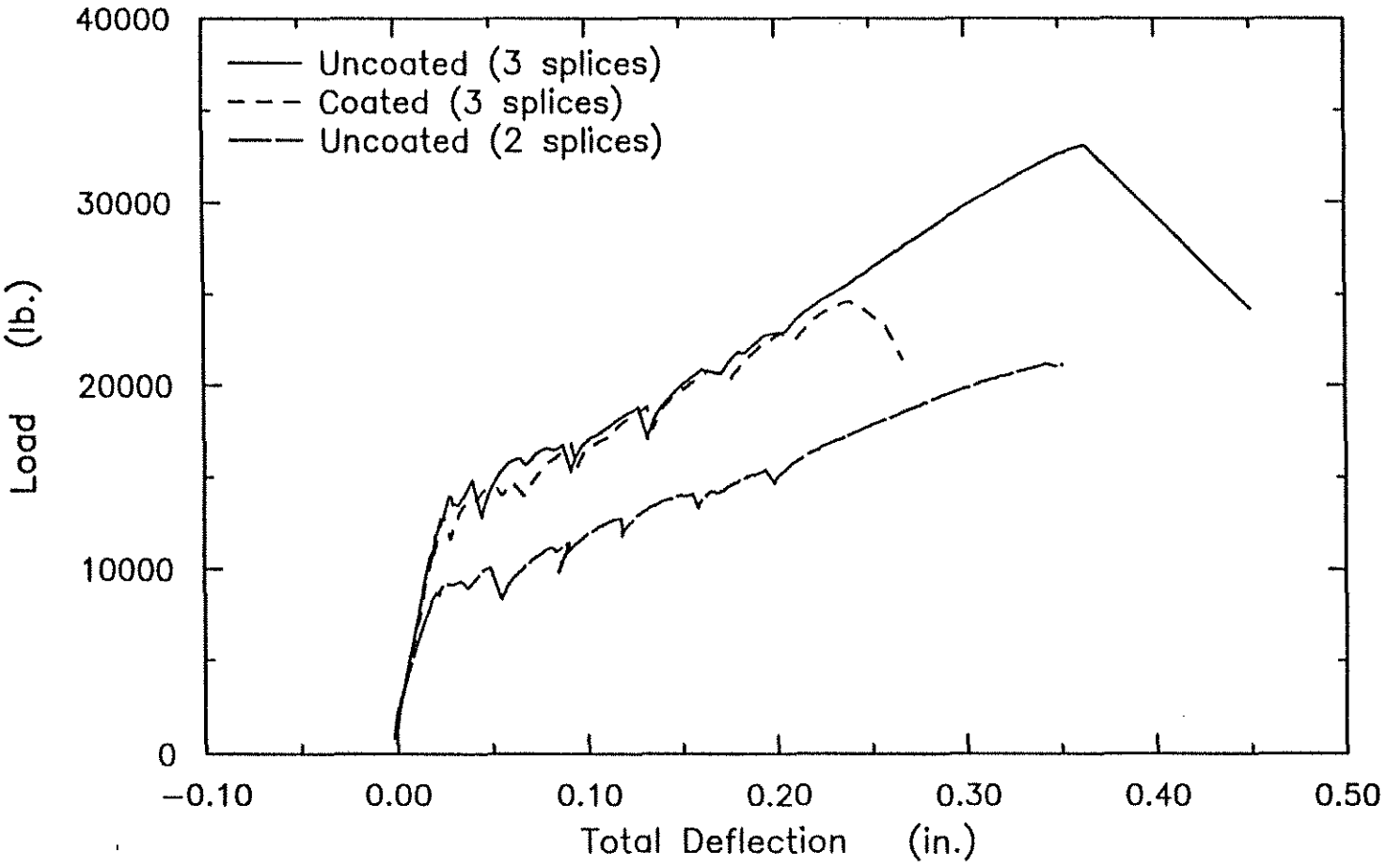

Fig. 2.8 Load–Deflection Curves of Beam Splice Specimens with N – pattern No. 5 Bars

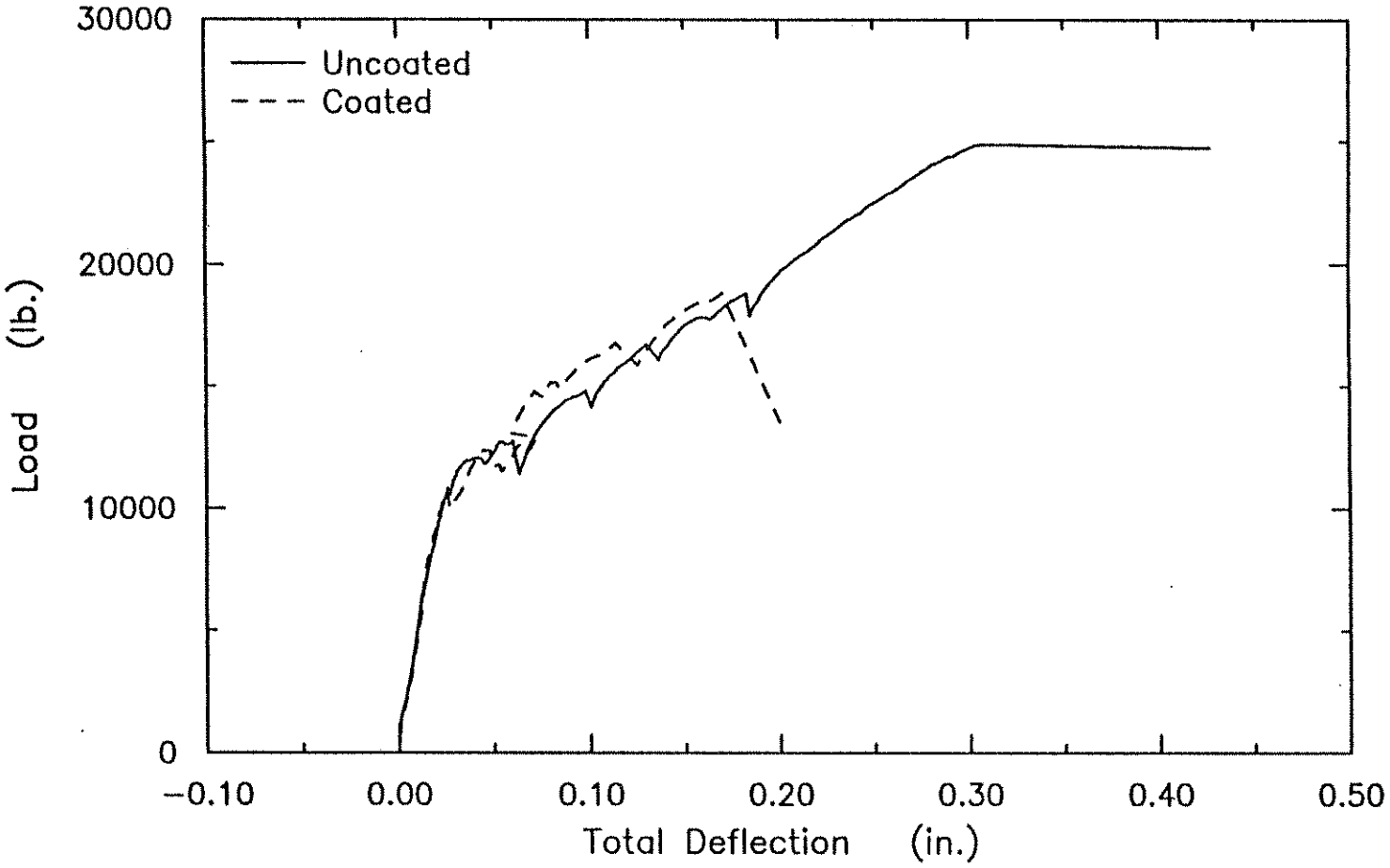

Fig. 2.9 Load–Deflection Curves of Beam Splice Specimens with C – pattern No. 6 Bars

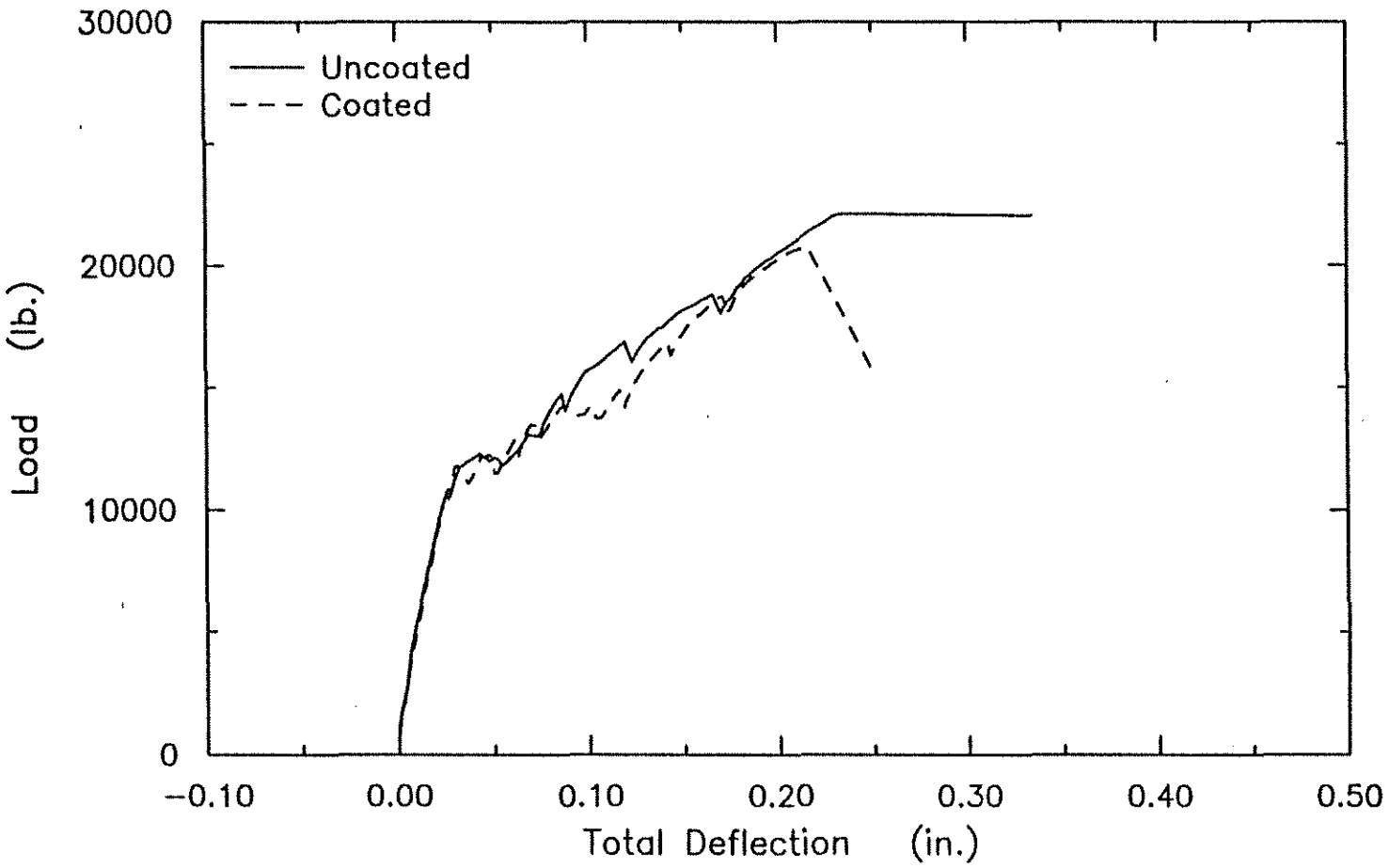

Fig. 2.10 Load–Deflection Curves of Beam Splice Specimens with S – pattern No. 6 Bars

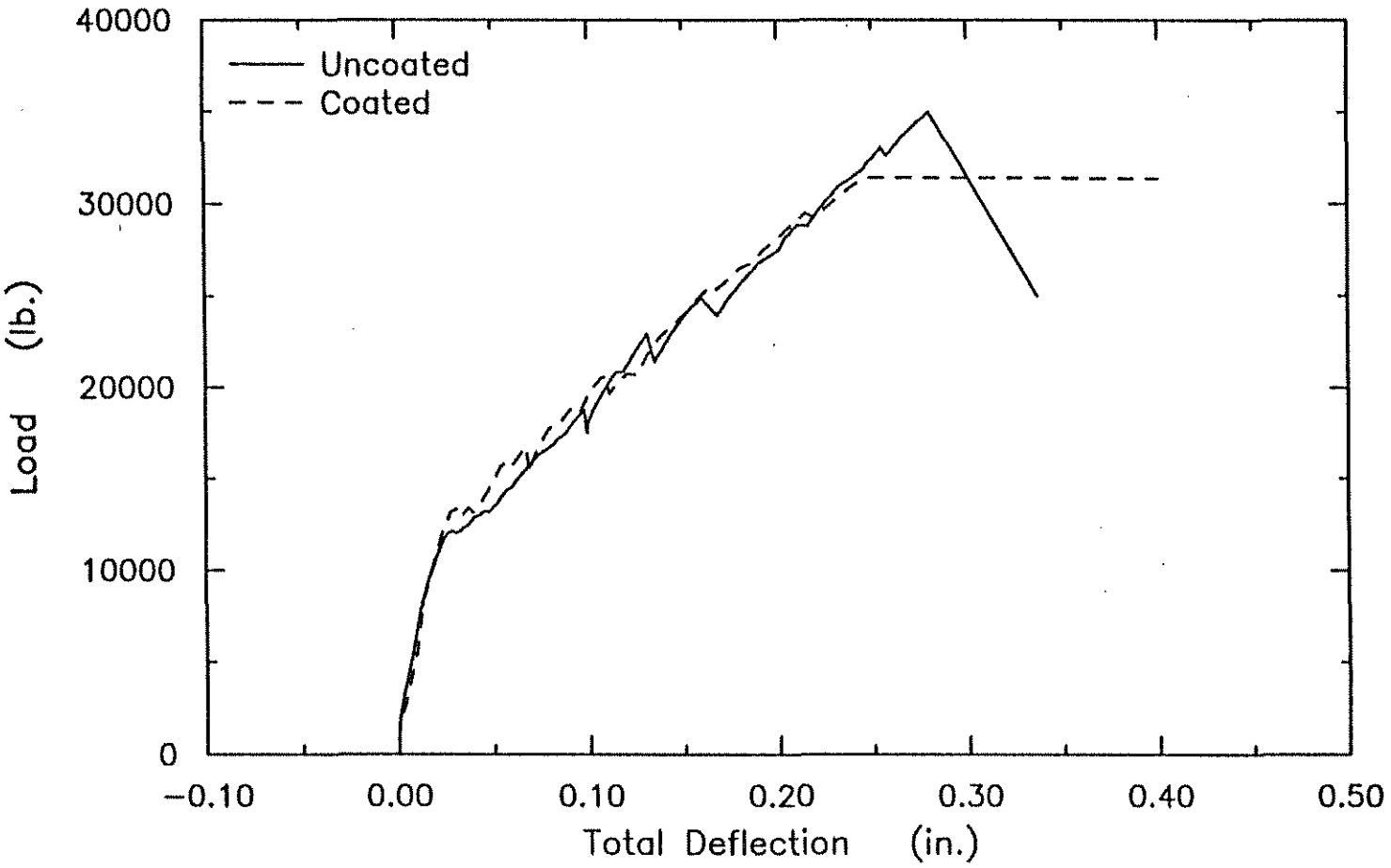

Fig. 2.11 Load–Deflection Curves of Beam Splice Specimens with S – pattern No. 8 Bars

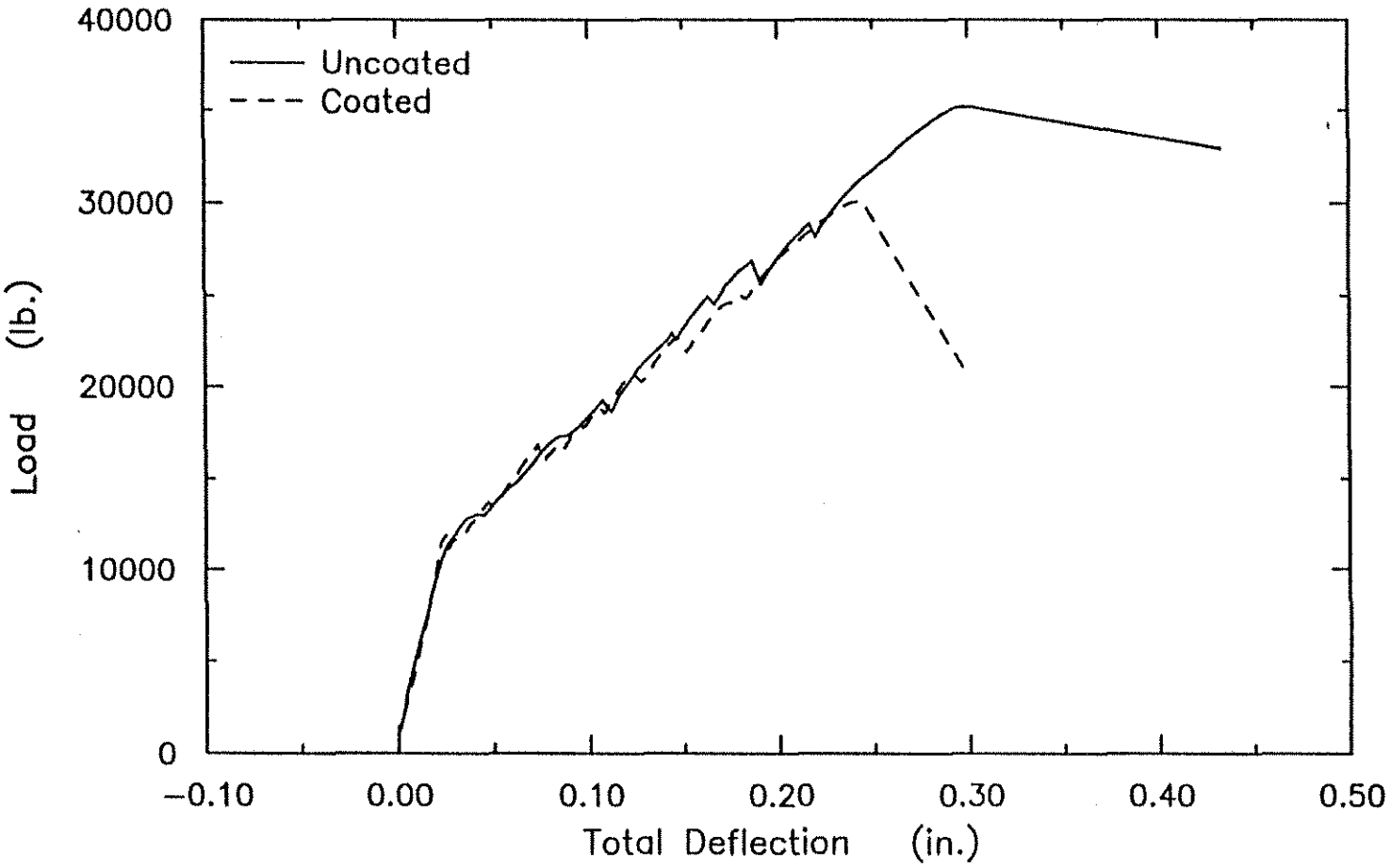

Fig. 2.12 Load–Deflection Curves of Beam Splice Specimens with N – pattern No. 8 Bars

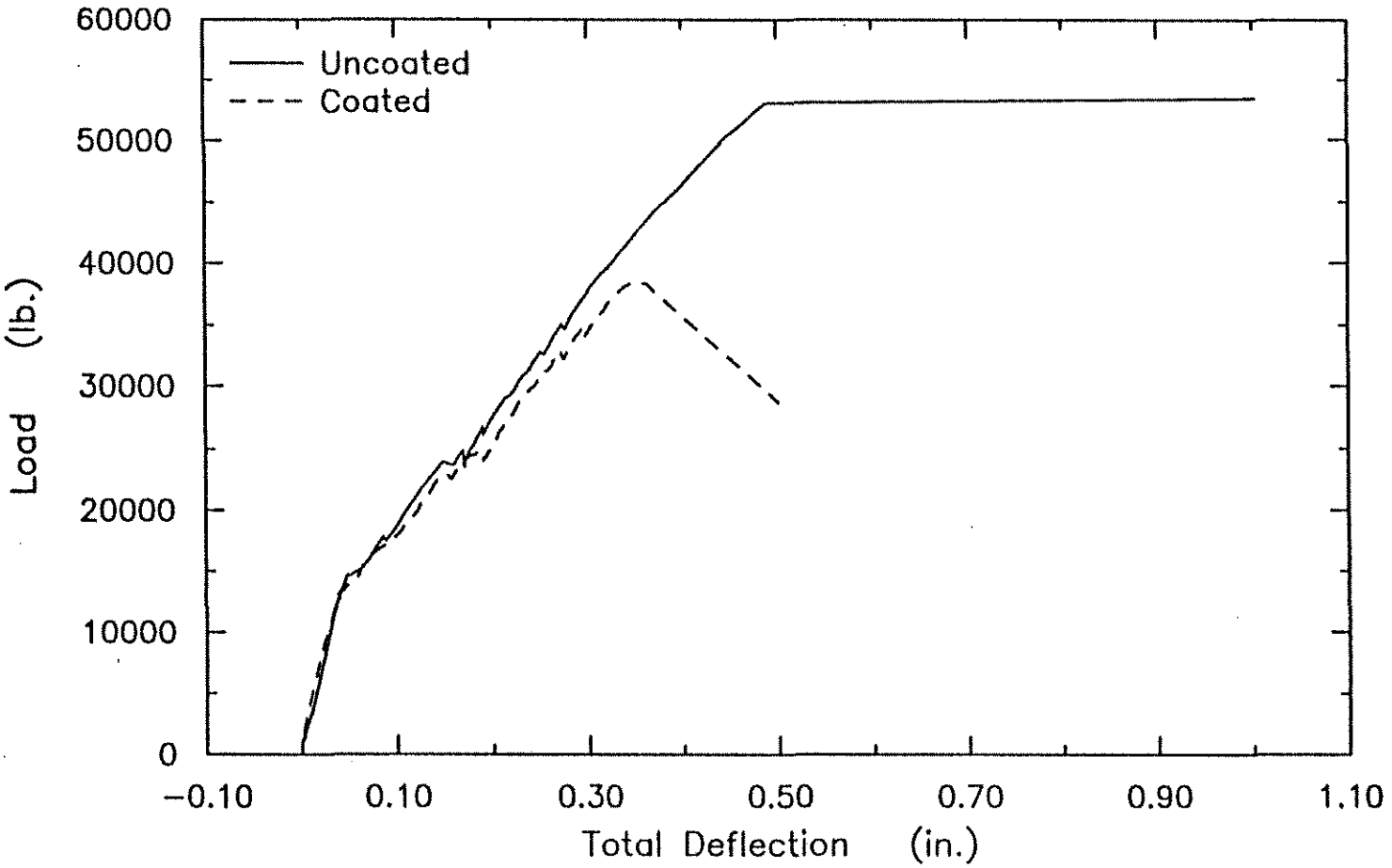

Fig. 2.13 Load–Deflection Curves of Beam Splice Specimens with S – pattern No. 11 Bars

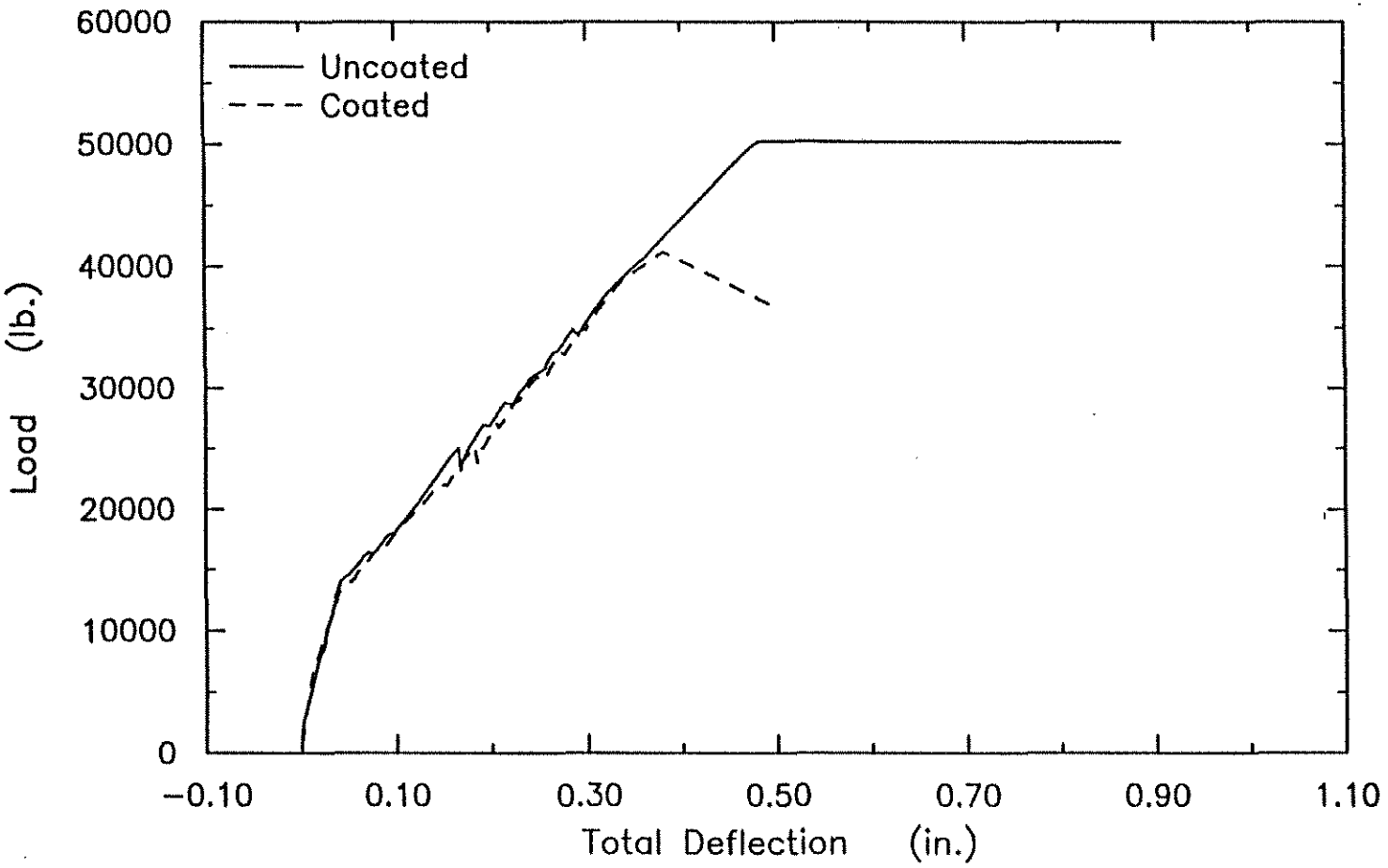

Fig. 2.14 Load–Deflection Curves of Beam Splice Specimens with C – pattern No. 11 Bars

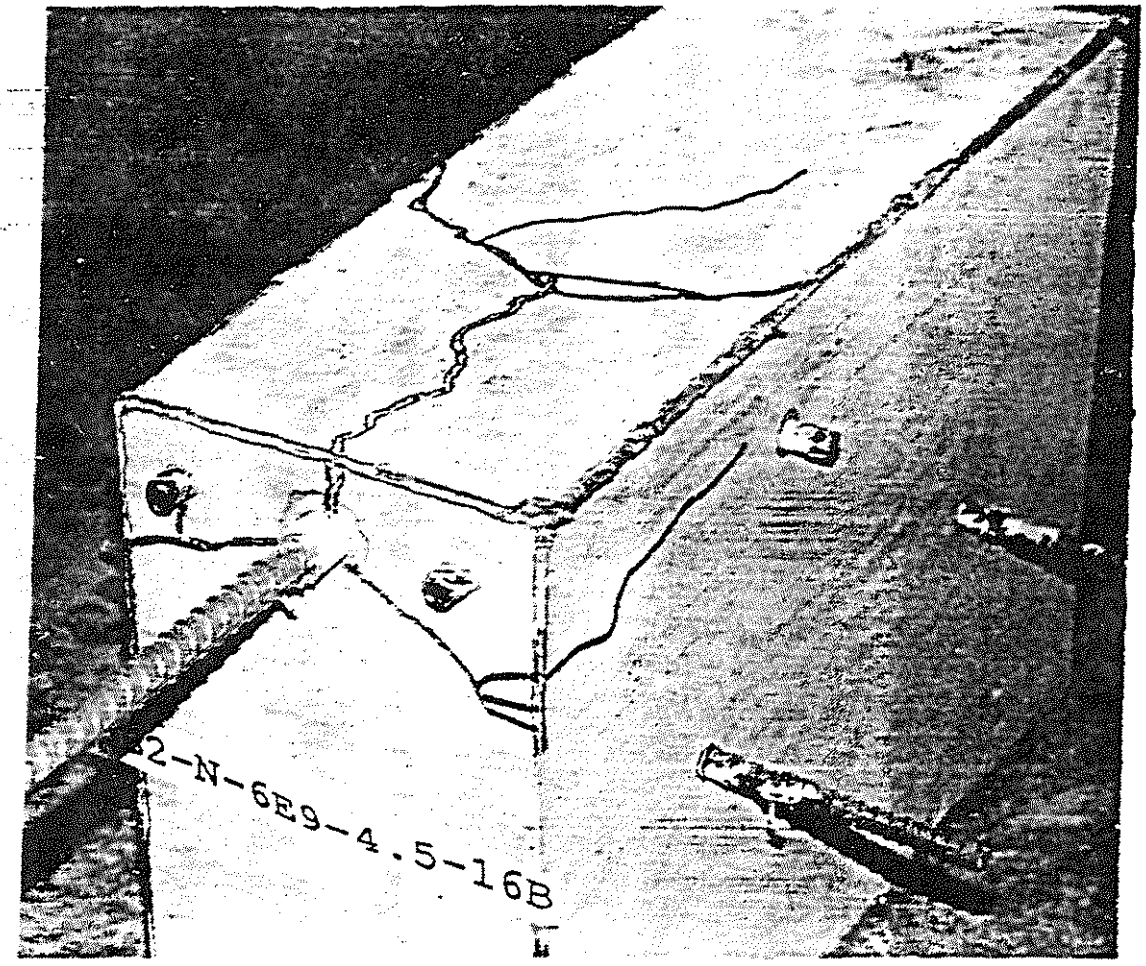

Fig. 2.15 Cracked Beam–end Specimen

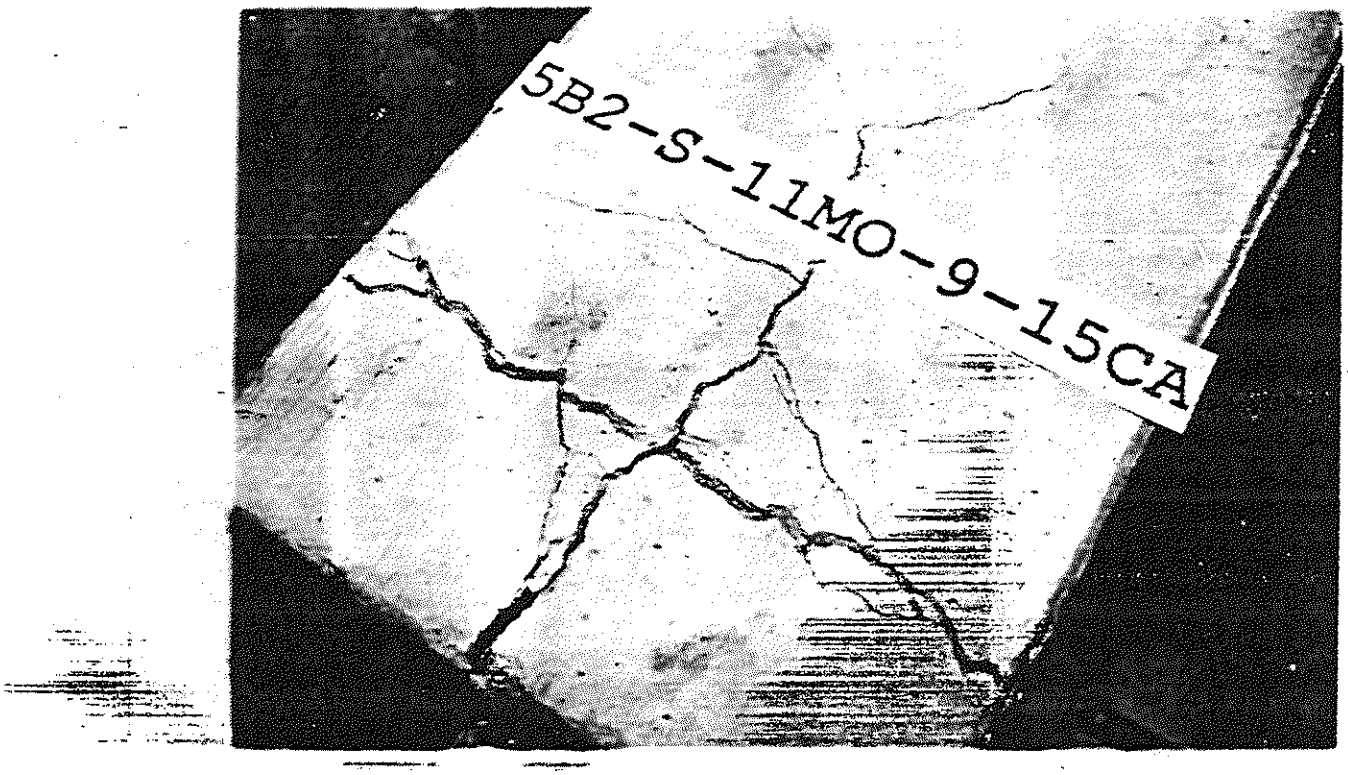

Fig. 2.16 Cracked Confined Beam–end Specimen

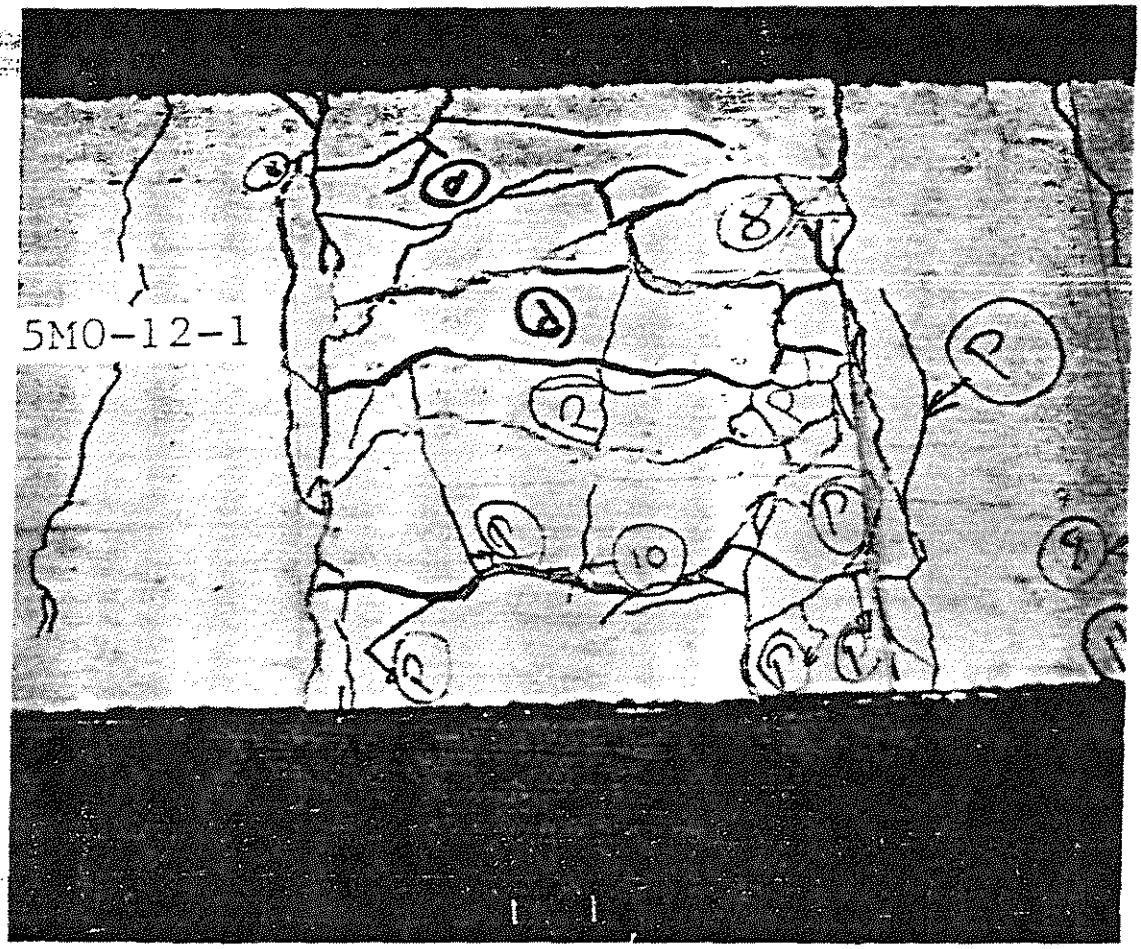

Fig. 2.17 Cracked Splice Specimen

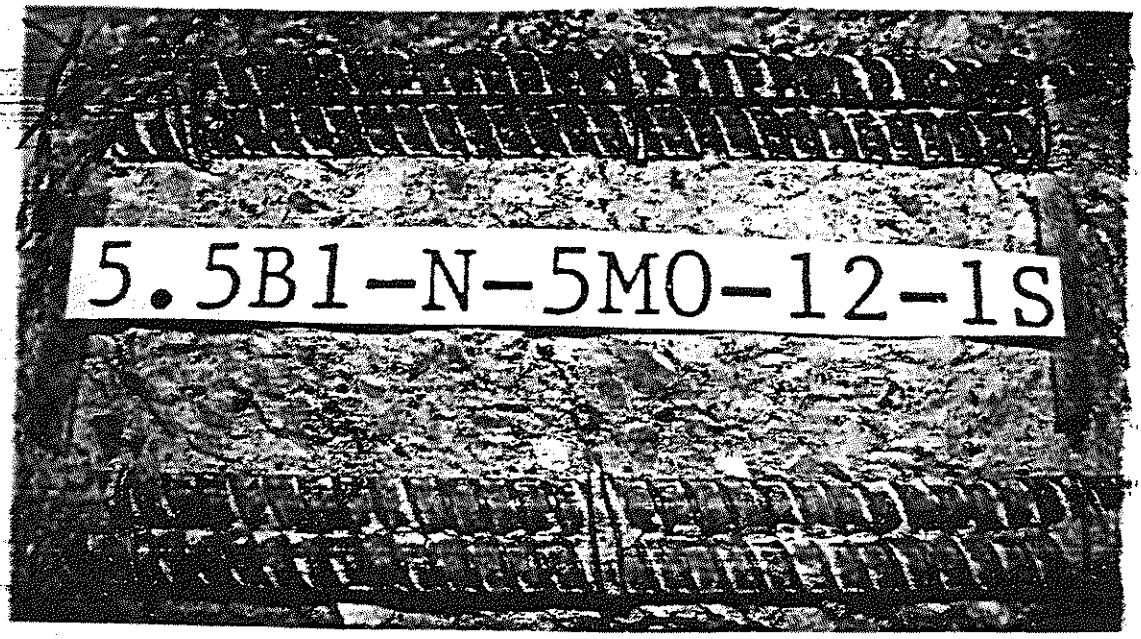

(a) Uncoated Bars

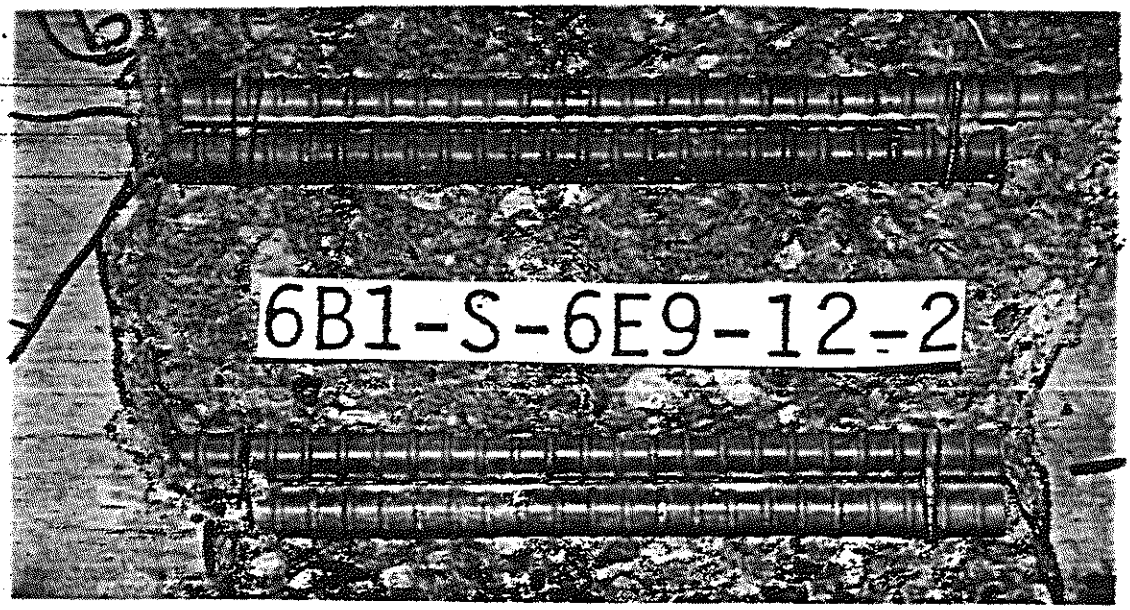

(b) Epoxy-Coated Bars

Fig. 2.18 Test Bar Appearance (beam splices)

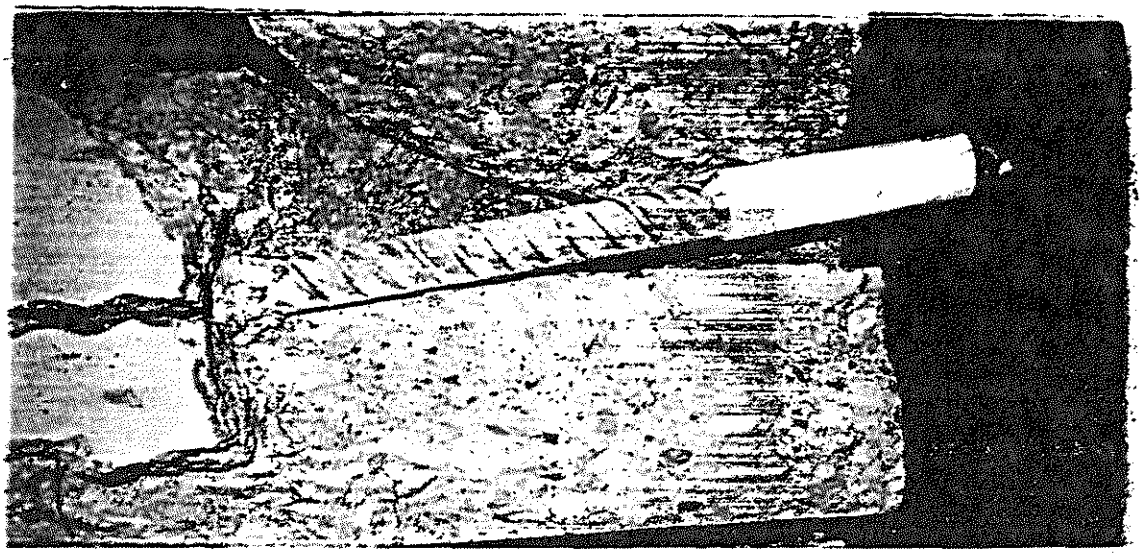

(a) Uncoated Bars

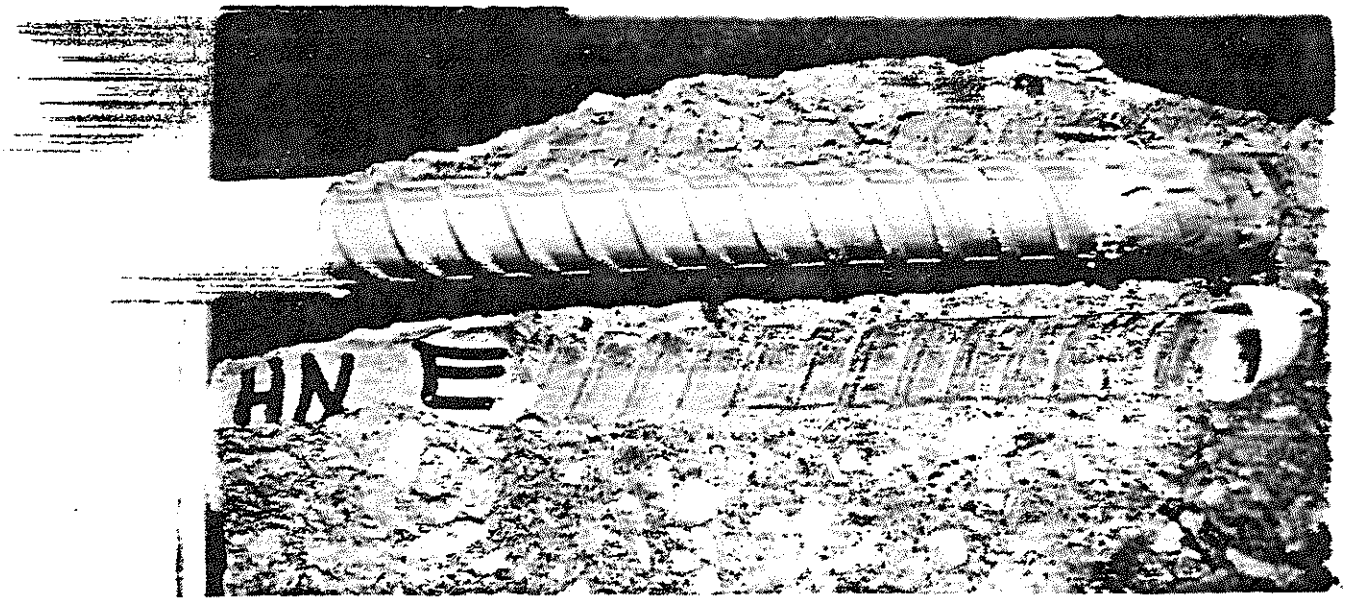

(b) Epoxy–Coated Bars

Fig. 2.19 Concrete Key Appearance After Testing (beam–end specimen)

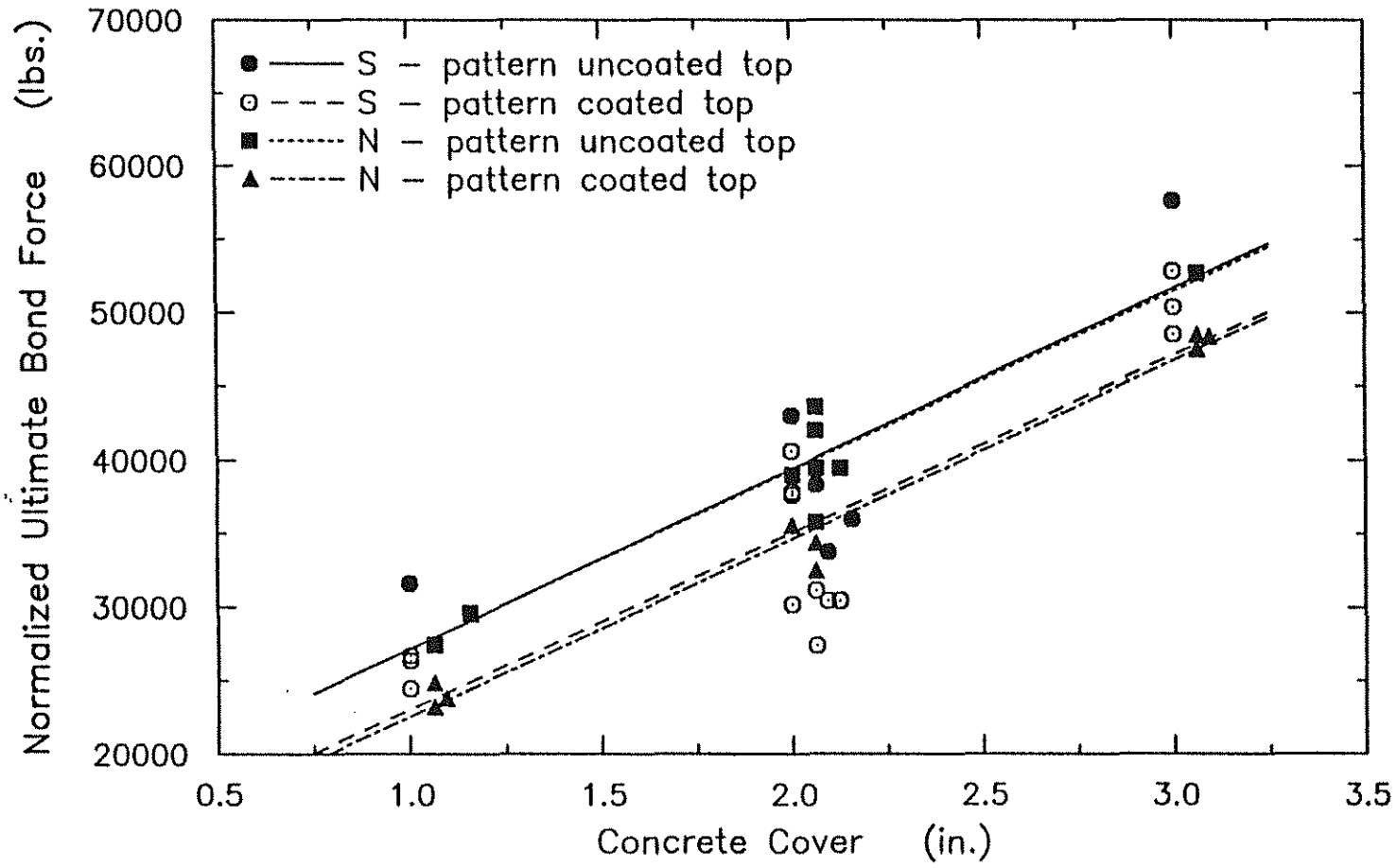

Fig. 3.1 Normalized Ultimate Bond Force versus Concrete Cover for No. 8 Bars

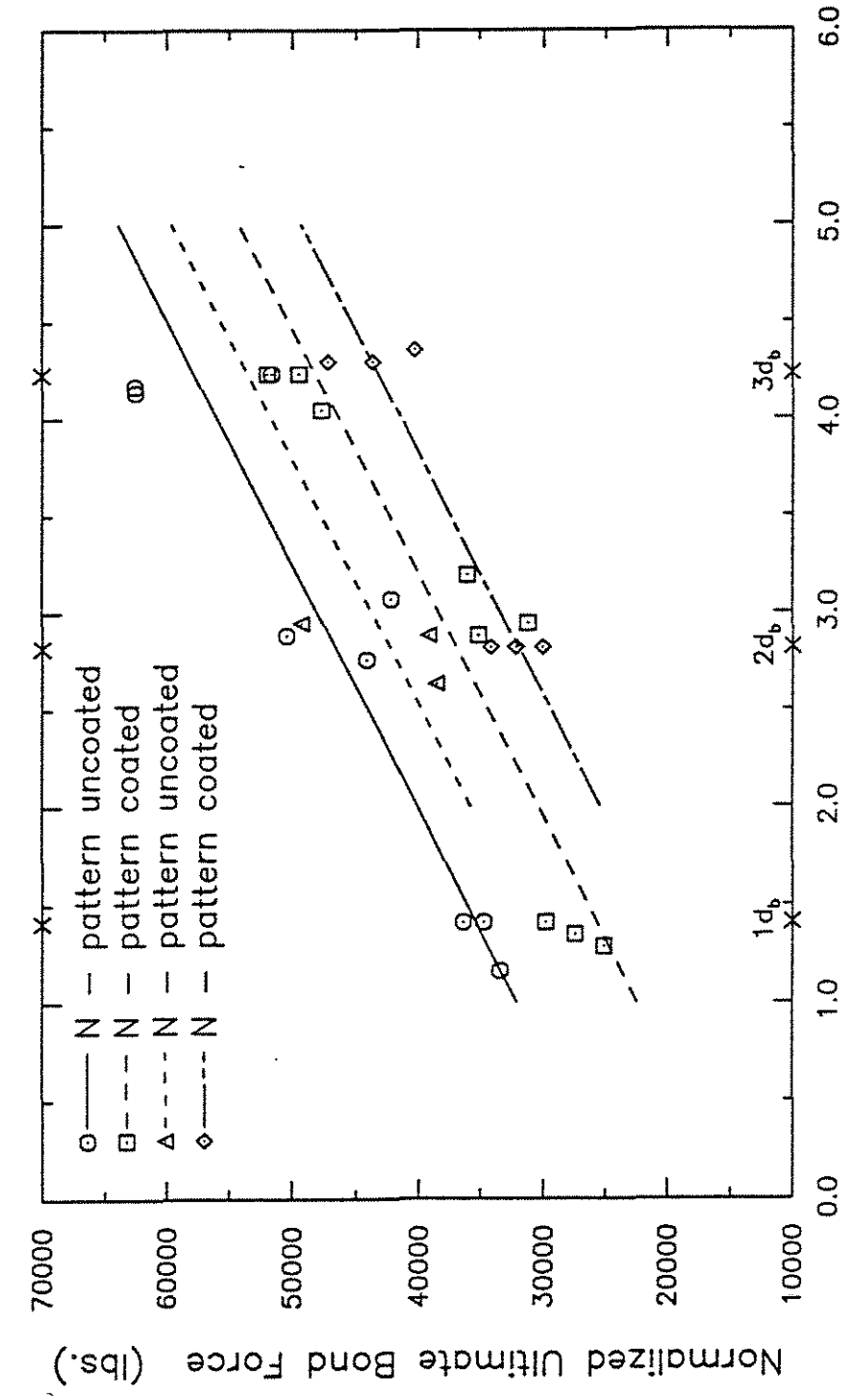

Fig. 3.2 Normalized Ultimate Bond Force versus Concrete Cover for No. 11 Bars Using Dummy Variable Technique

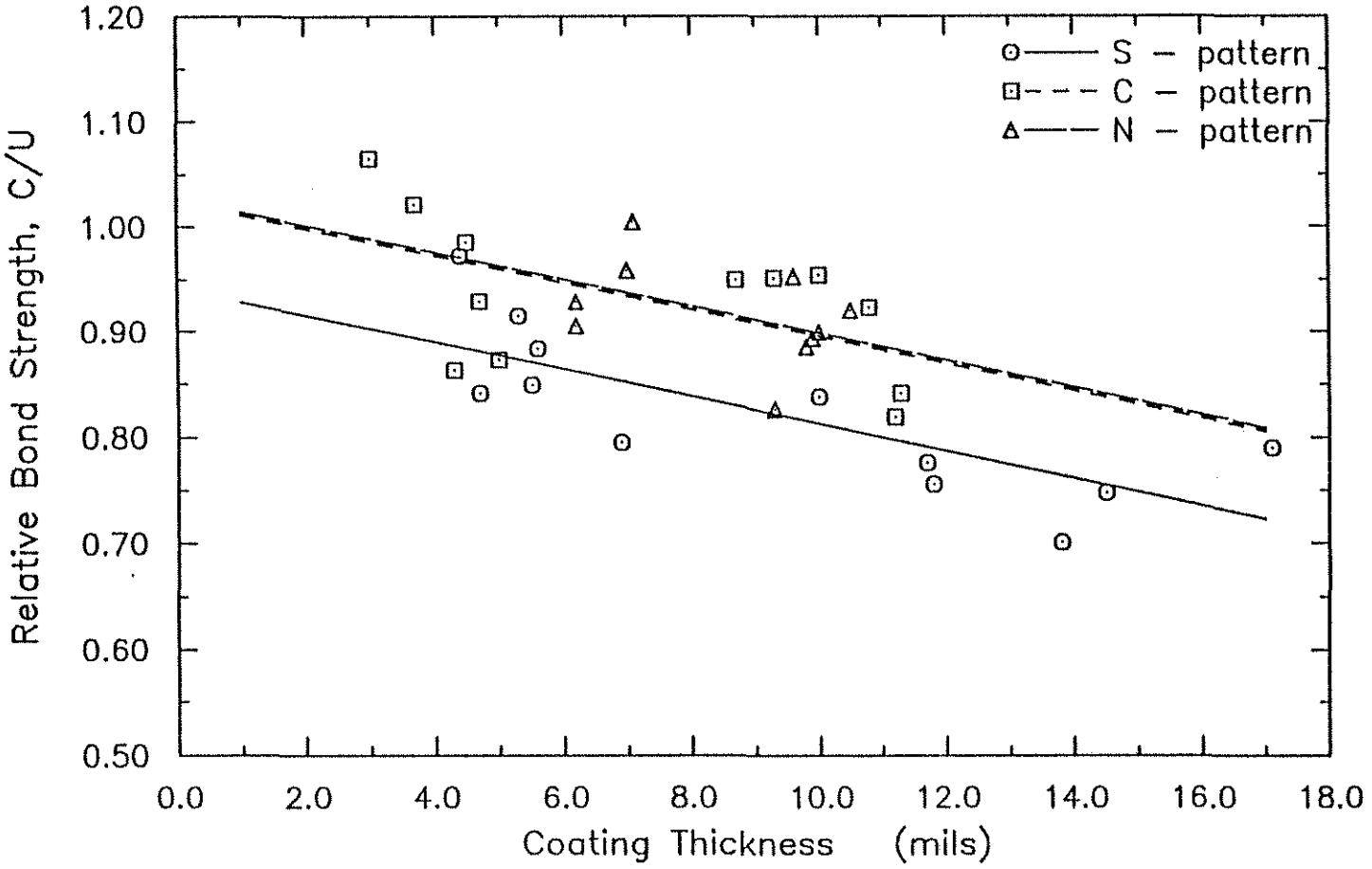

Fig. 3.3 Relative Bond Strength versus Coating Thickness for No. 5 Bars

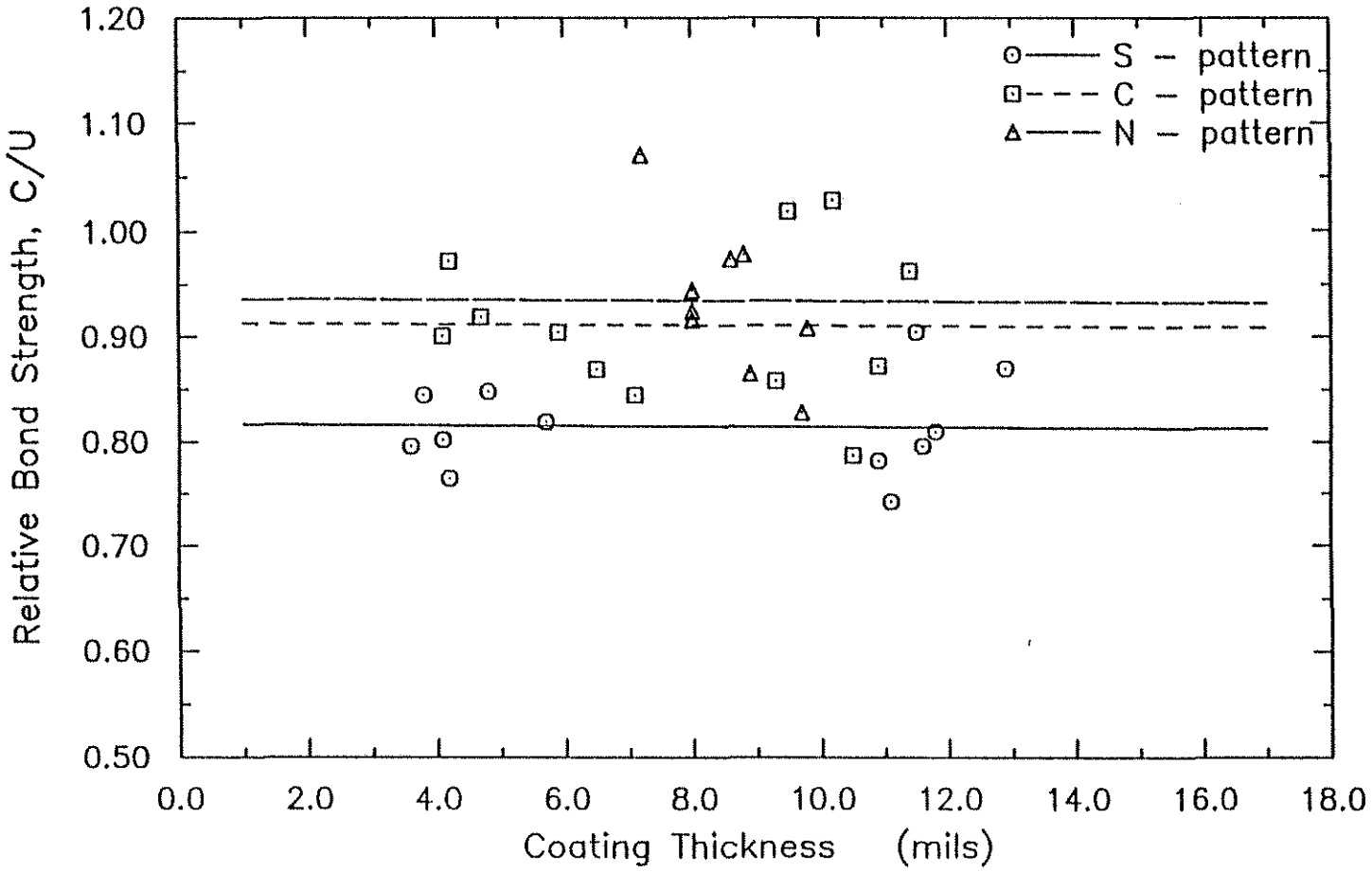

Fig. 3.4 Relative Bond Strength versus Coating Thickness for No. 6 Bars

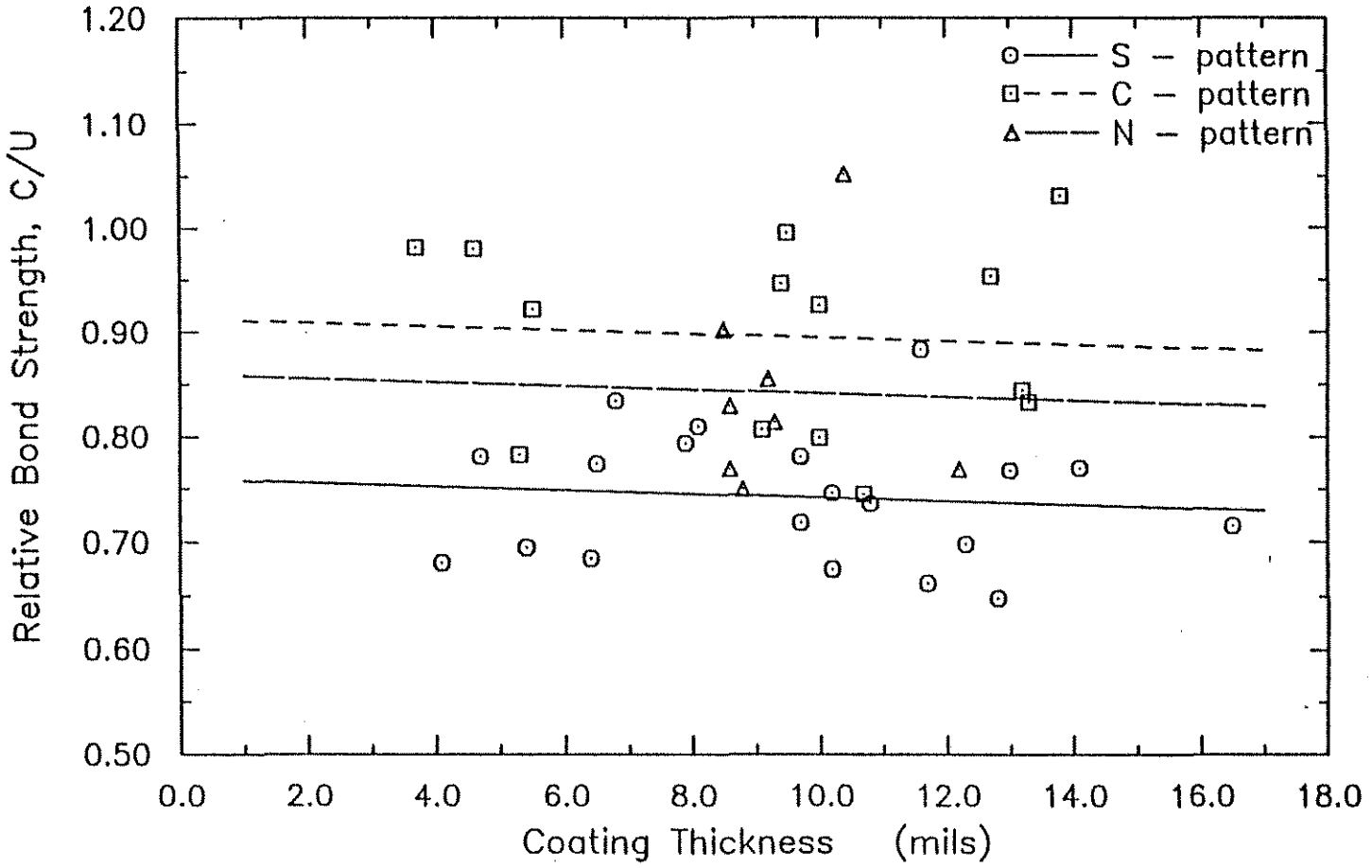

Fig. 3.5 Relative Bond Strength versus Coating Thickness for No. 8 Bars

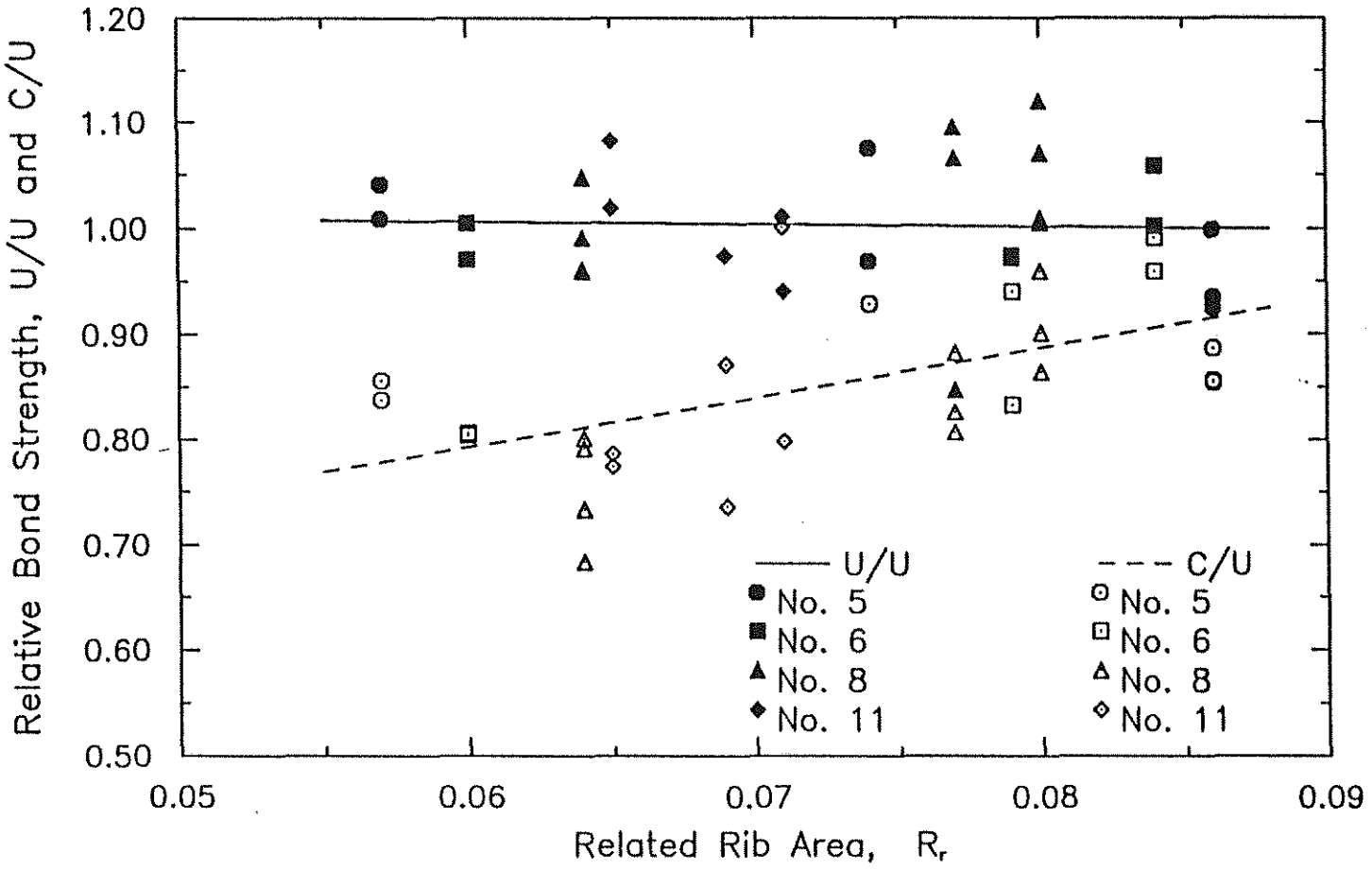

Fig. 3.6 Relative Bond Strength versus Related Rib Area

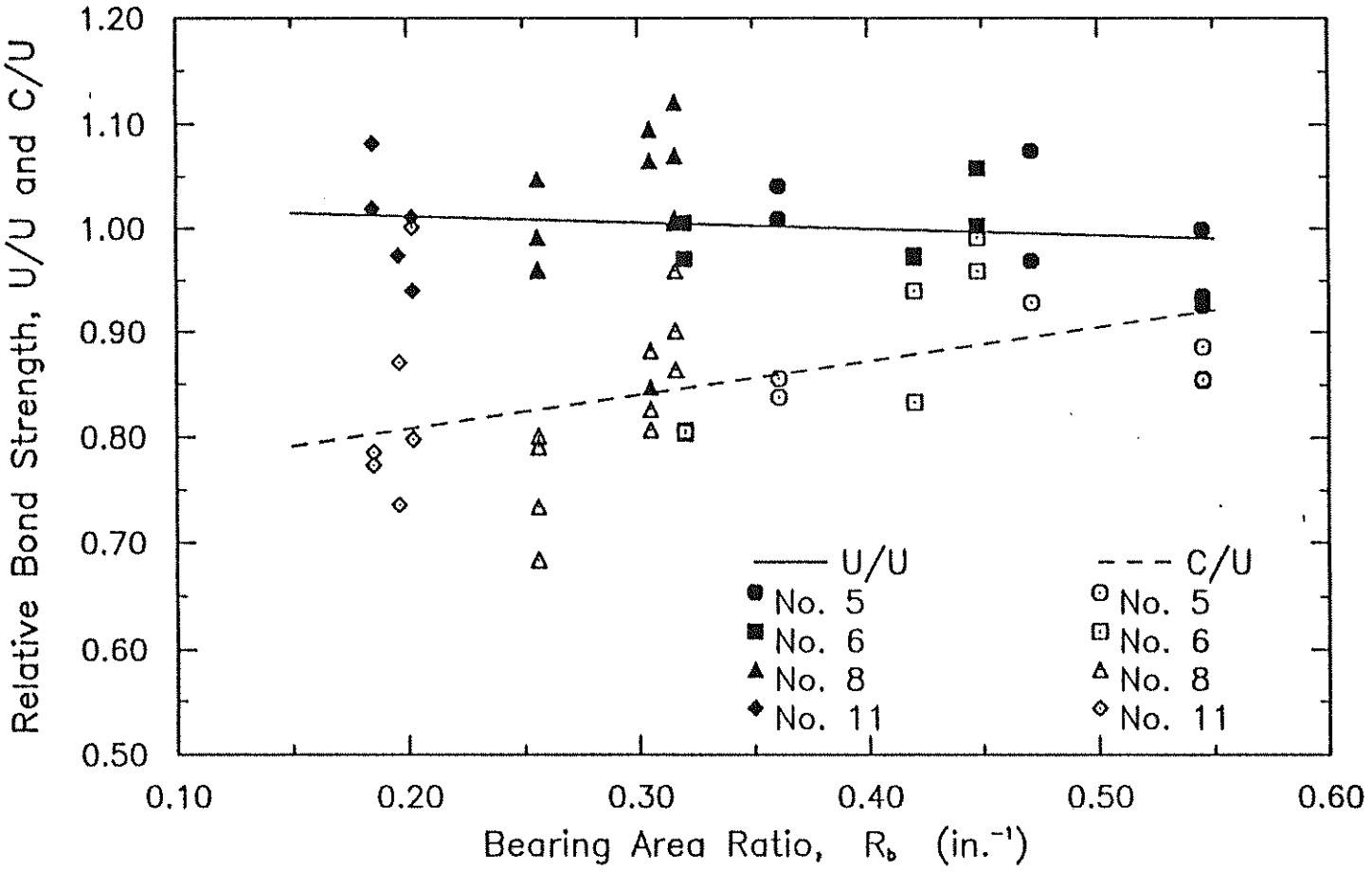

Fig. 3.7 Relative Bond Strength versus Bearing Area Ratio

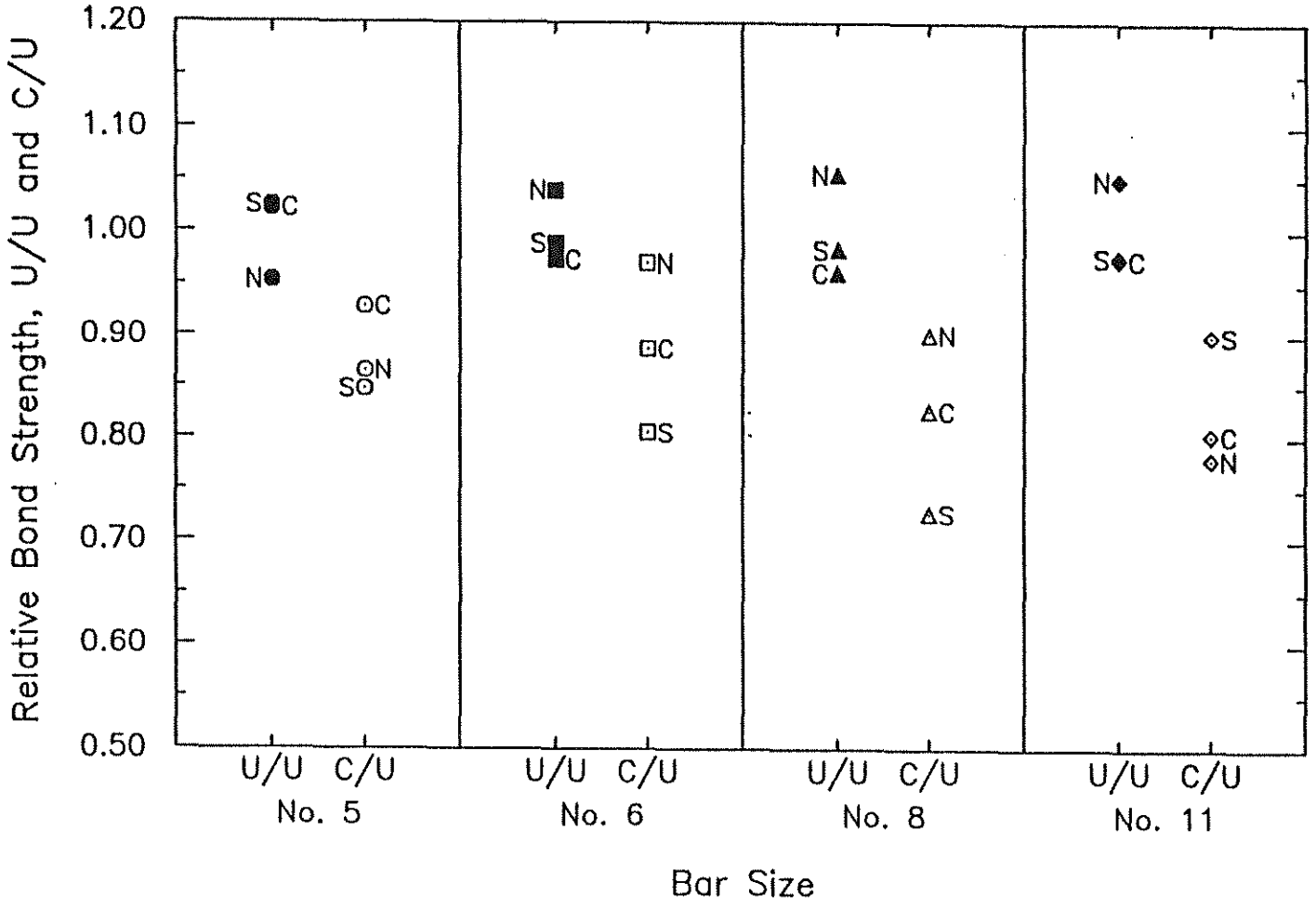

Fig. 3.8 Relative Bond Strength versus Bar Size

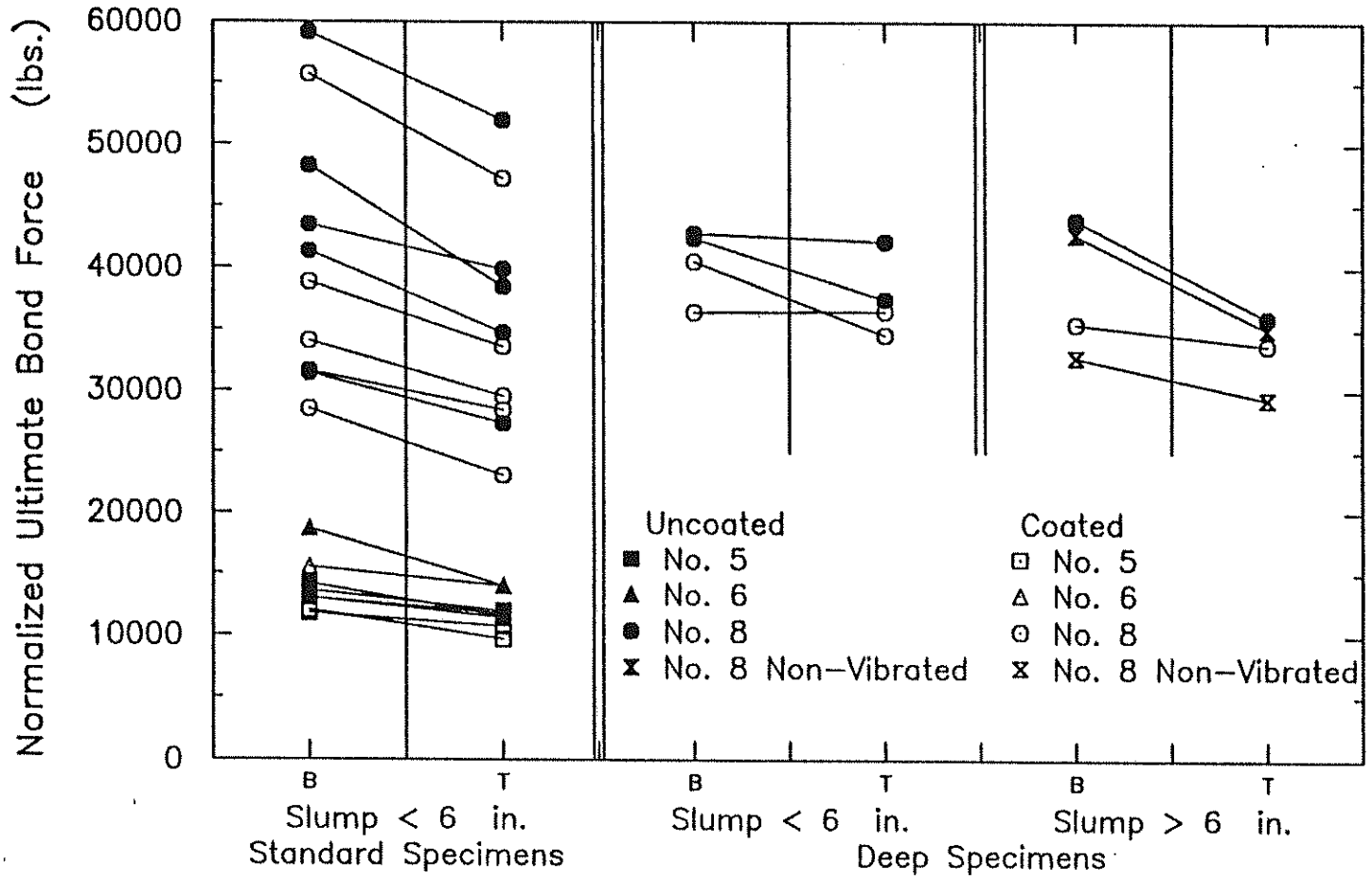

Fig. 3.9 Normalized Ultimate Bond Force for Bottom and Top-cast Bars for Different Slumps in Standard and Deep Specimens

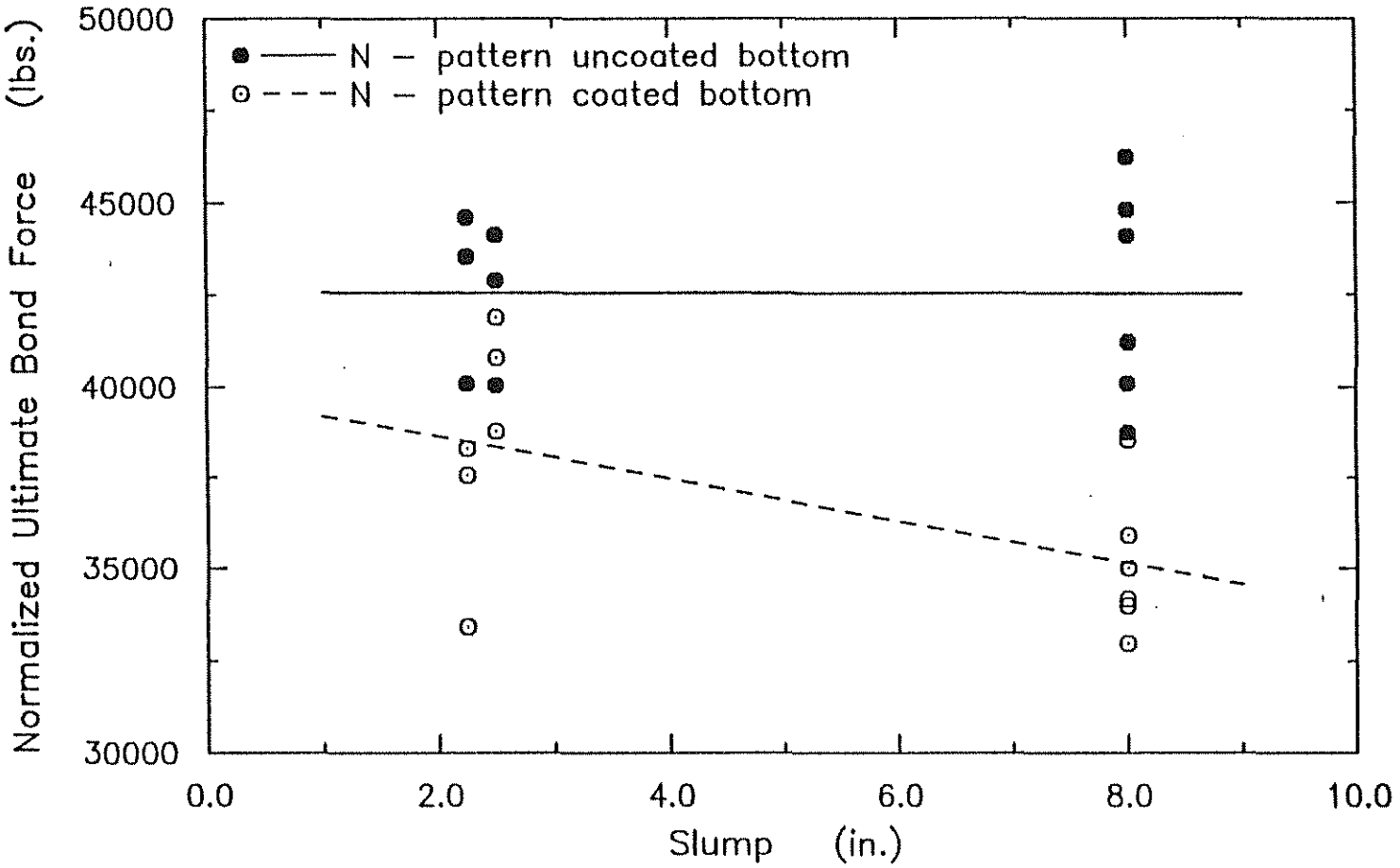

Fig. 3.10 Normalized Ultimate Bond Force of Bottom–cast Bars versus Slump for No. 8 Bars in Deep Specimens Only

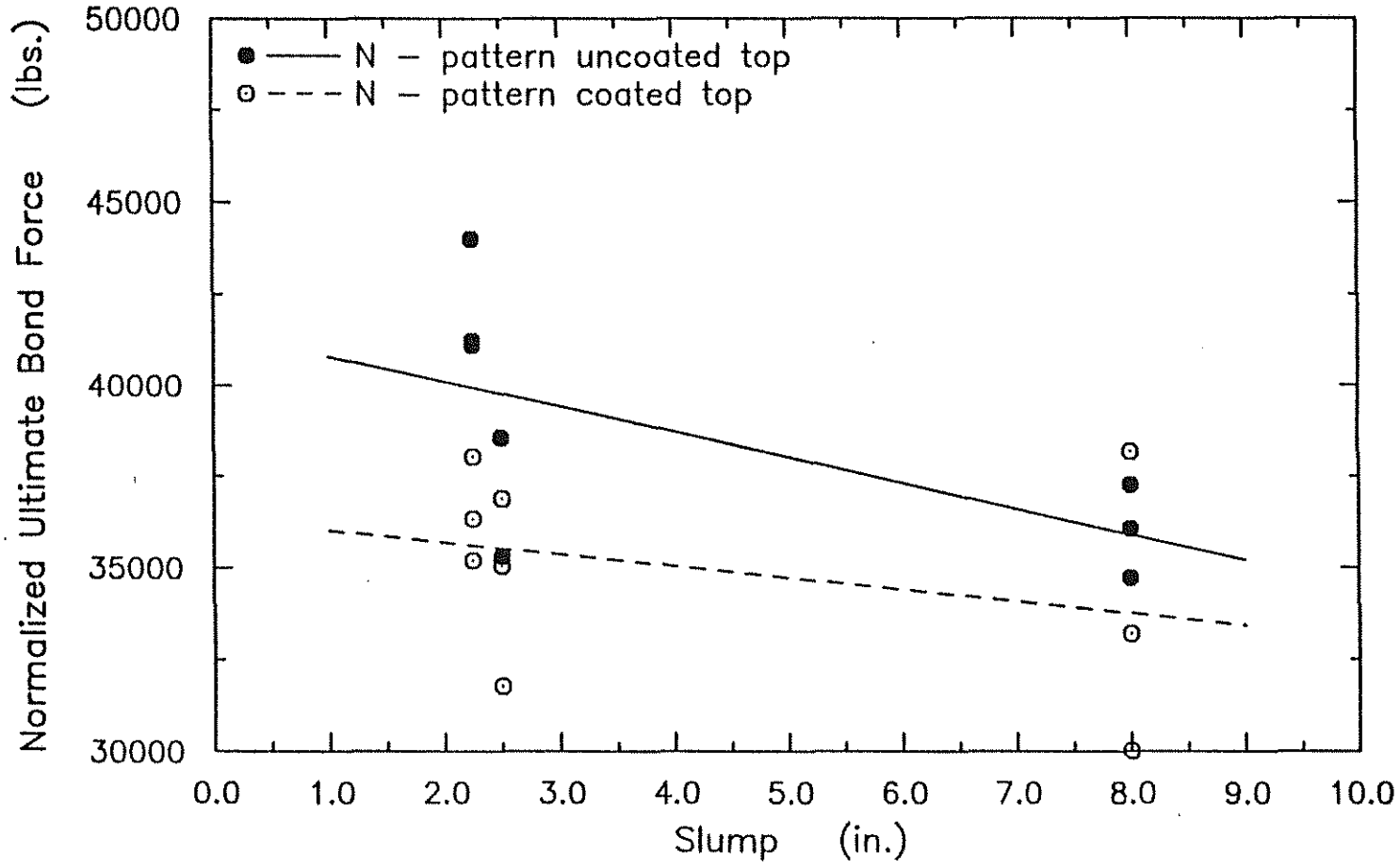

Fig. 3.11 Normalized Ultimate Bond Force of Top–cast Bars versus Slump for No. 8 Bars in Deep Specimens Only

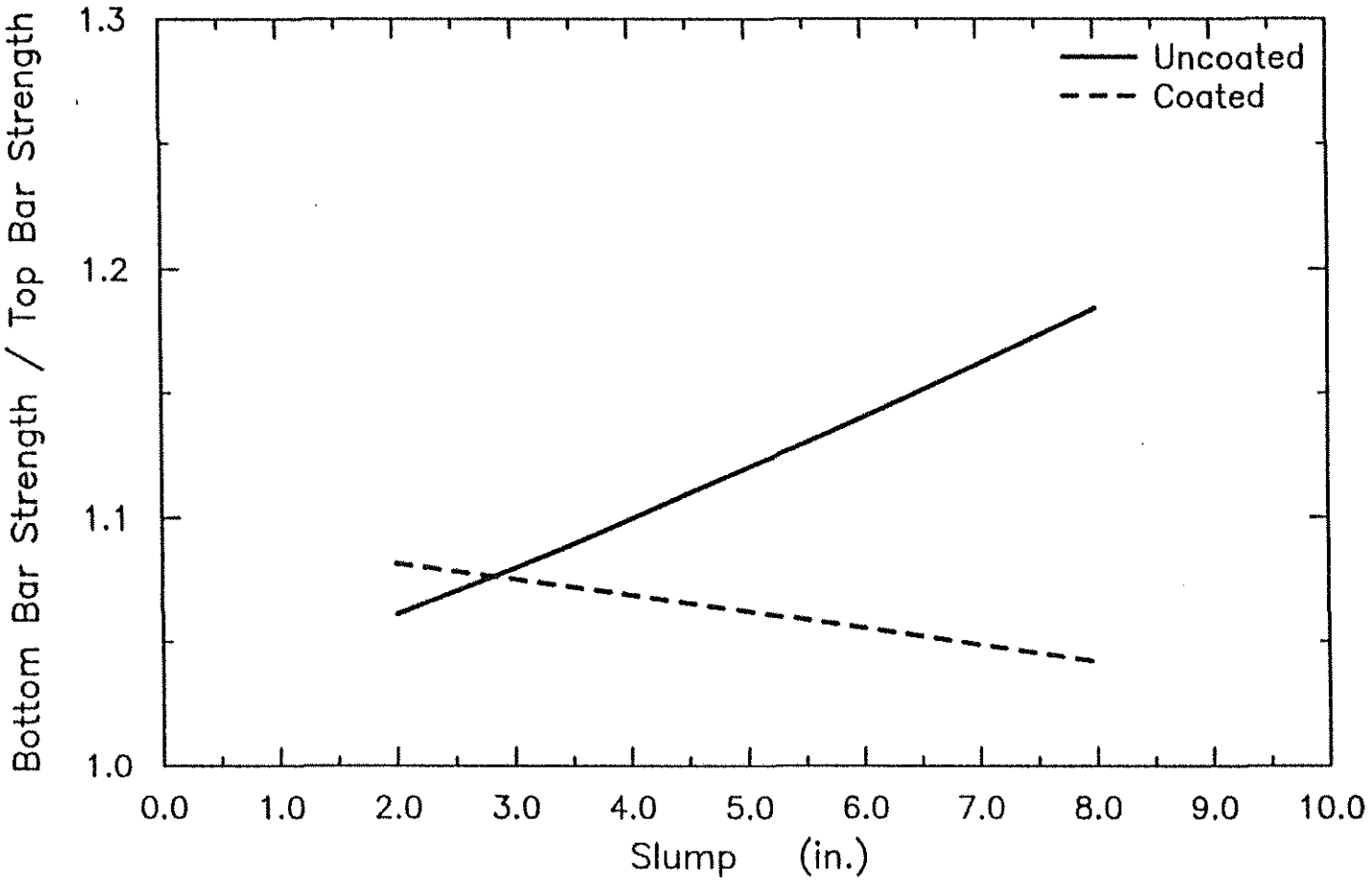

Fig. 3.12 Ratio of Bottom-cast Bar to Top-cast Bar Strength versus Slump for No. 8 Bars in Vibrated Deep Specimens Only

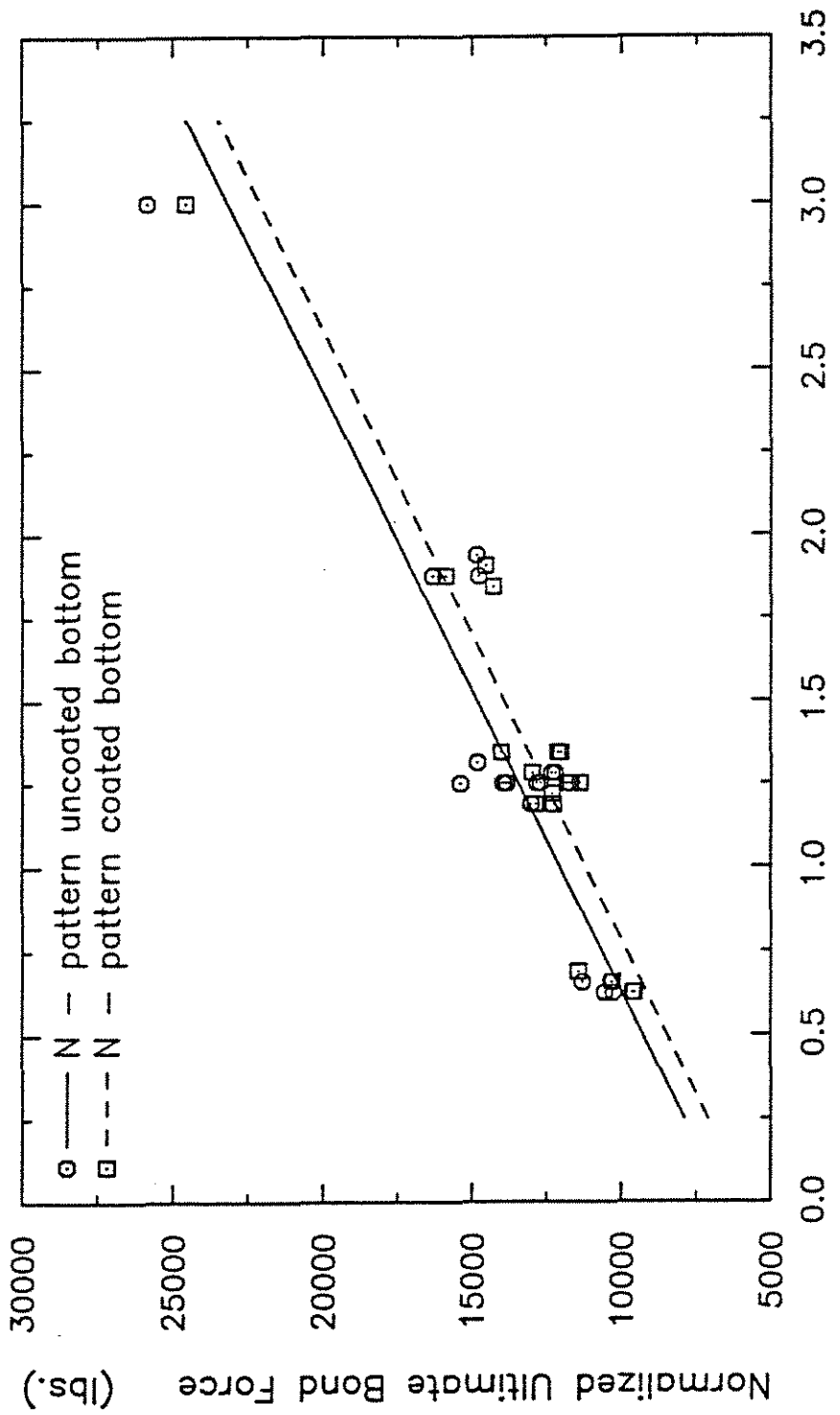

Fig. 3.13 Normalized Ultimate Bond Force versus Concrete Cover for No. 5 Bars

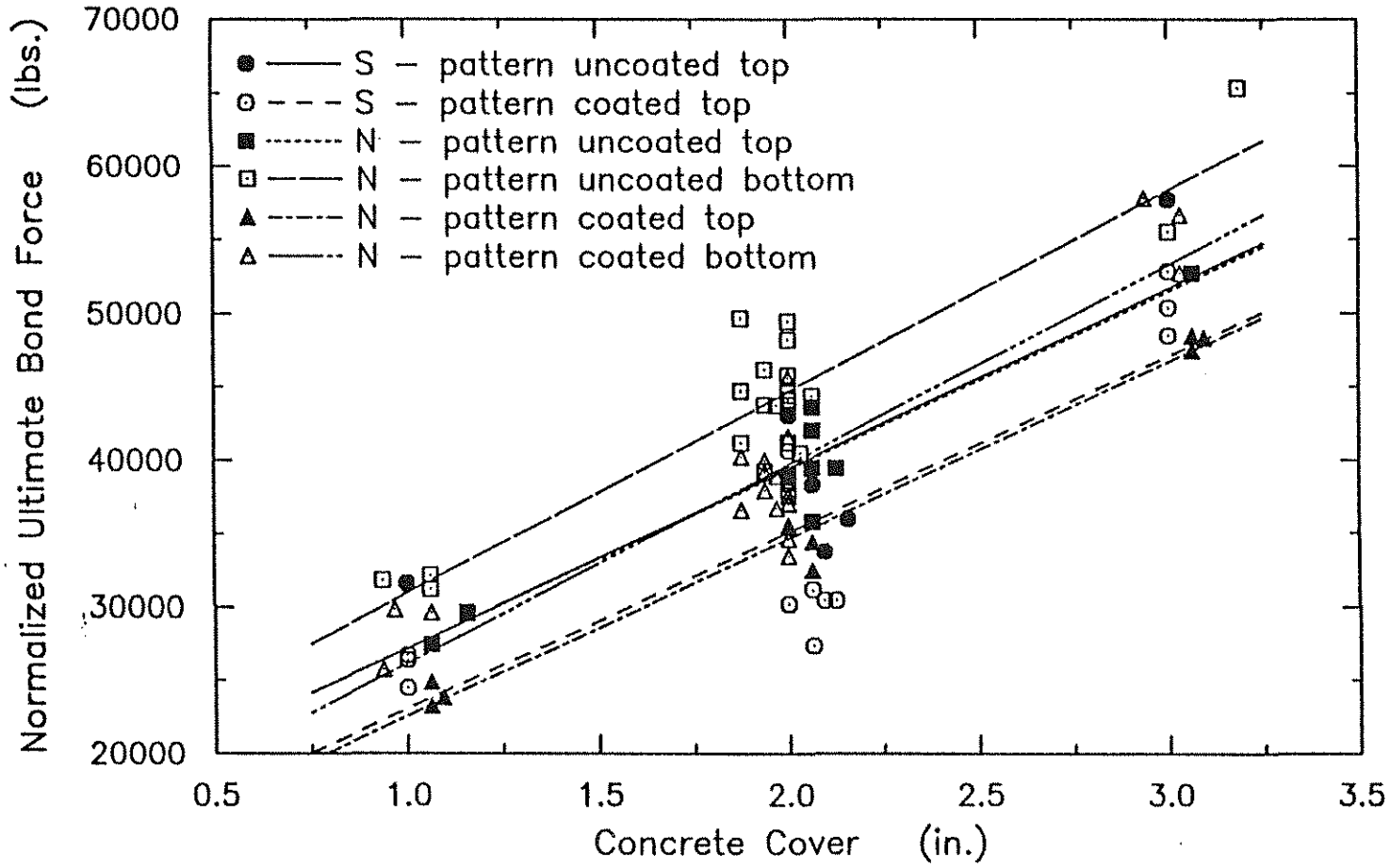

Fig. 3.14 Normalized Ultimate Bond Force versus Concrete Cover for No. 8 Bars

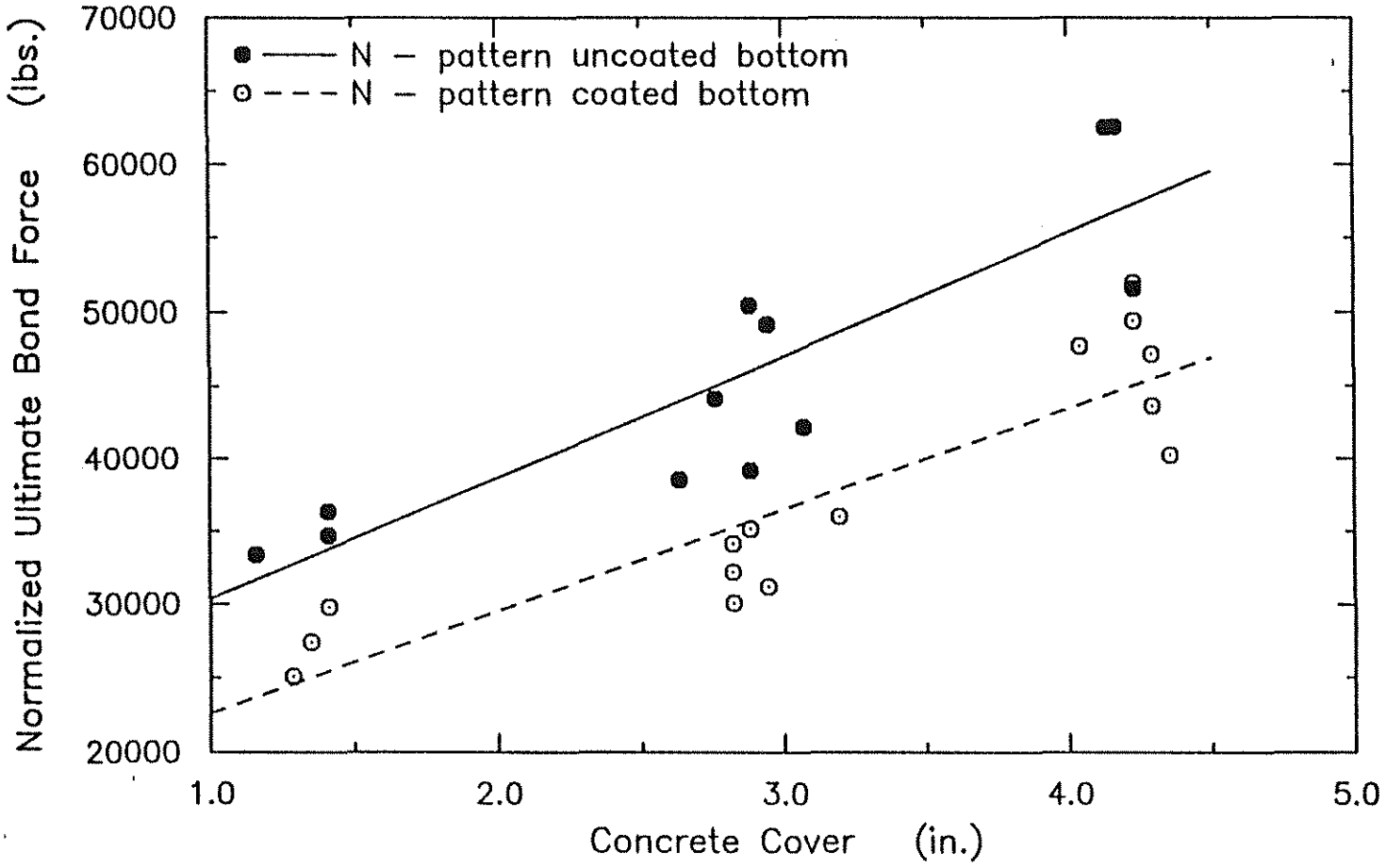

Fig. 3.15 Normalized Ultimate Bond Force versus Concrete Cover for No. 11 Bars

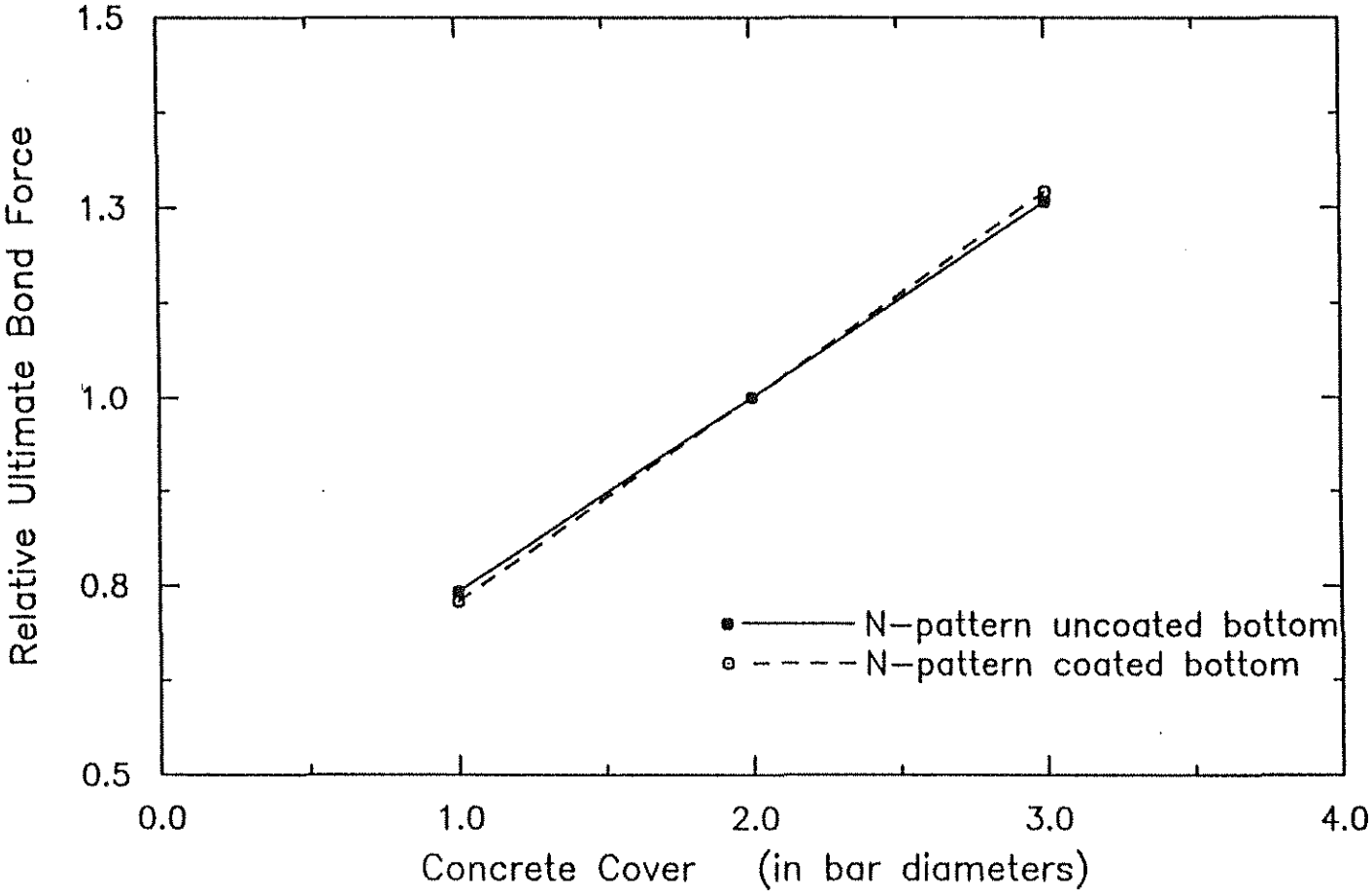

Fig. 3.16 Relative Ultimate Bond Force (normalized to 2db) versus Concrete Cover for No. 5 Bars

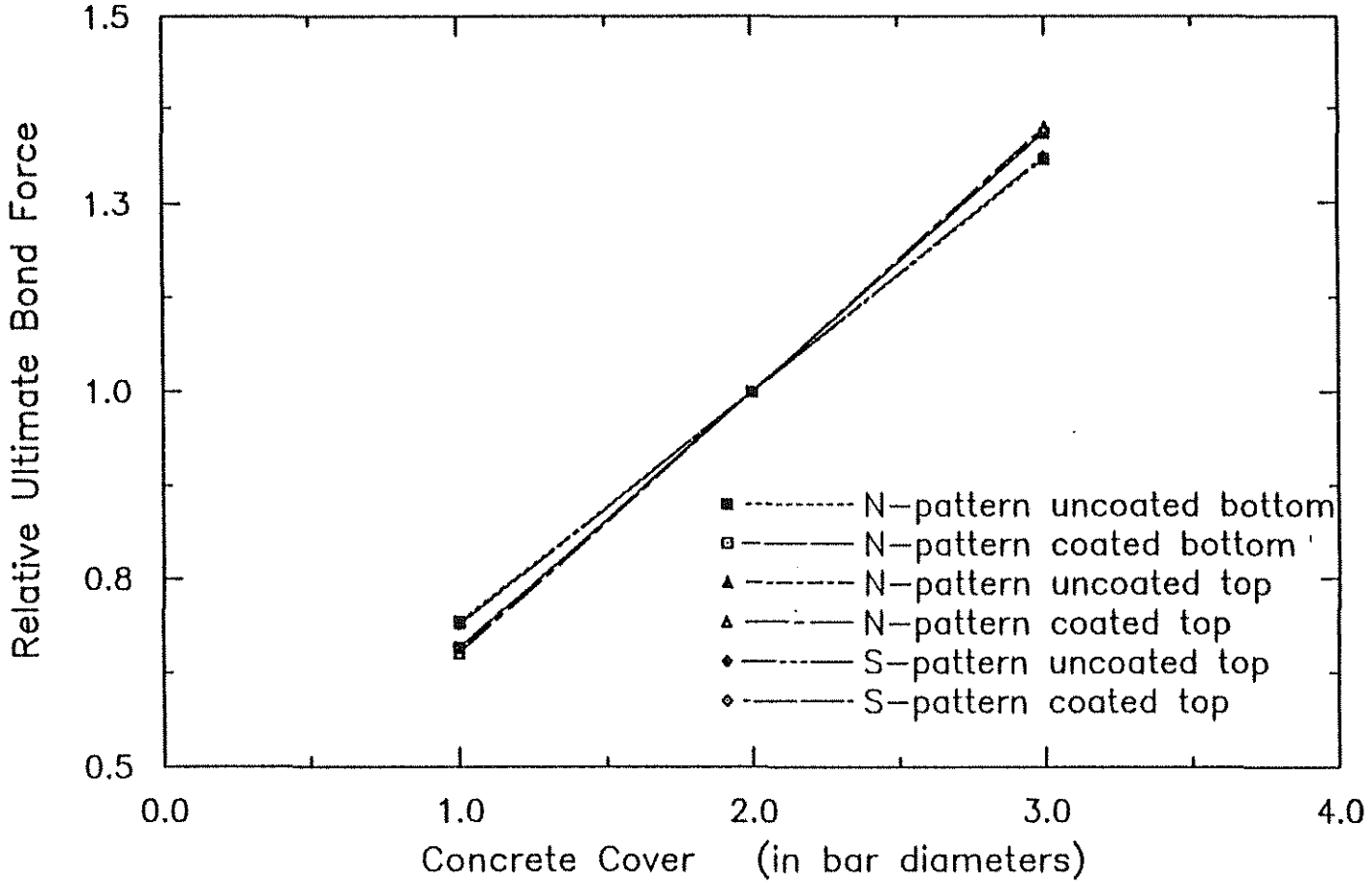

Fig. 3.17 Relative Ultimate Bond Force (normalized to 2db) versus Concrete Cover for No. 8 Bars

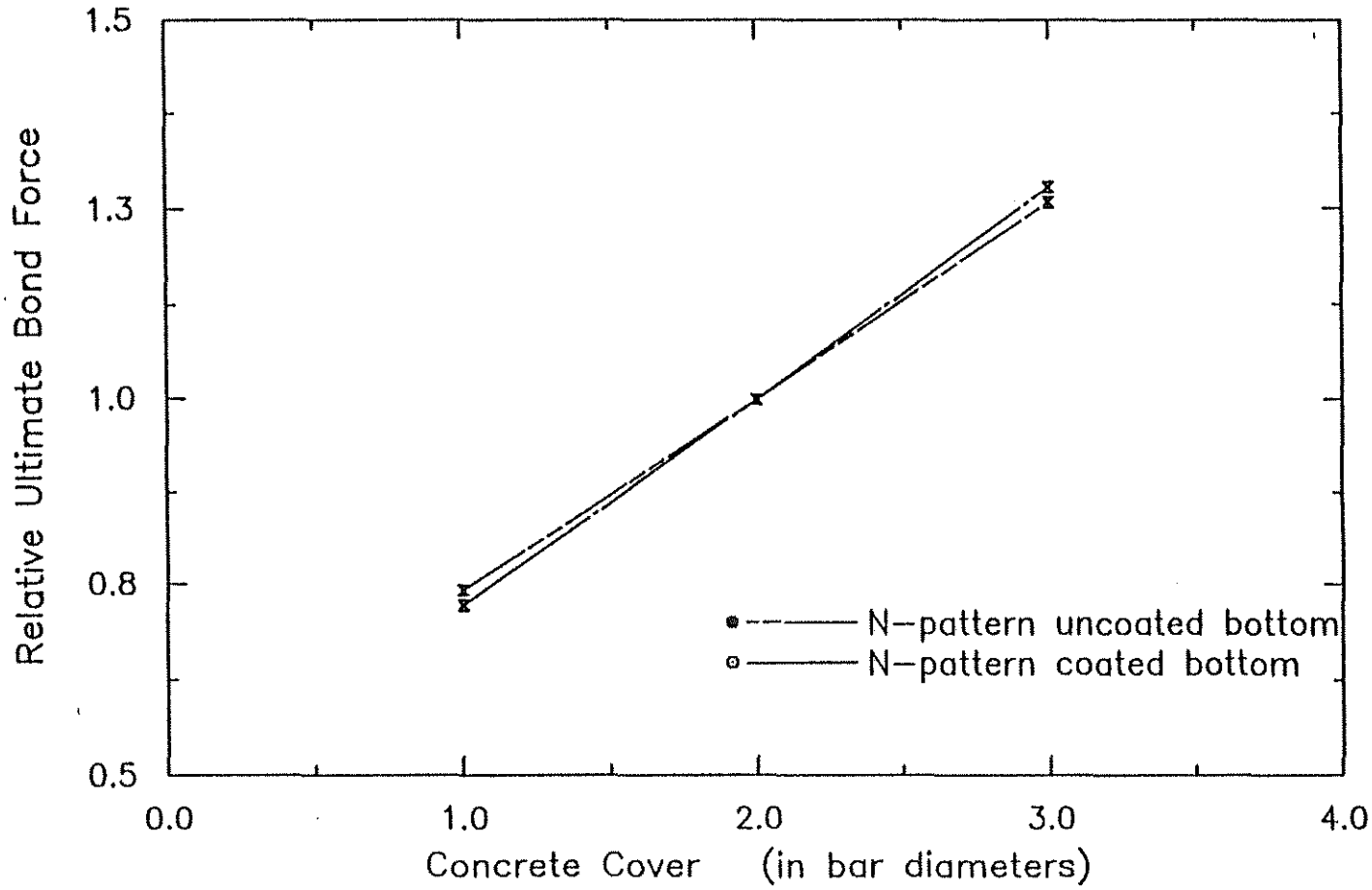

Fig. 3.18 Relative Ultimate Bond Force (normalized to 2db) versus Concrete Cover for No. 11 Bars

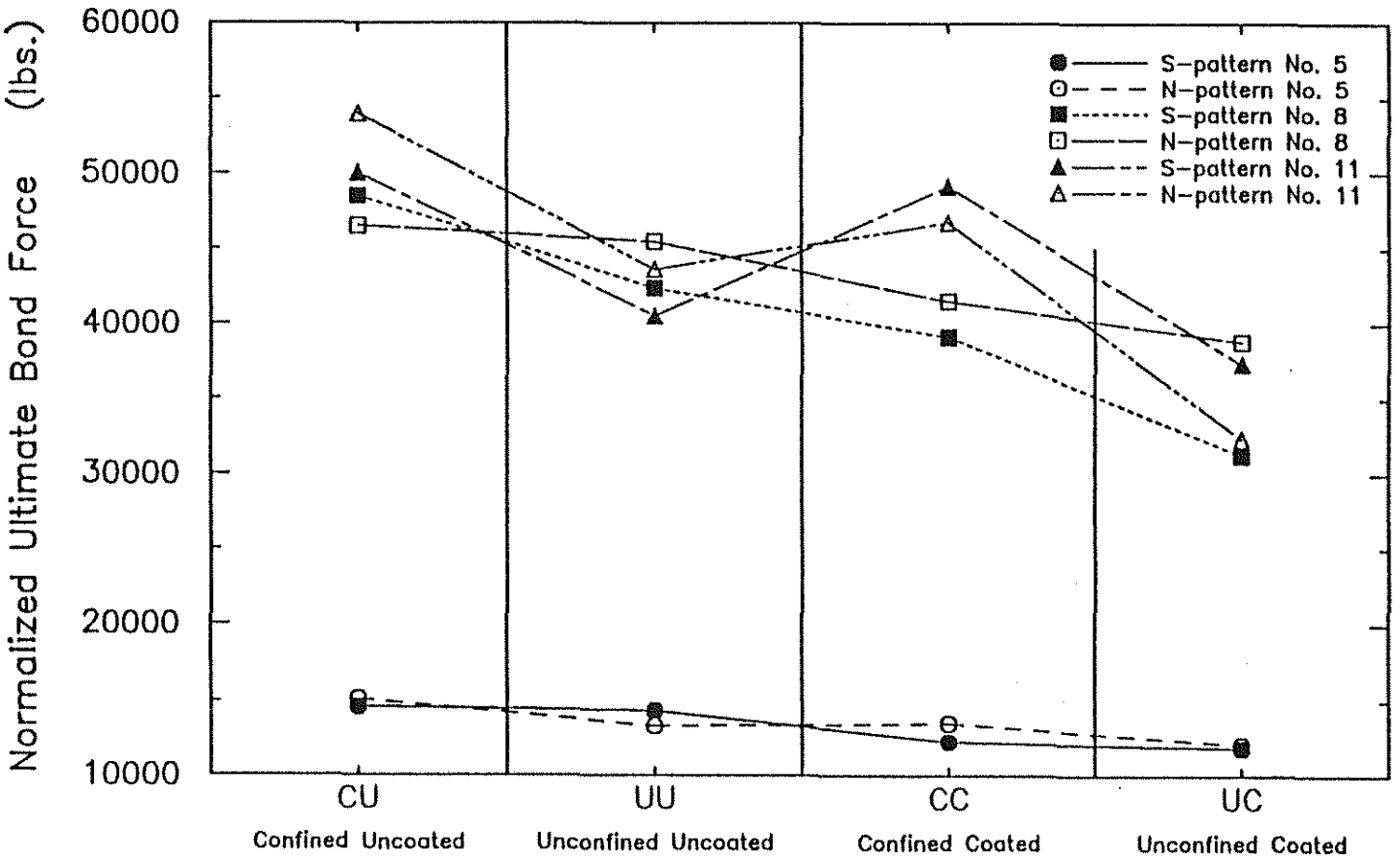

Fig. 3.19 Normalized Ultimate Bond Force for Uncoated and Coated Bottom-cast Bars With and Without Confinement

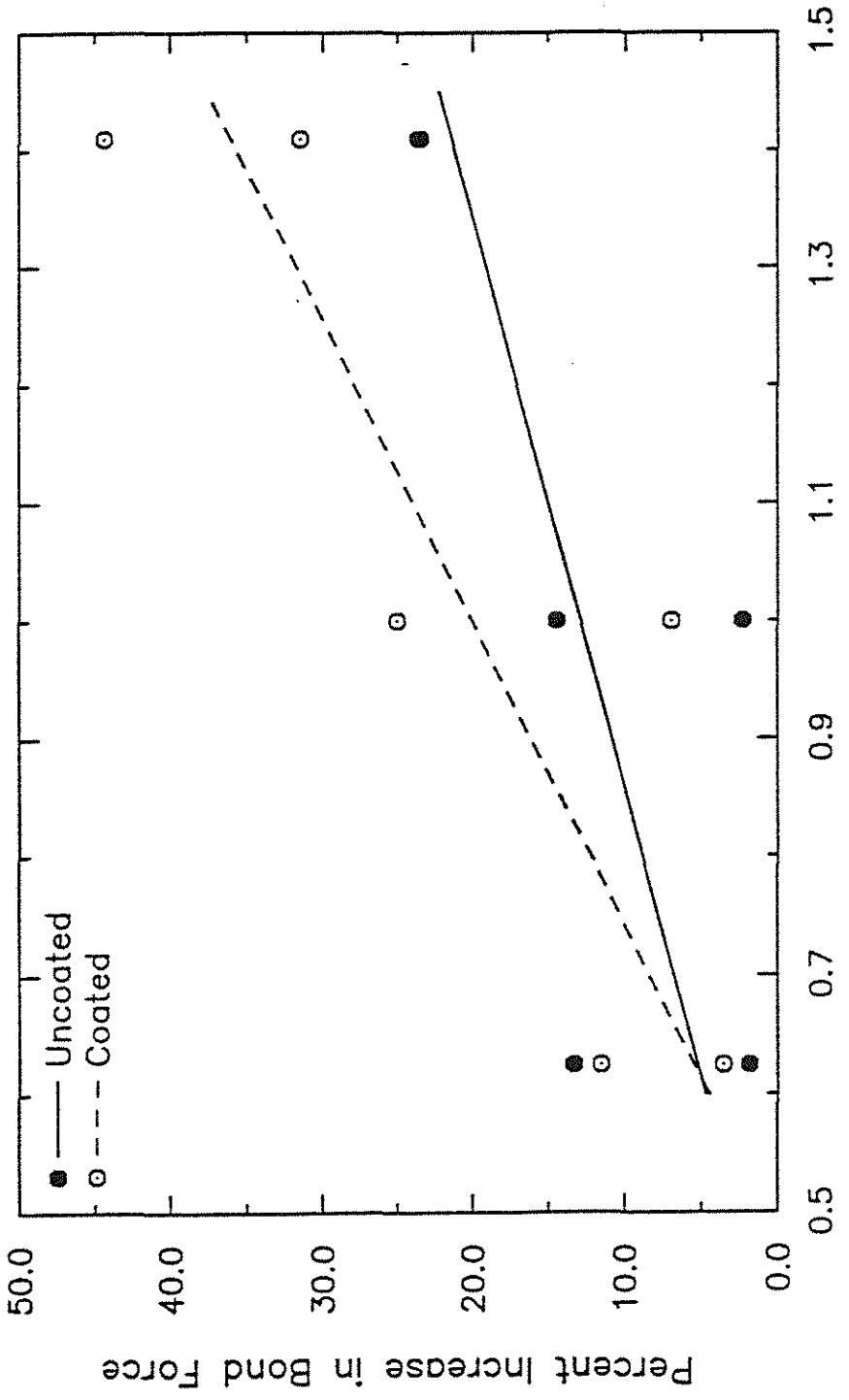

Fig. 3.20 Percent Increase in Bond Force due to Presence of Transverse Reinforcement versus Bar Diameter

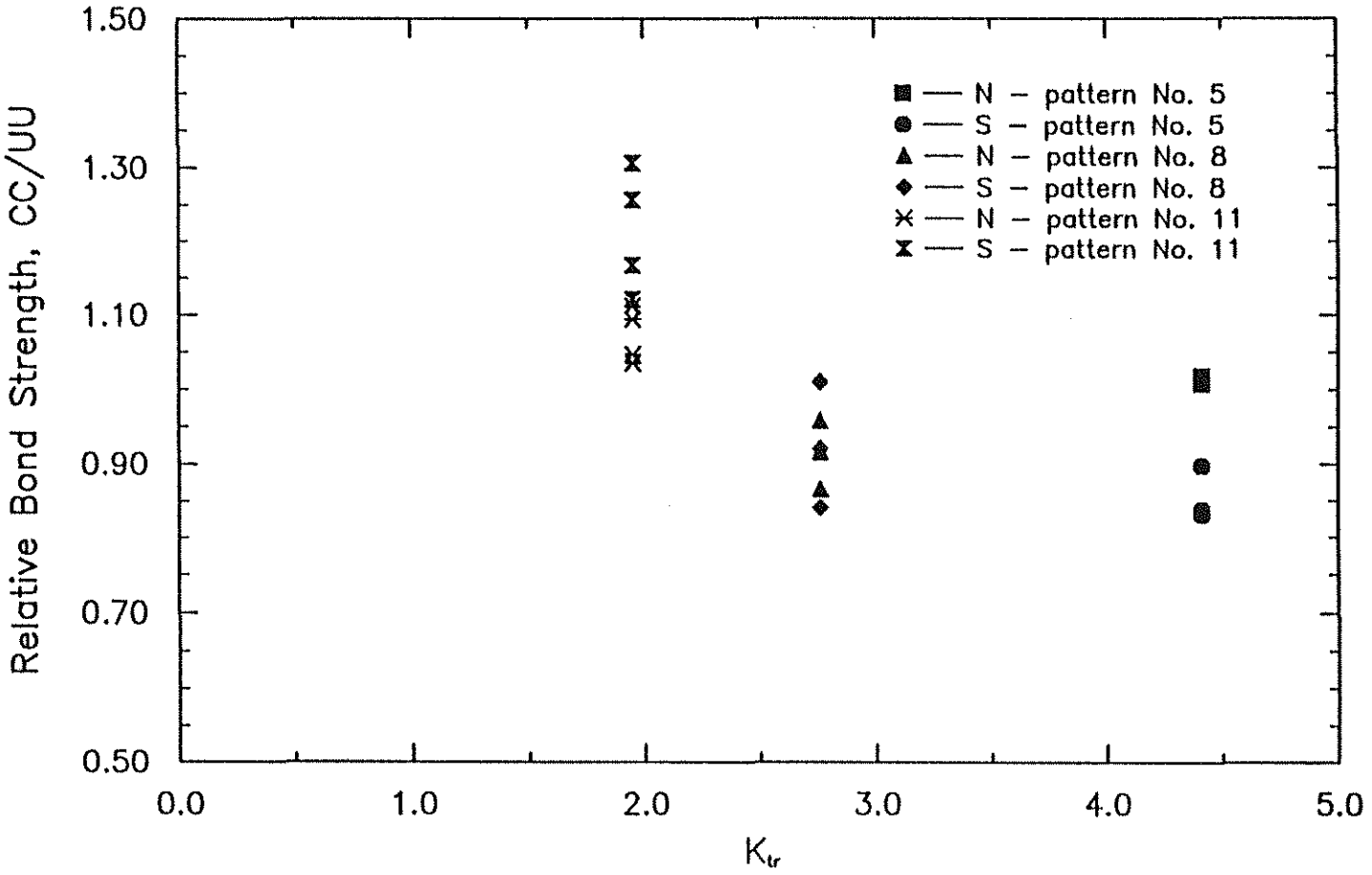

Fig. 3.21 Relative Bond Strength, Confined Coated / Unconfined Uncoated, versus K_{tr} (based on 5.5 in. spacing)

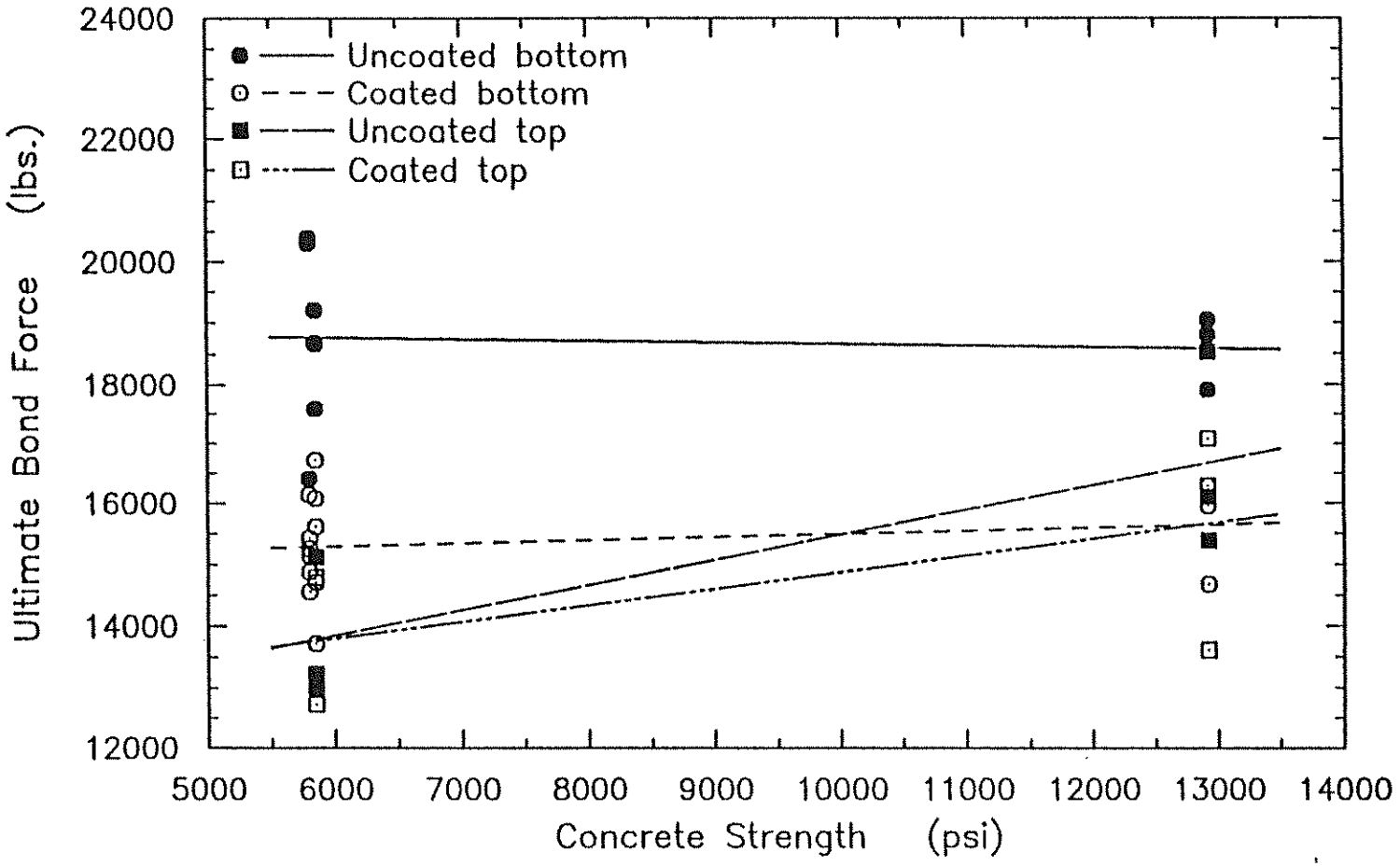

Fig. 3.22 Ultimate Bond Force versus Concrete Strength for S – pattern No. 6 Bars

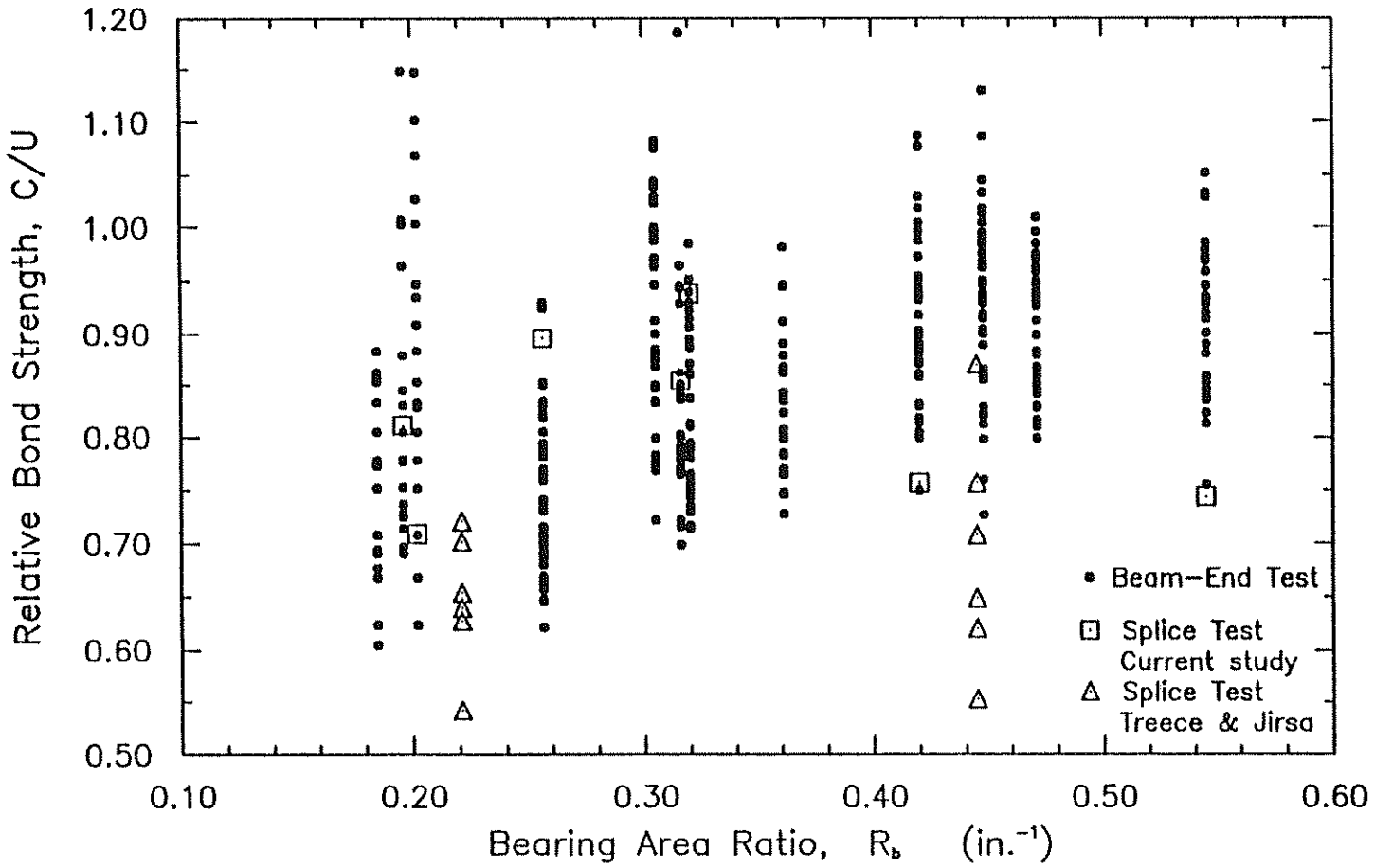

Fig. 3.23 Relative Bond Strength versus Bearing Area Ratio for Current Tests and Splice Tests by Treece and Jirsa (1987, 1989)

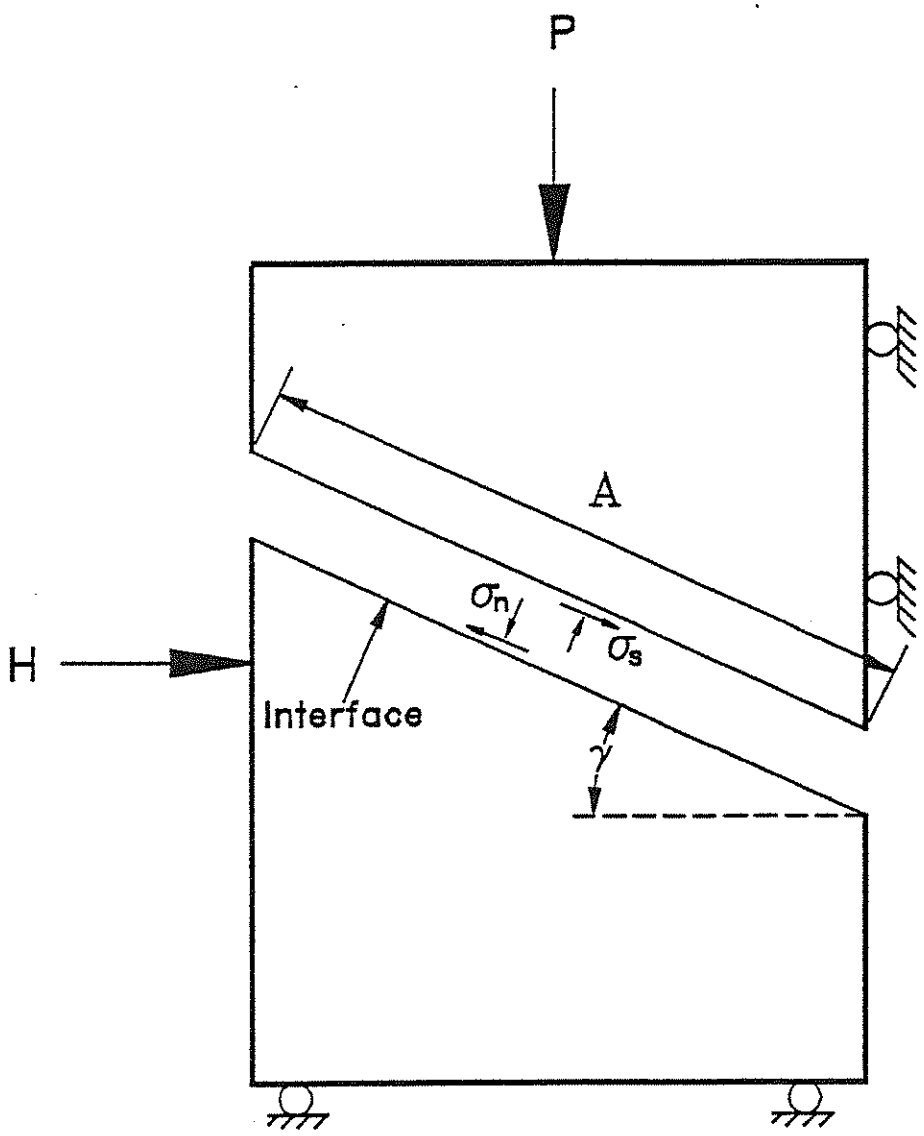

Fig. 4.1 Statical Model (Choi et al. 1990)

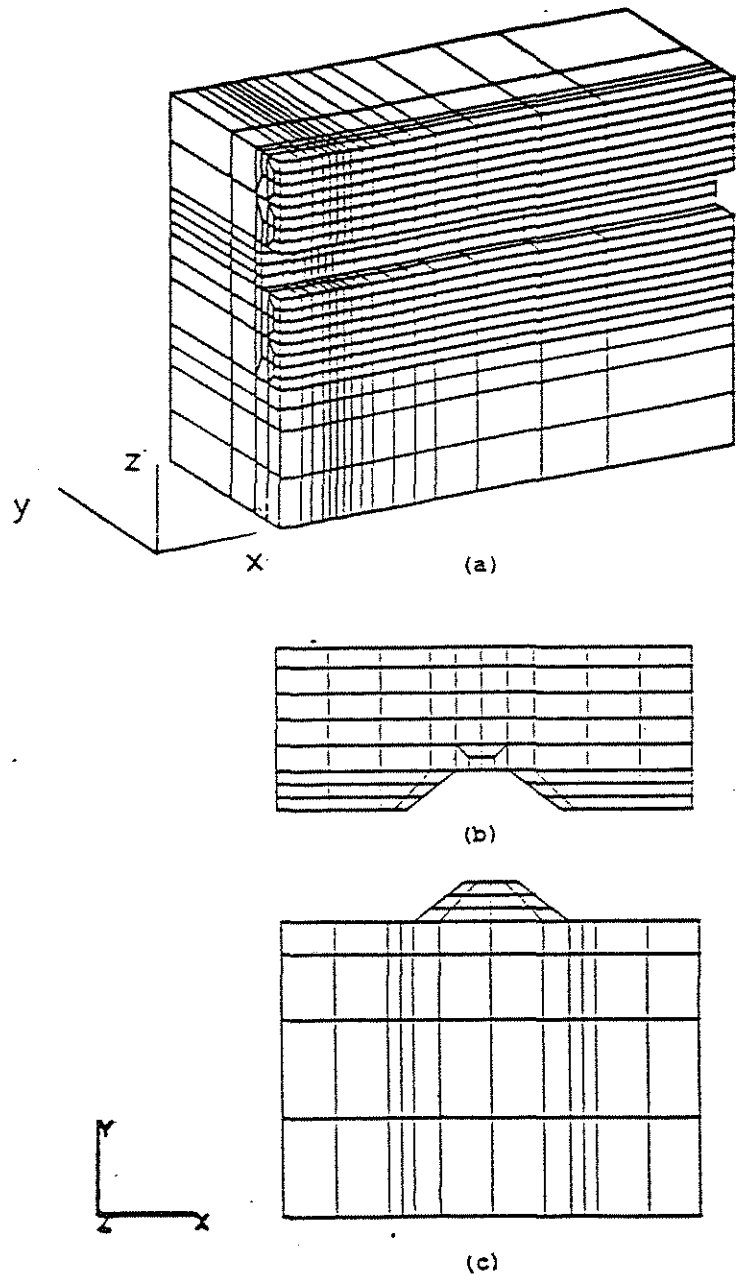

Fig. 4.2 Finite Element Model (Choi et al. 1990)

a) Exterior Concrete Substructure

b) Interior Concrete Substructure

c) Reinforcing Bar Substructure

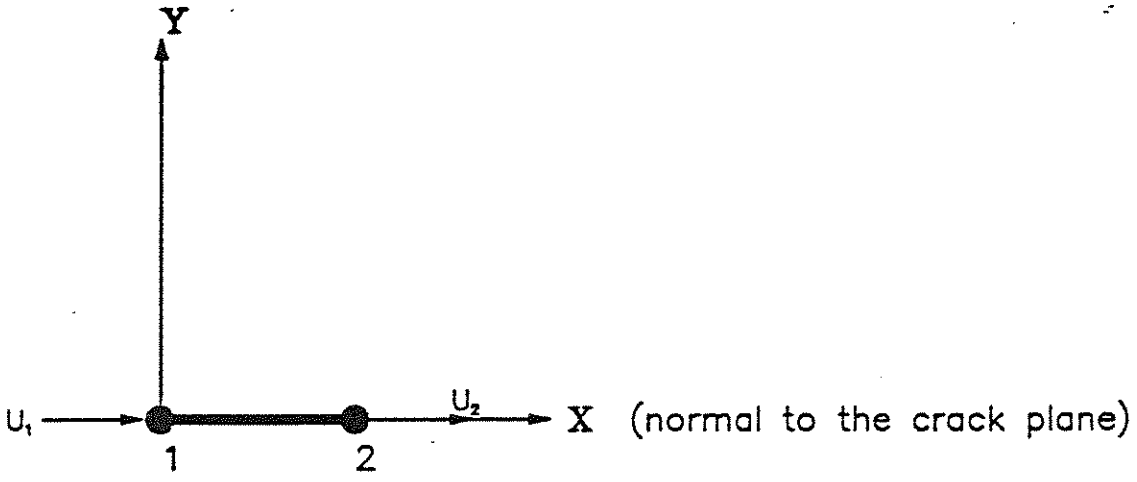

Fig. 4.3 Two Node Link Element

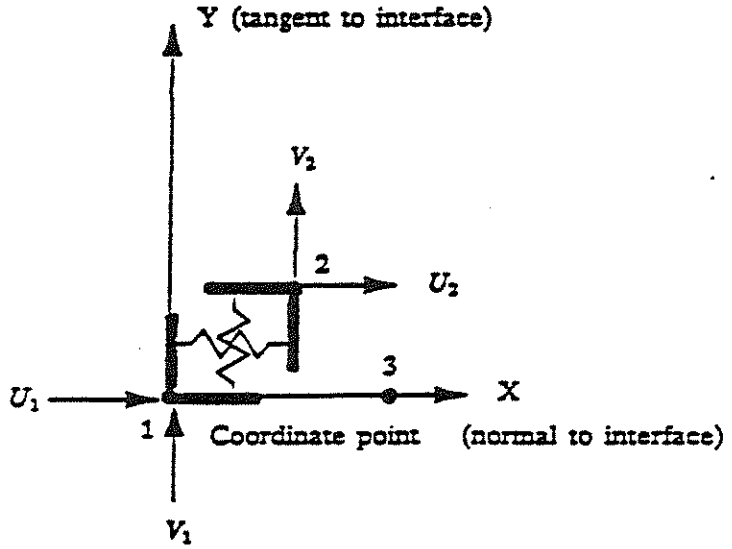

Fig. 4.4 Interface Link Element (Lopez et al. 1989)

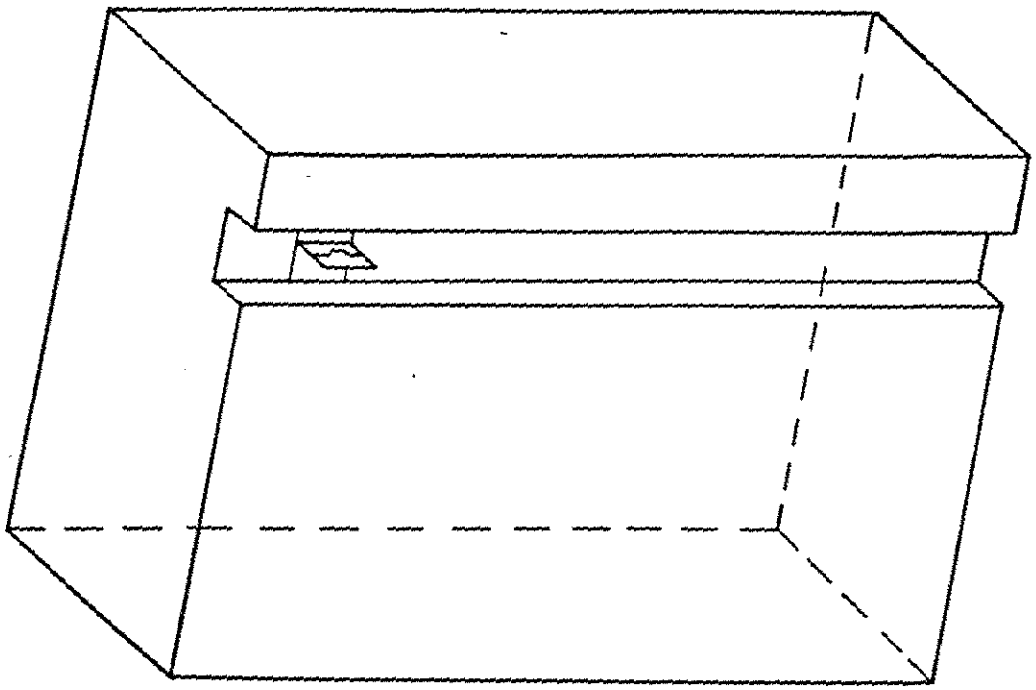

Fig. 4.5 Overall Finite Element Model of the Beam–end Specimen (Choi, Darwin, and McCabe 1990)

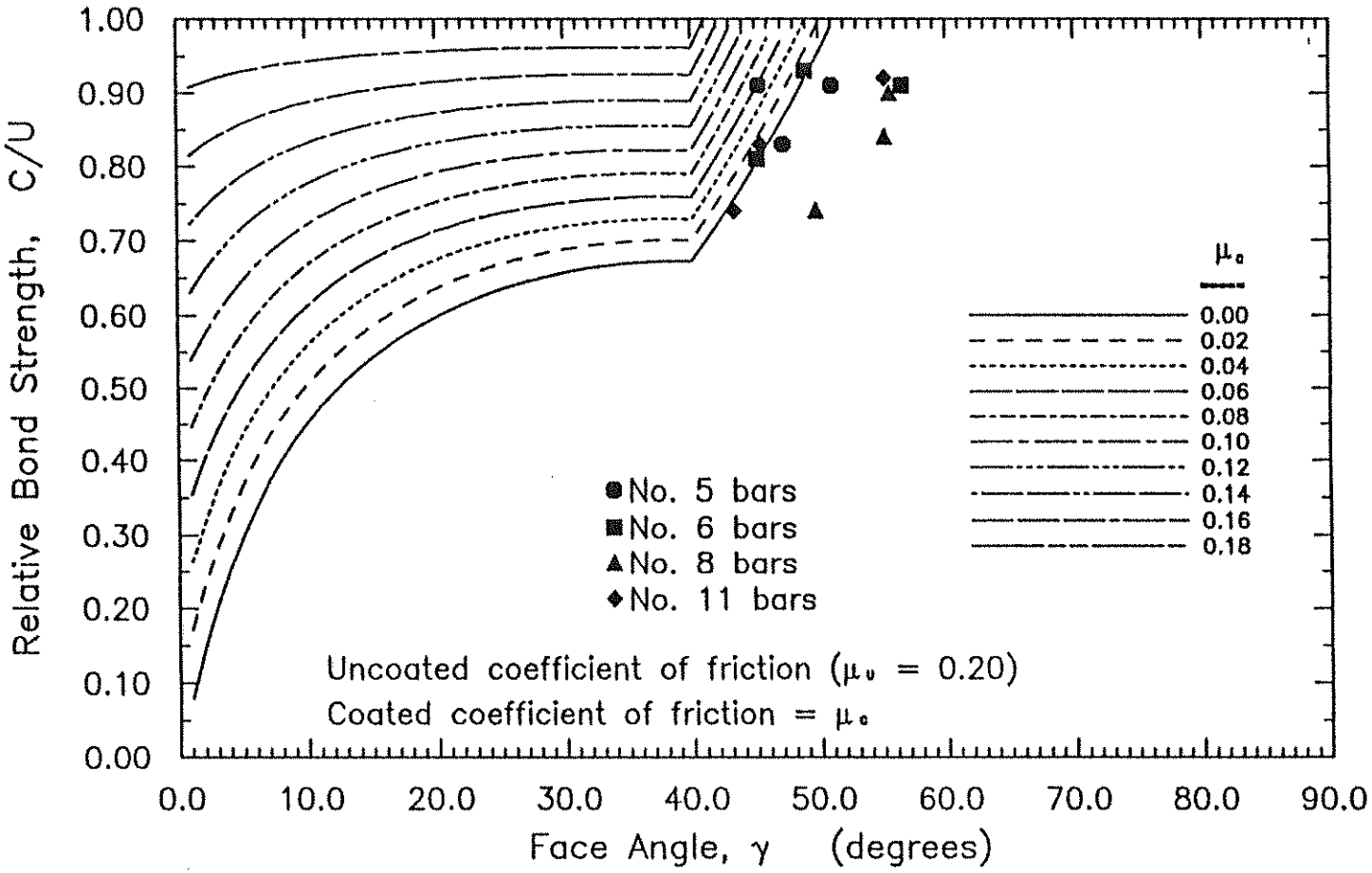

Fig. 4.6 Relative Bond Strength versus Face Angle With a Limitation of 40° on γ for Uncoated Bars, $\mu_u = 0.20$

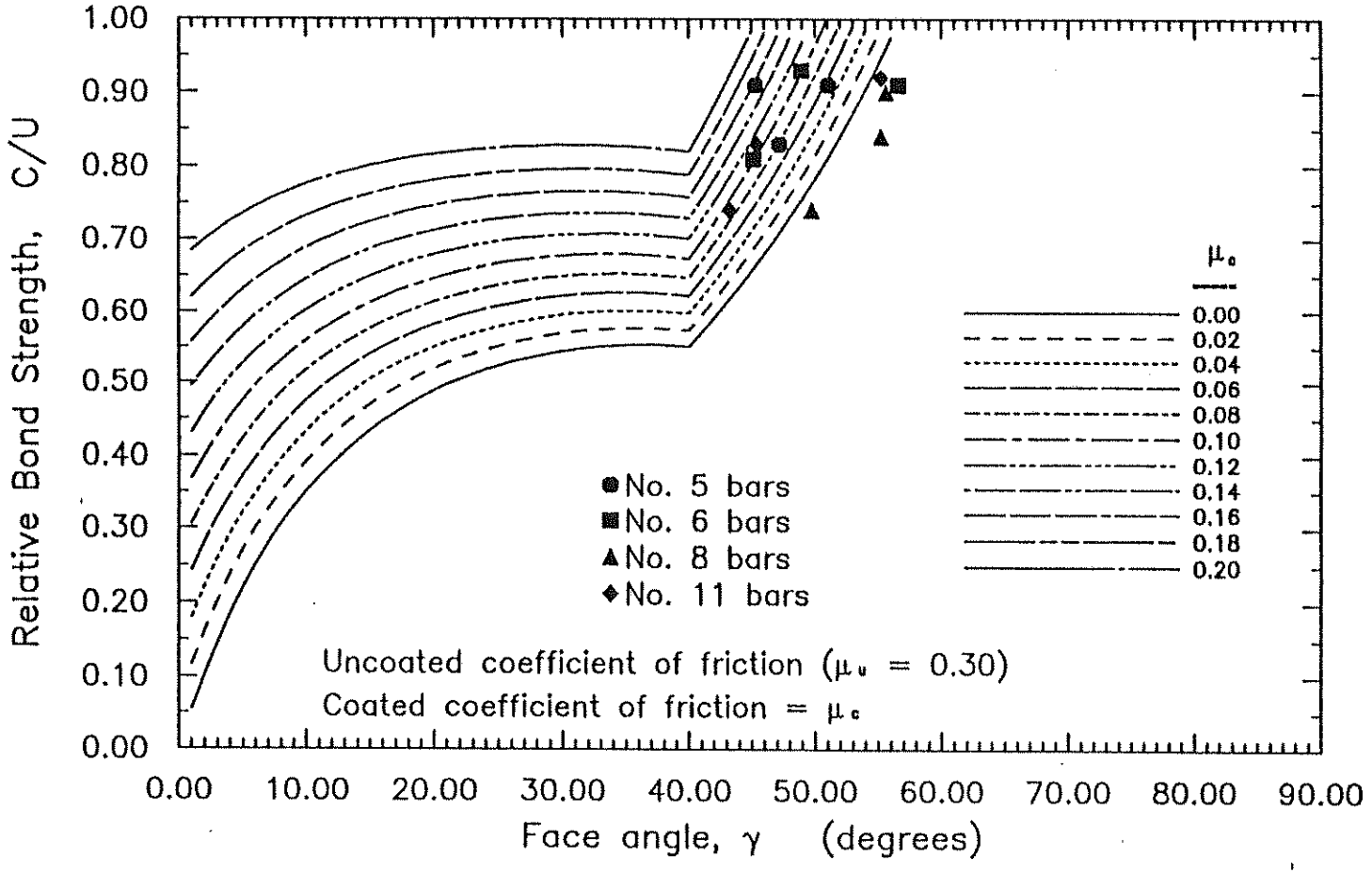

Fig. 4.7 Relative Bond Strength versus Face Angle With a Limitation of 40° on γ for Uncoated Bars, $\mu_u = 0.30$

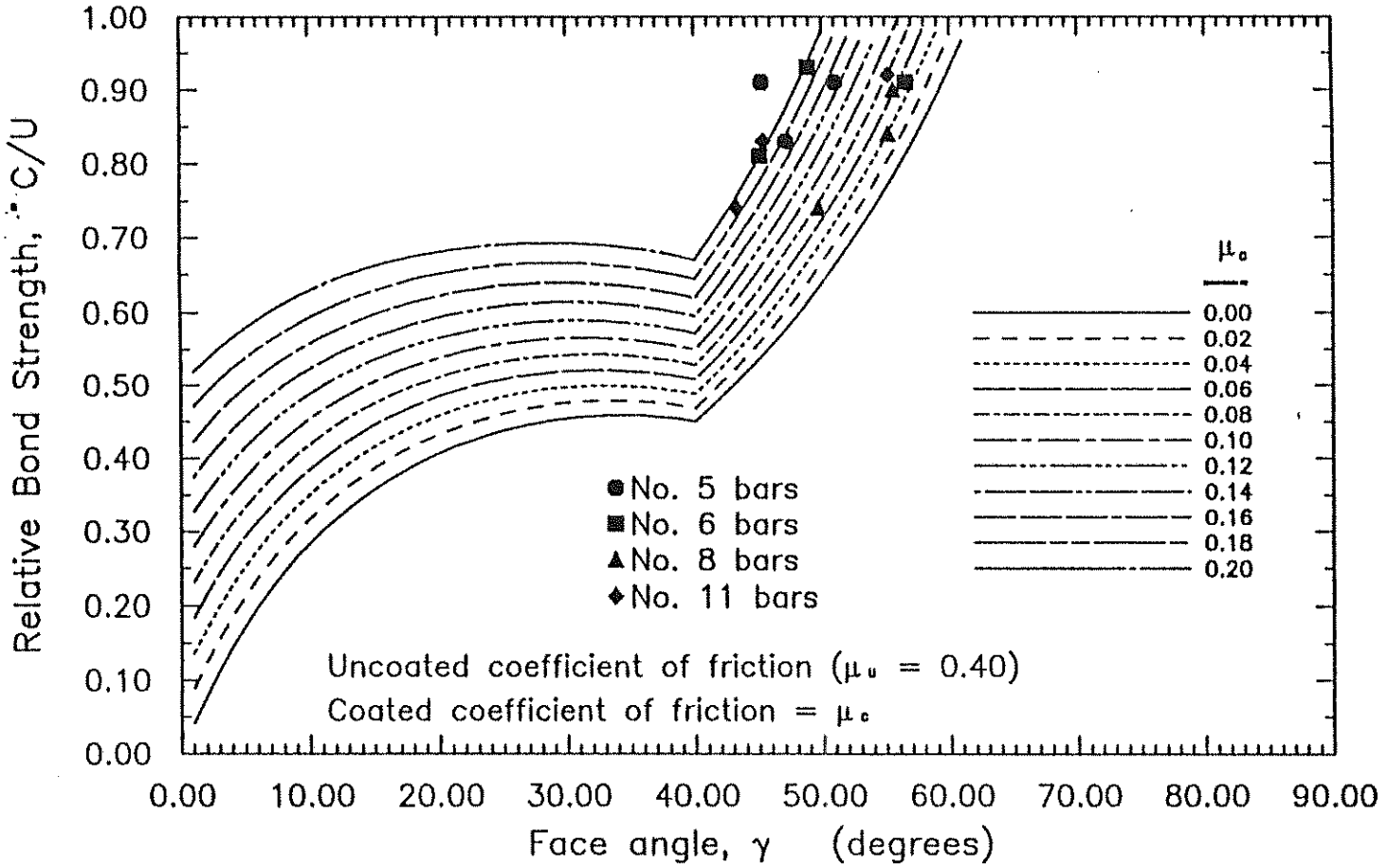

Fig. 4.8 Relative Bond Strength versus Face Angle With a Limitation of 40° on γ for Uncoated Bars, $\mu_u = 0.40$

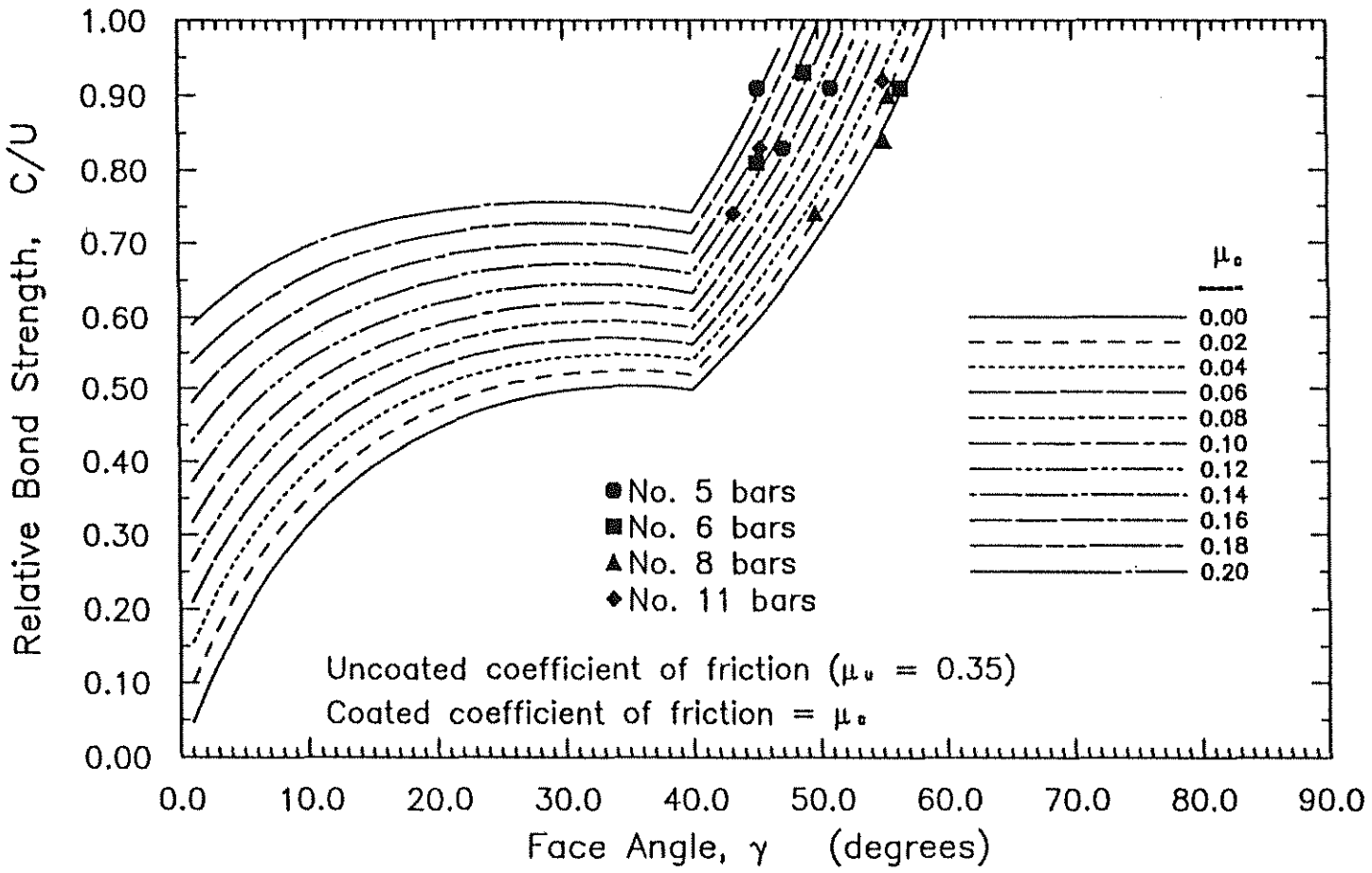

Fig. 4.9 Relative Bond Strength versus Face Angle With a Limitation of 40° on γ for Uncoated Bars, $\mu_u = 0.35$

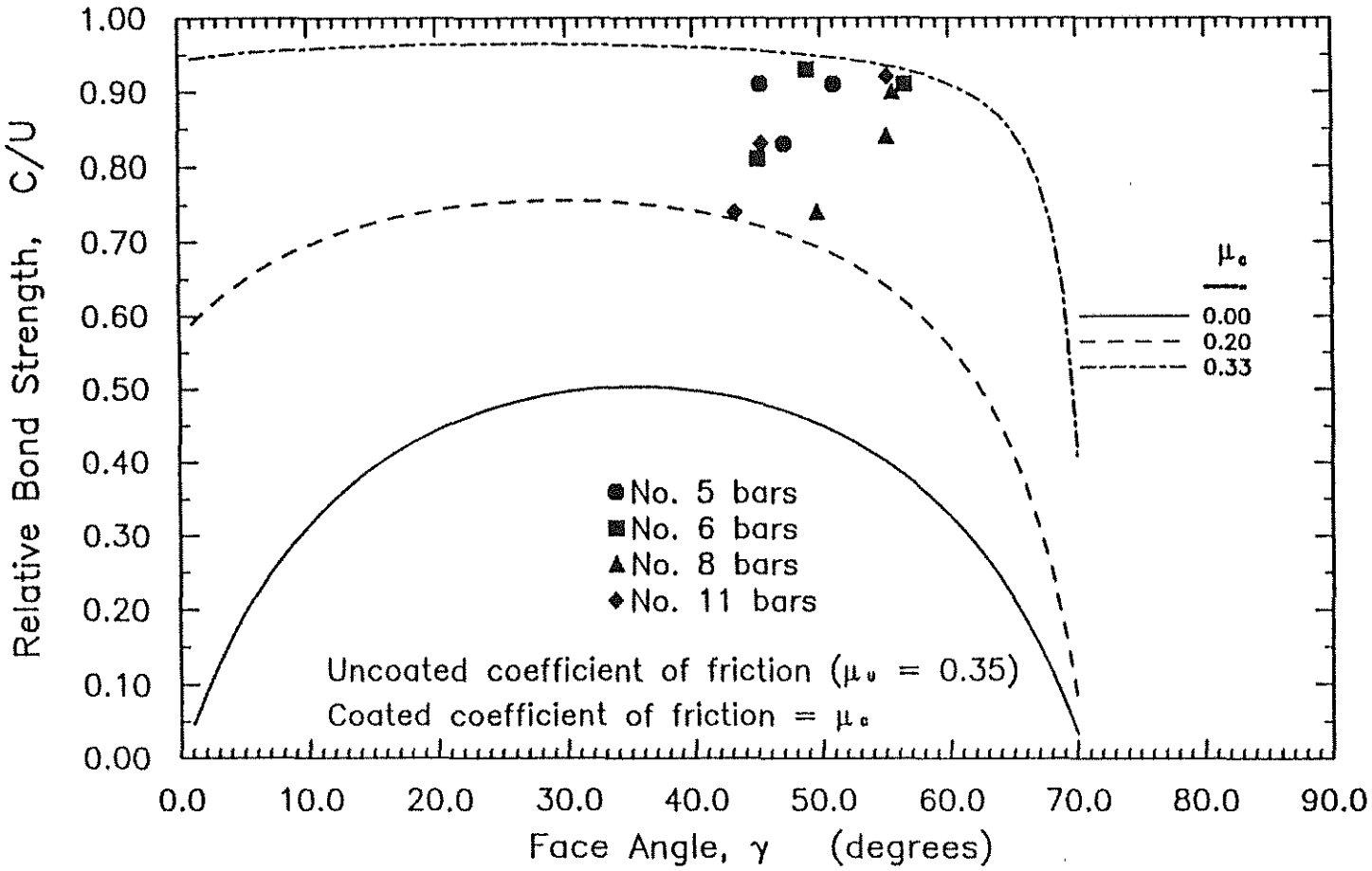

Fig. 4.10 Relative Bond Strength versus Face Angle With no Limitation on γ of Uncoated Bars, $\mu_u = 0.35$

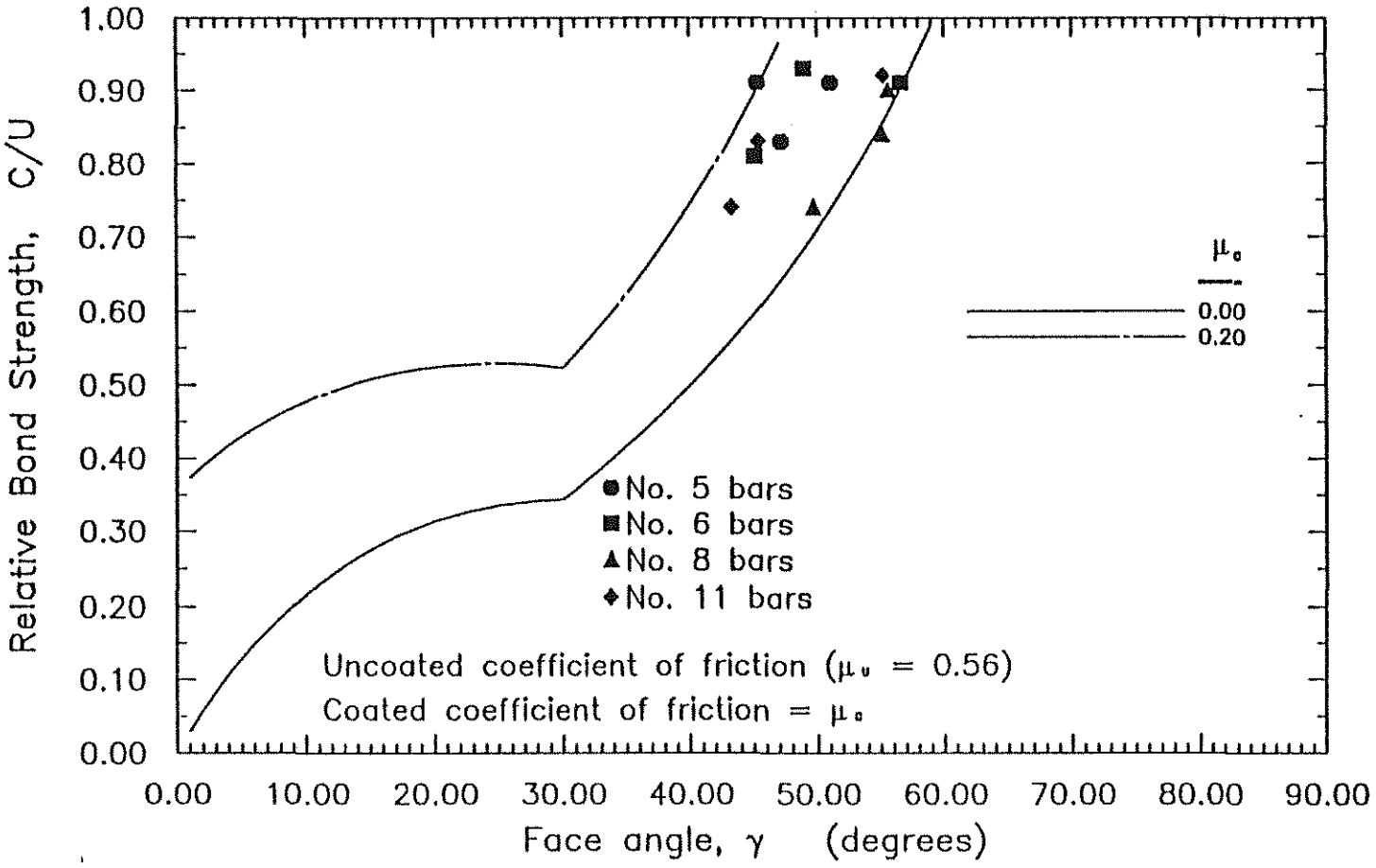

Fig. 4.11 Relative Bond Strength versus Face Angle With a Limitation of 30° on γ for Uncoated Bars, $\mu_u = 0.56$

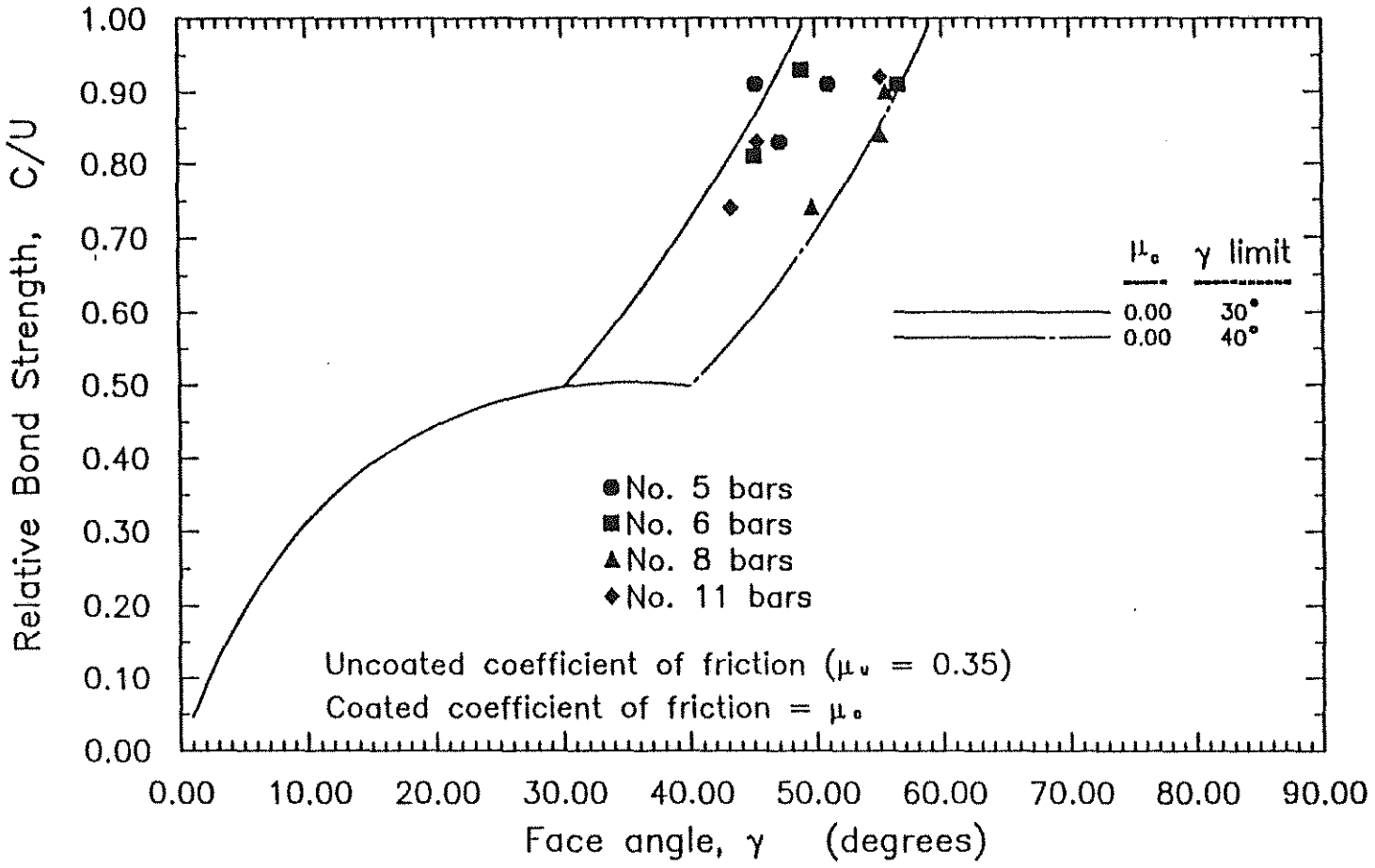

Fig. 4.12 Relative Bond Strength versus Face Angle, $\mu_u = 0.35$

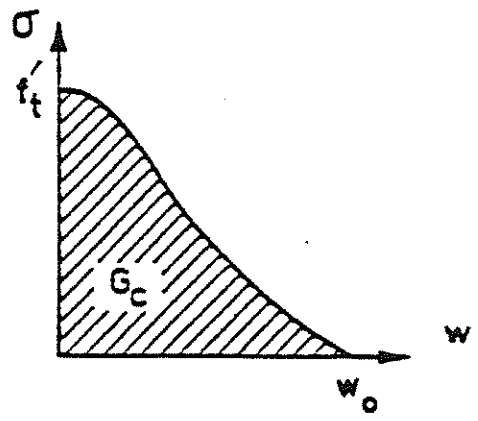

Fig. 4.13 Crack Opening Stress–Displacement Relationship (Petersson 1979)

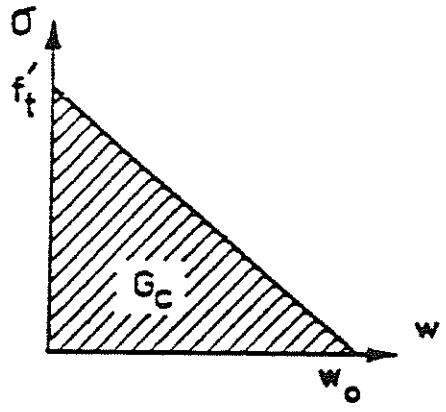

F Fig. 4.14 Straight–Line Approximation of Crack Opening Stress–Displacement Relationship (Petersson 1979)

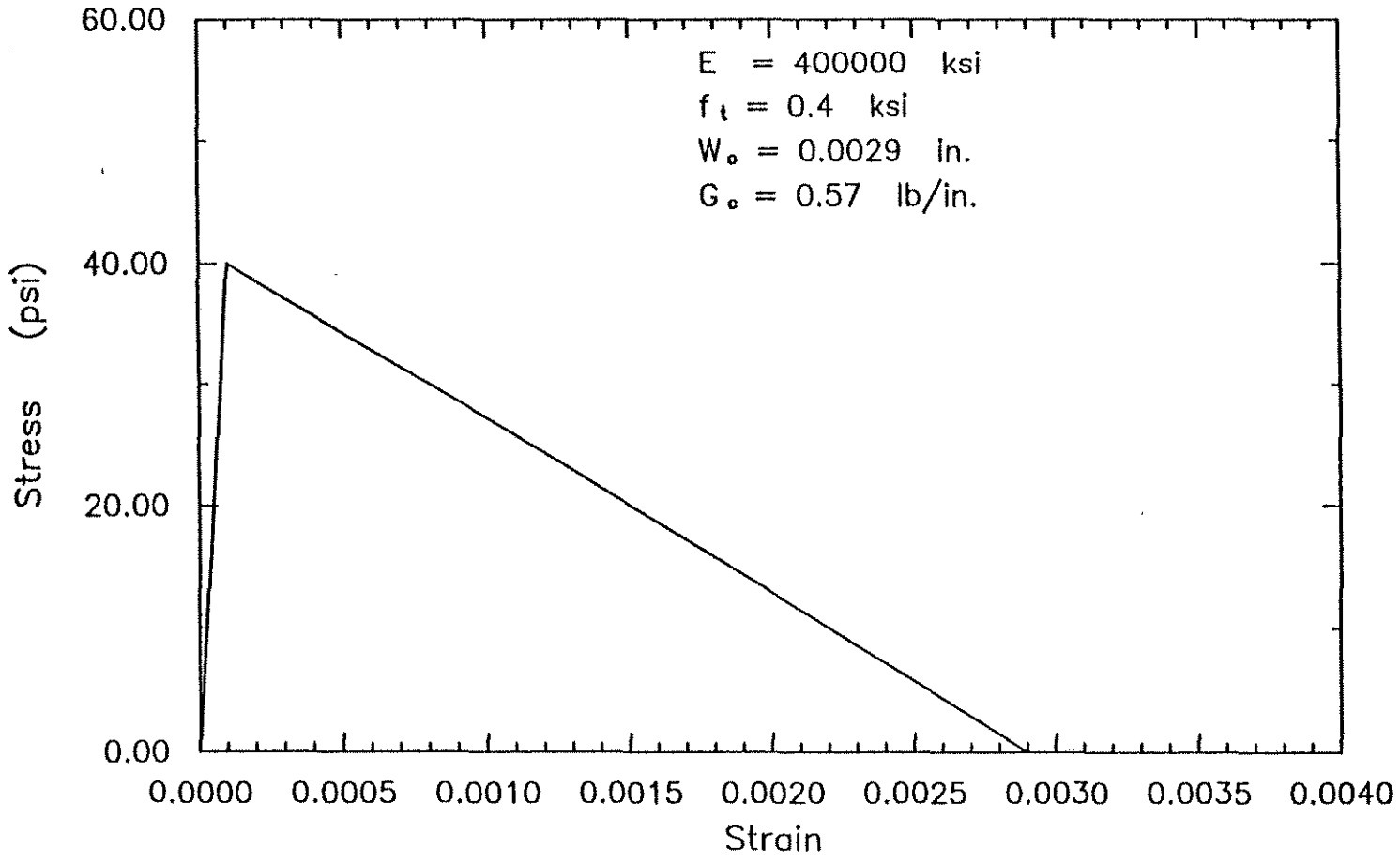

Fig. 4.15 Stress–Strain Function for Rod Elements

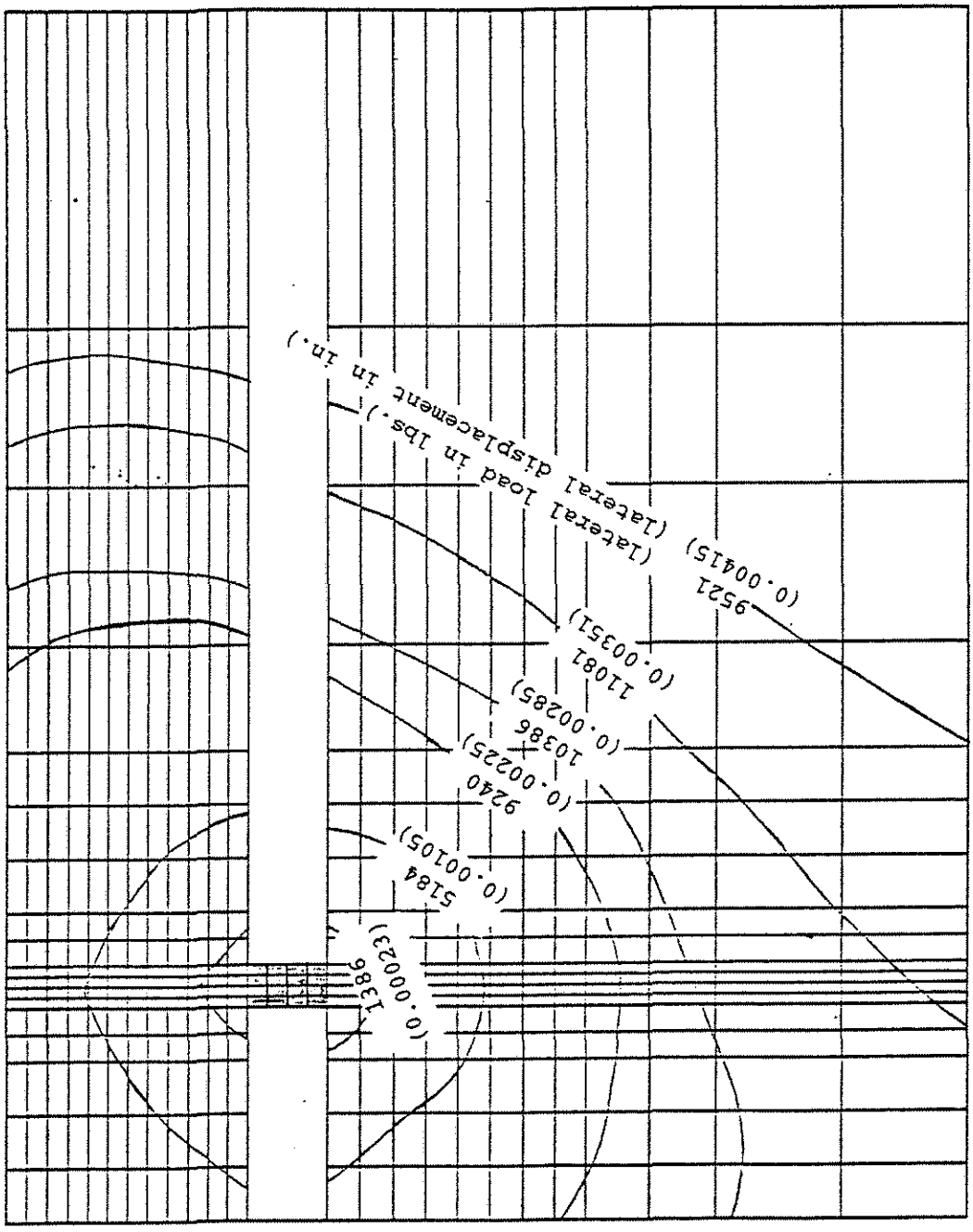

Fig. 4.16 Cracked Beam–end Specimen

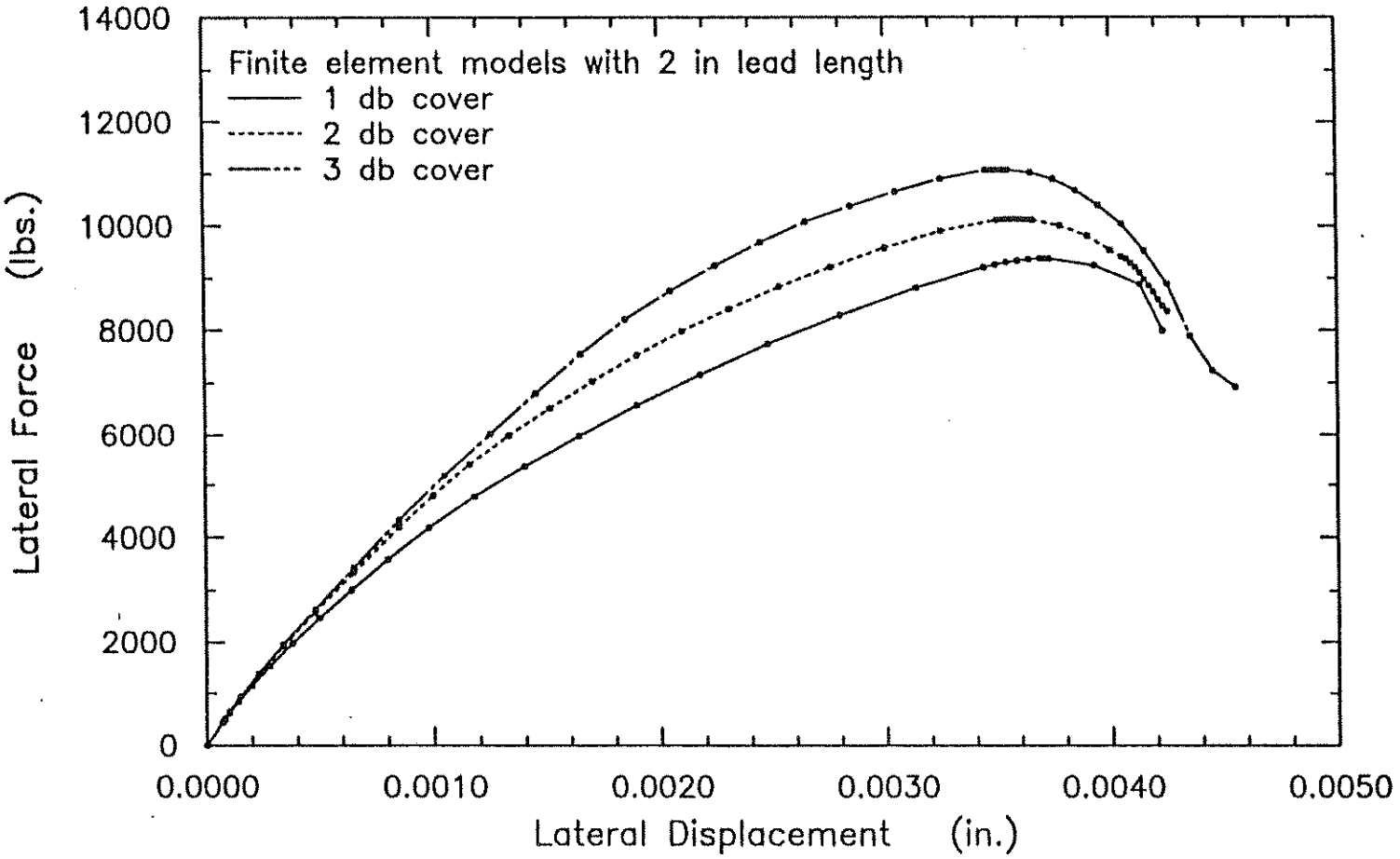

Fig. 4.17 Lateral Force versus Lateral Displacement for Finite Element Models with Different Covers

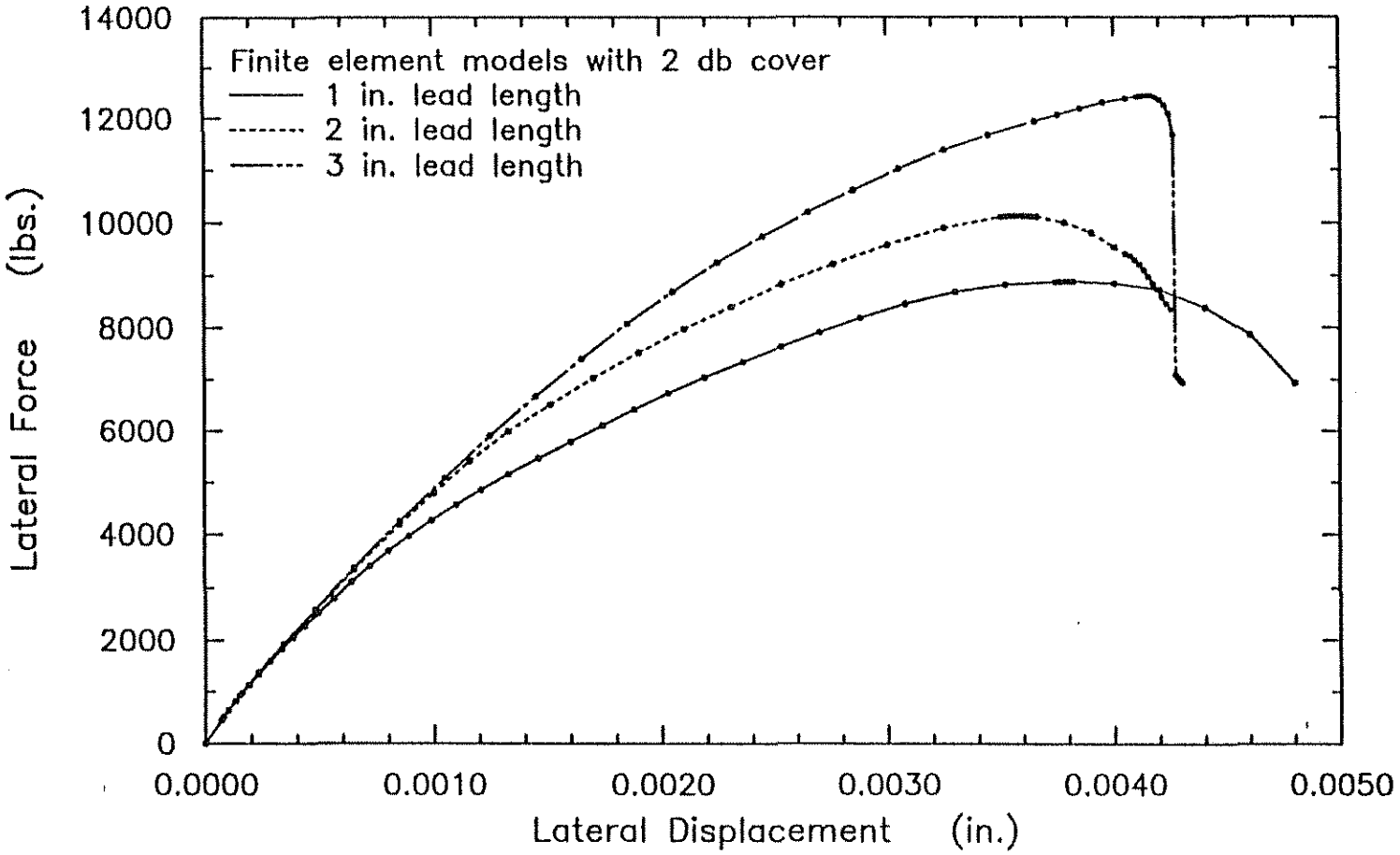

Fig. 4.18 Lateral Force versus Lateral Displacement for Finite Element Models with Different Lead Lengths

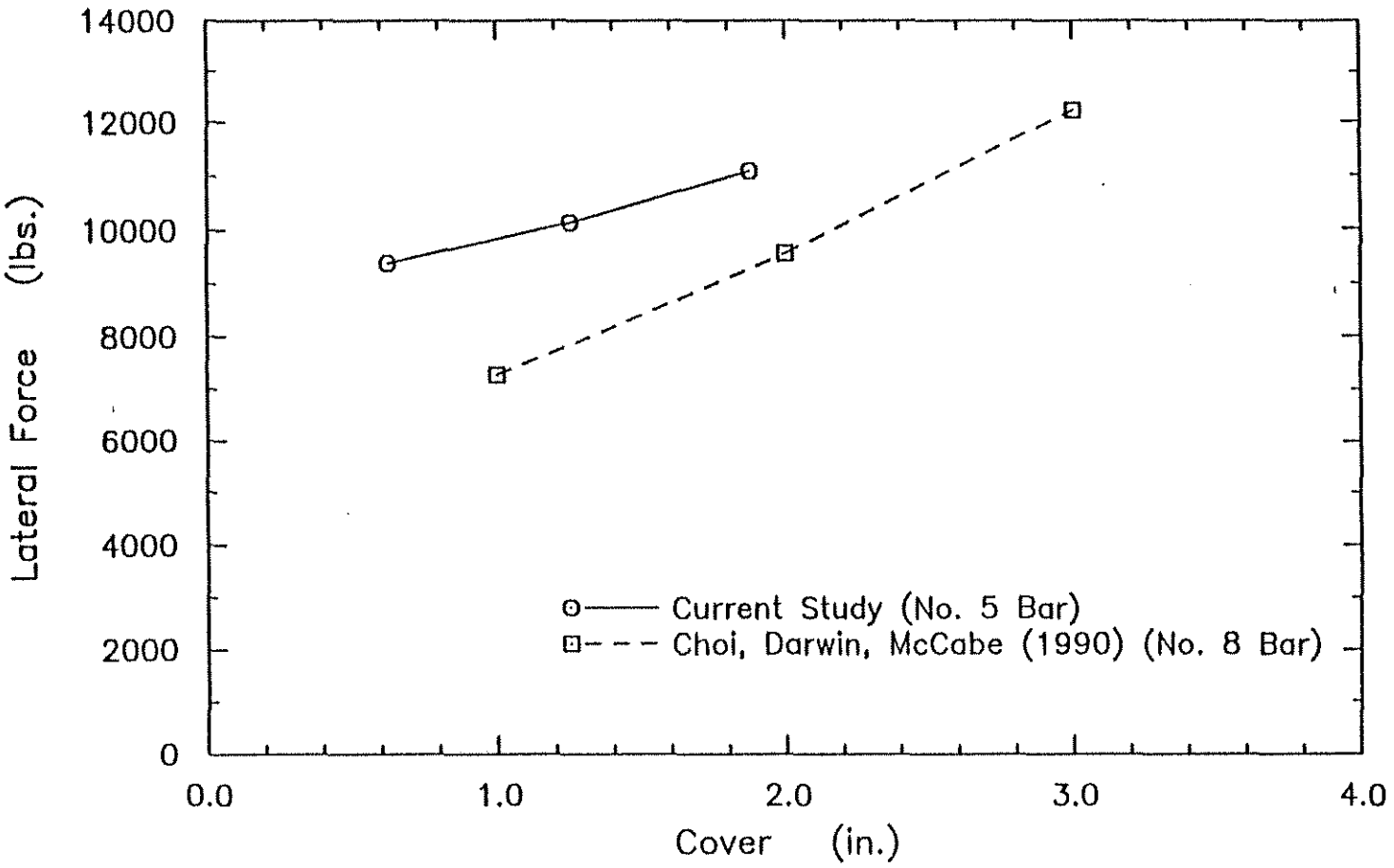

Fig. 4.19 Lateral Force versus Cover for Finite Element Models With Different Covers

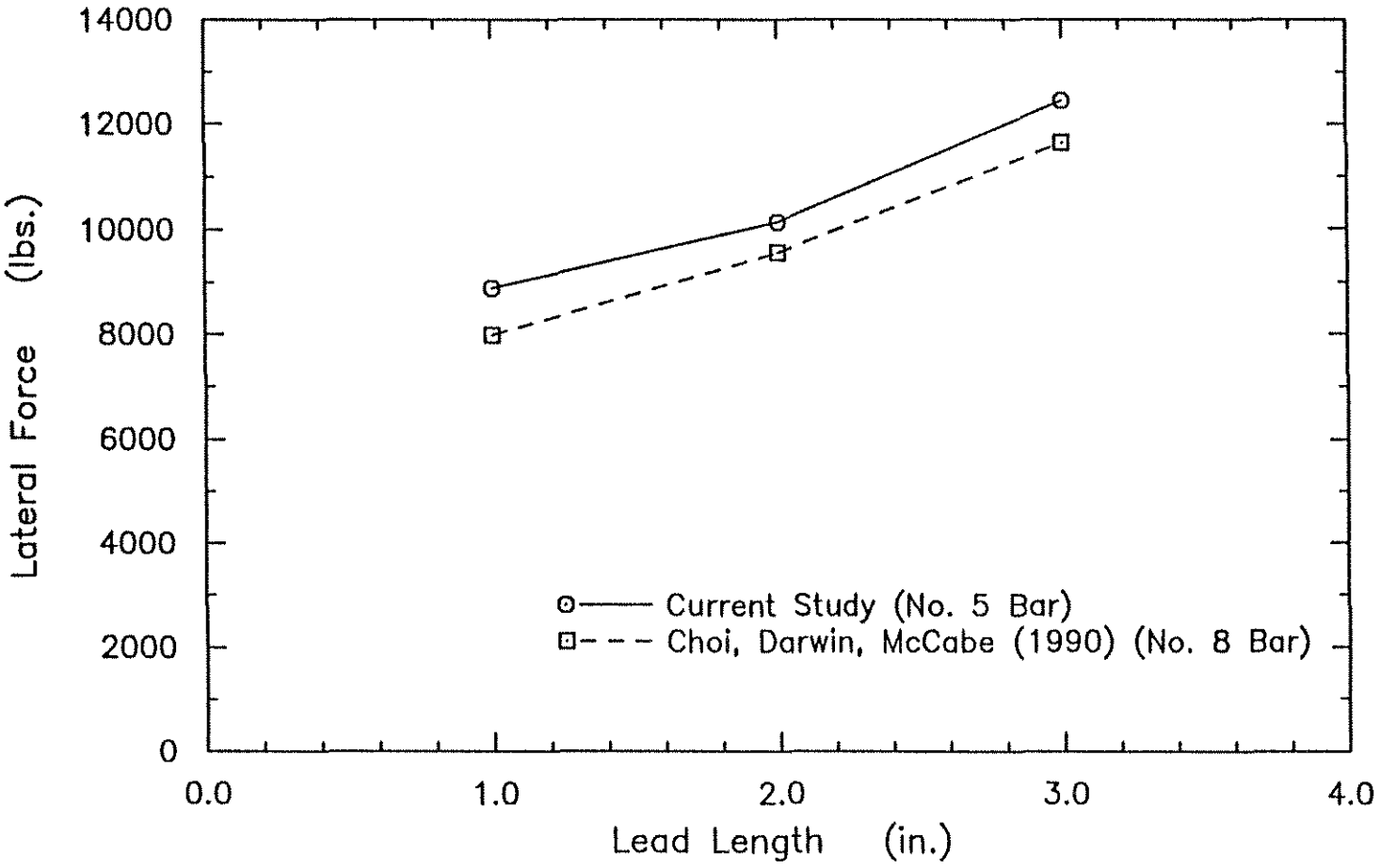

Fig. 4.20 Lateral Force versus Lead Length for Finite Element Models With Different Lead Lengths

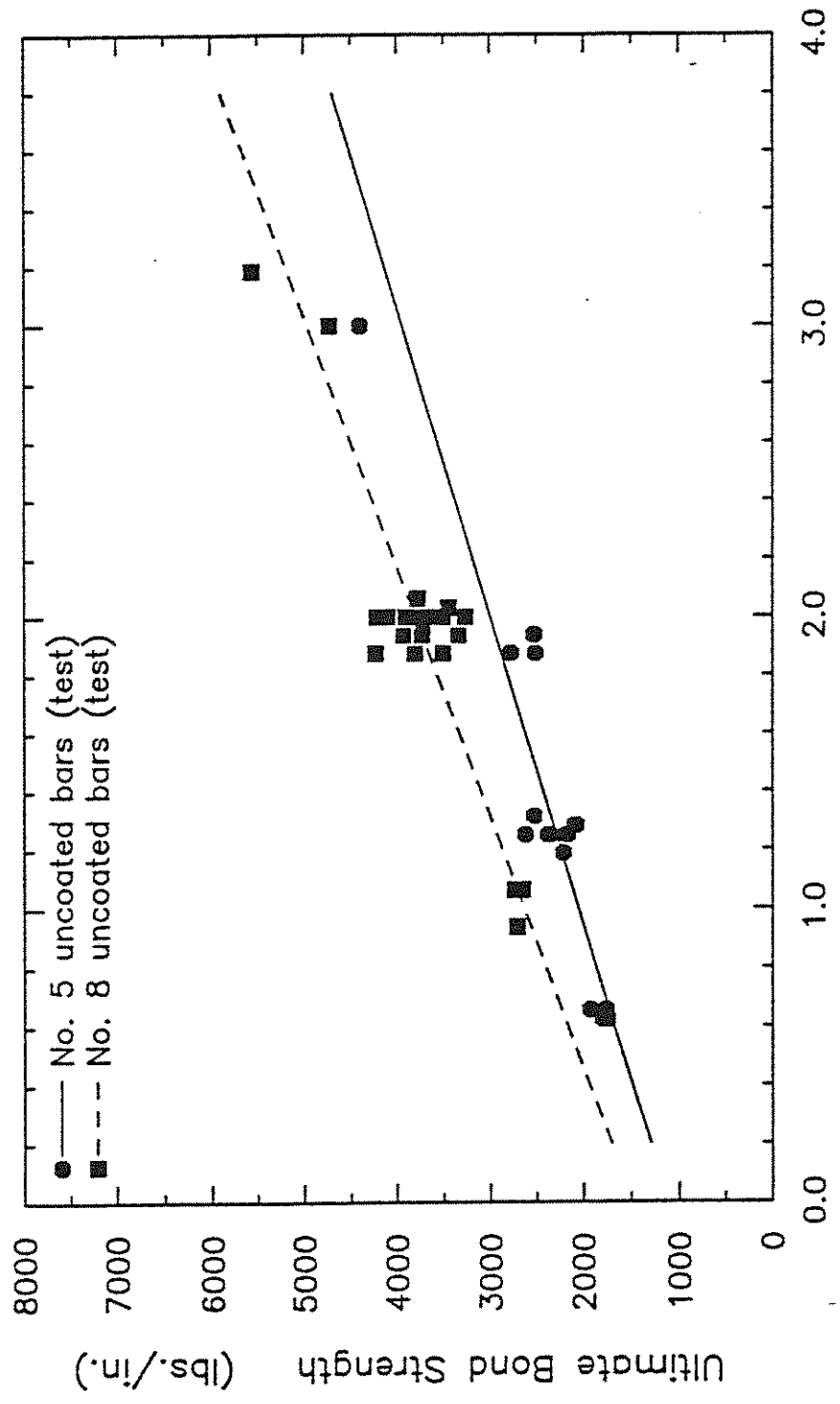

Fig. 4.21 Ultimate Bond Strength versus Cover for No. 5 and No. 8 test Bars

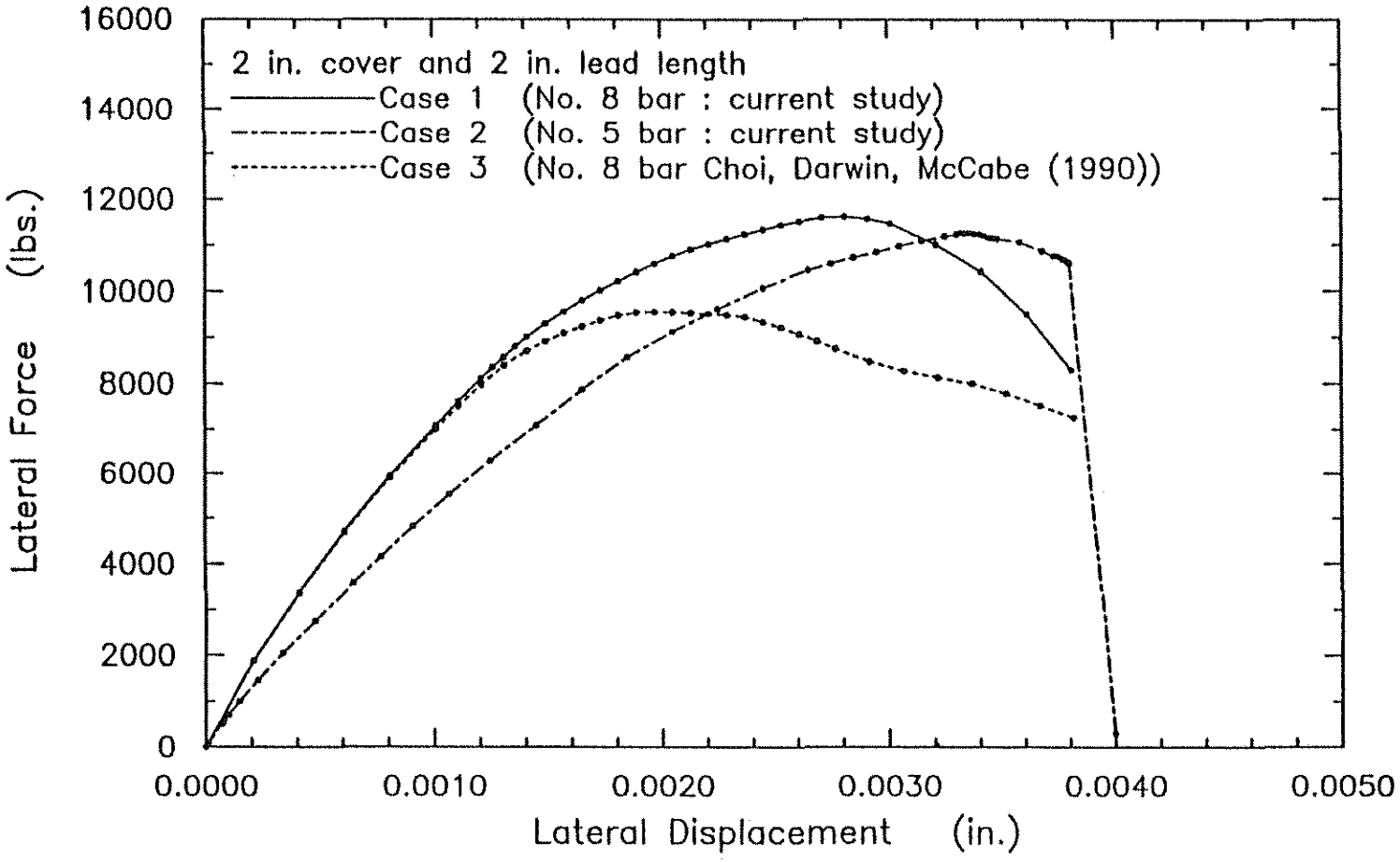

Fig. 4.22 Lateral Force versus Lateral Displacement for Different Finite Element Models

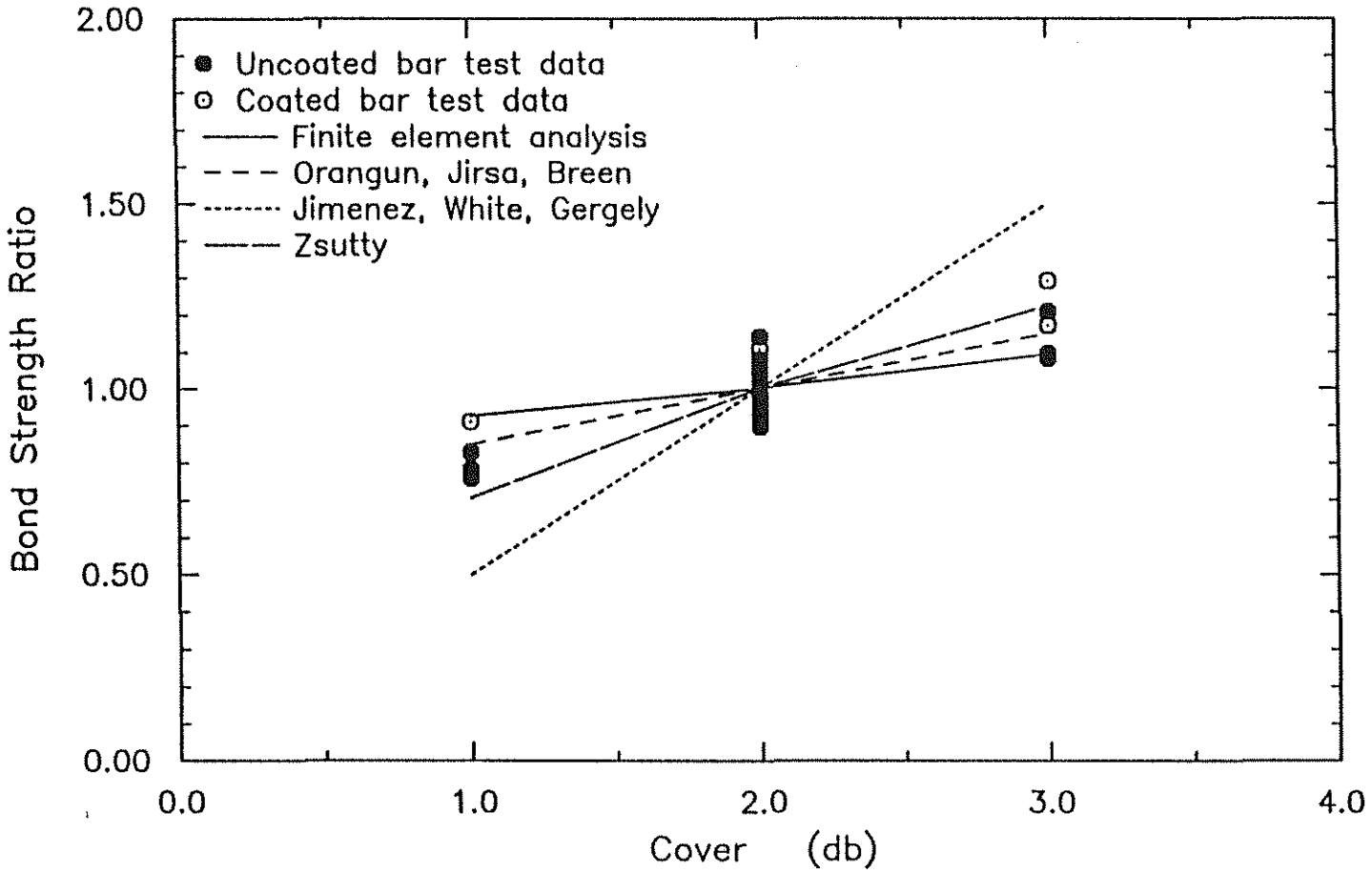

Fig. 4.23 Bond Strength Ratio for No. 5 Bars Normalized to 2 Bar Diameter Cover versus Cover

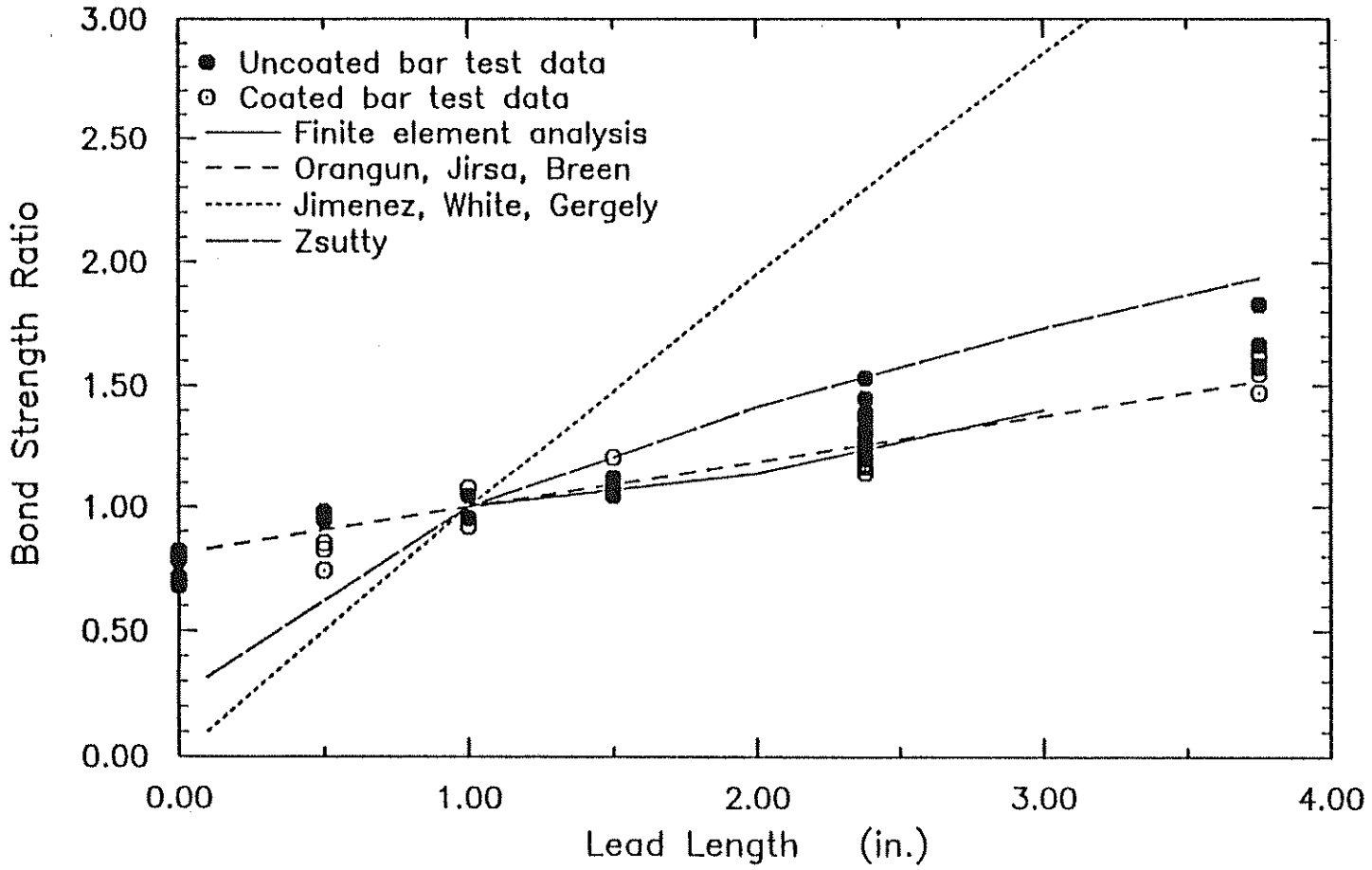

Fig. 4.24 Bond Strength Ratio for No. 5 Bars Normalized to 1.0 in. Lead Length versus Lead Length

APPENDIX A: BEARING AREA CALCULATION OF REINFORCING STEEL

An important characteristic of reinforcing bars is the bearing area of the deformations per unit length of the bar. There are no methods in ASTM A 615 (1987) for measuring the bearing area. Therefore, the following technique was developed for this task.

In this technique, the bearing area is calculated based on closely spaced measurements. As illustrated in Fig. A.1, the deformations are measured at n (typically 20) positions around the circumference. To carry out the measurements, the bars are mounted in a lathe as follows:

1) The bar is placed in the grip assembly of the lathe, which helps to match the center of the lathe and the bar. The wheel of the lathe is divided into n circumferential divisions of equal size, i.e., 20 divisions, 18° apart (Figs. A.1 and A.2).
2) Using a dial gage, the deformations are measured at points as illustrated in Figs. A.3 and A.4. At each division, dial gage readings are obtained with the tip of the dial gage at points A, C_1, D_1, M_1, B_1, B, B_2, M_2, D_2, C_2. The longitudinal dimensions of the ribs E_1, E_2, F, are measured. After each set of measurements, the lathe is rotated to the next division and the process is repeated. The widths of the longitudinal ribs (gaps) at the top and

the bottom of the deformation, G_{11}, G_{12}, G_{21}, G_{22} are measured with a caliper (Fig. A.1). The heights of the longitudinal ribs (not shown), d_1 and d_2, are measured with the dial gage. The width of the small longitudinal rib, G_4, is measured with caliper. To determine the height of the small longitudinal rib, d_3, the height of the rib, G_3, is measured with the dial gage. The values of G_{11}, G_{12}, G_{21}, G_{22}, G_3, and G_4 are the average of two values measured at each side of the deformation. Data from these measurements are shown in tables A.1 - A.26 for No. 5, 6, 8, and 11 bars with S, C, and N-pattern deformations. No. 3 bars are only C-pattern. Each bar size and deformation pattern is measured twice.

3) After the table is complete, the following steps are used to calculate the bearing area.

R = radius of the wheel of the lathe

X_1 = smaller value of C_1 and D_1

X_2 = smaller value of C_2 and D_2

Y = θ (Initializing the bearing area of divisions)

Step 1. Repeat from n = 1 to 20

$$W_{1(n)} = R - A + \frac{B_{(n)} + B_{1(n)} + B_{2(n)}}{3} \qquad (A.1)$$

$$W_{2(n)} = R - A + \frac{X_{1(n)} + X_{2(n)}}{2} \qquad (A.2)$$

$$W_{1(n+1)} = R - A + \frac{B_{(n+1)} + B_{1(n+1)} + B_{2(n+1)}}{3} \quad (A.3)$$

$$W_{2(n+1)} = R - A + \frac{X_{1(n+1)} + X_{2(n+1)}}{2} \quad (A.4)$$

$$Z_{(n)} = \frac{\pi}{20} \left[\left(\frac{W_{1(n)} + W_{1(n+1)}}{2} \right)^2 - \left(\frac{W_{2(n)} + W_{2(n+1)}}{2} \right)^2 \right] \quad (A.5)$$

$$Y = Y + Z_{(n)}$$

in which W_1 and W_2 are the measured radius of the top and the bottom deformation and Z is the bearing area of each division.

Step 2. Calculate the bearing area.

$$\text{Bearing Area} = \frac{Y - \left[d_1 \left(\frac{G_{11} + G_{21}}{2} \right) + d_2 \left(\frac{G_{12} + G_{22}}{2} \right) + \frac{d_3 G_4}{2} \right]}{\text{Spacing of the deformation}} \quad (A.6)$$

4) The face angle of the bars is calculated using three approaches. For every approach, the measurements of the deformations at 20 equal intervals around the circumference of the bar (Tables A.1 - A.26) are used for the determination of face angle of every bar. The three approaches are:

   a) In this approach, it is assumed that the line connecting the base of the deformation to the top of the deformation is a straight line (lines D_1B_1 and D_2B_2 in Fig. A.3). The face angle is the angle formed

by lines D_1B_1 or D_2B_2 and the longitudinal axis of the bar. The face angle calculated in this method for every bar is the average of the face angles at every interval (total of 20 intervals) at both sides of the deformation.

b) In this approach, the face angles at each interval are calculated exactly like the first approach. The face angle calculated in this method for every bar, however, is the maximum of the face angles at each interval (total of 20 intervals) at both sides of the deformation. The reason for using the maximum face angle is that it can be argued that it is the largest face angle value that controls the slip of the deformation, and in effect the slip of the bar relative to concrete.

c) In this approach, it is assumed that the line connecting the base of the deformation to the top of the deformation is not a straight line and is convex upward (lines D_1B_1 and D_2B_2 in Fig. A.3). Therefore, it is evident that the face angle at the base of the deformation is larger than that at the mid-height of the deformation and it is the face angle at the base of the deformation that controls the slip of the deformation against concrete. Therefore, the face angle calculated in this method for every bar is the

maximum of the face angles at the base of the deformation (the angle formed by lines D_1M_1 or D_2M_2 and the longitudinal axis of the bar) at each interval at both sides of the deformation.

As discussed in Section 4.3, the value of face angle calculated by the third approach is used as the face angle of the bars (Table 2.1).

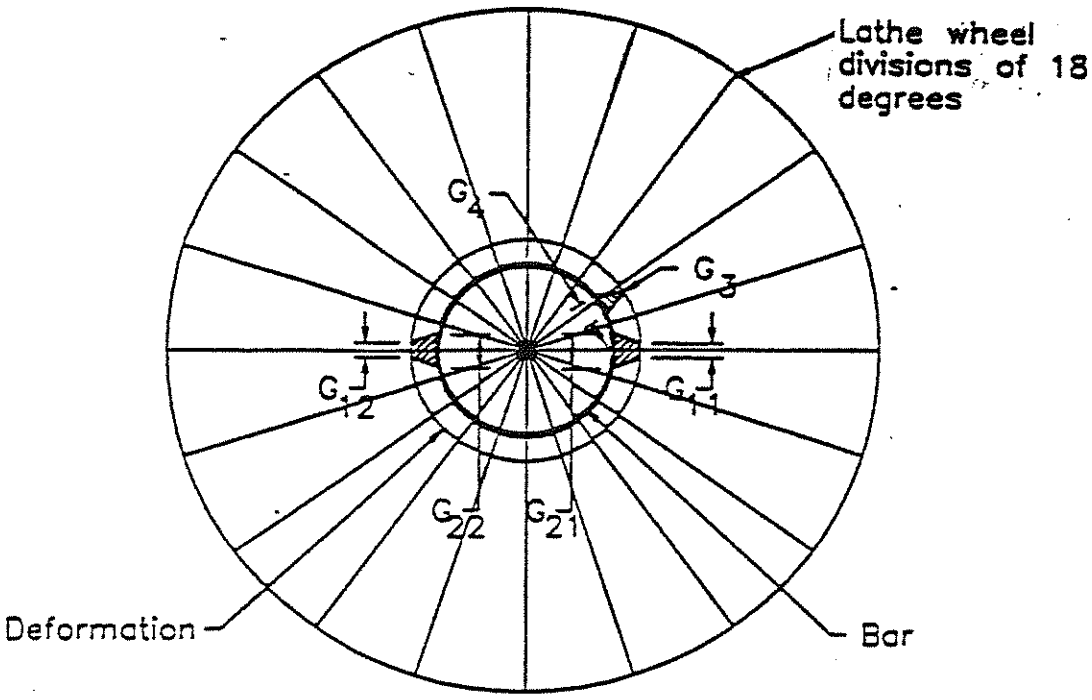

Fig. A.1 Equal Divisions for Deformation Measurement

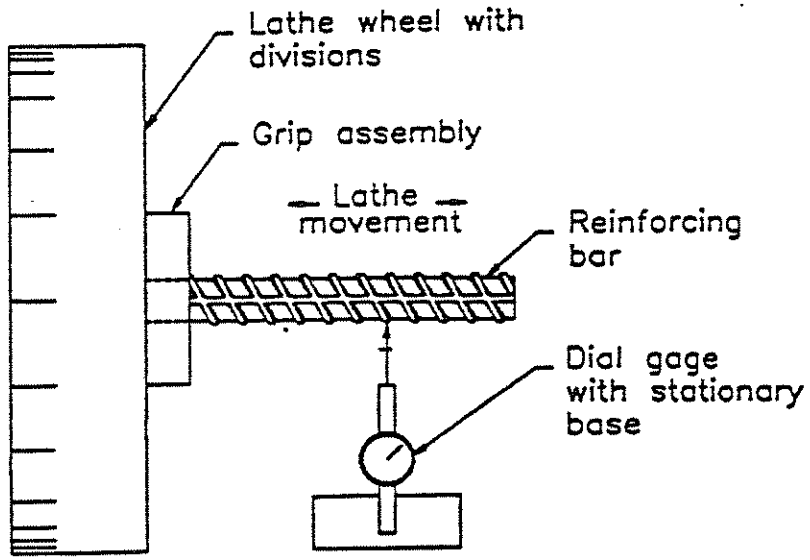

Fig. A.2 Instrument Set–up for Deformation Measurement

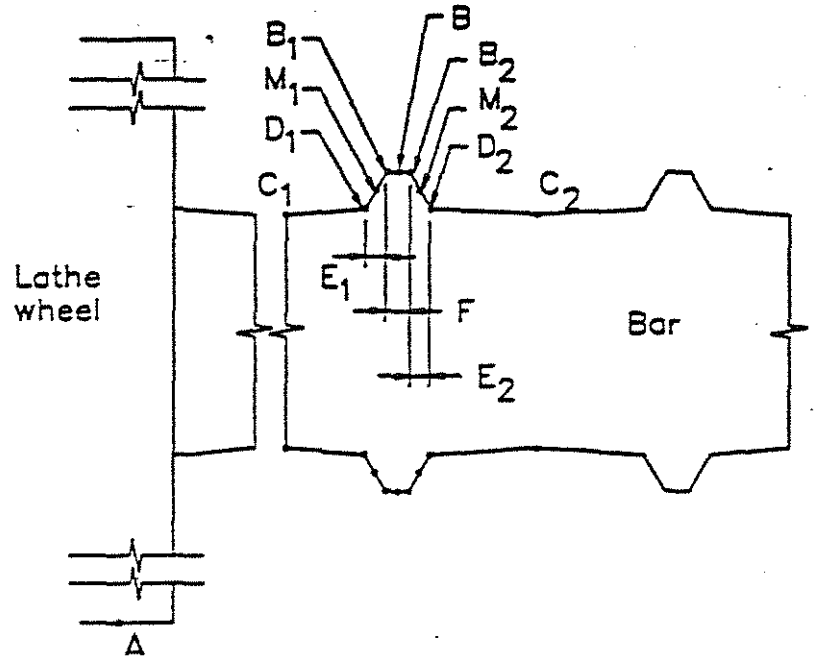

Fig. A.3 Side View of Measuring Points on the Reinforcing Bar

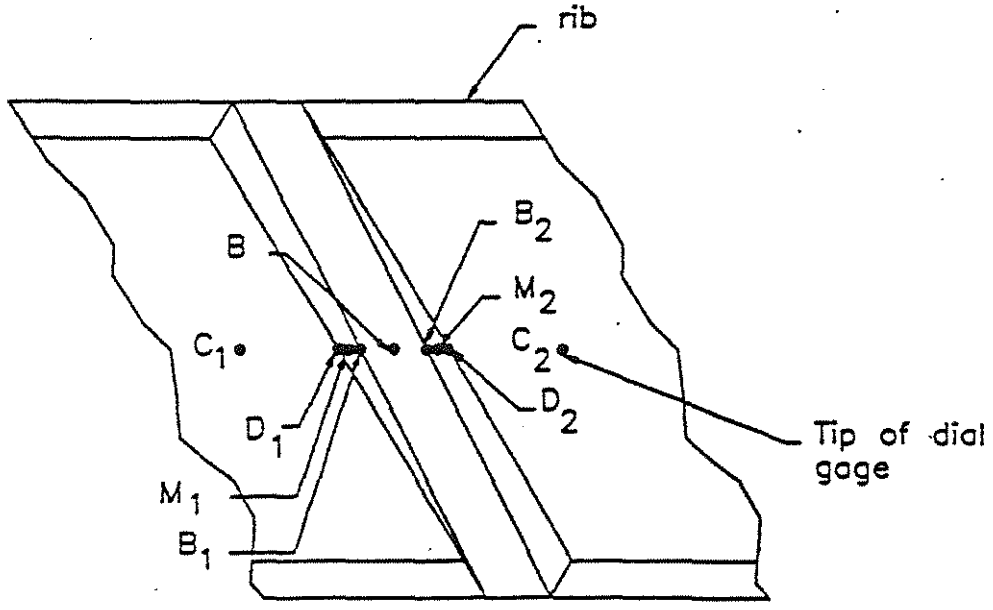

Fig. A.4 Front View of Measuring Points on the Reinforcing Bar

Table A.1 : Data for Deformation Measurements

Deformation Pattern : C
Surface Type : Mill scale
Bar size : No. 3 (first measurement)

P	A	B	B1	B2	C1	C2	D1	D2	M1	M2	E1	E2	F
1	5.714	1.772	1.770	1.771	1.751	1.751	1.752	1.751	---	---	0.044	0.060	0.048
2	5.714	1.766	1.766	1.762	1.748	1.747	1.752	1.749	---	---	0.039	0.058	0.047
3	5.714	1.769	1.767	1.766	1.750	1.746	1.747	1.744	---	---	0.038	0.045	0.035
4	5.714	1.770	1.767	1.768	1.760	1.759	1.761	1.760	---	---	0.033	0.023	0.037
5	5.714	1.767	1.766	1.765	1.758	1.755	1.760	1.758	---	---	0.030	0.029	0.041
6	5.714	1.769	1.766	1.768	1.758	1.757	1.758	1.758	---	---	0.019	0.027	0.048
7	5.714	1.772	1.770	1.772	1.756	1.754	1.758	1.751	---	---	0.046	0.037	0.041
8	5.714	1.774	1.772	1.772	1.754	1.752	1.757	1.750	---	---	0.021	0.082	0.038
9	5.714	1.777	1.774	1.776	1.760	1.759	1.767	1.760	---	---	0.036	0.035	0.037
* 10	5.714	1.780	1.779	1.782	1.761	1.761	1.765	1.763	---	---	---	---	---
11	5.714	1.790	1.791	1.789	1.770	1.771	1.772	1.769	---	---	0.019	0.030	0.035
12	5.714	1.796	1.795	1.797	1.778	1.780	1.778	1.776	---	---	0.046	0.061	0.046
+ 13	5.714	1.802	1.802	1.802	1.780	1.783	1.781	1.782	---	---	0.046	0.054	0.040
14	5.714	1.800	1.798	1.801	1.783	1.786	1.784	1.786	---	---	0.059	0.044	0.030
15	5.714	1.800	1.800	1.799	1.779	1.782	1.782	1.782	---	---	0.045	0.050	0.021
16	5.714	1.795	1.799	1.799	1.781	1.777	1.779	1.779	---	---	0.040	0.041	0.031
17	5.714	1.797	1.798	1.796	1.780	1.777	1.780	1.779	---	---	0.049	0.047	0.033
18	5.714	1.791	1.792	1.790	1.767	1.767	1.771	1.767	---	---	0.038	0.070	0.033
19	5.714	1.785	1.785	1.786	1.765	1.763	1.769	1.768	---	---	0.058	0.071	0.028
* 20	5.714	1.781	1.781	1.781	1.759	1.757	1.760	1.759	---	---	---	---	---

G11 = 0.093 G12 = 0.100 G3 = 1.800
G21 = 0.129 G22 = 0.132 G4 = 0.070

* Location of logitudinal ribs
+ Location of small longidudinal rib

Table A.2 : Data for Deformation Measurements

Deformation Pattern : C
Surface Type : Mill scale
Bar size : No. 3 (second measurement)

P	A	B	B1	B2	C1	C2	D1	D2	M1	M2	E1	E2	F
* 1	6.077	2.171	2.172	2.171	2.145	2.144	2.144	2.147	---	---	---	---	---
2	6.077	2.171	2.171	2.170	2.146	2.147	2.146	2.149	---	---	0.027	0.047	0.057
3	6.077	2.169	2.169	2.167	2.145	2.147	2.146	2.148	---	---	0.058	0.033	0.043
4	6.077	2.170	2.169	2.168	2.149	2.150	2.151	2.152	---	---	0.058	0.020	0.045
5	6.077	2.167	2.165	2.167	2.156	2.154	2.155	2.160	---	---	0.040	0.034	0.058
6	6.077	2.165	2.164	2.165	2.152	2.152	2.154	2.156	---	---	0.035	0.038	0.044
7	6.077	2.155	2.154	2.156	2.144	2.145	2.145	2.151	---	---	0.035	0.040	0.038
8	6.077	2.144	2.140	2.144	2.124	2.123	2.125	2.123	---	---	0.032	0.045	0.048
9	6.077	2.135	2.132	2.135	2.114	2.114	2.116	2.115	---	---	0.044	0.060	0.044
10	6.077	2.126	2.126	2.128	2.108	2.108	2.100	2.110	---	---	0.043	0.060	0.041
* 11	6.077	2.127	2.126	2.128	2.108	2.106	2.109	2.108	---	---	---	---	---
12	6.077	2.124	2.121	2.124	2.108	2.104	2.107	2.106	---	---	0.031	0.050	0.043
13	6.077	2.125	2.125	2.126	2.107	2.106	2.107	2.107	---	---	0.051	0.055	0.045
+ 14	6.077	2.130	2.130	2.130	2.115	2.114	2.115	2.115	---	---	0.015	0.037	0.038
15	6.077	2.137	2.136	2.136	2.122	2.121	2.124	2.124	---	---	0.027	0.050	0.038
16	6.077	2.137	2.136	2.136	2.121	2.121	2.125	2.128	---	---	0.045	0.033	0.049
17	6.077	2.145	2.143	2.143	2.128	2.128	2.129	2.133	---	---	0.023	0.049	0.030
18	6.077	2.152	2.153	2.150	2.132	2.133	2.132	2.133	---	---	0.040	0.037	0.048
19	6.077	2.160	2.161	2.158	2.136	2.137	2.137	2.138	---	---	0.035	0.052	0.041
20	6.077	2.165	2.165	2.165	2.143	2.141	2.142	2.145	---	---	0.031	0.052	0.054

G11 = 0.091 G12 = 0.094 G3 = 2.128
G21 = 0.141 G22 = 0.150 G4 = 0.081

* Location of logitudinal ribs
+ Location of small longidudinal rib

Table A.3 : Data for Deformation Measurements

Deformation Pattern : S

Surface Type : Mill scale

Bar size : No. 5 (first measurement)

P	A	B	B1	B2	C1	C2	D1	D2	M1	M2	E1	E2	F
1	4.269	0.670	0.669	0.670	0.640	0.640	0.640	0.640	0.657	0.657	0.076	0.050	0.041
2	4.269	0.675	0.672	0.674	0.642	0.642	0.641	0.643	0.657	0.655	0.072	0.062	0.032
3	4.269	0.676	0.674	0.674	0.645	0.645	0.645	0.645	0.660	0.661	0.081	0.065	0.012
4	4.269	0.679	0.676	0.677	0.647	0.648	0.646	0.648	0.660	0.665	0.078	0.066	0.026
5	4.269	0.682	0.677	0.681	0.649	0.649	0.648	0.650	0.655	0.660	0.066	0.067	0.022
6	4.269	0.675	0.672	0.674	0.648	0.649	0.649	0.649	0.659	0.664	0.054	0.064	0.047
* 7	4.269	0.679	0.682	0.680	0.648	0.650	0.651	0.650	0.663	0.665	---	---	---
8	4.269	0.680	0.676	0.677	0.646	0.646	0.647	0.648	0.656	0.660	0.050	0.046	0.055
9	4.269	0.668	0.667	0.665	0.647	0.648	0.647	0.648	0.656	0.655	0.050	0.024	0.066
10	4.269	0.682	0.676	0.678	0.648	0.650	0.647	0.648	0.664	0.662	0.065	0.056	0.035
11	4.269	0.681	0.678	0.680	0.650	0.650	0.650	0.650	0.666	0.662	0.063	0.061	0.039
12	4.269	0.684	0.683	0.682	0.649	0.650	0.650	0.649	0.670	0.663	0.089	0.051	0.028
13	4.269	0.683	0.682	0.683	0.649	0.648	0.649	0.647	0.665	0.664	0.075	0.084	0.037
14	4.269	0.680	0.678	0.679	0.648	0.648	0.648	0.647	0.665	0.666	0.088	0.066	0.033
15	4.269	0.674	0.669	0.674	0.645	0.642	0.644	0.644	0.659	0.655	0.055	0.057	0.034
16	4.269	0.663	0.660	0.662	0.642	0.641	0.641	0.641	0.649	0.651	0.043	0.048	0.039
* 17	4.269	0.670	0.670	0.670	0.642	0.641	0.642	0.642	0.650	0.649	---	---	---
18	4.269	0.652	0.655	0.649	0.631	0.633	0.633	0.631	0.636	0.636	0.042	0.056	0.067
19	4.269	0.654	0.655	0.654	0.634	0.633	0.633	0.633	0.641	0.644	0.051	0.048	0.057
20	4.269	0.665	0.664	0.665	0.636	0.635	0.636	0.636	0.651	0.650	0.079	0.054	0.093

G11 = 0.120 G12 = 0.127 G3 = ---

G21 = 0.190 G22 = 0.197 G4 = ---

* Location of logitudinal ribs

Table A.4 : Data for Deformation Measurements

Deformation Pattern : S
Surface Type : Mill scale
Bar size : No. 5 (second measurement)

P	A	B	B1	B2	C1	C2	D1	D2	M1	M2	E1	E2	F
1	4.100	0.312	0.310	0.310	0.280	0.279	0.279	0.279	0.296	0.303	0.063	0.044	0.050
2	4.100	0.320	0.319	0.318	0.289	0.290	0.291	0.289	0.306	0.310	0.042	0.043	0.059
3	4.100	0.323	0.320	0.324	0.294	0.296	0.296	0.297	0.311	0.315	0.046	0.039	0.063
4	4.100	0.324	0.322	0.323	0.296	0.296	0.296	0.297	0.311	0.312	0.044	0.045	0.059
5	4.100	0.325	0.320	0.321	0.294	0.295	0.296	0.295	0.306	0.313	0.046	0.035	0.067
6	4.100	0.324	0.318	0.320	0.290	0.291	0.291	0.280	0.305	0.307	0.076	0.031	0.060
7	4.100	0.315	0.313	0.314	0.284	0.283	0.283	0.284	0.301	0.301	0.056	0.036	0.060
8	4.100	0.305	0.301	0.304	0.274	0.274	0.276	0.274	0.288	0.290	0.052	0.045	0.060
* 9	4.100	0.300	0.302	0.305	0.270	0.269	0.280	0.274	0.290	0.295	---	---	---
10	4.100	0.290	0.294	0.295	0.965	0.964	0.270	0.266	0.279	0.283	0.054	0.044	0.057
11	4.100	0.289	0.285	0.286	0.260	0.259	0.260	0.258	0.267	0.270	0.053	0.031	0.064
12	4.100	0.286	0.281	0.286	0.255	0.253	0.255	0.254	0.266	0.267	0.050	0.046	0.055
13	4.100	0.285	0.281	0.280	0.251	0.251	0.251	0.251	0.264	0.266	0.052	0.046	0.060
14	4.100	0.290	0.286	0.283	0.254	0.253	0.253	0.252	0.266	0.267	0.054	0.039	0.066
15	4.100	0.286	0.270	0.282	0.250	0.250	0.251	0.251	0.266	0.267	0.064	0.042	0.057
16	4.100	0.284	0.282	0.283	0.251	0.251	0.251	0.251	0.268	0.265	0.041	0.051	0.061
17	4.100	0.286	0.281	0.281	0.253	0.253	0.252	0.253	0.268	0.269	0.063	0.044	0.053
18	4.102	0.284	0.287	0.282	0.257	0.256	0.258	0.257	0.272	0.272	0.054	0.037	0.068
* 19	4.100	0.294	0.291	0.290	0.260	0.262	0.259	0.261	0.275	0.276	---	---	---
20	4.100	0.303	0.301	0.300	0.270	0.271	0.269	0.270	0.286	0.290	0.053	0.043	0.053

G11 = 0.110 G12 = 0.107 G3 = ---
G21 = 0.210 G22 = 0.210 G4 = ---
* Location of logitudinal ribs

Table A.5 : Data for Deformation Measurements

Deformation Pattern : C
Surface Type : Mill scale
Bar size : No. 5 (first measurement)

P	A	B	B1	B2	C1	C2	D1	D2	M1	M2	E1	E2	F
1	4.269	0.664	0.664	0.663	0.631	0.632	0.633	0.633	0.648	0.638	0.098	0.046	0.102
2	4.269	0.675	0.674	0.674	0.630	0.629	0.631	0.631	0.653	0.650	0.108	0.058	0.044
3	4.269	0.677	0.674	0.674	0.632	0.631	0.632	0.633	0.660	0.658	0.057	0.049	0.152
4	4.269	0.676	0.672	0.672	0.636	0.637	0.636	0.636	0.653	0.650	0.063	0.052	0.054
5	4.269	0.676	0.672	0.674	0.641	0.641	0.645	0.642	0.658	0.652	0.059	0.048	0.057
6	4.269	0.678	0.679	0.677	0.644	0.646	0.648	0.648	0.663	0.658	0.065	0.066	0.045
+ 7	4.269	0.681	0.681	0.678	0.648	0.646	0.648	0.652	0.658	0.658	0.052	0.045	0.054
8	4.269	0.682	0.681	0.680	0.638	0.638	0.636	0.638	0.652	0.655	0.057	0.062	0.064
9	4.269	0.678	0.677	0.674	0.642	0.643	0.642	0.641	0.653	0.660	0.038	0.072	0.091
* 10	4.269	0.683	0.682	0.685	0.647	0.644	0.643	0.643	0.661	0.663	---	---	---
11	4.269	0.679	0.679	0.675	0.636	0.637	0.640	0.642	0.656	0.660	0.058	0.069	0.074
12	4.269	0.680	0.679	0.678	0.639	0.639	0.634	0.638	0.652	0.654	0.085	0.054	0.060
13	4.269	0.678	0.676	0.676	0.638	0.640	0.635	0.644	0.657	0.653	0.099	0.032	0.019
14	4.269	0.677	0.675	0.675	0.638	0.637	0.633	0.642	0.656	0.651	0.072	0.052	0.061
15	4.269	0.679	0.677	0.678	0.645	0.646	0.653	0.651	0.660	0.658	0.069	0.049	0.064
16	4.269	0.680	0.679	0.680	0.639	0.638	0.636	0.643	0.659	0.658	0.076	0.049	0.064
17	4.269	0.681	0.677	0.680	0.636	0.635	0.643	0.638	0.659	0.655	0.074	0.055	0.056
18	4.269	0.677	0.674	0.677	0.633	0.632	0.632	0.633	0.653	0.652	0.062	0.083	0.052
19	4.269	0.668	0.668	0.665	0.637	0.637	0.636	0.636	0.647	0.646	0.089	0.061	0.100
* 20	4.269	0.665	0.665	0.668	0.631	0.631	0.631	0.630	0.645	0.634	---	---	---

G11 = 0.118 G12 = 0.102 G3 = 0.662
G21 = 0.183 G22 = 0.175 G4 = 0.110

* Location of logitudinal ribs
+ Location of small longidudinal rib

Table A.6 : Data for Deformation Measurements

Deformation Pattern : C
Surface Type : Mill scale
Bar size : No. 5 (second measurement)

P	A	B	B1	B2	C1	C2	D1	D2	M1	M2	E1	E2	F
* 1	4.100	0.319	0.317	0.315	0.280	0.280	0.280	0.281	0.300	0.298	---	---	---
2	4.100	0.314	0.314	0.313	0.280	0.280	0.280	0.282	0.300	0.296	0.085	0.083	0.036
3	4.100	0.321	0.320	0.320	0.270	0.271	0.276	0.276	0.300	0.296	0.068	0.061	0.059
4	4.100	0.314	0.310	0.310	0.270	0.269	0.268	0.272	0.292	0.294	0.083	0.064	0.051
5	4.100	0.310	0.305	0.306	0.270	0.268	0.274	0.273	0.292	0.285	0.047	0.079	0.040
6	4.100	0.304	0.302	0.300	0.265	0.267	0.271	0.274	0.287	0.282	0.046	0.072	0.046
7	4.100	0.299	0.298	0.294	0.268	0.269	0.266	0.272	0.281	0.285	0.030	0.072	0.046
+ 8	4.100	0.290	0.298	0.288	0.257	0.257	0.254	0.261	0.273	0.272	0.050	0.088	0.048
9	4.100	0.288	0.288	0.286	0.245	0.245	0.241	0.249	0.264	0.258	0.060	0.096	0.054
10	4.100	0.282	0.281	0.275	0.242	0.239	0.244	0.242	0.258	0.261	0.065	0.100	0.050
* 11	4.100	0.290	0.286	0.277	0.241	0.240	0.244	0.241	0.260	0.261	---	---	---
12	4.100	0.292	0.289	0.285	0.249	0.248	0.248	0.250	0.265	0.266	0.055	0.103	0.067
13	4.100	0.295	0.292	0.293	0.256	0.255	0.254	0.259	0.270	0.271	0.052	0.079	0.057
14	4.100	0.296	0.293	0.294	0.257	0.257	0.256	0.260	0.270	0.272	0.049	0.071	0.045
15	4.100	0.302	0.299	0.300	0.264	0.260	0.264	0.266	0.270	0.275	0.043	0.073	0.036
16	4.100	0.308	0.309	0.307	0.273	0.274	0.281	0.281	0.286	0.288	0.033	0.088	0.044
17	4.100	0.316	0.312	0.314	0.274	0.274	0.275	0.277	0.290	0.291	0.054	0.068	0.057
18	4.100	0.323	0.317	0.321	0.276	0.276	0.289	0.280	0.302	0.300	0.066	0.072	0.056
19	4.100	0.320	0.320	0.319	0.278	0.280	0.282	0.280	0.301	0.300	0.091	0.077	0.055
20	4.100	0.319	0.319	0.318	0.279	0.281	0.280	0.280	0.300	0.301	0.076	0.124	0.044

G11 = 0.094 G12 = 0.110 G3 = 0.276
G21 = 0.174 G22 = 0.182 G4 = 0.139

* Location of logitudinal ribs
+ Location of small longidudinal rib

Table A.7 : Data for Deformation Measurements

Deformation Pattern : N
Surface Type : Mill scale
Bar size : No. 5 (first measurement)

P	A	B	B1	B2	C1	C2	D1	D2	M1	M2	E1	E2	F
1	4.269	0.678	0.678	0.670	0.649	0.650	0.650	0.654	0.662	0.664	0.039	0.069	0.043
2	4.269	0.671	0.672	0.664	0.642	0.641	0.641	0.643	0.651	0.654	0.032	0.073	0.044
3	4.269	0.671	0.669	0.668	0.631	0.629	0.630	0.629	0.648	0.657	0.034	0.061	0.039
4	4.269	0.663	0.661	0.660	0.622	0.619	0.621	0.620	0.637	0.636	0.034	0.044	0.057
5	4.269	0.654	0.654	0.651	0.616	0.613	0.615	0.615	0.626	0.624	0.055	0.046	0.047
6	4.269	0.652	0.649	0.651	0.612	0.609	0.611	0.613	0.626	0.627	0.055	0.031	0.032
7	4.269	0.649	0.647	0.649	0.608	0.605	0.612	0.610	0.625	0.628	0.040	0.037	0.051
8	4.269	0.651	0.653	0.651	0.608	0.606	0.608	0.609	0.626	0.626	0.057	0.044	0.050
9	4.269	0.653	0.657	0.649	0.614	0.609	0.614	0.612	0.634	0.625	0.037	0.055	0.063
* 10	4.269	0.622	0.659	0.659	0.606	0.604	0.606	0.607	0.624	0.624	---	---	---
11	4.269	0.667	0.668	0.665	0.633	0.631	0.633	0.632	0.647	0.640	0.073	0.056	0.045
12	4.269	0.674	0.671	0.672	0.633	0.633	0.634	0.633	0.650	0.644	0.076	0.052	0.058
13	4.269	0.687	0.685	0.684	0.641	0.639	0.639	0.639	0.658	0.653	0.055	0.044	0.057
14	4.269	0.698	0.696	0.697	0.645	0.649	0.647	0.651	0.669	0.666	0.060	0.036	0.054
15	4.269	0.694	0.690	0.690	0.652	0.655	0.657	0.654	0.664	0.668	0.050	0.064	0.050
16	4.269	0.697	0.695	0.696	0.656	0.659	0.657	0.657	0.671	0.672	0.036	0.065	0.050
+ 17	4.269	0.707	0.702	0.706	0.657	0.659	0.660	0.661	0.676	0.675	0.044	0.049	0.061
18	4.269	0.703	0.698	0.703	0.658	0.661	0.659	0.663	0.675	0.675	0.047	0.044	0.048
19	4.269	0.695	0.692	0.691	0.658	0.662	0.657	0.662	0.671	0.673	0.044	0.069	0.044
* 20	4.269	1.695	0.696	0.693	0.653	0.660	0.659	0.661	0.673	0.673	---	---	---

G11 = 0.088 G12 = 0.089 G3 = 0.687
G21 = 0.165 G22 = 0.150 G4 = 0.092

* Location of logitudinal ribs
\+ Location of small longidudinal rib

Table A.8 : Data for Deformation Measurements

Deformation Pattern : N

Surface Type : Mill scale

Bar size : No. 5 (second measurement)

P	A	B	B1	B2	C1	C2	D1	D2	M1	M2	E1	E2	F
1	4.100	0.264	0.263	0.262	0.219	0.219	0.220	0.220	0.240	0.236	0.056	0.039	0.066
2	4.100	0.264	0.263	0.262	0.222	0.221	0.222	0.223	0.244	0.240	0.063	0.057	0.055
* 3	4.100	0.278	0.277	0.276	0.230	0.228	0.228	0.227	0.246	0.242	---	---	---
4	4.100	0.295	0.294	0.293	0.255	0.255	0.256	0.256	0.272	0.267	0.058	0.080	0.045
5	4.100	0.311	0.310	0.308	0.280	0.282	0.283	0.284	0.297	0.291	0.055	0.093	0.037
6	4.100	0.326	0.325	0.325	0.287	0.289	0.288	0.289	0.305	0.306	0.059	0.058	0.036
7	4.100	0.332	0.330	0.330	0.290	0.291	0.289	0.290	0.309	0.312	0.055	0.058	0.036
8	4.100	0.337	0.335	0.335	0.289	0.291	0.289	0.290	0.308	0.312	0.041	0.063	0.058
9	4.100	0.333	0.330	0.330	0.286	0.288	0.287	0.285	0.310	0.310	0.041	0.066	0.056
+ 10	4.100	0.331	0.329	0.330	0.282	0.284	0.282	0.283	0.305	0.306	0.036	0.053	0.053
11	4.100	0.318	0.318	0.317	0.278	0.280	0.281	0.281	0.298	0.297	0.049	0.072	0.048
12	4.100	0.310	0.309	0.308	0.274	0.277	0.275	0.278	0.289	0.293	0.036	0.090	0.031
* 13	4.100	0.312	0.310	0.310	0.272	0.278	0.275	0.279	0.290	0.294	---	---	---
14	4.100	0.312	0.310	0.310	0.276	0.279	0.278	0.280	0.294	0.295	0.046	0.092	0.040
15	4.100	0.312	0.311	0.311	0.280	0.279	0.280	0.280	0.297	0.295	0.039	0.077	0.054
16	4.100	0.309	0.307	0.307	0.268	0.266	0.268	0.266	0.281	0.289	0.043	0.054	0.063
17	4.100	0.300	0.299	0.299	0.255	0.253	0.253	0.253	0.275	0.280	0.046	0.058	0.042
18	4.100	0.280	0.279	0.279	0.242	0.241	0.241	0.243	0.260	0.260	0.041	0.057	0.048
19	4.100	0.272	0.271	0.270	0.233	0.231	0.231	0.232	0.253	0.256	0.031	0.069	0.041
20	4.100	0.271	0.271	0.270	0.229	0.227	0.230	0.230	0.256	0.255	0.049	0.045	0.065

G11 = 0.116 G12 = 0.110 G3 = 0.292

G21 = 0.185 G22 = 0.220 G4 = 0.114

* Location of logitudinal ribs

\+ Location of small longidudinal rib

Table A.9 : Data for Deformation Measurements

Deformation Pattern : S
Surface Type : Mill scale
Bar size : No. 6 (first measurement)

P	A	B	B1	B2	C1	C2	D1	D2	M1	M2	E1	E2	F
1	4.269	0.719	0.715	0.716	0.678	0.676	0.677	0.678	0.695	0.695	0.083	0.064	0.042
2	4.269	0.723	0.718	0.720	0.685	0.684	0.682	0.684	0.697	0.701	0.079	0.064	0.046
3	4.269	0.727	0.725	0.725	0.692	0.691	0.696	0.691	0.709	0.706	0.075	0.064	0.051
4	4.269	0.733	0.732	0.731	0.700	0.697	0.699	0.695	0.719	0.716	0.078	0.069	0.026
5	4.269	0.741	0.741	0.738	0.704	0.705	0.711	0.703	0.726	0.719	0.069	0.066	0.038
6	4.269	0.749	0.746	0.746	0.712	0.713	0.713	0.714	0.735	0.737	0.065	0.066	0.049
* 7	4.269	0.759	0.759	0.760	0.718	0.716	0.718	0.724	0.735	0.737	---	---	---
8	4.269	0.746	0.740	0.743	0.712	0.714	0.712	0.713	0.724	0.728	0.077	0.067	0.045
9	4.269	0.745	0.745	0.744	0.712	0.713	0.714	0.714	0.725	0.728	0.053	0.062	0.060
10	4.269	0.749	0.748	0.746	0.711	0.714	0.718	0.718	0.732	0.727	0.078	0.063	0.063
11	4.269	0.751	0.751	0.751	0.713	0.716	0.715	0.715	0.735	0.737	0.079	0.061	0.061
12	4.269	0.752	0.747	0.749	0.713	0.715	0.714	0.716	0.732	0.735	0.086	0.070	0.032
13	4.269	0.749	0.748	0.749	0.708	0.710	0.711	0.711	0.729	0.730	0.076	0.063	0.046
14	4.269	0.749	0.747	0.747	0.707	0.709	0.711	0.707	0.728	0.726	0.070	0.071	0.053
15	4.269	0.739	0.738	0.738	0.701	0.700	0.704	0.701	0.702	0.701	0.078	0.070	0.035
16	4.269	0.733	0.731	0.727	0.696	0.693	0.698	0.695	0.715	0.705	0.072	0.064	0.048
* 17	4.269	0.729	0.726	0.725	0.690	0.690	0.694	0.686	0.611	0.604	---	---	---
18	4.269	0.725	0.711	0.718	0.682	0.680	0.686	0.682	0.696	0.692	0.074	0.072	0.033
19	4.269	0.709	0.709	0.707	0.675	0.673	0.675	0.674	0.667	0.691	0.060	0.080	0.077
20	4.269	0.719	0.715	0.717	0.673	0.672	0.675	0.674	0.697	0.705	0.095	0.071	0.048

G11 = 0.107 G12 = 0.119 G3 = ---
G21 = 0.190 G22 = 0.186 G4 = ---
* Location of logitudinal ribs

Table A.10 : Data for Deformation Measurements

Deformation Pattern : S

Surface Type : Mill scale

Bar size : No. 6 (second measurement)

P	A	B	B1	B2	C1	C2	D1	D2	M1	M2	E1	E2	F
1	3.936	0.215	0.213	0.213	0.181	0.183	0.183	0.183	0.200	0.199	0.057	0.054	0.054
* 2	3.936	0.213	0.211	0.213	0.176	0.177	0.179	0.179	0.196	0.196	---	---	---
3	3.936	0.211	0.208	0.212	0.170	0.170	0.175	0.176	0.191	0.193	0.044	0.104	0.087
4	3.936	0.215	0.211	0.212	0.165	0.166	0.169	0.170	0.191	0.192	0.072	0.038	0.098
5	3.936	0.211	0.207	0.208	0.162	0.161	0.166	0.166	0.188	0.189	0.069	0.063	0.092
6	3.936	0.208	0.204	0.205	0.158	0.157	0.165	0.167	0.186	0.185	0.055	0.073	0.080
7	3.936	0.207	0.202	0.202	0.160	0.158	0.165	0.166	0.185	0.185	0.059	0.058	0.093
8	3.936	0.205	0.200	0.199	0.160	0.159	0.166	0.165	0.186	0.185	0.058	0.058	0.083
9	3.936	0.205	0.201	0.200	0.158	0.158	0.165	0.165	0.185	0.186	0.060	0.061	0.074
10	3.936	0.206	0.202	0.201	0.156	0.157	0.163	0.164	0.185	0.186	0.068	0.063	0.084
11	3.936	0.205	0.202	0.204	0.159	0.159	0.165	0.166	0.183	0.184	0.071	0.067	0.088
* 12	3.936	0.204	0.202	0.203	0.158	0.158	0.162	0.163	0.177	0.177	---	---	---
13	3.936	0.181	0.178	0.179	0.156	0.157	0.158	0.160	0.170	0.170	0.057	0.055	0.067
14	3.936	0.185	0.183	0.182	0.158	0.159	0.161	0.162	0.172	0.172	0.044	0.055	0.056
15	3.936	0.190	0.188	0.188	0.160	0.161	0.163	0.164	0.175	0.174	0.057	0.055	0.056
16	3.936	0.198	0.195	0.196	0.165	0.165	0.167	0.168	0.180	0.181	0.063	0.041	0.090
17	3.936	0.206	0.201	0.202	0.171	0.172	0.173	0.173	0.186	0.188	0.050	0.049	0.065
18	3.936	0.209	0.207	0.206	0.176	0.177	0.178	0.177	0.194	0.193	0.057	0.057	0.051
19	3.936	0.215	0.212	0.211	0.181	0.181	0.182	0.182	0.200	0.201	0.072	0.044	0.068
20	3.936	0.216	0.213	0.212	0.180	0.181	0.182	0.183	0.198	0.199	0.052	0.050	0.062

G11 = 0.105 G12 = 0.110 G3 = ---

G21 = 0.200 G22 = 0.202 G4 = ---

* Location of logitudinal ribs

Table A.11 : Data for Deformation Measurements

Deformation Pattern : C

Surface Type : Mill scale

Bar size : No. 6 (first measurement)

P	A	B	B1	B2	C1	C2	D1	D2	M1	M2	E1	E2	F
1	4.269	0.716	0.712	0.715	0.687	0.686	0.687	0.686	0.693	0.699	0.039	0.055	0.166
2	4.269	0.725	0.726	0.719	0.686	0.684	0.685	0.685	0.695	0.702	0.036	0.058	0.130
3	4.269	0.737	0.735	0.734	0.687	0.685	0.687	0.686	0.706	0.705	0.057	0.064	0.100
4	4.269	0.739	0.734	0.740	0.693	0.692	0.695	0.693	0.712	0.709	0.080	0.059	0.076
5	4.269	0.739	0.737	0.738	0.696	0.695	0.697	0.696	0.715	0.711	0.045	0.046	0.079
6	4.269	0.743	0.735	0.741	0.700	0.700	0.702	0.696	0.717	0.714	0.062	0.023	0.078
7	4.269	0.745	0.738	0.744	0.701	0.701	0.702	0.697	0.719	0.715	0.049	0.035	0.073
8	4.269	0.740	0.734	0.739	0.700	0.701	0.701	0.702	0.715	0.716	0.033	0.042	0.095
* 9	4.269	0.739	0.738	0.742	0.703	0.706	0.708	0.706	0.717	0.715	---	---	---
10	4.269	0.737	0.733	0.739	0.690	0.691	0.691	0.690	0.705	0.714	0.047	0.033	0.086
11	4.269	0.725	0.718	0.726	0.685	0.687	0.690	0.687	0.703	0.700	0.042	0.026	0.117
+ 12	4.269	0.733	0.725	0.736	0.682	0.682	0.683	0.684	0.697	0.701	0.050	0.052	0.102
13	4.269	0.734	0.731	0.734	0.676	0.678	0.679	0.675	0.692	0.700	0.052	0.056	0.069
14	4.269	0.733	0.730	0.731	0.678	0.676	0.678	0.676	0.698	0.696	0.027	0.046	0.075
15	4.269	0.732	0.730	0.731	0.677	0.680	0.681	0.679	0.700	0.698	0.026	0.038	0.083
16	4.269	0.736	0.733	0.735	0.684	0.681	0.684	0.680	0.705	0.708	0.034	0.043	0.072
17	4.269	0.737	0.737	0.734	0.684	0.684	0.681	0.683	0.711	0.711	0.039	0.084	0.052
18	4.269	0.744	0.741	0.739	0.686	0.685	0.685	0.687	0.708	0.711	0.040	0.074	0.071
* 19	4.269	0.736	0.736	0.733	0.690	0.686	0.688	0.690	0.710	0.709	---	---	---
20	4.269	0.723	0.723	0.724	0.692	0.693	0.695	0.694	0.710	0.711	0.031	0.065	0.122

G11 = 0.140 G12 = 0.123 G3 = 0.732

G21 = 0.192 G22 = 0.188 G4 = 0.114

* Location of logitudinal ribs

\+ Location of small longidudinal rib

Table A.12 : Data for Deformation Measurements

Deformation Pattern : C
Surface Type : Mill scale
Bar size : No. 6 (second measurement)

P	A	B	B1	B2	C1	C2	D1	D2	M1	M2	E1	E2	F
1	3.936	0.205	0.205	0.200	0.160	0.162	0.165	0.162	0.180	0.177	0.066	0.073	0.078
2	3.936	0.208	0.208	0.205	0.165	0.163	0.166	0.165	0.183	0.182	0.057	0.084	0.078
3	3.936	0.209	0.207	0.208	0.169	0.172	0.171	0.173	0.186	0.188	0.049	0.083	0.074
4	3.936	0.214	0.213	0.213	0.175	0.177	0.180	0.181	0.190	0.192	0.066	0.088	0.086
5	3.936	0.218	0.216	0.217	0.177	0.179	0.178	0.180	0.195	0.194	0.065	0.094	0.081
6	3.936	0.220	0.219	0.218	0.180	0.182	0.181	0.184	0.198	0.199	0.118	0.084	0.083
7	3.936	0.220	0.219	0.218	0.175	0.177	0.176	0.178	0.195	0.194	0.062	0.092	0.079
8	3.936	0.212	0.212	0.212	0.170	0.169	0.172	0.170	0.191	0.189	0.034	0.104	0.081
* 9	3.936	0.210	0.209	0.209	0.160	0.159	0.162	0.160	0.185	0.182	---	---	---
10	3.936	0.207	0.205	0.205	0.150	0.149	0.153	0.150	0.179	0.174	0.058	0.085	0.058
11	3.936	0.200	0.200	0.198	0.145	0.146	0.146	0.147	0.175	0.171	0.043	0.089	0.071
12	3.936	0.193	0.191	0.194	0.141	0.140	0.142	0.140	0.170	0.168	0.049	0.089	0.059
13	3.936	0.186	0.185	0.184	0.137	0.136	0.138	0.138	0.160	0.161	0.067	0.093	0.062
14	3.936	0.182	0.179	0.181	0.135	0.138	0.134	0.136	0.154	0.151	0.064	0.083	0.084
15	3.936	0.184	0.184	0.181	0.138	0.140	0.131	0.138	0.158	0.156	0.075	0.070	0.127
+ 16	3.936	0.193	0.193	0.192	0.141	0.142	0.138	0.141	0.164	0.162	0.065	0.088	0.135
17	3.936	0.200	0.200	0.198	0.144	0.144	0.144	0.193	0.170	0.168	0.048	0.079	0.126
18	3.936	0.196	0.198	0.189	0.155	0.155	0.155	0.158	0.172	0.171	0.042	0.073	0.134
* 19	3.936	0.206	0.207	0.200	0.160	0.160	0.161	0.162	0.180	0.179	---	---	---
20	3.936	0.215	0.215	0.211	0.165	0.165	0.166	0.166	0.188	0.186	0.030	0.082	0.103

G11 = 0.062 G12 = 0.072 G3 = 0.186
G21 = 0.175 G22 = 0.177 G4 = 0.128

* Location of logitudinal ribs
+ Location of small longidudinal rib

Table A.13 : Data for Deformation Measurements

Deformation Pattern : N
Surface Type : Mill scale
Bar size : No. 6 (first measurement)

P	A	B	B1	B2	C1	C2	D1	D2	M1	M2	E1	E2	F
1	4.269	0.759	0.759	0.757	0.722	0.722	0.722	0.721	0.739	0.739	0.042	0.040	0.112
2	4.269	0.754	0.752	0.753	0.726	0.727	0.725	0.730	0.739	0.740	0.060	0.104	0.054
* 3	4.269	0.761	0.759	0.760	0.726	0.720	0.733	0.730	0.736	0.742	---	---	---
4	4.269	0.763	0.762	0.763	0.729	0.731	0.728	0.730	0.739	0.740	0.055	0.065	0.121
5	4.269	0.765	0.763	0.759	0.724	0.725	0.724	0.724	0.737	0.739	0.070	0.072	0.084
6	4.269	0.772	0.771	0.771	0.718	0.718	0.718	0.718	0.737	0.743	0.085	0.049	0.069
7	4.269	0.771	0.771	0.771	0.712	0.712	0.713	0.715	0.741	0.732	0.075	0.061	0.055
8	4.269	0.762	0.756	0.760	0.702	0.704	0.708	0.702	0.727	0.730	0.072	0.047	0.065
9	4.269	0.750	0.747	0.750	0.694	0.698	0.694	0.694	0.720	0.723	0.080	0.049	0.071
10	4.269	0.735	0.731	0.733	0.685	0.686	0.684	0.684	0.705	0.712	0.050	0.052	0.094
11	4.269	0.717	0.714	0.715	0.679	0.678	0.678	0.678	0.695	0.685	0.071	0.037	0.110
12	4.269	0.702	0.699	0.701	0.674	0.672	0.674	0.671	0.685	0.679	0.061	0.043	0.135
* 13	4.269	0.696	0.697	0.698	0.668	0.670	0.671	0.670	0.686	0.681	---	---	---
14	4.269	0.701	0.700	0.702	0.674	0.674	0.674	0.670	0.679	0.678	0.071	0.040	0.131
15	4.269	0.724	0.722	0.720	0.677	0.676	0.680	0.672	0.699	0.695	0.069	0.058	0.093
+ 16	4.269	0.743	0.741	0.738	0.685	0.685	0.690	0.680	0.715	0.708	0.057	0.054	0.074
17	4.269	0.752	0.748	0.751	0.694	0.694	0.697	0.694	0.724	0.728	0.049	0.054	0.072
18	4.269	0.757	0.754	0.755	0.701	0.701	0.707	0.710	0.725	0.724	0.059	0.052	0.062
19	4.269	0.760	0.760	0.758	0.709	0.709	0.712	0.708	0.730	0.725	0.044	0.040	0.088
20	4.269	0.763	0.763	0.760	0.716	0.717	0.717	0.717	0.734	0.737	0.038	0.044	0.100

G11 = 0.116 G12 = 0.144 G3 = 0.736
G21 = 0.208 G22 = 0.205 G4 = 0.121

* Location of logitudinal ribs
+ Location of small longidudinal rib

Table A.14 : Data for Deformation Measurements

Deformation Pattern : N

Surface Type : Mill scale

Bar size : No. 6 (second measurement)

P	A	B	B1	B2	C1	C2	D1	D2	M1	M2	E1	E2	F
1	3.936	0.211	0.208	0.207	0.169	0.168	0.171	0.167	0.186	0.186	0.056	0.118	0.057
2	3.936	0.225	0.223	0.224	0.168	0.168	0.170	0.170	0.188	0.189	0.049	0.099	0.063
3	3.936	0.224	0.222	0.223	0.166	0.166	0.168	0.167	0.190	0.192	0.042	0.077	0.074
4	3.936	0.224	0.221	0.222	0.165	0.164	0.170	0.171	0.194	0.195	0.048	0.085	0.066
5	3.936	0.220	0.219	0.218	0.163	0.164	0.164	0.165	0.193	0.194	0.056	0.086	0.066
6	3.936	0.215	0.215	0.211	0.161	0.161	0.164	0.165	0.194	0.193	0.062	0.088	0.070
7	3.936	0.198	0.197	0.196	0.161	0.162	0.162	0.164	0.185	0.182	0.057	0.098	0.058
8	3.936	0.197	0.194	0.192	0.162	0.162	0.163	0.164	0.181	0.181	0.040	0.115	0.057
9	3.936	0.197	0.195	0.194	0.163	0.164	0.165	0.167	0.181	0.182	0.060	0.110	0.050
* 10	3.936	0.206	0.204	0.204	0.164	0.165	0.166	0.169	0.181	0.181	---	---	---
11	3.936	0.210	0.208	0.209	0.165	0.166	0.167	0.168	0.181	0.182	0.062	0.090	0.075
12	3.936	0.216	0.214	0.213	0.166	0.168	0.168	0.169	0.182	0.183	0.063	0.078	0.069
+ 13	3.936	0.231	0.229	0.231	0.168	0.170	0.171	0.173	0.189	0.189	0.059	0.075	0.070
14	3.936	0.229	0.225	0.229	0.170	0.171	0.174	0.177	0.195	0.194	0.055	0.071	0.072
15	3.936	0.230	0.227	0.226	0.169	0.170	0.172	0.173	0.194	0.196	0.049	0.081	0.059
16	3.936	0.225	0.223	0.222	0.170	0.171	0.172	0.173	0.188	0.189	0.055	0.071	0.067
17	3.936	0.220	0.219	0.219	0.174	0.174	0.177	0.177	0.184	0.185	0.061	0.092	0.064
18	3.936	0.213	0.211	0.210	0.175	0.176	0.176	0.178	0.186	0.187	0.063	0.126	0.046
19	3.936	0.209	0.206	0.207	0.171	0.172	0.173	0.172	0.186	0.187	0.066	0.130	0.064
* 20	3.936	0.204	0.201	0.201	0.165	0.167	0.170	0.169	0.186	0.187	---	---	---

G11 = 0.100 G12 = 0.100 G3 = 0.216

G21 = 0.210 G22 = 0.195 G4 = 0.125

* Location of logitudinal ribs

\+ Location of small longidudinal rib

Table A.15 : Data for Deformation Measurements

Deformation Pattern : S
Surface Type : Mill scale
Bar size : No. 8 (first measurement)

P	A	B	B1	B2	C1	C2	D1	D2	M1	M2	E1	E2	F
1	5.344	1.751	1.748	1.752	1.711	1.712	1.712	1.715	1.727	1.726	0.053	0.120	0.065
* 2	5.344	1.754	1.750	1.756	1.710	1.711	1.712	1.713	1.728	1.728	---	---	---
3	5.344	1.749	1.745	1.750	1.708	1.709	1.711	1.710	1.728	1.729	0.060	0.120	0.070
4	5.344	1.757	1.757	1.754	1.701	1.702	1.704	1.701	1.725	1.731	0.069	0.120	0.080
5	5.344	1.750	1.754	1.748	1.694	1.694	1.696	1.696	1.717	1.720	0.067	0.110	0.080
6	5.344	1.743	1.742	1.741	1.690	1.689	1.690	1.690	1.716	1.715	0.095	0.075	0.079
7	5.344	1.743	1.743	1.743	1.685	1.685	1.690	1.687	1.721	1.715	0.095	0.069	0.088
8	5.344	1.732	1.730	1.730	1.676	1.676	1.679	1.675	1.708	1.711	0.089	0.066	0.099
9	5.344	1.730	1.729	1.727	1.673	1.674	1.677	1.673	1.705	1.699	0.080	0.066	0.105
10	5.344	1.727	1.724	1.725	1.673	1.672	1.677	1.675	1.702	1.697	0.083	0.106	0.070
11	5.344	1.723	1.720	1.723	1.677	1.677	1.680	1.680	1.696	1.703	0.085	0.120	0.074
* 12	5.344	1.731	1.730	1.731	1.692	1.693	1.691	1.690	1.711	1.712	---	---	---
13	5.344	1.732	1.730	1.732	1.693	1.693	1.693	1.693	1.711	1.713	0.066	0.110	0.080
14	5.344	1.745	1.743	1.743	0.696	1.695	1.697	1.697	1.723	1.722	0.067	0.096	0.099
15	5.344	1.758	1.757	1.758	1.703	1.703	1.704	1.702	1.732	1.732	0.077	0.078	0.100
16	5.344	1.762	1.756	1.758	1.709	1.708	1.709	1.709	1.740	1.733	0.090	0.050	0.102
17	5.344	1.763	1.761	1.761	1.710	1.711	1.713	1.709	1.734	1.732	0.089	0.050	0.095
18	5.344	1.768	1.766	1.767	1.714	1.714	1.714	1.715	1.739	1.743	0.076	0.060	0.110
19	5.344	1.763	1.763	1.762	1.713	1.714	1.714	1.710	1.740	1.742	0.095	0.080	0.098
20	5.344	1.763	1.763	1.761	1.714	1.714	1.714	1.713	1.737	1.737	0.072	0.102	0.051

G11 = 0.141 G12 = 0.135 G3 = ---
G21 = 0.221 G22 = 0.224 G4 = ---
* Location of logitudinal ribs

Table A.16 : Data for Deformation Measurements

Deformation Pattern : S
Surface Type : Mill scale
Bar size : No. 8 (second measurement)

P	A	B	B1	B2	C1	C2	D1	D2	M1	M2	E1	E2	F
1	3.812	0.228	0.224	0.225	0.174	0.174	0.174	0.174	0.194	0.195	0.076	0.056	0.105
2	3.812	0.224	0.222	0.221	0.171	0.172	0.171	0.172	0.193	0.192	0.088	0.071	0.096
3	3.812	0.223	0.222	0.221	0.171	0.173	0.171	0.174	0.193	0.194	0.075	0.107	0.056
4	3.812	0.220	0.218	0.218	0.173	0.174	0.170	0.174	0.194	0.194	0.054	0.126	0.057
* 5	3.812	0.219	0.218	0.217	0.169	0.170	0.168	0.172	0.190	0.188	---	---	---
6	3.812	0.206	0.206	0.201	0.150	0.150	0.152	0.151	0.184	0.180	0.050	0.155	0.062
7	3.812	0.215	0.208	0.213	0.158	0.156	0.160	0.160	0.191	0.188	0.065	0.119	0.077
8	3.812	0.211	0.209	0.209	0.155	0.156	0.155	0.158	0.188	0.185	0.070	0.110	0.082
9	3.812	0.209	0.207	0.208	0.155	0.155	0.153	0.157	0.186	0.187	0.089	0.077	0.077
10	3.812	0.207	0.205	0.205	0.154	0.154	0.150	0.156	0.185	0.184	0.101	0.065	0.091
11	3.812	0.208	0.205	0.206	0.155	0.154	0.155	0.155	0.180	0.181	0.089	0.061	0.094
12	3.812	0.201	0.200	0.207	0.156	0.156	0.157	0.158	0.178	0.179	0.080	0.062	0.111
13	3.812	0.205	0.202	0.203	0.157	0.158	0.159	0.160	0.180	0.181	0.089	0.100	0.077
14	3.812	0.202	0.201	0.202	0.160	0.160	0.161	0.162	0.182	0.180	0.080	0.115	0.075
* 15	3.812	0.200	0.202	0.201	0.158	0.160	0.159	0.160	0.182	0.179	---	---	---
16	3.812	0.194	0.192	0.189	0.150	0.151	0.152	0.152	0.175	0.170	0.066	0.119	0.081
17	3.812	0.203	0.202	0.203	0.156	0.156	0.158	0.161	0.180	0.179	0.070	0.093	0.097
18	3.812	0.210	0.207	0.208	0.159	0.158	0.160	0.161	0.182	0.181	0.070	0.075	0.092
19	3.812	0.218	0.216	0.216	0.163	0.162	0.165	0.163	0.184	0.183	0.083	0.050	0.106
20	3.812	0.220	0.218	0.219	0.166	0.166	0.169	0.170	0.185	0.186	0.084	0.057	0.101

G11 = 0.136 G12 = 0.139 G3 = ---
G21 = 0.218 G22 = 0.212 G4 = ---
* Location of logitudinal ribs

Table A.17 : Data for Deformation Measurements

Deformation Pattern : C

Surface Type : Mill scale

Bar size : No. 8 (first measurement)

P	A	B	B1	B2	C1	C2	D1	D2	M1	M2	E1	E2	F
1	5.344	1.785	1.780	1.786	1.724	1.726	1.729	1.722	1.755	1.748	0.065	0.104	0.070
* 2	5.344	1.786	1.780	1.789	1.722	1.725	1.726	1.724	1.754	1.754	---	---	---
3	5.344	1.773	1.764	1.772	1.702	1.703	1.706	1.703	1.727	1.729	0.090	0.130	0.090
4	5.344	1.759	1.751	1.752	1.699	1.699	1.700	1.698	1.721	1.720	0.080	0.150	0.060
+ 5	5.344	1.752	1.753	1.751	1.690	1.692	1.695	1.687	1.720	1.727	0.070	0.137	0.080
6	5.344	1.738	1.738	1.736	1.682	1.679	1.680	1.675	1.708	1.700	0.100	0.140	0.060
7	5.344	1.737	1.737	1.736	1.680	1.679	1.686	1.682	1.714	1.705	0.090	0.120	0.059
8	5.344	1.728	1.730	1.729	1.669	1.666	1.671	1.671	1.701	1.701	0.095	0.125	0.070
9	5.344	1.724	1.725	1.716	1.664	1.663	1.667	1.666	1.694	1.691	0.105	0.129	0.085
10	5.344	1.723	1.725	1.725	1.663	1.662	1.662	1.662	1.698	1.691	0.115	0.120	0.079
11	5.344	1.715	1.716	1.714	1.669	1.665	1.667	1.669	1.667	1.694	0.105	0.140	0.075
* 12	5.344	1.713	1.711	1.713	1.673	1.674	1.680	1.674	1.689	1.693	---	---	---
13	5.344	1.712	1.714	1.715	1.667	1.667	1.670	1.666	1.686	1.690	0.099	0.175	0.065
14	5.344	1.716	1.716	1.712	1.660	1.659	1.659	1.657	1.683	1.686	0.120	0.130	0.095
15	5.344	1.738	1.737	1.730	1.670	1.668	1.669	1.667	1.701	1.695	0.115	0.121	0.096
16	5.344	1.745	1.742	1.742	1.681	1.679	1.683	1.673	1.715	1.708	0.085	0.145	0.085
17	5.344	1.758	1.754	1.759	1.694	1.696	1.700	1.691	1.730	1.723	0.080	0.140	0.060
18	5.344	1.722	1.768	1.772	1.708	1.709	1.709	1.698	1.742	1.738	0.075	0.130	0.069
19	5.344	1.779	1.775	1.779	1.714	1.716	1.715	1.711	1.748	1.746	0.077	0.135	0.071
20	5.344	1.787	1.783	1.785	1.722	1.724	1.724	1.721	1.745	1.752	0.060	0.138	0.068

G11 = 0.145 G12 = 0.161 G3 = 1.735

G21 = 0.254 G22 = 0.248 G4 = 0.118

* Location of logitudinal ribs

+ Location of small longidudinal rib

Table A.18 : Data for Deformation Measurements

Deformation Pattern : C
Surface Type : Mill scale
Bar size : No. 8 (second measurement)

P	A	B	B1	B2	C1	C2	D1	D2	M1	M2	E1	E2	F
1	3.812	0.215	0.210	0.214	0.153	0.152	0.160	0.145	0.170	0.167	0.071	0.133	0.058
2	3.812	0.216	0.210	0.214	0.150	0.151	0.154	0.150	0.174	0.170	0.071	0.138	0.079
3	3.812	0.217	0.212	0.215	0.152	0.152	0.155	0.149	0.175	0.172	0.080	0.130	0.076
4	3.812	0.216	0.210	0.216	0.160	0.160	0.162	0.160	0.180	0.181	0.063	0.140	0.066
5	3.812	0.213	0.208	0.214	0.159	0.158	0.156	0.155	0.176	0.177	0.070	0.135	0.070
* 6	3.812	0.210	0.202	0.208	0.150	0.148	0.150	0.149	0.171	0.173	---	---	---
7	3.812	0.209	0.203	0.208	0.149	0.148	0.151	0.150	0.172	0.173	0.083	0.143	0.088
8	3.812	0.208	0.204	0.206	0.147	0.148	0.152	0.148	0.174	0.172	0.071	0.152	0.070
+ 9	3.812	0.204	0.205	0.201	0.149	0.149	0.155	0.152	0.176	0.176	0.071	0.151	0.069
10	3.812	0.210	0.208	0.207	0.150	0.149	0.057	0.155	0.177	0.179	0.088	0.156	0.050
11	3.812	0.124	0.213	0.211	0.151	0.152	0.160	0.161	0.184	0.184	0.096	0.115	0.066
12	3.812	0.220	0.217	0.215	0.153	0.154	0.160	0.161	0.186	0.186	0.101	0.133	0.075
13	3.812	0.222	0.223	0.218	0.158	0.158	0.158	0.159	0.188	0.186	0.120	0.135	0.081
14	3.812	0.215	0.214	0.214	0.162	0.161	0.163	0.164	0.188	0.186	0.177	0.123	0.077
15	3.812	0.207	0.205	0.209	0.154	0.148	0.147	0.147	0.175	0.178	0.114	0.160	0.073
* 16	3.812	0.204	0.201	0.203	0.138	0.135	0.136	0.135	0.167	0.170	---	---	---
17	3.812	0.209	0.207	0.204	0.140	0.139	0.140	0.139	0.172	0.172	0.090	0.182	0.063
18	3.812	0.209	0.208	0.208	0.140	0.140	0.141	0.142	0.176	0.173	0.112	0.127	0.089
19	3.812	0.210	0.209	0.208	0.144	0.144	0.145	0.146	0.173	0.169	0.113	0.110	0.094
20	3.812	0.211	0.208	0.210	0.148	0.148	0.153	0.147	0.172	0.167	0.087	0.143	0.080

G11 = 0.135 G12 = 0.145 G3 = 0.177
G21 = 0.250 G22 = 0.249 G4 = 0.140

* Location of logitudinal ribs
+ Location of small longidudinal rib

Table A.19 : Data for Deformation Measurements

Deformation Pattern : N
Surface Type : Mill scale
Bar size : No. 8 (first measurement)

P	A	B	B1	B2	C1	C2	D1	D2	M1	M2	E1	E2	F
+ 1	5.344	1.756	1.757	1.752	1.708	1.705	1.705	1.703	1.723	1.719	0.065	0.070	0.080
2	5.344	1.756	1.754	1.754	1.691	1.691	1.701	1.700	1.723	1.720	0.050	0.077	0.095
3	5.344	1.761	1.757	1.756	1.690	1.693	1.698	1.697	1.730	1.725	0.048	0.088	0.080
4	5.344	1.760	1.760	1.758	1.693	1.694	1.699	1.694	1.733	1.721	0.075	0.089	0.060
5	5.344	1.760	1.756	1.758	1.694	1.696	1.699	1.697	1.625	1.625	0.058	0.110	0.040
6	5.344	1.747	1.744	1.747	1.696	1.695	1.698	1.694	1.719	1.718	0.044	0.138	0.069
7	5.344	1.750	1.745	1.750	1.700	1.703	1.702	1.704	1.719	1.717	0.080	0.120	0.070
* 8	5.344	1.756	1.753	1.756	1.702	1.704	1.706	1.708	1.726	1.724	---	---	---
9	5.344	1.752	1.750	1.749	1.702	1.701	1.704	1.702	1.726	1.716	0.075	0.113	0.063
10	5.344	1.754	1.752	1.751	1.693	1.694	1.695	1.696	1.721	1.722	0.099	0.082	0.060
11	5.344	1.750	1.746	1.748	1.687	1.687	1.690	1.687	1.720	1.719	0.040	0.105	0.045
12	5.344	1.746	1.742	1.744	1.688	1.687	1.692	1.696	1.722	1.719	0.090	0.085	0.067
13	5.344	1.742	1.741	1.738	1.682	1.683	1.691	1.691	1.722	1.718	0.050	0.099	0.080
14	5.344	1.741	1.742	1.740	1.682	1.681	1.686	1.680	1.714	1.716	0.062	0.079	0.080
15	5.344	1.741	1.741	1.742	1.686	1.685	1.693	1.687	1.712	1.715	0.070	0.080	0.077
16	5.344	1.736	1.736	1.735	1.684	1.683	1.686	1.689	1.720	1.716	0.052	0.089	0.095
17	5.344	1.733	1.731	1.733	1.689	1.689	1.692	1.693	1.711	1.715	0.060	0.100	0.111
* 18	5.344	1.742	1.742	1.744	1.697	1.694	1.698	1.698	1.725	1.722	---	---	---
19	5.344	1.744	1.745	1.743	1.696	1.695	1.699	1.698	1.726	1.726	0.067	0.130	0.080
20	5.344	1.754	1.755	1.755	1.694	1.694	1.700	1.695	1.727	1.724	0.064	0.080	0.105

G11 = 0.115 G12 = 0.095 G3 = 1.737
G21 = 0.243 G22 = 0.209 G4 = 0.146

* Location of logitudinal ribs
+ Location of small longidudinal rib

Table A.20 : Data for Deformation Measurements

Deformation Pattern : N

Surface Type : Mill scale

Bar size : No. 8 (second measurement)

	P	A	B	B1	B2	C1	C2	D1	D2	M1	M2	E1	E2	F
	1	3.812	0.224	0.221	0.218	0.165	0.165	0.172	0.172	0.198	0.199	0.051	0.091	0.084
	2	3.812	0.225	0.224	0.223	0.167	0.168	0.170	0.170	0.202	0.200	0.071	0.085	0.054
	3	3.812	0.228	0.226	0.224	0.170	0.170	0.174	0.172	0.204	0.198	0.058	0.116	0.046
	4	3.812	0.229	0.226	0.227	0.172	0.172	0.175	0.174	0.205	0.204	0.044	0.136	0.067
	5	3.812	0.221	0.220	0.220	0.170	0.169	0.170	0.169	0.201	0.202	0.072	0.121	0.071
*	6	3.812	0.219	0.218	0.218	0.165	0.164	0.165	0.165	0.191	0.194	---	---	---
	7	3.812	0.213	0.211	0.210	0.160	0.162	0.161	0.163	0.180	0.185	0.075	0.113	0.063
	8	3.812	0.219	0.219	0.219	0.158	0.156	0.161	0.158	0.188	0.190	0.096	0.078	0.056
+	9	3.812	0.217	0.217	0.216	0.151	0.150	0.152	0.150	0.181	0.181	0.042	0.103	0.051
	10	3.812	0.210	0.208	0.207	0.143	0.144	0.148	0.146	0.174	0.172	0.084	0.091	0.062
	11	3.812	0.209	0.207	0.207	0.142	0.142	0.149	0.150	0.174	0.173	0.044	0.091	0.085
	12	3.812	0.210	0.208	0.209	0.145	0.144	0.148	0.149	0.176	0.177	0.059	0.082	0.074
	13	3.812	0.210	0.209	0.210	0.144	0.145	0.150	0.150	0.177	0.176	0.066	0.088	0.078
	14	3.812	0.207	0.206	0.207	0.148	0.147	0.151	0.150	0.178	0.177	0.048	0.091	0.095
	15	3.812	0.204	0.200	0.201	0.150	0.150	0.153	0.149	0.177	0.179	0.055	0.104	0.112
*	16	3.812	0.210	0.204	0.207	0.153	0.154	0.156	0.155	0.176	0.179	---	---	---
	17	3.812	0.211	0.203	0.206	0.160	0.162	0.162	0.164	0.174	0.178	0.067	0.130	0.082
	18	3.812	0.220	0.215	0.216	0.160	0.161	0.160	0.162	0.179	0.180	0.064	0.087	0.109
	19	3.812	0.224	0.218	0.219	0.158	0.160	0.160	0.161	0.188	0.190	0.066	0.082	0.088
	20	3.812	0.222	0.219	0.221	0.163	0.164	0.170	0.174	0.194	0.197	0.047	0.077	0.090

G11 = 0.100 G12 = 0.092 G3 = 0.193

G21 = 0.210 G22 = 0.236 G4 = 0.146

* Location of logitudinal ribs

\+ Location of small longidudinal rib

Table A.21 : Data for Deformation Measurements

Deformation Pattern : S
Surface Type : Mill scale
Bar size : No. 11 (first measurement)

P	A	B	B1	B2	C1	C2	D1	D2	M1	M2	E1	E2	F
1	4.269	1.066	1.061	1.067	0.990	0.988	0.984	0.989	1.029	1.031	0.131	0.066	0.138
2	4.269	1.051	1.050	1.054	0.984	0.980	0.977	0.983	1.020	1.020	0.153	0.061	0.113
3	4.269	1.043	1.041	1.042	0.979	0.975	0.976	0.978	1.013	0.105	0.113	0.081	0.119
4	4.269	1.044	1.042	1.044	0.978	0.975	0.973	0.977	1.013	1.008	0.122	0.085	0.112
5	4.269	1.055	1.053	1.050	0.982	0.978	0.972	0.980	1.026	1.013	0.121	0.057	0.110
6	4.269	1.064	1.055	1.059	0.983	0.982	0.981	0.984	1.028	1.020	0.108	0.087	0.103
7	4.269	1.063	1.063	1.056	0.993	0.990	0.992	0.993	1.039	1.020	0.104	0.100	0.099
* 8	4.269	1.076	1.076	1.077	0.990	0.988	0.993	0.997	1.042	1.036	---	---	---
9	4.269	1.101	1.103	1.101	1.032	1.034	1.035	1.035	1.070	1.058	0.116	0.132	0.112
10	4.269	1.125	1.125	1.125	1.044	1.042	1.047	1.045	1.086	1.077	0.115	0.101	0.140
11	4.269	1.143	1.132	1.143	1.060	1.059	1.065	1.062	1.100	1.092	0.103	0.101	0.141
12	4.269	1.143	1.141	1.142	1.069	1.070	1.071	1.069	1.106	1.104	0.098	0.118	0.131
13	4.269	1.143	1.138	1.144	1.072	1.073	1.070	1.075	1.100	1.105	0.072	0.119	0.113
14	4.269	1.141	1.138	1.138	1.066	1.070	1.063	1.072	1.112	1.104	0.103	0.074	0.134
15	4.269	1.133	1.129	1.132	1.056	1.058	1.057	1.057	1.105	1.093	0.127	0.072	0.110
16	4.269	1.121	1.116	1.120	1.042	1.041	1.044	1.043	1.090	1.080	0.135	0.077	0.115
17	4.269	1.096	1.095	1.094	1.020	1.023	1.027	1.026	1.072	1.060	0.115	0.087	0.113
* 18	4.269	1.104	1.107	1.107	1.012	1.012	1.018	1.015	1.061	1.050	---	---	---
19	4.269	1.083	1.082	1.084	1.004	1.001	1.009	1.004	1.050	1.039	0.134	0.074	0.127
20	4.269	1.075	1.074	1.077	0.995	0.993	0.994	0.994	1.040	1.034	0.117	0.065	0.111

G11 = 0.158 G12 = 0.155 G3 = ---
G21 = 0.270 G22 = 0.266 G4 = ---

* Location of logitudinal ribs

Table A.22 : Data for Deformation Measurements

Deformation Pattern : S
Surface Type : Mill scale
Bar size : No. 11 (second measurement)

P	A	B	B1	B2	C1	C2	D1	D2	M1	M2	E1	E2	F
1	3.930	0.558	0.557	0.556	0.485	0.487	0.490	0.484	0.522	0.520	0.119	0.066	0.148
2	3.930	0.565	0.564	0.563	0.485	0.488	0.489	0.484	0.529	0.525	0.114	0.084	0.149
3	3.930	0.570	0.568	0.568	0.485	0.489	0.483	0.483	0.533	0.530	0.119	0.070	0.167
4	3.930	0.565	0.565	0.564	0.480	0.482	0.482	0.482	0.528	0.527	0.139	0.055	0.163
5	3.930	0.560	0.558	0.559	0.476	0.478	0.482	0.481	0.522	0.524	0.122	0.076	0.169
6	3.930	0.573	0.549	0.550	0.473	0.474	0.478	0.478	0.517	0.519	0.128	0.090	0.157
* 7	3.930	0.543	0.539	0.540	0.470	0.470	0.474	0.474	0.512	0.513	---	---	---
8	3.930	0.550	0.547	0.546	0.475	0.476	0.477	0.478	0.517	0.517	0.130	0.086	0.150
9	3.930	0.555	0.550	0.548	0.480	0.479	0.487	0.477	0.517	0.520	0.116	0.078	0.140
10	3.930	0.554	0.552	0.553	0.483	0.482	0.485	0.484	0.516	0.519	0.119	0.085	0.137
11	3.930	0.552	0.553	0.548	0.486	0.489	0.487	0.486	0.520	0.518	0.124	0.084	0.124
12	3.930	0.558	0.555	0.556	0.487	0.487	0.489	0.487	0.524	0.523	0.116	0.104	0.116
13	3.930	0.565	0.564	0.560	0.488	0.485	0.489	0.486	0.528	0.525	0.099	0.091	0.089
14	3.930	0.561	0.560	0.558	0.486	0.488	0.488	0.489	0.524	0.522	0.129	0.110	0.109
15	3.930	0.560	0.555	0.558	0.485	0.484	0.490	0.486	0.520	0.521	0.139	0.093	0.129
16	3.930	0.565	0.549	0.550	0.478	0.479	0.484	0.481	0.518	0.519	0.111	0.114	0.133
* 17	3.930	0.544	0.543	0.542	0.471	0.474	0.477	0.475	0.515	0.516	---	---	---
18	3.930	0.550	0.548	0.549	0.475	0.478	0.477	0.479	0.517	0.516	0.124	0.088	0.149
19	3.930	0.562	0.558	0.559	0.421	0.482	0.484	0.481	0.520	0.518	0.119	0.080	0.148
20	3.930	0.560	0.558	0.560	0.483	0.482	0.484	0.485	0.520	0.518	0.115	0.075	0.143

G11 = 0.150 G12 = 0.160 G3 = ---
G21 = 0.277 G22 = 0.280 G4 = ---

* Location of logitudinal ribs

Table A.23 : Data for Deformation Measurements

Deformation Pattern : C
Surface Type : Mill scale
Bar size : No. 11 (first measurement)

P	A	B	B1	B2	C1	C2	D1	D2	M1	M2	E1	E2	F
1	4.269	1.082	1.067	1.081	1.004	1.000	1.003	1.005	1.031	1.042	0.217	0.156	0.069
2	4.269	1.020	1.020	1.012	0.967	0.962	0.967	0.964	0.993	0.993	0.164	0.224	0.047
3	4.269	0.970	0.974	0.970	0.939	0.390	0.936	0.934	0.955	0.947	0.136	0.268	0.030
4	4.269	0.954	0.957	0.953	0.921	0.912	0.920	0.915	0.936	0.929	0.070	0.194	0.016
* 5	4.269	0.935	0.932	0.931	0.903	0.893	0.903	0.896	0.917	0.910	---	---	---
6	4.269	0.941	0.941	0.941	0.895	0.888	0.895	0.889	0.917	0.910	0.089	0.163	0.034
7	4.269	0.954	0.953	0.952	0.896	0.887	0.894	0.890	0.915	0.918	0.111	0.131	0.042
8	4.269	0.962	0.964	0.966	0.907	0.900	0.905	0.905	0.930	0.935	0.084	0.162	0.040
9	4.269	1.001	1.003	1.000	0.930	0.925	0.931	0.927	0.962	0.964	0.079	0.137	0.072
10	4.269	1.041	1.043	1.038	0.958	0.956	0.959	0.962	0.996	0.990	0.100	0.110	0.091
11	4.269	1.077	1.077	1.072	0.997	0.997	1.003	1.001	1.035	1.020	0.090	0.113	0.066
+ 12	4.269	1.103	1.102	1.096	0.009	1.012	1.020	1.015	1.046	1.045	0.060	0.109	0.081
13	4.269	1.134	1.128	1.133	1.068	1.074	1.065	1.071	1.093	1.099	0.075	0.117	0.127
14	4.269	1.161	1.166	1.168	1.098	1.105	1.098	1.103	1.123	1.123	0.048	0.217	0.120
* 15	4.269	1.187	1.180	1.175	1.127	1.135	1.130	1.134	1.153	1.146	---	---	---
16	4.269	1.202	1.200	1.195	1.129	1.137	1.132	1.131	1.156	1.153	0.178	0.150	0.087
17	4.269	1.196	1.195	1.195	1.121	1.131	1.122	1.129	1.157	1.153	0.194	0.138	0.092
18	4.269	1.185	1.182	1.175	1.101	1.108	1.104	1.107	1.142	1.140	0.238	0.120	0.095
19	4.269	1.162	1.161	1.158	1.074	1.074	1.075	1.078	1.114	1.117	0.238	0.110	0.081
20	4.269	1.120	1.115	1.122	1.037	1.037	1.037	1.038	1.080	1.083	0.246	0.111	0.084

G11 = 0.130 G12 = 0.171 G3 = 1.096
G21 = 0.234 G22 = 0.235 G4 = 0.173

* Location of logitudinal ribs
+ Location of small longidudinal rib

Table A.24 : Data for Deformation Measurements

Deformation Pattern : C
Surface Type : Mill scale
Bar size : No. 11 (second measurement)

P	A	B	B1	B2	C1	C2	D1	D2	M1	M2	E1	E2	F
1	3.930	0.562	0.558	0.560	0.470	0.471	0.477	0.474	0.513	0.516	0.107	0.101	0.232
2	3.930	0.560	0.557	0.555	0.480	0.479	0.482	0.481	0.515	0.516	0.099	0.136	0.214
3	3.930	0.559	0.555	0.552	0.483	0.483	0.486	0.483	0.516	0.517	0.100	0.155	0.194
4	3.930	0.555	0.551	0.553	0.488	0.489	0.491	0.491	0.517	0.517	0.069	0.173	0.189
5	3.930	0.549	0.540	0.549	0.491	0.494	0.496	0.493	0.518	0.518	0.069	0.209	0.170
* 6	3.930	0.556	0.550	0.549	0.487	0.489	0.490	0.490	0.514	0.513	---	---	---
7	3.930	0.540	0.531	0.536	0.482	0.483	0.483	0.486	0.510	0.507	0.093	0.142	0.082
8	3.930	0.548	0.541	0.546	0.477	0.480	0.481	0.480	0.511	0.510	0.098	0.150	0.089
+ 9	3.930	0.548	0.541	0.545	0.472	0.473	0.476	0.477	0.512	0.511	0.092	0.118	0.104
10	3.930	0.548	0.541	0.544	0.466	0.466	0.470	0.474	0.513	0.512	0.087	0.112	0.107
11	3.930	0.545	0.541	0.542	0.463	0.464	0.468	0.469	0.508	0.507	0.089	0.111	0.114
12	3.920	0.525	0.524	0.524	0.461	0.461	0.465	0.466	0.496	0.497	0.099	0.114	0.082
13	3.920	0.525	0.525	0.522	0.462	0.462	0.465	0.466	0.495	0.496	0.087	0.147	0.104
14	3.920	0.516	0.517	0.515	0.465	0.464	0.465	0.465	0.488	0.489	0.059	0.180	0.099
15	3.920	0.505	0.505	0.500	0.470	0.468	0.469	0.468	0.486	0.487	0.043	0.213	0.078
* 16	3.920	0.510	0.505	0.500	0.467	0.465	0.468	0.466	0.486	0.486	---	---	---
17	3.920	0.508	0.504	0.500	0.466	0.464	0.467	0.465	0.485	0.485	0.052	0.237	0.148
18	3.920	0.538	0.539	0.534	0.466	0.463	0.468	0.467	0.491	0.492	0.104	0.159	0.203
19	3.920	0.549	0.549	0.548	0.464	0.464	0.466	0.467	0.500	0.501	0.105	0.137	0.218
20	3.920	0.554	0.552	0.548	0.466	0.465	0.475	0.474	0.503	0.505	0.103	0.122	0.221

G11 = 0.163 G12 = 0.136 G3 = 0.517
G21 = 0.293 G22 = 0.241 G4 = 0.176

* Location of logitudinal ribs
+ Location of small longidudinal rib

Table A.25 : Data for Deformation Measurements

Deformation Pattern : N

Surface Type : Mill scale

Bar size : No. 11 (first measurement)

P	A	B	B1	B2	C1	C2	D1	D2	M1	M2	E1	E2	F
1	4.269	1.705	1.071	1.074	0.997	0.994	1.004	0.999	1.040	1.025	0.183	0.088	0.058
2	4.269	1.075	1.072	1.074	1.007	1.006	1.009	1.010	1.048	1.040	0.190	0.098	0.034
* 3	4.269	1.081	1.079	1.077	1.028	1.025	1.030	1.031	1.053	1.049	---	---	---
4	4.269	1.092	1.094	1.093	1.033	1.032	1.034	1.037	1.062	1.055	0.161	0.158	0.038
5	4.269	1.092	1.088	1.092	1.038	1.039	1.038	1.042	1.070	1.060	0.127	0.193	0.073
6	4.269	1.131	1.126	1.133	1.050	1.051	1.048	1.052	1.092	1.092	0.153	0.131	0.135
7	4.269	1.141	1.133	1.144	1.052	1.058	1.063	1.060	1.092	1.088	0.156	0.076	0.108
8	4.269	1.134	1.127	1.133	1.050	1.056	1.057	1.055	1.098	1.090	0.118	0.104	0.100
9	4.269	1.130	1.128	1.128	1.050	1.054	1.061	1.062	1.097	1.092	0.139	0.106	0.095
+ 10	4.269	1.128	1.127	1.130	1.057	1.058	1.054	1.059	1.093	1.081	0.117	0.111	0.083
11	4.269	1.125	1.119	1.119	1.037	1.040	1.035	1.040	1.066	1.074	0.090	0.079	0.083
12	4.269	1.078	1.077	1.072	1.020	1.018	1.024	1.021	1.053	1.047	0.081	0.141	0.088
* 13	4.269	1.071	1.072	1.072	1.011	1.010	1.020	1.012	1.048	1.036	---	---	---
14	4.269	1.055	1.055	1.052	0.998	0.997	1.003	0.999	1.023	1.022	0.101	0.177	0.127
15	4.269	1.044	1.043	1.035	0.983	0.980	0.990	0.982	1.020	1.006	0.138	0.141	0.094
16	4.269	1.055	1.052	1.051	0.978	0.973	0.983	0.976	1.018	1.007	0.127	0.136	0.071
17	4.269	1.048	1.044	1.049	0.974	0.969	0.985	0.972	1.014	1.012	0.116	0.090	0.088
18	4.269	1.043	1.042	1.046	0.974	0.967	0.979	0.976	1.010	1.005	0.128	0.130	0.086
19	4.269	1.043	1.039	1.040	0.977	0.972	0.979	0.978	1.002	1.008	0.098	0.164	0.076
20	4.269	1.058	1.057	1.060	0.986	0.982	0.995	0.987	1.023	1.017	0.113	0.121	0.092

G11 = 0.111 G12 = 0.112 G3 = 1.097

G21 = 0.262 G22 = 0.265 G4 = 0.202

* Location of logitudinal ribs

+ Location of small longidudinal rib

Table A.26 : Data for Deformation Measurements

Deformation Pattern : N
Surface Type : Mill scale
Bar size : No. 11 (second measurement)

	P	A	B	B1	B2	C1	C2	D1	D2	M1	M2	E1	E2	F
	1	3.930	0.552	0.550	0.547	0.471	0.471	0.489	0.481	0.518	0.513	0.103	0.083	0.154
	2	3.930	0.558	0.555	0.556	0.475	0.476	0.486	0.484	0.518	0.516	0.101	0.096	0.171
	3	3.930	0.561	0.558	0.556	0.480	0.481	0.488	0.484	0.517	0.521	0.108	0.103	0.136
	4	3.930	0.550	0.544	0.546	0.483	0.484	0.490	0.494	0.512	0.515	0.087	0.148	0.129
	5	3.930	0.535	0.525	0.531	0.486	0.488	0.490	0.488	0.505	0.509	0.072	0.225	0.099
*	6	3.930	0.541	0.528	0.530	0.483	0.484	0.485	0.485	0.508	0.508	---	---	---
	7	3.930	0.533	0.530	0.529	0.480	0.479	0.480	0.481	0.510	0.507	0.095	0.219	0.103
	8	3.930	0.558	0.555	0.554	0.478	0.481	0.488	0.483	0.515	0.510	0.111	0.130	0.114
+	9	3.930	0.568	0.565	0.565	0.477	0.478	0.487	0.479	0.515	0.514	0.136	0.094	0.111
	10	3.930	0.559	0.557	0.557	0.475	0.474	0.485	0.475	0.515	0.517	0.112	0.098	0.143
	11	3.930	0.545	0.544	0.544	0.465	0.465	0.471	0.473	0.510	0.514	0.110	0.112	0.167
	12	3.930	0.547	0.545	0.544	0.464	0.463	0.468	0.470	0.510	0.513	0.103	0.103	0.179
	13	3.930	0.557	0.555	0.551	0.463	0.460	0.466	0.467	0.512	0.510	0.118	0.086	0.174
	14	3.930	0.522	0.523	0.518	0.457	0.455	0.464	0.459	0.491	0.494	0.098	0.157	0.160
	15	3.930	0.502	0.502	0.499	0.460	0.456	0.464	0.456	0.472	0.479	0.092	0.241	0.124
*	16	3.930	0.517	0.507	0.505	0.461	0.459	0.467	0.456	0.480	0.482	---	---	---
	17	3.930	0.513	0.511	0.510	0.461	0.461	0.470	0.465	0.488	0.485	0.081	0.194	0.167
	18	3.930	0.540	0.540	0.540	0.466	0.464	0.468	0.466	0.499	0.503	0.111	0.145	0.162
	19	3.930	0.550	0.550	0.546	0.468	0.465	0.475	0.470	0.507	0.500	0.109	0.097	0.155
	20	3.930	0.550	0.546	0.547	0.471	0.469	0.478	0.477	0.509	0.510	0.116	0.075	0.176

G11 = 0.120 G12 = 0.115 G3 = 0.516
G21 = 0.270 G22 = 0.275 G4 = 0.208

* Location of logitudinal ribs
+ Location of small longidudinal rib

APPENDIX B: HYPOTHESIS TESTING

Bond tests naturally exhibit a great deal of data variation. Therefore, some form of statistical analysis is needed to determine whether observed data variations are statistically significant, that is, the result of actual performance differences, or not significant and the result of data scatter. In this study, hypothesis testing is employed to make this determination. Specifically, the hypothesis that the mean bond strength of one population (μ_1) is equal to the mean bond strength of another population (μ_2) is tested against another hypothesis that these means are not equal. Hypothesis testing is applied to two population means using what is known as the two-sample t-test. In the following, concepts of this statistical method are discussed and examples are given to illustrate the procedures.

In order to apply hypothesis testing, the two hypotheses in a comparison must be conflicting, that is, these hypotheses must be constructed so that if one hypothesis is true, the other is false, and vice versa. The two hypotheses are normally known as the null hypothesis, H_o, and the alternative hypothesis, H_a. The objective of hypothesis testing is to test the null hypothesis H_o, $\mu_1 = \mu_2$, against the alternative hypothesis, H_a, $\mu_1 \neq \mu_2$. From the hypothesis testing, a decision is made whether to accept or to reject the null hypothesis with some level of confidence. The mean bond strength of one population can be equal to the mean bond strength of another population, or these means may not be equal.

The hypothesis tests which we make are based on certain probability assumptions. Specifically, let X_1 be the ultimate bond strength for bars in population No. 1, and X_2 be the ultimate bond strength for bars in population No. 2. Then X_1 and X_2 are random variables which have certain distributions. For the purposes of our tests we assume that X_1 and X_2 are normally distributed with means μ_1 and μ_2 and standard deviations σ_1 and σ_2. We consider the bars which we test to constitute random samples, of sizes n_1 and n_2, respectively, from populations No. 1 and No. 2. Once we have tested the bars in our samples, we can calculate the sample means $\bar{x}_1$ and $\bar{x}_2$ and sample standard deviations s_1 and s_2. Due to random variations, the two sample means $\bar{x}_1$ and $\bar{x}_2$ will in general be different. We want to decide whether the difference between $\bar{x}_1$ and $\bar{x}_2$ is so great as to indicate that $\mu_1 \neq \mu_2$, or whether the difference between $\bar{x}_1$ and $\bar{x}_2$ is small enough that it is consistent with the hypothesis $\mu_1 = \mu_2$.

In the cases which we need to consider, we do not know σ_1 or σ_2. Also, we usually have small sample sizes (n_1 and n_2) each less than 30), so we do not want to assume $\sigma_1 = s_1$ and $\sigma_2 = s_2$. However, it does seem reasonable to assume, in our cases, that $\sigma_1 = \sigma_2$. Therefore, we make this assumption, i.e., that the population standard deviations are unknown, but equal. Under these assumptions, if the null hypothesis H_o: $\mu_1 = \mu_2$, is true, then the statistic:

$$T = \frac{\bar{x}_1 - \bar{x}_2}{\sqrt{\left(\frac{n_1 - 1}{n_1 + n_2 - 2} s_1^2 + \frac{n_2 - 1}{n_1 + n_2 - 2} s_2^2\right)\left(\frac{1}{n_1} + \frac{1}{n_2}\right)}} \qquad (B.1)$$

has a t-distribution with $n_1 + n_2 - 2$ degrres of freedom (Harnett 1975). It is this statistic T which we use in the two-sample t-test.

Our decision procedure is then as follows. After we have tested the bars in our samples, we calculate $\bar{x}_1$, $\bar{x}_2$, s_1, s_2, and, from these, the observed value of the T-statistic defined above, call it t_{obs}. Due to the fact that T has a t-distribution if H_o is true, we regard extreme values of t_{obs} as evidence that H_o is false, i.e., H_a is true. Specifically, we define a critical region for the test, i.e., a set C of values for T such that if t_{obs} lies in C, then we reject H_o. We take:

$$C = \{t: |t| > t_{\frac{\alpha}{2}, n_1 + n_2 - 2}\}. \qquad (B.2)$$

The number α is called the level of significance of the test; it is the probability that we will reject H_o when in fact H_o is true. Note that if t_{obs} is such that we reject H_o even for small values of α (say $\alpha = .001$), then we have strong evidence that H_o is false. On the other hand, if t_{obs} is such that we accept H_o even for relatively large values of α (say $\alpha = .20$), then we do not have even mildly strong evidence against H_o; in this case, our test results

are entirely consistent with the hypothesis $\mu_1 = \mu_2$. Note that in this second case we have not proved that $\mu_1 = \mu_2$; we can say just that our test results are consistent with this hypothesis.

Once the two-sample t-test was performed on the data, the sets of data that the t-test proved to be not significant, are put through a more stringent test utilizing the σ_1 and σ_2. The coefficient of variation (COV) for uncoated and coated bars in each group of specimens is calculated by $\text{COV} = \frac{\sigma}{\bar{x}}$ in which $\sigma = \sqrt{\frac{\Sigma_i (x_i - \bar{x})^2}{n}}$ in which x_i is the individual bond test and $\bar{x}$ is the mean of n uncoated or coated bars within a group. Once the COV is calculated for all the groups, for every bar size, a combined COV is calculated by

$$(\text{COV})_{\text{combined}} = \sqrt{\frac{\Sigma_i (n_i \ \text{COV}_i^2)}{\Sigma_i (n_i)}} \qquad \text{(B.3)}$$

in which COV_i is the COV of uncoated or coated bars in group i and n_i is the number of uncoated or coated bars in group i. The obtained values of $(\text{COV})_{\text{combined}}$ for No. 5 bars are 0.046399 and 0.045414 for uncoated and coated bars, respectively. The respective values for No. 6, No. 8, and No. 11 bars are, 0.06 and 0.050377, 0.053917 and 0.057981, and 0.073695 and 0.074853, respectively. Then, for uncoated and coated bars of different sizes, a very good estimate of σ is $\sigma = (\text{COV})_{\text{combined}} \cdot \bar{x}$. The value of σ has to be estimated since the sample size is usually small (less than 30).

Once the values of $\bar{x}_1$, $\bar{x}_2$, σ_1, and σ_2 are known, then the statistic

$$Z = \frac{\bar{x}_1 - \bar{x}_2}{\sqrt{(\frac{\sigma_1^2}{n_1}) + (\frac{\sigma_2^2}{n_2})}} \tag{B.4}$$

has a normal distribution. It is this statistic Z which we use in the more stringent significance test, let's call it two-sample z-test. Once a value of z, call it z_{obs}, is calculated, then if H_o is true, we regard extreme values of z_{obs} as evidence that H_o is false, i.e., H_a is true. Again, we define a critical region for the test, i.e., a set D of values for Z such that if z_{obs} lies in D, then we reject H_o. We take:

$$D = (Z: |Z| > Z_{\frac{\alpha}{2}}). \tag{B.5}$$

The number α is called the level of significance of the test, same as in Eq. (B.2).

As an example of this procedure, the significance of casting position on bond strength is studied for coated N-pattern No. 8 bars. The two samples included six coated bottom-cast bars with ultimate bond forces of 33,417, 38,275, 37,548, 40,805, 38,763, and 41,893 lbs. and six coated top-cast bars with ultimate bond forces of 36,351, 38,016, 35,205, 36,917, 35,018, and 31,796 lbs. The

sample mean ultimate bond forces for bottom and top-cast bars in our samples are 38,450 and 35,551 lb., with sample standard deviations of 2955 and 2149 lb., respectively. The sample sizes for this analysis include 6 bottom-cast bars and 6 top-cast bars. It is assumed that the alternative is two-sided (covers situations where μ_1 can be greater than or less than μ_2) and that $\alpha = 0.05$. The critical values in this case from the table of the t-distribution are

$$\pm t_{(\alpha/2,\ n_1 + n_2 - 2)} = \pm t_{(0.025,\ 10)} = \pm 2.228. \qquad (B.6)$$

in which n_1 and n_2 are sample sizes. These critical values can be compared with the calculated value of t. Using Eq. B.1, and $\bar{x}_1 = 38,450$, $\bar{x}_2 = 35,551$, $s_1^2 = 2955^2$, and $s_2^2 = 2149^2$, the calculated t value is obtained as 1.944. The calculated t value does not fall in the critical region; thus the null hypothesis, that the mean bond strength of bottom and top-cast coated N-pattern No. 8 bars are equal, cannot be rejected with 0.05 level of significance. The test results show that the difference in these two sample mean bond strengths may be attributed to scatter, and a significant difference in bond strength does not exist between bottom-cast and top-cast coated bars with the same bar size.

As another example, we apply the more stringent two-sample z-test to the previous example. The sample mean ultimate bond forces for bottom and top-cast bars in our samples are 38,450 and 35,551

lb., with estimated standard deviations of 2229 and 2061 lb., respectively [$\sigma_1 = \sigma_{bottom} = (COV)_{combined} \cdot \bar{x}_1 = 0.057981\ (38,450) = 2229$ and $\sigma_2 = \sigma_{top} = (COV)_{combined} \cdot \bar{x}_2 = 0.057981\ (35,551) = 2061$]. The sample sizes are 6 bottom-cast bars and 6 top-cast bars. It is assumed that the alternative is two-sided and that $\alpha = 0.05$. The critical values in this case from the table of the normal distribution are

$$\pm z_{\frac{\alpha}{2}} = \pm z_{0.025} = \pm 1.960 \qquad (B.7)$$

The calculated z value, 2.339 from Eq. B.4, does fall between the critical values of z; thus the null hypothesis, that the mean bond strengths of bottom and top-cast coated N-pattern No. 8 bars are equal, can be rejected. There are significant differences in the sample mean bond strengths, between bottom and top-cast bars in our samples due to the effect of casting position.

Because bond tests naturally exhibit a great deal of scatter, it is important to establish whether differences in test results are caused by normal variability in bond properties or by a systematic cause. Hypothesis testing is used to make this distinction. The two-sample t-test and Z-test, as used in this study, are effective in evaluating test results, especially the variations in bond strength accompanying changes in bar surface condition, bar position, concrete slump, and consolidation of concrete.